MODELLING DISTRICT HEATING IN A RENEWABLE ELECTRICITY SYSTEM

Salman Siddiqui

Bartlett School of Environment, Energy and Resources
Energy Institute
University College London

A dissertation submitted in fulfilment of the requirements
for the degree of
Doctor of Philosophy

August 2022

Declaration

I, Salman Siddiqui, confirm that the work presented in this thesis is my own. Where information has been derived from other sources, I confirm that this has been indicated in the thesis.

Signed:_____

Date:_____

Abstract

With the decarbonisation of electricity generation, large scale heat pumps are becoming increasingly viable for district heating combined with thermal energy storage, district heating can provide flexibility to the electricity grid by decoupling demand from supply. This thesis examines how district heating with heat pumps and thermal energy storage can integrate with and provide a benefit to an electricity system with predominantly renewable generation. The scope of work comprises three interlinked models underpinned by the same set of meteorology data, fundamentally coupling supply and demand.

First, heat load data are surveyed, and an hourly demand profile is simulated. Disaggregation of district heating loads from the national demand is accomplished via segmentation of the building stock to model heat demand at high spatiotemporal resolution.

Second, a novel method of pricing hourly electricity in a zero carbon, capital-intensive renewable system with electricity storage is developed and applied to a dispatch simulation to generate hourly electricity prices.

Third, a dynamic model of district heating is constructed to simulate the meeting of heat loads with different design configurations using electricity as the energy source. Model predictive control is applied with varying forecast horizons so as to minimise the cost of electricity to meet the heat demand given a time series of hourly prices and consequently optimising the capacity of thermal energy storage. It was found that a thermal energy storage capacity equivalent to 1.3% of annual demand is sufficient to minimise operating costs.

Finally, the potential impact of district heating on balancing the electricity system is analysed and an equivalence between thermal and electric storage is examined. While this is highly dependent on annual conditions, it can be as much as 3.5 units of thermal storage for every unit of electrical grid storage on the system. This could potentially reduce the investment in grid storage by £36 billion, underlining the significant financial benefits of thermal storage to the whole system. The research highlights the important potential of district heating to the UK's energy system strategy.

Impact Statement

The decarbonisation of the UK economy necessitates a transition away from fossil fuels. This provides a challenge to managing the electricity grid which must balance the variability of renewable generation with time varying demand. For space heating in buildings, electrification is a promising method to achieve decarbonisation. However, the electricity requirements for heat pumps will be substantial and may impact the security of the electricity grid. The central premise of this work is the exploration of how heat pumps in district heating systems with thermal energy storage can support the electricity grid and help to accommodate larger fractions of renewable generation by allowing greater flexibility of operation via large scale thermal energy storage. The results presented here should be of interest to policymakers, highlighting the importance of district heating to the energy system.

The investigation was conducted by developing a set of models to simulate heat loads, the electricity system, and district heating. The methods used and datasets produced in designing these models will be of interest to the modelling research community. The study has produced a dataset of national hourly heat loads, disaggregated by area, which can be utilised for early feasibility work by city energy planners in various other applications as model inputs.

The electricity cost model introduces a novel method for calculating marginal electricity generation costs for capital intensive systems that may aid other modelling studies. It was shown that the marginal costs of electricity supply in a highly renewable system can be within a manageable range and that they are largely driven by capital costs of both renewables and storage. This has implications on policy and tariff design for bodies such as Ofgem who could ensure that storage is adequately rewarded so that sufficient capacities are built.

For industry and district heating operators, the simulation of district heating has provided a practical grasp of operating costs in a highly renewable electricity system. It was shown that optimal thermal energy storage costs represent a small fraction of the capital investment. The operational costs of electricity import amount to a tenth of the total cost of supplying heat from district heating. For policy and public planners, this is comparable to current and future counterfactual options and shows that district heating is a viable option for cost-effective heat in urban areas. It is hoped that these results will feed into future economic analyses of district heating deployment.

The conclusions show that the widespread deployment of district heating can have an important function in the national energy system and that thermal energy storage is able to displace a significant amount of grid storage, thereby reducing total system costs. This alone warrants that it is investigated as part of an energy system strategy. The issues raised in this thesis directly impact organisations such as the National Grid. They are also important for the district heating industry as well as government policymakers and for the Climate Change Committee who advise them, both of whom ultimately shape the direction of energy policy and research in the UK.

Publications

Siddiqui, S., Macadam, J., Barrett, M., 2020. A novel method for forecasting electricity prices in a system with variable renewables and grid storage. International Journal of Sustainable Energy Planning and Management. https://doi.org/10.5278/IJSEPM.3497

Siddiqui, S., Barrett, M., Macadam, J., 2021. A High Resolution Spatiotemporal Urban Heat Load Model for GB. Energies 14, 4078. https://doi.org/10.3390/en14144078

Siddiqui, S., Macadam, J., Barrett, M., 2021. The operation of district heating with heat pumps and thermal energy storage in a zero-emission scenario. Energy Reports. https://doi.org/10.1016/j.egyr.2021.08.157

Acknowledgements

I have been fortunate enough to have been given a chance to undertake a PhD and work with some extraordinary people, namely my esteemed supervisors Professor Mark Barrett and John Macadam, to whom I am forever grateful. This thesis was only possible with their support, wise guidance and painstaking supervision. Mark took me under his wing, gave me the opportunity to explore ideas and his enthusiasm for the subject and confidence in my abilities invigorated this work. John has been an absolute fountain of knowledge to which I have been incredibly lucky to have had access to. Laying much of the theoretical framework, his expertise, persistent and meticulous examination of outputs has shaped much of this work.

This research was made possible by the EPSRC Centre for Doctoral Training in Energy Demand (LoLo). The support provided by the LoLo management and peers within the Energy Institute provided the ideal research environment with welcome breaks full of stimulating discussions on a multitude of topics beyond energy and academic discourse.

I must also thank my friends and family for their unwavering support, particularly my parents and siblings, and especially my wife, Rahma who encouraged me to begin this journey, helped me overcome many challenges throughout and had an endless supply of patience.

Contents

1 INTRODUCTION 1
1.1 The Decarbonisation of Heating 1
1.2 Integrated Energy Systems 8
1.3 Energy System and District Heating Modelling 12
1.4 Research Design 15
1.5 Thesis Structure 18
2 HEAT LOAD MODEL 19
2.1 Model Objectives 19
2.2 Literature Review of Heat Load Modelling 20
2.3 Archetype Development 25
2.4 Thermal Model Development 33
2.5 Results 39
2.6 Discussion 45
3 ELECTRICITY COST MODEL 47
3.1 Renewable Energy and Grid Balancing 47
3.2 Review of Renewable Electricity Price Variance 49
3.3 Modelling Methodology 50
3.4 Dispatch model 51
3.5 Marginal cost method development 52
3.6 Model Validation 55
3.7 Scenario Development 60
3.8 Discussion 67
4 DISTRICT HEATING MODEL 69
4.1 Review of District Heating Modelling 69
4.2 Modelling Methodology 74
4.3 Operating Algorithm Development 82
4.4 Algorithm comparison 97
4.5 District Heating Network Configuration 99
4.6 Discussion 101
5 CONCLUSIONS: A SYSTEM PERSPECTIVE 105
5.1 Thesis Summary 105
5.2 District Heating and the Electricity System 106
5.3 Key Findings and Contributions 111
5.4 Future Work 114
5.5 Epilogue 115
REFERENCES 117
APPENDICES 135

List of Tables

TABLE 1.1 ADVANTAGES AND DISADVANTAGES OF THREE OPTIONS FOR FUTURE UK HEAT DELIVERY 3
TABLE 1.2 STUDIES ON DISTRICT HEATING'S POTENTIAL IN THE UK 6
TABLE 1.3 REVIEW OF ELECTRICITY GRID FLEXIBILITY STUDIES 10
TABLE 1.4 COMPARISON OF EXISTING MODELS' FUNCTIONALITY 14
TABLE 2.1 SUMMARY OF DATA SOURCES USED FOR HELOM 25
TABLE 2.2 ARCHETYPES USED IN COMPARATIVE STUDIES 27
TABLE 2.3 DOMESTIC ARCHETYPE DATA SOURCES 28
TABLE 2.4 SUMMARY OF MODELLED REGIONS 32
TABLE 2.5 UK HOURLY WEATHER OBSERVATIONS - REGIONAL STATIONS 34
TABLE 2.6 MONTHLY FACTOR FOR DOMESTIC HOT WATER VARIATION 36
TABLE 2.7 AVERAGE CALIBRATION FACTORS PER REGION 37
TABLE 2.8 COMPARISON OF 2010 HEAT DEMAND WITH PREVIOUS ESTIMATES 40
TABLE 2.9 ECUK 2010 HEATING CONSUMPTION ESTIMATES 40
TABLE 3.1 COMPARISON OF 2016 LOW CARBON GENERATION WITH MODELLED GENERATION 56
TABLE 3.2 NATIONAL GRID FES SCENARIOS COMPARISON 56
TABLE 3.3 PRICE COMPARISON WITH RENEWABLE CAPACITY AND STORAGE 56
TABLE 3.4 AVERAGE PRICE COMPARISON FOR HIGH AND LOW-COST CASES 60
TABLE 3.5 CT BASE SCENARIO AND ADJUSTED NZ GENERATION AND STORAGE CAPACITY 65
TABLE 4.1 TES PERCENTAGE AND PEAK HOURS EQUIVALENCE FOR MODELLED DHN 86

List of Figures

FIGURE 1.1 COMPARISON OF ENERGY STORAGE COSTS WITH TES ADAPTED FROM LUO ET AL. (2015) 5

FIGURE 1.2 OVERVIEW OF THE EVOLUTION OF DISTRICT HEATING ADAPTED FROM LUND ET AL. (2014)..... 8

FIGURE 1.3 MODELLING SYSTEM BOUNDARIES.....16

FIGURE 2.1 DWELLING TYPES IN THE UK HOUSING STOCK.....26

FIGURE 2.2 DWELLING BUILT PERIOD IN THE UK HOUSING STOCK 27

FIGURE 2.3 NORMALISED DOMESTIC OCCUPANCY PROFILES.....29

FIGURE 2.4 COUNT AND FLOOR AREA PER ACTIVITY CLASSIFICATION IN THE CARB2 DATABASE 29

FIGURE 2.5 NONDOMESTIC CLASSIFICATION SHARE IN SCOTLAND (SCOTTISH GOVERNMENT, 2018) 30

FIGURE 2.6 PROPORTION OF NONDOMESTIC ARCHETYPES IN MODELLED URBAN AREAS.....30

FIGURE 2.7 MODELLED GB MSOA LOCATIONS 32

FIGURE 2.8 LOCATIONS OF REGIONAL WEATHER STATIONS USED.....34

FIGURE 2.9 NORMALISED DAILY LOAD PROFILES FOR DOMESTIC HOT WATER.....36

FIGURE 2.10 COMPARISON BETWEEN CARB2 COUNT AND NONDOMESTIC GAS METERS PER MSOA 38

FIGURE 2.11 MODELLING STEPS FOR AGGREGATING DOMESTIC AND NONDOMESTIC DEMAND 38

FIGURE 2.12 SENSITIVITY OF THERMAL MODEL PARAMETERS 39

FIGURE 2.13 MODELLED NATIONAL HOURLY HEAT DEMAND FOR 2010.....40

FIGURE 2.14 COMPARISON OF NATIONAL COLDEST DAY AND MEAN DECEMBER DEMAND PROFILE 40

FIGURE 2.15 DOMESTIC AND NONDOMESTIC NATIONAL HEAT DEMAND DURATION CURVES FOR 2010.....41

FIGURE 2.16 MODELLED NATIONAL HOURLY HEAT LOAD 2010-2015 42

FIGURE 2.17 COMPARISON OF THE NATIONAL AND URBAN HEAT DEMAND DURATION CURVE FOR 2010 43

FIGURE 2.18 AVERAGE WINTER LOAD PROFILE COMPARISON 43

FIGURE 3.1: ORDER OF OPERATION TO CALCULATE MARGINAL COSTS FOR EACH HOUR TYPE.....52

FIGURE 3.2: RESIDUAL RENEWABLE GENERATION (ABOVE) AND RESULTING CYCLING OF STORAGE AND COSTS (BELOW) FOR SCENARIO A 2016.....57

FIGURE 3.3: SCENARIO A AND B COST DURATION CURVES 2013.....58

FIGURE 3.4: SCENARIO A 2013 PRICE DURATION CURVE WITH ADJUSTED DSP HOUR COSTS.....58

FIGURE 3.5: RESIDUAL RENEWABLE GENERATION FOR SCENARIO A AND B 2013.....59

FIGURE 3.6: SCENARIO A 24-HOUR ROLLING AVERAGE OF MODELLED COSTS AND TRENDLINE 2006-2016.....59

FIGURE 3.7: SCENARIO B WITH HIGH AND LOW-COST PROJECTIONS (CLIPPED FOR DETAIL).....60

FIGURE 3.8 DAILY ELECTRIC VEHICLE DEMAND PROFILE FOR THE NZ SCENARIO 61

FIGURE 3.9 MODELLED 2012 DAILY ELECTRICITY DEMAND FOR THE NZ SCENARIO.....62

FIGURE 3.10 OFFSHORE CAPACITY FACTORS BEFORE (TOP) AND AFTER (BOTTOM) TRANSFORMATION.....63

FIGURE 3.11 BASE SCENARIO ADJUSTMENT FACTORS EXPERIMENTATION.....64

FIGURE 3.12 CUMULATIVE DEMAND AND GENERATION FOR NZ 2010.....65

FIGURE 3.13 DAILY TOTAL DEMAND AND GENERATION FOR NZ 2010.....65

FIGURE 3.14 NZ SCENARIO DAILY MEAN ELECTRICITY COSTS 66

FIGURE 3.15 DURATION CURVE OF ELECTRICITY PRICES AND GENERATION COSTS FOR NZ 2010.....67

FIGURE 4.1 MODELLING OF DH NETWORK OPERATING MODES 75
FIGURE 4.2 COSTS PER UNIT VOLUME FOR TTES AND PTES 79
FIGURE 4.3 SCHEMATICS OF PARTIALLY BURIED TTES (LEFT) AND PTES (RIGHT) ADAPTED FROM (SØRENSEN AND SCHMIDT (2018) 79
FIGURE 4.4 SPECIFIC HEAT LOSSES FROM MODELLED TES 80
FIGURE 4.5 MODELLED DAILY MEAN COPS COMPARED TO AMBIENT AND GROUND TEMPERATURES 82
FIGURE 4.6 COMPARISON OF WINTER SEASON WIND CAPACITY FACTORS AND MEAN TEMPERATURE 83
FIGURE 4.7 FIVE DAY ROLLING AVERAGE OF ELECTRICITY COSTS AND HEAT DEMAND 84
FIGURE 4.8 12 HOUR ROLLING DEMAND AND PRICES FOR SELECTED PERIODS 85
FIGURE 4.9 CORRELATION BETWEEN HEAT DEMAND AND ELECTRICITY COST 86
FIGURE 4.10 THE EFFECT OF RELATIVE TES AND HP SIZE ON COST (HP+TES ANNUITISED CAPITAL) 87
FIGURE 4.11 THE IMPACT OF VARYING HP AND TES WITH OPTIMAL TRIGGER PRICES ON TOTAL COST (A) AND ELECTRICITY COSTS ONLY (B) FOR THE PERIOD 2014-2015 88
FIGURE 4.12 HOURLY OPERATION OF 0.1% TES FOR BSC (TOP), TRG (MIDDLE), DOA (BOTTOM) 90
FIGURE 4.13 COMPARISON OF FIVE-DAY ROLLING AVERAGE OF ELECTRICITY COSTS WITH VARIOUS TES SIZES USING DOA FOR 2010-2011 (TOP) AND 2013-2014 (BOTTOM) 91
FIGURE 4.14 HOURLY OPERATION OF 1% TES FOR BSC (TOP), TRG (MIDDLE), DOA (BOTTOM) 92
FIGURE 4.15 COMPARISON OF 24-HOUR ROLLING AVERAGE OF ELECTRICITY COSTS WITH VARIOUS TES SIZES USING DOA FOR SELECT PERIODS 93
FIGURE 4.16 IMPLEMENTATION OF PRODYN OPTIMISATION ALGORITHM WITH HELOM 95
FIGURE 4.17 TES OPERATION AT VARIOUS TES SIZES USING THE RDOA FOR THE PERIOD 2014-2015 96
FIGURE 4.18 FREQUENCY ANALYSIS OF TES CYCLES USING A 0.1% TES (TOP) AND 1% (BOTTOM) WITH SUPER-DIURNAL CYCLES INSET FOR THE 2014-2015 PERIOD 97
FIGURE 4.19 COMPARISON OF ELECTRICITY COSTS OF ALL ALGORITHM FROM THE PERIODS 2010-2011 (TOP) AND 2013-2014 (BOTTOM) 98
FIGURE 4.20 OPERATING ELECTRICITY COSTS FOR EACH PERIOD USING THE RDOA 99
FIGURE 4.21 TOTAL ANNUITISED CAPITAL, O&M, AND ELECTRICITY ANNUAL COSTS PER MWH OF DELIVERED HEAT FOR VARYING TES CAPACITIES 99
FIGURE 4.22 COMPARISON OF ANNUAL COMPONENT COST PER MWH OF DELIVERED HEAT FOR LOW, MEDIUM AND HIGH COST SENSITIVITY RANGES 100
FIGURE 4.23 MEDIUM CASE ANNUAL OPERATING COSTS DISTRIBUTION 100
FIGURE 4.24 AERIAL VIEW OF THE KENNINGTON GAS HOLDERS (GOOGLE MAPS, 2021) 103
FIGURE 5.1 PEAK AND TOTAL ELECTRICITY DEMAND WITH DH DEPLOYMENT 106
FIGURE 5.2 CHANGE IN THE MEAN (SOLID) AND MAXIMUM (DASHED) MARGINAL GENERATION COSTS 107
FIGURE 5.3 CHANGE IN THE AVERAGE UNIT (TOP) AND TOTAL ANNUAL (BOTTOM) COST OF ELECTRICITY FOR HEATING 108
FIGURE 5.4 CHANGE IN RENEWABLE SURPLUS AND DEFICIT AFTER INTEGRATION 109
FIGURE 5.5 GRID RESIDUAL DURATION CURVES FOR NZ SCENARIO AND INTEGRATION OF DH (2010) 110

List of Boxes

BOX 1.1 ECONOMIC TERMINOLOGY: THE DIFFERENCE BETWEEN COST AND PRICE....18
BOX 2.1 OUTPUT AREAS AND GEOGRAPHIC SUBDIVISIONS....21
BOX 2.2 DIVERSITY FACTORS AND PEAK DEMAND....35
BOX 3.1 DEFINITIONS OF COST AND PRICE IN CONTEXT....48
BOX 4.1 DYNAMIC PROGRAMMING - DP....74
BOX 4.2 CHALLENGES OF DEVELOPING THE RDOA....95

List of Abbreviations and Acronyms

BSC	Basic algorithm
CCGT	Combined cycle gas turbine
CCS	Carbon capture and storage
CHP	Combined heat and power
CHR	Charge hours
COP	Coefficient of performance
DCHf / DCHp	Discharge hours – full / partial
DH	District heating
DiHeM	District heating model
DOA	Dynamic optimisation algorithm
DP	Dynamic programming
DSPp /DSPo	Dispatch hours – peak /off-peak
ElCoM	Electricity cost model
HDD	Heat demand density
HeLoM	Heat load model
HP	Heat pump
HV	High voltage
LP	Linear programming
MILP	Mixed-integer linear programming
MINLP	Mixed-integer nonlinear programming
MPC	Model predictive control
NLP	Nonlinear programming
NZ	Net zero (scenario)
RDOA	Rolling dynamic optimisation algorithm
SRP	Surplus hours
TES	Thermal energy storage
TRG	Trigger algorithm
TTES	Tank thermal energy storage
VRE	Variable renewable energy

Nomenclature

Chapter 2 Nomenclature

Symbols

ach	Air Changes per hour
A	Area (m^2)
h_c	Wall convection coefficient ($Wm^{-2}K^{-1}$)
M_{th}	Thermal mass (WhK^{-1})
N_b	Number of buildings
P_h	Hourly occupancy
Q	Heat transfer (W)
T	Temperature (K)
U	Thermal transmittance ($Wm-^2K^{-1}$)
V_b	Building volume (m^3)
v_w	Wind speed (ms^{-1})
f	Adjustment factor
G_t	Glazing transmittance factor (%)
I_r	Incident irradiance (W/m^2)

Subscripts

s	Denotes value per surface/wall
f	Floor area (m^2)
amb	Ambient temperature (K)
ext	External wall temperature (K)
h	Hourly factor
int	Internal wall temperature (K)
set	Setpoint temperature (K)
cond	Conduction heat transfer per surface (W)
conv	Convection heat transfer per surface (W)
gain	Thermal gains (W)
dem	Building Heat demand (W)
HW	Hot water demand (W)
inf	Infiltration heat transfer (W)
m	Monthly factor
sol	Solar (W)
tot	Total heat transfer (W)

Chapter 3 Nomenclature

Symbols

A	Availability/Capacity Factor (%)
C	Capacity, (MW or MWh)
D	Demand (MWh)
E	Efficiency (%)
F	Fixed Costs (£/MW/annum)
G	Generation (MWh)
K	Cost of grid storage (£/MWh)
L_{DST}	Distribution Loss
M	Constrained-down loss (£/MWh)
MC	Marginal Cost (£/MWh)
N	Number of hours count
Q	Charge/Discharge quantity (MWh)
R	Forced outage rate (%)
T_{amb}	Ambient temperature (K)
V	Variable Costs (£/MWh)

Subscripts

BSL	Baseload
CAR	Carnot efficiency
CDD	All Charge, Discharge and Dispatch hours
CHR	Charge hours All
CHRc	Charge hours in cycle
D	Dispatchable generator
DCH	Discharge hours,
DCHf/ DCHp	Discharge hours, full cycle/ part cycle
DSP	Dispatch hours
DSPp/ DSPo	Dispatch hours, peak / off peak
E	Electrical
H	Heating
i	Hour i
LCB	Low Carbon Generation
m	Marginal renewable generator
n	Incremental renewable generator
OFS	Offshore wind
ONS	Onshore wind
s	Storage
SOL	Solar PV
SRP	Surplus hours

Chapter 4 Nomenclature

Symbols

c	Specific Heat capacity ($Whkg^{-1}K^{-1}$)
E	Electricity demand (MWh)
J	Cost (£)
L	Heat load (MW)
M	Mass (kg)
$\dot{M}$	Mass flow rate (kgs^{-1})
P	Price of electricity (£/MWh)
Q	Heat transfer (MW)
T	Temperature (K)
U	Decisions variable
X	TES state

Subscripts

c	TES cold water
f	Flow
h	TES hot water
hp	Heat pump
i	Time
m	Mixture
r	Return
s	Source
v	Sequence
w	Water
η	Efficiency

1 INTRODUCTION

The Climate Change Act (2008) set a target for the UK to reduce greenhouse gas emissions by 80% from 1990 baseline levels. The government has since committed to a net-zero target or 100% reduction (UK Parliament, 2019). Nearly half of the energy demand in the UK is for the provision of heat, with the majority of this coming from the combustion of fossil fuels and this accounts for around a fifth of UK emissions (BEIS, 2017a; DECC, 2013). Hence, it is widely recognised that to meet the emissions target, heating for buildings will need to be nearly fully decarbonised as it is easier to reduce emissions from heat than other harder to decarbonise sectors such as aviation.

The government has outlined several strategies towards decarbonising the UK economy. This includes a high degree of electrification of some sectors such as low temperature heat demand (BEIS, 2020a). The decarbonisation targets necessitate a large deployment of renewable power generation for the electricity grid. Some analysis has left room for natural gas as a transition fuel, but its long term viability is sensitive to the successful deployment of carbon capture and sequestration (CCS) (Hull and Kane, 2016; National Grid, 2017a).

Renewable power generation is variable by nature. This variability provides a challenge to managing the grid which must be balanced at all times by matching supply to demand. Offshore wind is likely to prominently feature in the generation mix. With wind power being uncontrollable and hence inflexible, flexibility must be provided elsewhere. Provisions for flexibility can take many forms such as storage on the grid, or on the demand side (such as demand side response). There is currently a limited capacity to accommodate variable renewable electricity generation. This may cause an increase in the cost of power generation as it limits the ability to fully utilise all the available renewable generation (Strbac et al., 2016). Heating may provide an important vector for economically integrating variable renewable electricity.

1.1 The Decarbonisation of Heating

The predominant source of heating in the UK has been from natural gas. Although the vast majority of homes and buildings in the UK have a gas boiler, the transition away from gas boilers is underway and will not feature in a zero-carbon future for heating (BEIS, 2021a; McGlade et al., 2014). All decarbonisation pathways provide an infrastructure challenge. This includes the expansion of district heating (DH) networks in the UK (also widely referred to as ‘heat networks’ in the literature).

The government has kept its options open, pursuing the paths of least regret and its policy direction is yet to be settled (Climate Change Committee, 2016). Questions remain over the viability of switching to hydrogen. This concerns the infrastructure requirements and potential "lock-in" of hydrogen technology. To make hydrogen heating low carbon will require long term planning due to hydrogen production methods and this may also be contingent on the successful deployment of CCS (ERP, 2016).

Electrification is a promising method to facilitate the decarbonisation of heating (Connolly, 2017). However, the electricity requirement for heat, particularly peak load, could be substantial. This may impact the security of the electricity grid from a supply and transmission perspective (Quiggin and Buswell, 2016; Wilson et al., 2013). The successful integration of electrified heating into the grid will need both load reduction and demand side management (Eyre and Baruah, 2015).

1.1.1 District heating and thermal energy storage

Heat electrification opens the possibility of using variable renewable generation with thermal energy storage (TES). Electrification via efficient heat pumps can achieve load reductions and facilitate demand flexibility. Flexibility can be attained through thermal inertia of buildings and TES. This in effect decouples demand from supply, to a degree depending on store size and performs the role of demand side management.

DH networks allow the distribution of centralised heat generation and enables the use of large-scale TES. Centralised heat generation allows buildings to connect to multiple sources of heat such as reusing low exergy waste heat from industrial processes with economic, technical, efficiency and safety advantages. This diversity of sources can be advantageous in providing security of supply and eliminating reliance on a single energy source (Radov et al., 2010). Similar reasoning applies to large, centralised TES in DH networks. Additionally, economies of scale can result in higher efficiencies and lower costs (capital and operating) at a district level.

TES can play a role in the energy system if there is a wider adoption of DH networks, due to its potential in grid balancing and managing demand. Currently, the most mature form of heat storage is sensible heat storage (as opposed to latent heat), commonly in the form of water stored in tanks, pits, or aquifers. TES can be sized to shift peak loads by several hours or to be very large inter-seasonal heat stores (BEIS, 2016a; Eames et al., 2014). The sizing of these heat stores is then an important factor and thus the control method, of how best to utilise and optimise heat stores would play a significant role.

Table 1.1 Advantages and disadvantages of three options for future UK heat delivery

	Centralised, District Heating Large - scale HP	Decentralised, Individual Heat Pumps	Decentralised, Individual Hydrogen (with Boilers/CHP)
Infrastructure	New	New/upgraded electric distribution	New/upgraded gas distribution pipes
Heat source	Multiple switchable, can use waste heat recovery	Single delivered energy source	Single delivered energy source
Capital Costs	Low individual cost High network cost	High consumer cost High production and distribution cost	Low consumer cost High production and distribution cost
Heat storage	Unrestricted low cost	Consumer restricted high cost	Consumer restricted high cost
System efficiency	High because of scale economies and basic heat pump & CHP efficiency.	Medium because of small units and availability of environmental heat sources	Low due to the need to make hydrogen
Operational Flexibility	High flexibility	Low flexibility	Low flexibility
Consumer practicality	Little space, noiseless	Significant space, potentially noisy	Significant space, potentially noisy
Economies of scale	Network and TES efficiency benefits from economies of scale	No economies of scale	Requires a scaled-up supply chain to be viable
Integration with cooling	Requires a cooling loop	Can be reversible	No cooling
Electricity Transmission	High efficiency HV transmission – lower transmission costs	LV transmission, higher losses	HV losses if electrolytic H2
Connection requirements	Requires high percentage connection to be financially viable	Can be installed progressively and upgraded later	Requires high percentage connection to be financially viable

1.1.2 Current district heating

Many of the DH networks in the UK are supplied from natural gas powered 'CHP (combined heat and power) and recovered waste heat' (DECC, 2013). CHP plants are commonly natural gas turbines or engines. In industrial application they provide electricity while recovering heat from combustion of fuel. Recovering heat from electricity generation in this way leads to a significant reduction in the carbon intensity of heat. CHP based DH systems are amongst the lowest cost per tonne of CO_2 when compared to other heating technologies. But with the continuing decarbonisation of the electricity grid, any carbon abatement from fossil fuel based (e.g. gas) CHP will eventually diminish (Foster et al., 2015; Lowe, 2011), though CHP using low or zero carbon fuels such as biomass or hydrogen may continue to play an important role.

With the current trend of high renewable deployment and government policies, indications are that electricity will continue to decarbonise (BEIS, 2020a). The use of CHP for the provision of power may be limited to in the short term to replace highly emitting peaking plants. DH allows

a flexibility of sources enabling 'low regret' measures. In the eventuality that gas CHPs are superseded, it is possible to incorporate other heat sources once the DH infrastructure is in place (Committee on Climate Change, 2015).

While the current power capacity would be unable to meet peak electrical heating loads if all heating were electric, CHP is likely to play a central role in DH in the medium-term. The deployment of CHP will be dependent on the extent of electricity decarbonisation and fuel prices (Li, 2013). In Denmark where renewable deployment is high, it appears that CHP units are being phased out. The capacity of CHP in 2018 was lower than in 2013 and the remaining units are envisaged to serve as backup for the Danish power grid. In addition, the number of full-load hours for CHPs has been declining to less than half the hours than observed in 2010 although this is aided by the fact that it is connected to a wider international grid (Helin et al., 2018).

DH as a technology means that CHP and heat pumps are not mutually exclusive. The sizing and control of TES in CHP and heat pump systems will not be the same. In CHP based systems, the goal is to minimise fuel consumption and maximise electricity revenue. Heat pump systems will aim to reduce the cost of electricity imports and reduce peak loads. At the consumer scale heat pumps installations are expected to rapidly increase (HM Government, 2020). The pairing of consumer heat pumps with consumer TES incurs high capital costs and space requirements. Additionally, a consumer heat store of 200-400 litres would store several hours of heat demand at best, as compared to days or weeks for a DH TES.

Projections of widespread electrification of heat would provide "favourable" conditions for TES. It would facilitate the integration of electric heating. BEIS (2016a) identify the potential for larger inter-seasonal TES. They note the potential for coupling conventional (tank) TES with CHP and/or HP systems and that the exploitation of electricity prices provides financial incentives for the adoption of TES. The benefits of TES for the energy system and carbon emissions are uncertain. Knowledge gaps and lack of experience in the UK of TES and inter-seasonal TES have been cited as a limitation to further development of TES. This thesis aims to address these gaps. The BEIS (2016a) report states:

> *"At a whole system level, it would require complex system-modelling to justify any statements about a unit of TES (a kWh or kW) equating to a quantity of saved carbon"*

In the present system, TES may lead to a small increase in emissions for the DH system as it is not 100% efficient. But the balance of emissions should also consider the fraction of low emission electricity generation facilitated by the TES. Given the predicted levels of renewable deployment and DH penetration, it should in principle, be possible to estimate the impact of TES. This is dependent on the operational methods to control heat dispatch and minimise costs. It should also be possible to optimise the level of TES, but this will depend on many variables. This includes not just the overall heat load, but on the profile of this load and how this harmonises with the variability of renewable generation. Strbac et al. (2012) identified that different storage types fulfil different functions in the energy system. They show that the value of electricity grid storage increases non-linearly with increased renewable deployment and that the marginal value diminishes rapidly beyond 6 hours of storage – enough to reduce peak loads. However, the cost of TES is far lower than conventional grid scale storage as demonstrated in Figure 1.1. As the round-trip conversion of power-heat-power is not feasible, TES is not suitable to replace all grid scale storage. But it will be able to displace conventional storage to a theoretical maximum of the electrical heating load. Physical TES volumes can become very large. Unless there are significant improvements in thermochemical or latent heat storage technologies, the capacities required to efficiently accommodate TES are only feasible in DH networks.

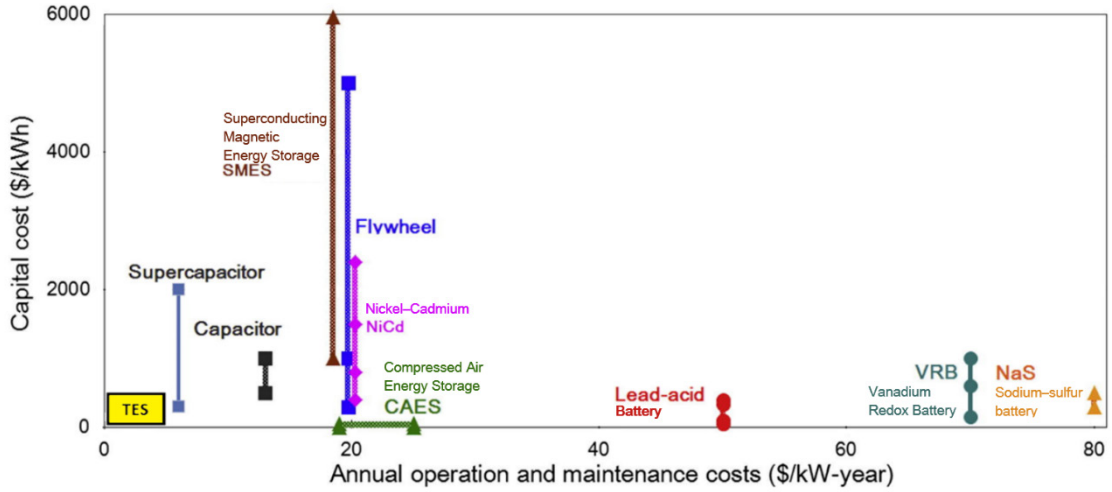

Figure 1.1 Comparison of energy storage costs with TES adapted from Luo et al. (2015)

1.1.3 The potential of district heating

Numerous recent studies have assessed the potential for DH in the UK. These studies have largely been techno-economic assessments for the viability of DH. An overview of these is presented in Table 1.2.

Poyry (2009) conducted an economic analysis that concluded DH is currently economically uncompetitive. However, this was sensitive to the cost of carbon. The analysis consisted mainly of gas-CHP and their analysis finds that DH is economically competitive in areas with heat demand density (HDD) of 3 MW/km^2 or higher. Using this metric, they show that DH currently has the potential to supply up to 14% of the national space heating demand.

DECC's (2013) 'Future of Heating' report, was more optimistic, estimating that "over 20%" of national demand or 50 TWh annually of heat could be provided by DH. They used Poyry's (2009) demand density to determine the economic competitiveness cut-off for DH take up compared to individual heating technologies.

Restricted to the domestic sector, Arran and Slowe (2012) conducted a scenario analysis for Delta-ee. They combined a building stock model with technology performance data to estimate the uptake of DH as an economic decision per household. DH was not the primary focus of the study; hence they cover a full range of heat generation and distribution technologies. In their most optimistic scenario for full electrification of heating, 34% of domestic heating is from DH networks.

The ETI conducted a spatial analysis of heat demand in Britain to identify zones suitable for DH (Woods, 2012). They used a lower threshold for HDD of 2 MWh/km^2 based on experience in other countries. The identification was used to determine the cost of DH based on the physical network and CHP technologies and concluded that as much as 43% of domestic demand could be from DH.

Ricardo-AEA conducted a similar nationwide assessment of district heating potential in the UK (Abu-Ebid, 2015). Their scenario analysis leads to a maximum potential of 42% share of heat load. They undertook a geographic survey of heating and cooling density and potential sources of waste heat. This enabled them to vary the minimum HDD based on geographic conditions.

Redpoint Energy analysed the potential for different heating technologies under various scenarios (Greenleaf and Sinclair, 2012). Using their RESOM model, they show that 11% of domestic and 9% of non-domestic heating can be provided by DH in a 2050 least cost scenario.

BuroHappold have taken another approach to estimating DH development in the UK. Using National Grid's scenarios, they show up to 60% of heat delivered via DH (Grainger, 2016). The

geographic analysis, while being a cost benefit analysis also captured the transient evolution of DH networks. This included practical constraints such as limited construction speeds and the stage of infrastructure development.

In a study commissioned by the Committee on Climate Change, Foster et al. (2015) conducted an in depth analysis of DH potentials and projections. This included an economic analysis of the heat and energy market, identifying barriers and externalities that affect the uptake of DH. The scenarios used reflect their economic analysis with differing levels of policy interventions to facilitate uptake. They also looked at the effect on uptake of DH with electricity grid capacity limitations.

Table 1.2 Studies on district heating's potential in the UK

Institution/Author	Method/Study	2050 Technical potential	Technologies
(DECC, 2013) DECC Future of heat	Building stock Cost benefit analysis	20% domestic	Gas-CHP
(Greenleaf and Sinclair, 2012) Redpoint	Resom least cost optimisation	11% domestic 9% non-domestic	Full technology range
Macadam et al. (2009) Poyry 2009	Building stock Cost benefit analysis	14% of national	Primarily gas CHP
(Arran and Slowe, 2012) Delta EE	Building stock Cost benefit analysis	34% domestic	Full technology range
(Woods, 2012) ETI	Geographic HDD survey	43% of national	Primarily gas CHP, HP, and waste heat recovery
(Abu-Ebid, 2015) Ricardo	Geographic HDD survey Cost benefit analysis	42% of national	Primarily gas and biomass CHP, HP, and waste heat recovery
(Grainger, 2016) Buro Happold	Geographic spatial optimisation capturing evolution	60% - Gone green 50% - Slow Pro 25% - Consumer Power	Full range but Primarily HP
(Foster et al., 2015) Element energy for the CCC	Spatial cost benefit analysis and TIMES least cost optimisation	25% - High scenario 18% - Central scenario	Full technology range

In summary, there have been two main approaches that have been used to analyse the potential uptake of DH in the UK. The majority of studies use a full geographic analysis of HDD and suitable locations for DH. Then use this as the basis of a cost benefit analysis with varied detail in the geographic survey and the economics of DH against counterfactual heat supply options. The geographic analysis is typically based on a highly disaggregated bottom-up model of the building stock such as Arran and Slowe (2012) or Woods (2012). The other main form of geographic analysis is a GIS survey of heat maps and waste heat locations, identifying suitable zones such as in Grainger (2016) or Foster et al. (2015). The cost benefit analysis here was largely based on the estimated levelised cost of DH compared to either existing or other low carbon technology options.

While some of these studies recognise the benefits of TES, they are only able to, at best, estimate the cost reduction of heat supply that is enabled by the extra flexibility provided by storage. Similarly, the operating costs of DH are estimated based on prior experience and projections of fuel and electricity costs. These assumptions can be critical to a cost benefit analysis of DH. On the other hand, the integrated cost optimisation models that do look at system costs, such as Greenleaf and Sinclair (2012) or Foster et al. (2015) do not capture the benefits of TES to the electricity supply and thus may overestimate the required generation or grid storage capacity.

To obtain a more accurate depiction of DH operating costs, a high temporal resolution analysis is needed. This enables the exploration of cost reduction benefits from increasing flexibility. Any such analysis with HP based DH must also be an integrated analysis covering the electricity sector. This is because the capacity requirements and generation mix will affect the resulting system's electricity costs. These costs in turn, are what would drive the operation of DH heat pumps in conjunction with TES.

1.1.4 The future of district heating

There has been much speculation as to why DH is not established in the UK. Kelly and Pollit (2010) posit that this has resulted from competition from other fuels and has suffered from privatisation of the electricity sector and the government's failure to create a heat market. Another factor is said to be that the limited availability of capital for long term investments. In 2015 the UK government made available £320 million of funding through the Heat Network Investment Programme (HNIP). The HNIP is expected to drive a further £2 billion in investment for the construction of new DH (BEIS, 2016b). The government's clean growth strategy (BEIS, 2017a) recognises the need for a complete decarbonisation of heating to meet its emissions targets. The report presents a number of scenarios where it envisages 1 in 5 domestic and non-domestic buildings connected to low carbon DH.

While the current DH infrastructure is limited, an electrified future for heating requires coordinated integration with the electricity system. A higher DH penetration will certainly have a significant impact on the national energy system. There is an urgent need to transition towards low carbon heat. The Committee on Climate Change (2016) recommends that low regret measures be taken now to meet the UK's emission targets. DH are a low regret option in that can enable immediate gains through efficiencies of scale and do not cause long-term fuel lock-in.

Any route towards decarbonising heat will have to be preceded by planning for both the national and local infrastructure. Whether this is for expansion of power generation capacity and reinforcement of the grid, hydrogen production and storage facilities, or DH networks. This raises the question of how to approach the expansion of DH in the country. The current decade has been described as a period of experimentation before commitment to any single strategy (Climate Change Committee, 2016). Table 1.1 demonstrates that there are many advantages to the adoption of DH in the UK. Recent policy and incentives such as the HNIP are indicative of government support towards DH networks.

It is thus in this context that this study aims to explore and broaden the understanding of the potential for DH in the UK. This includes how to build out DH to minimise system costs, emissions and ensure long-term resilience of DH systems. With the increasing deployment of renewables, flexibility is becoming increasingly important. The integration of DH with the electricity system will need to be assessed to explore the role of DH in low carbon system.

1.2 Integrated Energy Systems

To determine the role of DH in a low carbon system, requires modelling the heating sector in conjunction with the wider energy system. If the provision of heat were to become dependent on the supply of electricity, it is crucial that they work in coordination to ensure security of supply. A central supposition of this research is that electrification of heating can provide valuable flexibility for the electricity grid to achieve this. This coordinated operation of an integrated energy system is often referred to as a 'smart grid' or 'smart energy system' (Lund et al., 2014).

Much of the recent research into DH has been led by the Department of Planning at Aalborg University, Denmark. They have instigated a new paradigm in DH centric research, 4th generation DH, and host the largest annual conference on the subject. A key aspect of 4th generation DH includes the ability to aid in decarbonising energy systems and that they should be built to facilitate this (Lund et al., 2014). This is echoed by various other authors who identify that the direction of research should focus on integration with renewable sources and other supply grids (EKRC, 2014; Rezaie and Rosen, 2012).

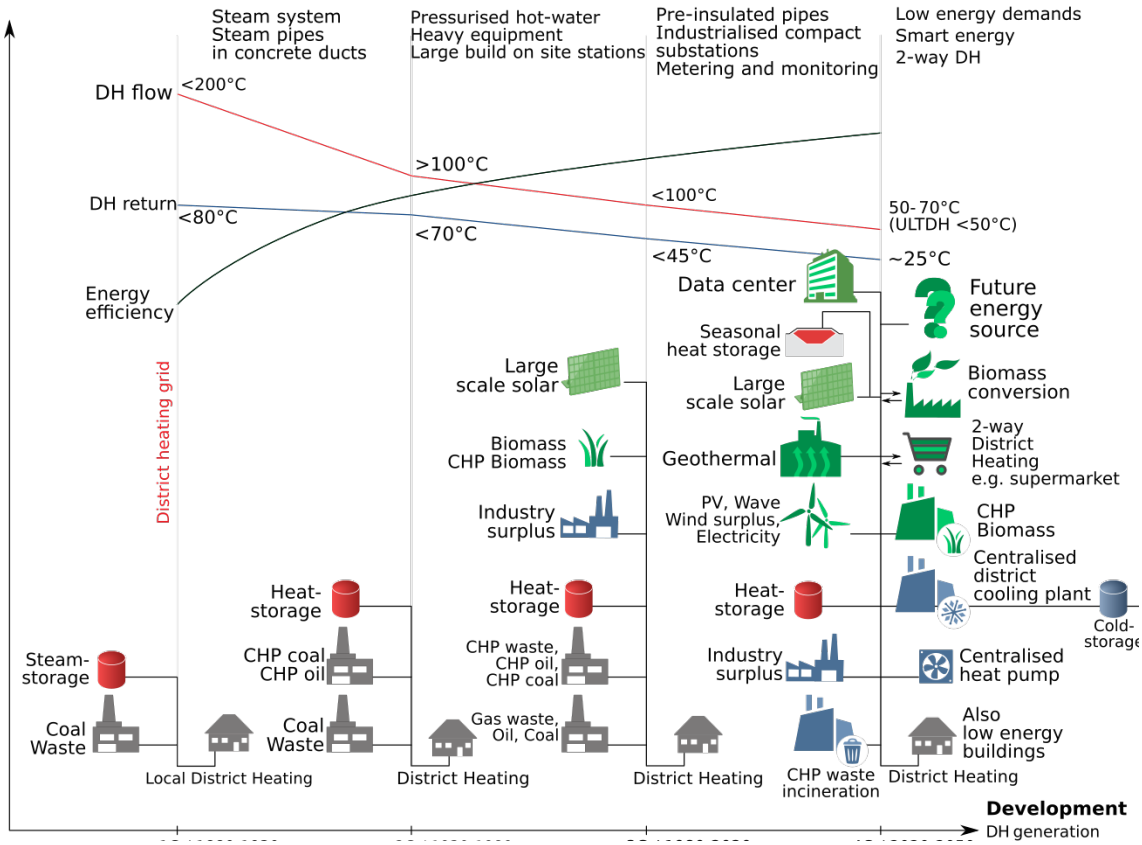

Figure 1.2 Overview of the evolution of district heating adapted from Lund et al. (2014)

The Heat Roadmap for Europe argues the case for DH networks to feature significantly in a decarbonised system (Connolly et al., 2014). The authors emphasise the need for integration and harmonisation with the electrical network. To achieve high levels of system efficiency, it is necessary to manage peak loads on the electrical grid and harmonise it with DH. For large scale integration of DH, it is essential to meet the challenge of coordinating energy production. Whether that be from CHP or heat pumps as this will have an impact on the electric grid.

Improved forecasting now enables more accurate predictions of renewable generation. When paired with demand forecasting, such a system would operate through coordinated and intelligent control of resources. There has been a recent growth in published work and review papers on the development of DH (Galatoulas et al., 2018; Lake et al., 2017; Rezaie and Rosen, 2012; Rismanchi, 2017; Sayegh et al., 2017; Tereshchenko and Nord, 2018). There has also been interest from many large city municipalities in the use of DH to decarbonise urban areas (Rismanchi, 2017). These reviews all present a variant on the idea of integrating DH for future energy systems.

1.2.1 Integrated energy system studies

The focus on integration of heating with the electricity system has grown alongside emissions targets. Renewable generation technologies provide a clear route to decarbonising electricity. Lund (2018) explores various renewable heating strategies and their significance for system flexibility. The study shows the superiority of a whole-system approach to decarbonise electricity. For example, the inherent storage capacity of the existing gas and DH networks is far larger than the electrical network.

Sneum and Sandberg (2018) considered the financial incentives of integration with the electricity system in Nordic countries. The authors argue that DH operators should be economically incentivised (by the grid) to provide flexibility. They consider revenue from heat and electricity comparing plant configuration and flexibility. They find that TES is essential to reduce costs. In the context of this research, they show that this can be achieved via dynamic tariffs. This would incentive DH operators to provide flexibility.

Electrified DH in Sweden was investigated by Schweiger et al. (2017). The authors stated that there is little analysis on the electrification of DH in Sweden. They identify that there is a difference in the theoretical potential to electrify - which amounts to the total heat load from DH, and the technical potential - which is the total of the negative residual load from renewable generation. The study simulated the operation and loads of the Swedish power and DH networks using fixed electricity costs. Their model prioritised TES charging when storage capacity was low. They found that access to TES substantially increased the technical potential and concluded that Sweden has favourable conditions for the electrification of DH. Another Swedish based study on DH used hourly electricity spot prices to determine the levelised cost of heat for DH. They consider several scenarios and investigate their economic feasibility (Hennessy et al., 2018).

A study of DH in Germany looked at integrating DH with renewable electricity (Böttger et al., 2014). They compare hourly heat demand to the negative residual loads from renewable generation. Looking at various scenarios, the investigation consisted of a synthesised heat load and they assumed a constant electricity demand. Where negative residual loads coincided with heat demand, this was used directly for heat. Further surplus generation is allocated to storage. The authors conclude that around 50% of the current DH load in Germany can be efficiently electrified.

Gudmundsson et al. (2018) looked at the role of DH in integrating renewable generation in Denmark. They concluded that increased use of heat pumps would necessitate the better integration of the two sectors.

1.2.2 Flexibility and thermal energy storage

The subject of flexibility for the electricity system is under increased examination, particularly in places where renewable deployment is high. The key issues from an energy systems perspective are: determining a measure of flexibility, how much flexibility is required and how this flexibility can be provided? Kondziella and Bruckner (2016) state that identifying an accurate quantification of flexibility requirements is a complex problem. They classify flexibility options as falling within six broad categories:

1. Fast ramping power generators (supply side)
2. Increasing the spatial range of the grid (supply side)
3. Grid scale energy storage (supply side)
4. Curtailing surplus renewable generation (supply side)
5. Demand side management (demand side)
6. Integration of other energy sectors (demand side)

Table 1.3 Review of electricity grid flexibility studies

Study	Location	Flexibility type	Key result
Comaty (2013)	Pan-European	Spatial range	Savings from distributed renewable generators.
Connolly et al. (2012)	Ireland	Grid scale storage	Pumped hydro can permit 20% wind penetration at no increased operation cost.
Denholm and Hand (2011)	Texas, USA	Grid scale storage	Storage capacity equivalent to daily demand needed to limit curtailment below 10%
Silva Monroy and Christie (2011)	Model 'Isolated island'	Grid scale storage	Storage alone able to increase wind penetration up to 1/3.
Villavicencio (2017)	France	Grid scale storage	Storage reduces costs of integrating renewable generation into system.
Drysdale et al. (2015)	UK	Domestic demand side management	DSM measures potentially 60 TWh of flexibility.
Strbac et al. (2012)	UK	Grid scale storage	Value of storage increases non-linearly with increased variable renewable generation.
Sanders et al.(2016)	UK	Multiple flexibility options	Flexibility reduces cost of balancing and improves utilisation of renewables

Table 1.3 is an overview of some studies on achieving flexibility for renewable electricity. Each flexibility option has its own costs and technical limitation. Determining a hierarchy for flexibility options is not straightforward. To efficiently achieve high fractions of renewable generation will require a combination of these. Among the integration of other sectors, the provision for heat supply has a very large potential capacity. TES increases the flexibility of heat demand and has been studied as an option for providing flexibility in other mainly European countries.

An analysis of the German electricity system identified that a higher level of integration between heat and power sectors is a 'favourable' solution (Gils, 2015). This was particularly the case with large amounts of wind generation.

The use of TES with CHP as a method to increase flexibility has been the subject of many studies (Anna et al., 2018; Fang and Lahdelma, 2016; Hast et al., 2017; Noussan et al., 2014; Reynolds et al., 2018; Wang et al., 2015). Research that has looked at TES in the context of the energy system has demonstrated its ability to reduce system-wide emissions. In Denmark, it is shown that the flexible demands of heating can enable the country to reach very high levels of

decarbonisation with the use of TES and has holistic benefits as a flexibility solution (Hedegaard et al., 2012; Lund et al., 2010).

In the UK, it is recognised that it will become increasingly difficult to incorporate larger amount of renewable generation without sufficient flexibility and this may limit the growth of renewables (Cox, 2009). A report for the Carbon Trust assessed a range of flexibility options for the UK electricity system (Sanders et al., 2016). It factored the uncertainty of generation capacities and long-term demand. The main findings highlight that deployment of flexibility systems in the UK can have a significant cost saving. They reduce the cost of system balancing and improve the utilisation of renewable generation. The cost savings were estimated to be in the region of £2 billion per year in operational costs and the avoided costs of not having to increase generation capacity and network reinforcement. The authors highlight that faced with uncertainty; the safest strategy is to utilise a mixture of flexibility initiatives. This includes extension of the grid with extra interconnector capacity.

Barrett and Spataru (2013) studied the storage requirements for the UK with a whole systems model. The authors described a high renewable scenario with a range of storage types and noted that their performance can be highly nonlinear. Storage from multiple sectors such as transport was included. They estimate that the building stock contains in its fabric 1 TWh of thermal energy storage per degree of temperature change. Altogether, the storage capacity was estimated to be around 6.8 TWh. It was concluded that thermal and chemical stores have a larger capacity potential than electrical storage. Finding the appropriate configuration of storage, accounting for power ratings, performance and timescales remains a key challenge. Other estimates show that if every dwelling in the UK had three hours provision of TES, this would be equivalent to 36 GWh of storage for the grid (Eames et al., 2014). Quiggin and Buswell (2016) modelled the electrification of space and water heating to investigate demand side management in the UK. They cite that existing studies to date had failed to capture the problem in sufficient resolution. They suggest that demand side management alone is not adequate to ensure security of supply and heat demand must be reduced to achieve this.

Strbac et al. (2020) identified the challenges of a highly variable renewable system. They highlight the importance of flexibility and review the various options to achieve a low carbon system. The authors present findings from prior studies. They estimate the value of energy storage and suggest that 25 GWh of capacity could be worth £15 billion per year to the system by 2050. They also show that sector coupling such heat and power is imperative to achieve highly renewable systems. A complementary study by Pöyry demonstrated that under 2030 emissions targets, flexibility solutions could potentially be worth £4.7 billion per year (Shakoor et al., 2017). This was via a reduction in capacity requirements and lower operating costs. Another study for the Climate Change Committee (Strbac et al., 2018b) highlighted the importance of system flexibility. They show that 58 GW_{th} of domestic TES reduces the electricity storage requirements from 55 to 10 GW_e.

1.2.3 Flexibility research gaps

There is plenty of recent research on flexibility requirements for renewable systems in the UK. But research into TES has largely focused on individual DH systems or domestic storage. There exists a gap in the research with respect to using large scale TES as a provision for flexibility for the electricity system. This includes to what extent it could be integrated into the energy system.

Researching the potential of TES requires the use of adequate tools and investigation techniques. This needs to combine heat and electricity sectors as well as adequately capturing the dynamics of storage. Many existing models that combine both sectors inadequately embody storage potential. This is largely due to their low temporal resolution or only focusing on one solution in isolation(Grünewald et al., 2012).

TES with heat pumps, in addition to decarbonising heating can also increase flexibility for the electrical system. DH enables the connection of large, centralised capacities of both. However,

the use of TES as a means for providing flexibility as an energy storage mechanism requires more analysis.

1.3 Energy System and District Heating Modelling

Classifying models can help identify what kind of model is appropriate for a given purpose. Some models can fall into more than one category. A first such category can be assigned by identifying the purpose of the model. This normally relates to the questions they were created to answer such as forecasting or exploration. Forecasting models are essentially those models whose primary purpose is to make predictions of future outcomes based on observations and extrapolations of historical data. These models are generally suitable for short term predictions, using constant parameters (Van Beeck, 2000). Exploration models are typically used for scenario analysis. The effect of interventions or altering actions to the base case are measured. Assumptions or measures are required to determine the effect of interventions. Typically a sensitivity analysis is provided to quantify assumptions (Neshat et al., 2014).

Complementing these classifications, Pfenninger et al. (2014) identify the underlying methodology and paradigms used in these models. They state that simulation methods are best used in forecasting models to predict the evolution of a system from the current base case. Accounting methods are usually seen in exploration models. This is where the modelling accounts for the effect of interventions and does not necessarily produce optimisations. As a subcategory of exploration models, backcasting methods are usually used for more long-term analysis. This is where future scenarios or specific targets are constructed, such as an emissions level. The model then determines the steps or path required to achieve this state. This is an alternative method to forecasting and is typically used with economic optimisation models (Bibri, 2018). In backcasting, the optimisation methods are used to form normative scenarios and typically involve a large range of variables to find cost or energy optimal combinations to achieve a particular scenario.

Another distinction is the analytical approach in constructing the model, bottom-up or top-down. In the context of energy models this differs with the level of detail and data in the construction of the model. Top down approaches are typically less data intensive, with less detail in their construction. Functions are described as aggregates of variables such as the total energy demand of a sector. Bottom up approaches tend to require more data and are a more descriptive. They account for each variable in a function, such as a disaggregation of energy demand from each actor in a sector. Simplifications need to be made as the real world can never be fully simulated. There is always a trade off between speed and accuracy in computation. The distinction is important depending on the aim of the model such as prediction or exploration and models can include a combination of each approach (Vega, 2018).

Another classification is the approach towards uncertainty in the model - deterministic or stochastic. Pfenninger et al. (2014) differentiate between aleatory uncertainty, i.e. random events and epistemic uncertainty, such as insufficient data. Aleatory uncertainty can be dealt with using deterministic methods and varying parameters to determine sensitivities. But another approach is to allow variables to take a distribution of ranges rather than fixed-deterministic values and building probability into functions – the stochastic approach.

There are many more classifications and categories of models that can be described. Some of the fundamental distinctions concerned with energy models are covered here. It is important to note that very rarely does a model fit neatly into one category with many large models incorporating methods that could fall into multiple categories. The choice of what approach to use is driven by the aim of the model, the data available and the epistemic approach to building the model.

1.3.1 Modelling approaches

A review of modelling approaches is conducted prior to developing a custom research model. The review is limited to selected, major, current models that include heat and electricity sectors. They are assessed for both methods and viability in aiding the research. This review can be approached in two ways; with respect to studies that have explored similar questions, and those which have used similar methods, but explore a different topic.

The reviewed models are categorised into two main types; there are a group of exploration models that cover the whole energy system. These are typically designed bottom-up with a focus on long term analyses of technology uptake. As a result, these normally have low temporal resolution. They also usually focus on economics and are used as policy guidance tools such as UK Times, ESME, RESOM and Balmorel. These types of models compare the costs of various technologies and their trade-offs and can aid in system design. The representation of DH is normally basic and not used to make any inferences about the design of DH. The other group of models tend to be forecasting models, normally with a narrower sector focus. They require a higher temporal resolution. Examples include SIVAEL, Enneralt, GTMax and RAMSES, all of which simulate the electricity network. These models can aid in the design and configuration of DH from the perspective of the operator. Table 1.4 contains an overview of the functionality of relevant models covered in the review.

The UK Times, RESOM and ESME models are all bottom-up exploration tools for the UK energy system. They consist of large databases of technologies and economically optimise variables based on given constraints. These models capture elements of DH and renewable electricity generation. But the detail and temporal resolution make them an unsuitable analysis tool for the research problem. A similar assessment can be made of OSeMoSYS. Even though it is open source, significant changes and adaptations would be needed. Balmorel is an economic analysis tool that covers the whole system. It has a detailed representation of DH as it has been used mostly in Baltic and Scandinavian countries. The temporal resolution is flexible depending on the type of analyses required. Variable renewable generation, however, is not represented endogenously. It is primarily an economic analysis tool and a UK localisation does not yet exist.

DynEMo is a versatile model and has a high temporal resolution. It couples heating with renewable generation and captures storage dynamics. It has a whole system approach; hence it does not model DH in great detail. Enneralt a forecasting model, is primarily built for the Nordic electricity sector. It has a high temporal resolution, but DH representation is primarily for CHP based networks. Similar features and approaches are seen in other forecasting models - SIVAEL, GTMax and RAMSES. EnergyPRO is a commercial package but only suitable for single plant operation and analysis.

EnergyPlan is a whole system model with localisations for many countries, including the UK available. It simulates the operation of the national system at hourly resolution and has a full representation of DH and TES. The operation and heat dispatch have been programmed based on heuristics. This keeps computation times to a minimum and is thus fully deterministic. EnergyPlan is suitable to address the wider research area. It could be an alternative to compare with, particularly to analyse integration of TES into the electricity system. Remod-D also has many desirable features for the context of this research project. It is a whole system forecasting model but simulates at high temporal resolution. Includes a detailed representation of DH, including TES. It is primarily used to find a cost optimal solution of the energy system (Fraunhofer, 2019). A strength of this model is the ability to capture the investment of building retrofit measures.

Many of the models were not available for use. Some were commercially available or charged for licenses, while others were for internal use only. The only models that are publicly available or open source that were reviewed are Balmorel, Osemosys and EnergyPlan. The Balmorel and Osemosys are open-source models that could potentially be adapted for use, but significant

adaptation of the models is required. EnergyPlan and Remod-D should be studied to aid the development of this research.

Table 1.4 Comparison of existing models' functionality

Model	Focus	DH Included	Dispatch optimis-ation	Electric. spot prices	Include TES	High Temp Reso-lution	Can use historic time-series	UK local-isation	Couples Heat & RenGen
DynEMo	Whole system	Yes	Yes	No	Yes	Yes	No	Yes	Yes
Balmorel	Whole system	Yes	Yes	Yes	Yes	Yes	No	No	No
Enneralt	Electricity	Yes	Yes	Yes	No	Yes	No	No	No
UK Times	Whole system	Yes	No	No	No	No	No	Yes	No
SIVAEL	Power	Yes	Yes	No	No	Yes	No	No	Yes
RAMSES	Electricity and DH	Yes	Yes	Yes	No	Yes	No	No	No
EnergyPlan	Whole system	Yes	No	No	Yes	Yes	Yes	Yes	No
EnergyPro	Electricity	Yes	Yes	No	No	Yes	No	Yes	No
REMod-D	DH and electricity	Yes	Yes	No	Yes	Yes	Yes	No	No
OSeMOSYS	Whole system	No	No	No	No	No	No	Yes	No
RESOM	Whole system	Yes	No	No	Yes	No	No	Yes	No
ESME	Whole system	Yes	Yes	No	Yes	No	No	Yes	No
GTMax	Electricity and DH	Yes	Yes	Yes	No	Yes	No	No	No

1.3.2 Modelling conclusions

Table A-1 in Appendix A contains a detailed overview of all the models covered in the review, emphasis is given to the purpose of the models from the classifications described, the methods to model electricity generation, heat demand and DH allocation as well as the optimisation methods employed. The availability and suitability to address the research area was also scrutinised. The models are restricted to those covering the power and heat sectors, either on its own or representing DH as a subsector of the heat sector. None of the models explicitly couple heating demands and renewable electricity generation with meteorological data, nor do any models simulate the operation of heat pumps and thermal energy storage based on electricity spot prices, thus considering the configuration of the electricity system.

This research addresses these gaps by developing a model that optimises DH configuration for electrified heat by operational costs from electricity network spot prices, therefore including the configuration of the electricity system. The inclusion of electricity spot for operation has been a feature of existing models, however the novelty here comes from the predicted spot prices for

a future energy system. As many of the whole system models have previously done, DH penetration will be modelled from a system perspective but with higher detail in the potential of TES to manage residual variable generation and reduce electricity generation costs. Moreover, the novelty introduced by this project will include a realistic coupling of renewable generation and heating loads via the use of hourly weather data. The hourly resolution has been used in existing models and is sufficient to capture the dynamics of storage.

1.4 Research Design

Research on the national potential for DH deployment has typically not analysed it from a systems perspective. The studies that have done so, do not fully capture the benefits of integrating heat with the electricity and the trade-offs for TES as a means of flexibility. Most of the cost-benefit analyses have not been able to fully account for the cost benefits of TES. Further, the current research has given little guidance on how these systems should be designed to ensure future proofing and harmonising with the wider system. The research that has given guidance on what kind of heating technologies to use, for similar reasons have not fully incorporated the effects of TES and renewable variability on operation.

Flexibility has been shown to be vital in achieving high penetrations of renewable generation in the electricity system. Despite this, there has yet to be a full investigation into the effectiveness of TES to support this. Finally, the review of existing tools and models has shown their limitations to analyse the impact of large-scale TES incorporated into DH networks on the electricity grid.

This thesis aims to address these knowledge gaps. It will fill a gap in research on the use of TES and DH to manage grid flexibility. Investigating the configuration of DH for a future low carbon system while maximising benefits and minimising operation costs to uncover their full potential. This will be achieved by developing a high-resolution DH and electricity network model for the UK that directly couples the variability of heat demand and renewable generation through the underlying weather patterns.

1.4.1 Research aims

The aim of this thesis is to investigate the role of electrified DH in a future low emission and high renewable energy system in Great Britain (GB – England, Scotland and Wales, excluding Northern Ireland which has a separate grid). Highly renewable systems are likely to have variable electricity generation. This variability will lead to fluctuations in electricity prices. Under the assumption that DH networks will be designed and operated on a cost minimisation bases:

> *To what extent can DH with heat pumps and TES exploit the variability in demand and electricity prices to minimise operating costs and how should they be designed to achieve this?*

To address this, a series of studies and models will be required with several sub-objectives:

1. The Heat Load Model (HeLoM):
    a. Creates a representative time variable DH heat demand considering the areas suitable for DH deployment and the mix of demand this comprises
    b. Synthesises an hourly national (GB) heat demand profile to provide inputs for further modelling
    c. Determines how the DH load profile differs from the national profile.
2. The Electricity Cost Model (ElCoM):
    a. Collates a suitable scenario to determine the demand characteristics and generation mix of a highly renewable, all-electric, net zero compatible scenario.
    b. Provides a storage or flexibility baseline to later contrast with the inclusion of DH.
    c. Devises a methodology to estimate the time varying cost of electricity supply and estimates the resulting cost of electricity supplied to DH and consumers.

3. The District Heating Model (DiHeM):
    a. Devises a suitable DH simulation with control algorithms using hourly heat demand and electricity costs as inputs to minimise operating costs.
    b. Determines the optimal DH configuration in terms of HP and TES capacity.
    c. Estimates the resulting levelised cost of heat from DH.

An extension of this modelling will be to analyse how a significant DH presence may impact the electricity system. This can be used to assess the impact of DH and TES on the national electricity system to explore the value of flexibility provided by DH as described in the review:

What is the impact of a significant DH deployment on the electricity system, how much flexibility can it provide and to what extent can it supplant grid storage?

This will require using the outputs from DiHeM as input for ElCoM and the integration and coordinated operation of the two models.

4. Model integration:
    a. Devise a suitable coordinated operating regime for the integrated system.
    b. Estimate the change in peak and total electricity demand for heat with increased DH deployment.
    c. Assess the change in the cost of heat provision with varying DH deployment.
    d. Estimate the impact of DH in reducing the renewable generation deficit and the ability of TES to replace grid electrical storage.

1.4.2 Research design

The design is driven by the need to investigate the potential of DH considering the effects of integration with the electricity system. As the variability of renewable generation, particularly wind, can occur at over the time period of hours, the full impact of operating DH with TES can only be realised at high resolutions. Figure 1.3 shows the system boundaries of the project and the detailed modelling requirement that is needed to simulate the impact of each sector on the other.

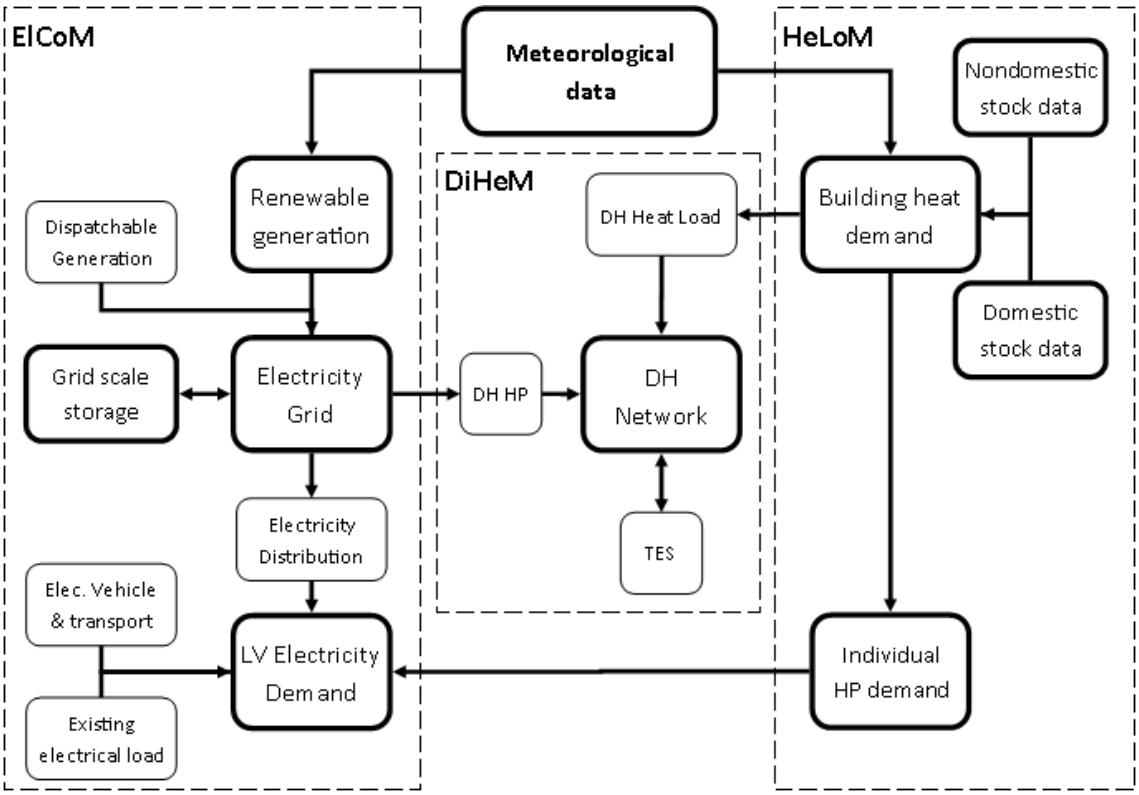

Figure 1.3 Modelling system boundaries and energy flows

The three models are-soft linked with data flowing from HeLoM and ElCoM models into DiHeM. An integrated exploration of the impact of DiHeM on ElCoM system is later undertaken. Meteorological data is an exogenous input for both the heat loads and electricity module. Using meteorological data, couples the heat demand to renewable power generation. This coupling is a fundamental feature of this study that distinguishes it from other such studies. Another novel inclusion in this model is the operation of DH based on upstream cost signals from the electricity network. A summary of the modelling assumptions used in this study is provided in Table A-2.

1.4.3 Heat Load Model - HeLoM

The Heat Load Model – HeLoM, takes meteorology variables - hourly ambient temperature, wind speed and solar irradiation, combined with heat use activity patterns as an input and outputs heat load. This forms an input for the other modules. It will be constructed bottom-up, using building archetypes applied to a thermal simulation, which needs to capture a high temporal resolution. The development will draw on existing archetypes and building surveys. It needs to be disaggregated by area to split out urban-DH heat loads.

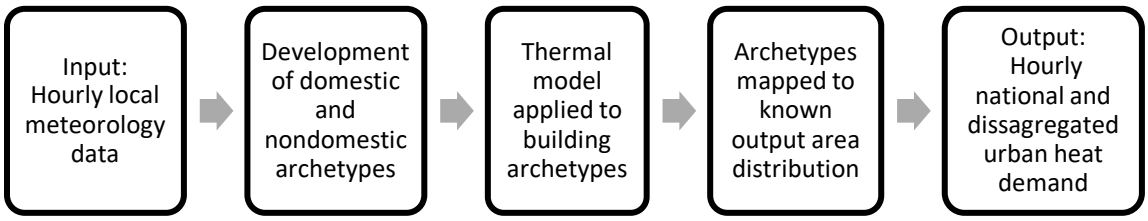

1.4.4 Electricity Cost Model - ElCoM

The Electricity Cost Model - ElCoM, inputs capacity factors that have been correlated to meteorology to simulate the grid and output marginal costs. It is defined using scenarios to set the generation and storage mix. The electricity market prices are assumed to reflect marginal costs. This work will be an original contribution of this project. The electricity market prices are intended to be used by the DH module to operate and control the dispatch of heat.

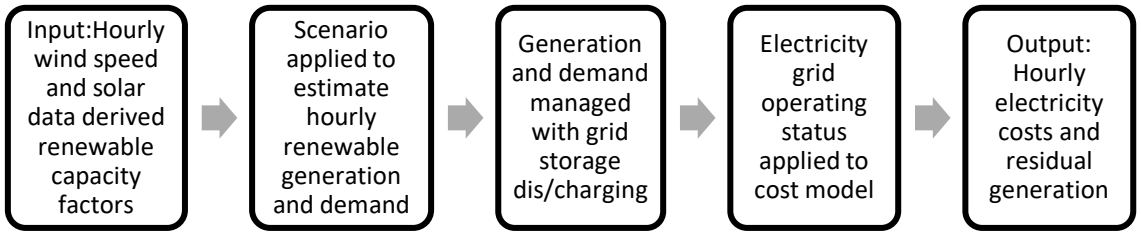

1.4.5 District Heating Model - DiHeM

The District Heating Model - DiHeM connects the supply and demand components from the other modules. It will take the data provided from the other modules and output costs based on the configuration of DH for which it has been designed to explore. The design of the operational control method will form an important aspect of this module. It is initially proposed that this be a standalone module. As an extension, integrating this with ElCoM would be necessary to analyse the impact on the electricity system.

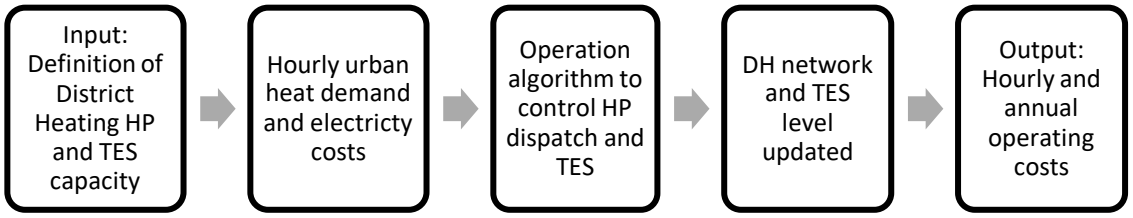

Box 1.1 Economic terminology: the difference between Cost and Price

The terms 'cost' and 'price' are used frequently in this thesis from Chapter 3 onwards. The distinction between them is significant in the context of this research. In common parlance, they are used interchangeably. The Oxford English Dictionary (2001) gives the following definition:

> *"A Price is the amount of money required or given in payment for a commodity or service" and the "Cost is the expense incurred to attain a particular goal"*

Expanding upon this in the context of this research, a cost refers to the value of inputs to an enterprise and following from this, marginal costs represents the value of adding a unit of production to a system which might have multiple enterprises.

The price refers to the value paid for an output of an enterprise. In theory, in an efficient market, this is equal to the marginal cost. For the marginal consumer (at the intersection of the supply and demand curves) this price is exactly what they are willing to pay for the good. All other consumers consuming would have been prepared to pay a higher price. The cumulative difference between these higher prices and the optimal price is known as the Consumer Surplus, a measure of the benefit to consumers collectively.

Similarly, the optimal price is paid to all producers producing the good. For the marginal producer (at the intersection of the supply and demand curves) the price exactly equals their total cost of production. All other producers producing have lower production costs than this. The difference between such a lower cost and the optimal price is the profit made by the producer; the marginal producer makes no profit (and no loss). The cumulative profit is known as the Producer Surplus, a measure of the benefit to producers collectively.

1.5 Thesis Structure

Chapter 1 has covered the rationale and defined the research problem for this thesis. Chapter 2 covers the development of Heat Load Model - HeLoM which serves as the basis for demand in the following chapters. Chapter 3 is the Electricity Cost Model - ElCoM. This develops the dispatch and cost methodology for electricity prices which are used to operate DH. It also develops a zero-emission scenario in which the heat load forms the basis of consumer HP demand. Chapter 4 covers the District Heating Model - DiHeM. DH simulation and operational control of the HP-TES system is developed. Chapters 2, 3 and 4 are designed such that they can be read independently as standalone sections. An exploration of system integration is covered in Chapter 5 with a discussion of the work presented in this thesis with key conclusions and recommendations.

2 HEAT LOAD MODEL

Chapter Summary

This chapter details the development of the Heat Load Model (HeLoM). Estimation of spatially disaggregated heat demand is needed for the development of local energy distribution infrastructure. A significant heat pump deployment would require the electricity distribution network to have sufficient capacity, and similarly in the event of hydrogen heating. It can also aid in identifying and planning areas suitable for district heating infrastructure. The temporal variation of heat demand is important when considering the operation of storage within district heating and the electrical grid. The difference between the national and urban heat demands profiles will vary due to the type and occupancy of buildings leading to temporal variations which have not been widely surveyed. A review of existing national and urban heat load modelling is first presented with a focus on the modelling methods and datasets used. This leads towards identifying the appropriate datasets, archetype segmentation and characterisation for the domestic and nondomestic building stock. The segmentations and archetypes for both domestic and nondomestic stock are described alongside the spatial disaggregation used. 20 domestic and 12 nondomestic archetypes in 11 GB weather regions are applied to a thermal model and calibrated on the local scale using gas consumption statistics. The annual national heat demand was closely aligned to other estimates and the peak demand was estimated at 219 GW_{th}. The urban heat demand was found to have a lower peak to trough ratio than the national demand. This may have important implications for the uptake and design of district heating.

2.1 Model Objectives

Hourly space heat and hot water demand estimates are required as an input to the modelling in following chapters. This includes the electrified heat load for electricity scenarios and for district heating (DH) loads. These demand profiles will differ. The DH loads will primarily be composed of urban areas. The remaining load can be assumed representative of the national demand and extrapolated as such. These requirements can be summarised as:

a. Capture the entire hourly national space heat and hot water load based on historic meteorological data
b. Disaggregate the urban load as a proxy for DH demand

The demand is to be derived from meteorology data, primarily external temperatures, and wind speeds. Urban loads are split out as these are typically the areas with the highest heat demand density (HDD). DH networks are generally more economically feasible in these high HDD areas

with lower costs per unit of heat. The disaggregation of urban heat loads will be achieved through a spatial disaggregation with the highest ranked HDD areas assumed as being urban.

The temporal variation is crucial when considering the operation of energy storage. It is surmised that there will be differences in the shape of the daily load profile between the urban and non-urban areas. This is due to the differences in the type and occupancy of buildings. The differing use patterns will lead to temporal variations. This difference has not been widely surveyed. Thus, the requirement is for the model to encompass both a high spatial and temporal – 'spatiotemporal' – resolution.

Industrial and (some high-temperature service sector) heat loads are omitted from this study. They are likely to fall outside of urban areas and the heat demand is usually of a higher temperature than that of space and water heat, or what would be appropriate to be supplied by DH.

2.2 Literature Review of Heat Load Modelling

Most recent national heat demand studies have focused on domestic heating. Space and hot water heating accounts for 40% of energy demand in the UK with the domestic sector making up just over two-thirds of this (BEIS, 2020b; Climate Change Committee, 2016). Building stock energy simulations range from highly detailed simulations of individual buildings which require detail in geometry, fabric, and usage, up to the scale of the entire building stock containing many built form types, ages, construction methods and uses in which limited data exist on the characteristics and spatiotemporal energy demand.

In building energy modelling, top-down models normally explore the inter-relationship of demand with key factors such as construction age or demography, this can be described as a deductive method (Sousa et al., 2017). Bottom-up models tend to disaggregate the components of energy demand into its various components, often employing a building physics based approach (Kavgic et al., 2010). A notable example used for the UK is the BRE's Domestic Energy Model (BREDEM) and has been extensively validated (Anderson, 2002; Henderson and Hart, 2013). At higher spatial resolutions, the impact of an individual building is greater and thus the need for accuracy increases. The bottom-up approach is hence preferred by designers and planners. However, it can be difficult to calibrate and validate such models without large scale data collection, which can often be impractical on such a scale. For this reason, many building stock energy models use building archetypes as a representation of a statistically average form of a typology that can be multiplied to the national stock scale. Most building energy models aggregate energy demand from many buildings and can provide estimates of energy use if the ratio of built form types is altered.

To highlight the growing importance of this field, there have been several reviews of building stock energy models conducting in recent years (Kavgic et al., 2010; Keirstead et al., 2012; Reinhart and Davila, 2016; Sousa et al., 2017). Reinhart and Davila (2016) review the design of existing bottom-up building stock energy models. They describe the steps required to construct such models as:

1. Data input and organisation
2. Thermal modelling
3. Result validation

They identify the information that is required to generate building energy models. This includes regional weather data, building form, construction and operation data and finally building occupancy or usage. To estimate future demand, inferences have to be made regarding the building stock and climate conditions. The authors state that the biggest challenge for such models is in the definition of the archetypes to recreate the simulated building stock

In the review of Kavgic et al. (2010), the authors compared eight different bottom-up energy stock models, including five UK based models. All the UK models derived their calculation from

a version of the BREDEM. All the models reviewed output data at either an annual resolution or in two cases, a monthly resolution. They vary in the number of archetypes or dwelling types, ranging from just two age categories to over 8000 unique combinations of dwelling type including age, form, construction, and heating method. Of these, only the Community Domestic Energy Model (Firth et al., 2010) contained a spatial resolution higher than the national scale but only for the existing stock while most others were used for some form of scenario analysis.

Sousa et al. (2017) comprehensively analysed 29 housing stock energy models. Their conclusions are critical of the current approaches noting that they are limited in scope due to a lack of transparency, a sentiment shared by Kavgic et al. (2010). Much of this is due to the scale of the challenge, with some 25 million homes in the UK and a limited number of cross-sectional surveys from which to base modelling assumption and data validation. There exists a large variation in their designs, both spatially and temporally (Keirstead et al., 2012). None of the UK based models however, disaggregated urban loads from the national at an hourly resolution. The authors conclude that improved data collection standards are needed as well as computational resources to capture detail at high spatial and temporal resolutions.

Box 2.1 Output areas and geographic subdivisions

Output areas (OA) have been used for data collection in England and Wales since the 2001 Census. They are the smallest geographical unit for which data is collected and designed to be largely homogenous. Small area statistics are reported at the Lower Super Output Area (LSOA), consisting of multiple adjacent OAs and Middle Super Output Area (MSOA), constructed from adjacent LSOAs. LSOAs are designed to have a population of 1000-3000 and MSOAs 5000-15000.

The Scottish equivalents of LSOA and MSOA are Data Zones (DZ) and Intermediate Zones (IZ). For convenience only the former terminology will be used. Scottish DZ are also smaller than LSOAs, each DZ contains approximately 500-1200 residents and IZs between 2500-6000.

Another common subdivision used is the local authority (LA) which are governmental subdivisions. There are 397 LAs in Great Britain of varied area and population.

2.2.1 National demand

Prediction of peak demand with electrification is a key aim in many assessments of the national heat load. One of the few spatiotemporal studies has been conducted by Eggiman et al. (2019). They developed a high spatiotemporal resolution heat and electricity demand model to study the diffusion of heat pumps in the UK. The authors noted that the need to balance resolution with computing requirements and data availability is one of the main contributing factors towards the lack of spatiotemporal projections of UK heat demand. They use the LA subdivision and disaggregate between domestic, service, and industrial sectors. The temporal variation for electricity was calibrated via electricity transmission system data. Similar data is not available for gas transmission, and therefore it was not validated. They use a heating degree day method to estimate heat demand and like most studies of this kind, they used a combination of yearly and daily load profiles to decompose annual energy use data into hourly temporal demand. A strength of this study is the use of technology specific load profiles; they have differentiated between gas boiler demand profiles and heat pump profiles, notably using measured heat pump load profiles.

Another recent contribution towards national spatiotemporal heat demand modelling was conducted by Clegg and Mancarella (2019). They also use the LA level and heat demand was simulated for a single year in EnergyPlus using four domestic archetypes and four nondomestic archetypes to derive load profiles. These were mapped to the building stock with statistical variations in occupancy and in thermal performance characteristics to recreate demand

diversity. It was found that regional half hourly peaks were 200% larger than the average daily demand. The authors use this to analyse the impact of the evolution of heating technologies on the gas and electricity network. A similar method using EnergyPlus generated profiles was applied at the postcode level and aggregated to city level demand (Wang and Mancarella, 2016).

Taylor et al. (2014b) created a high resolution (1 km square) spatial mapping of heat and electricity demand to study the diffusion of heating technologies, particularly heat pumps. They used output area socio-economic census data combined with historic energy demand data (LSOA for domestic and MSOA for nondomestic). Assumptions were made to increase the spatial resolution of demand, but the analysis was static with no temporal simulation of demand, capturing only annual demand at high spatial resolutions. 2009 was used as the base year for demand modelling and the authors estimate future demands extrapolating from a base year using scenario factors.

Quiggin and Buswell (2016) used historic weather data to analyse the impact of heat electrification. The authors note that hourly demand modelling is vital to investigate the impact of electrified heating. They combined a heating degree day with measured DH demand to generate domestic load profiles and flat constant nondomestic load. The authors concluded that peak electricity demand will be significant, and that demand side management can provide an important balancing function.

Other notable contributions in estimating national heat demand includes the work of Sansom (2014). A regression analysis was conducted using 2010 weather and daily gas demand data to estimate national heat load. The daily heat demand was combined with load profiles obtained from boilers and CHP (combined heat and power) plants to create a half hourly demand profile for 2010. The synthesised demand data was used for analysis of heat decarbonisation pathways and the impact of electrification (Sansom and Strbac, 2012).

Many studies focus exclusively on either the domestic or nondomestic building stock. It is estimated that there are over 2 million nondomestic buildings in the UK compared to over 27 million dwellings but comprises around a fifth of the space and water heat demand (BEIS, 2017a). The studies that primarily focus on the domestic sector in the UK outnumber the studies in nondomestic modelling. Reasons for this include the oft-cited complexity of the nondomestic building stock (Bruhns et al., 2000; Liddiard et al., 2008; Smith, 2009; Steadman, 1997).

2.2.2 Domestic modelling

There are a several commonly used bottom up domestic energy models for the national housing stock (Cheng and Steemers, 2011). Most are based on the English Housing Survey EHS (and prior to that the English House Condition Survey) which is an ongoing stratified random national survey covering the housing stock (DCLG, 2017). The segmentations used in the survey are commonly used in modelling assumptions. It provides the main input to the Cambridge Housing Model (CHM), a policy advice tool to estimate energy demand from the housing stock and also provides the basis for other studies (BEIS, 2010).

Cheng and Steemers (2011) note that a common weakness of the current bottom up stock models is the use of generic occupant behaviour. Considering this, a large differentiating factor in their model—the Domestic Energy and Carbon Model (DECM), has been the use of multiple occupancy profiles based on employment status from socio-economic census data. DECM disaggregates output down to the LA level. The heat demand is estimated based on the SAP method from the BRE (2009), due to this, only yearly results are output from the model. They find that dwelling type and socio-economic factors can account for 85% of the variation in consumption between LAs.

BREDEM is described as a methodology to calculate domestic building energy consumption for different end uses and has widely employed as the core of other domestic energy models due to its adaptability (Kavgic et al., 2010). It uses heat balances and simple empirical relationships

that can be expanded upon to estimate annual domestic energy consumption (Arababadi, 2012). Examples that use BREDEM include the Community Domestic Energy Model (CDEM) (Firth et al., 2010). CDEM combines archetypes with the BREDEM method to investigate efficiency interventions. Another model utilised GIS tools to infer built form and orientation to model the energy consumption using BREDEM at the neighbourhood scale (Rylatt et al., 2003). The use of GIS based methods to analyse and gather data is becoming prevalent in building stock modelling. Oikonomou et al. (2012) looked at the urban heat island effect for London and the risk of overheating in dwellings. They use GIS data of building form and orientation to conduct simulations in EnergyPlus. Occupancy profiles were based on the work of Yao and Steemers (2005), incorporating socio-economic factors. Another GIS based approach applied polygon information, LIDAR, and thermal imaging to the Cambridge Housing Model to produce energy demand profiles at the neighbourhood level (Calderón et al., 2015). There is potential to use this methodology on a wider scale by city planners but the large computing requirements when scaled to larger areas remains a key challenge (Rosser et al., 2019).

In contrast to the bottom-up models presented, Watson et al. (2019) use a top-down approach to determine a regression model using historical gas demand and weather data. This is combined with load profiles obtained from measured heat pump profiles and differentiated by mean outdoor temperature. The study modelled a high temporal resolution, and the results can provide a useful comparison for national heat demand.

2.2.3 Nondomestic modelling

The difficulties involved in modelling the nondomestic stock include the high degree of heterogeneity, both within and across use categories. Perhaps the biggest challenge involves the availability of quality data (Taylor et al., 2014b). The energy end use is more varied, meaning measurements of gas consumption cannot be reliably used as a proxy for heating. The most comprehensive resource available is the property taxation database collected by the Valuation Office Agency (VOA). However, this does not identify all floor area in nondomestic sites such as hospitals or libraries and omits certain use categories such as agricultural buildings or places of worship. A second important data source are Display Energy Certificates (DECs) for public access properties in England and Wales, but these can also be inaccurate for many of the same reasons (Evans et al., 2017). In 2014 DECC commissioned the Building Energy Efficiency Survey (BEES) (BEIS, 2016c) to assess and understand how energy is used in the nondomestic stock across the different use categories. A comprehensive review of nondomestic stock modelling in the UK has been covered in Steadman et al. (2020). These have typically been in the form of a building database containing activity class and floor areas. The energy demand has then typically been estimated by simple steady state equations, such as energy intensities per floor area for a given activity class.

The CaRB2 model operates on this basic principle, using data from the above-mentioned sources, combined with a consumption data per activity type that was obtained from prior surveys (Liddiard, 2018). However, as it draws upon the VOA data, it only covers England and Wales. The Cambridge Nondomestic Energy Model (CNDM) has been developed with similar methods to the CHM (Armitage et al., 2015). This is achieved by segmenting the nondomestic stock into different building archetypes and applying a steady state energy model. The segmentation included built form, HVAC type, building age, location and use which resulted in some 35,000 combinations. The CNDM also uses the taxation database and output is disaggregated to a regional level but the energy model only produces annual demand with a breakdown of end use.

GIS approaches are also being used in nondomestic stock modelling, albeit on a smaller scale. The approach taken by Taylor et al. (2014a) involves combining the existing nondomestic data sources with ordnance survey data to create polygons of buildings for Leicester city centre. The 3DStock model is intended as a whole stock model but its treatment of the nondomestic stock

merits attention (Evans et al., 2017). It uses a GIS approach to combine a detailed representation of the urban building stock in select sub-city areas with taxation data, DECs and energy consumption data. A key feature of 3DStock is that the model differentiates between buildings and premises for nondomestic sites. A single premise can be part of a building, or multiple buildings, and the same building can have multiple premises. The energy consumption data in the form of annual gas and electricity readings for all premises modelled (a database few other models have access to) is then matched to the 3D representation of the buildings. It has so far only been applied to several sub-city areas and provides a high spatial resolution snapshot of urban energy consumption.

2.2.4 District scale models

There have been attempts at mapping the heat demand intensity for urban areas in the UK at a high spatial resolution such as the now defunct National Heat Map developed by the Centre for Sustainable Energy (2010) for DECC which was designed with an emphasis on the location of heat networks and waste heat potential. Internationally, other such tools exist at the city scale however these are only snapshots of heat demand intensity or annual consumption (Fremouw, 2017; Prieto et al., 2018). Tools such as CitySim (Robinson et al., 2009) or Huber and Nytsch-Geusen (2011) have been developed to aid urban planning and have been demonstrated with application to case studies, however these localised tools require extensive modelling data input. Numerous examples exist in the literature of localised studies to forecast heat load in DH systems that use a variety of methods from detailed network simulation to statistical and machine learning methods (Calikus et al., 2019; Dahl et al., 2017; Dalipi et al., 2016; Guelpa et al., 2019; Idowu et al., 2016). As these are localised for specific districts and existing networks, these models can't be applied directly to modelling districts in the UK without extensive data input and large assumption. Methods of creating spatiotemporal energy demand for districts have been achieved by applying known spatial consumption to temporal profiles based on the distribution of building archetypes but the temporal profile can be difficult to validate particularly without comparative data at the same spatial resolution (Mikkola and Lund, 2014).

As already shown, GIS based methods to generate three-dimensional polygons to model districts and urban centres are prevalent in the literature. Nouvel et al. (2015) compared two methods, a thermal model applied to 3D reorientations and a statistical method using 2D GIS. They combined these methods to develop a framework to study heat loads at higher spatial resolutions, using the statistical method at the lower spatial resolution then applying a thermal model to 3D representations for higher spatial resolutions. Dogan and Reinhart (2017) applied GIS to a mixed used neighbourhood in Boston, USA. They generated 3D models that are then simulated in EnergyPlus to create hourly load profiles. Nageler et al. (2017) applied a GIS to open source mapping data of an Austrian district to generate polygonal representations of buildings. Demand profiles were assigned to building using a thermal model and a database of archetypes. The authors of this study noted that computational resources were the main limiting factors on enlarging the modelled area.

2.2.5 Conclusion of review

Building stock energy models in the UK are well established, particularly in the domestic sector. The segmentation of the building stock into archetypes is widely used in the analyses, except in cases where a regression has been applied to historical data. The main data sources that are drawn upon are census data, historical consumption and the EHS. Many studies and tools that map energy demand do so with a static state energy method or mapping historical annual consumption. Two recent studies have created a spatiotemporal analysis of energy demand (Clegg and Mancarella, 2019; Eggimann et al., 2019). The heat load modelling was achieved via either application of load profiles to heating degree day calculations or the generation of load profiles through building physics models with a reduced set of archetypes.

Achieving high accuracy is difficult due to the lack of data. In the case of buildings, data on occupancy and when heating systems are operated is essential. This is one of the primary reasons that nondomestic modelling is a harder than the well understood domestic sector. With (non-hourly metered) gas being the main heating vector in the UK, it has not been possible to use historical consumption alone to determine hourly loads, as is the case with electricity. With the increasing uptake in heat pumps however, this may be less of an issue in future. DH load profiles are available and have been drawn upon in the literature to provide urban heat load profiles. However, the composition of the local building stock varies between locations.

The aim of HeLoM is to generate weather derived spatially disaggregated hourly national heat load profiles for domestic and nondomestic buildings. This provides the bases for national demand and the disaggregation enables the urban demand to be extracted as a proxy for DH demand. It is not possible to use or adapt the existing highly spatiotemporal models for the purposes of this study. Others that can be adapted are only national in scale, as is the case with the regression models.

2.3 Archetype Development

Each building is unique, not just in terms of the physical construction, orientation, exposure and location, but also in its occupancy and use. This model follows the approach of segmenting the stock into building archetypes. Once building archetypes are defined, a transient thermal simulation is developed. The purpose of the simulation to calculate the hourly heat demand using historical weather data. The advantages of using a custom a thermal model for simulating buildings is that it allows the efficacy of interventions such as altering insulation to be evaluated and enables the use of custom weather data to simulate heat demand. While individual building will be simulated, results will be stored at an aggregated level (LSOA or MSOA). Diversity is achieved by stochastically varying occupancy and application of known diversity factors.

A fundamental challenge in modelling the building stock is in the level of detail and attention afforded towards grouping similar constructions into segments or archetypes. The archetype approach is a widely utilised framework in bottom-up building stock modelling. A building stock can be represented by a sample of building archetypes that represent a statistical average for the archetype within the stock (Mata et al., 2014).

Table 2.1 Summary of data sources used for HeLoM

Data	Level	Source
Dwelling build period	LSOA/DZ	CTSOP4.1 (Valuation Office Agency, 2020) (Scottish Government Statistics, 2020)
Dwelling type	LSOA/DZ	QS402EW (Office for National Statistics, 2020) QS402SC (Scottish Government Statistics, 2020)
Domestic Heating type	LSOA/DZ	QS415EW (Office for National Statistics, 2020) QS415SC (Scottish Government Statistics, 2020)
UK Domestic and Nondomestic Gas Consumption	LSOA/DZ MSOA/IZ	Sub-national gas consumption (BEIS, 2020c)
Nondomestic floor areas	Building	CaRB2 from (Valuation Office Agency, 2020) (Scottish Government, 2018)
Standard Area measurements	MSOA/IZ	(Office for National Statistics, 2020) (Scottish Government Statistics, 2020)
Weather data	Regional	(Met Office, 2019)

To develop archetypes, appropriate segmentations need to be identified prior to characterisation of thermal properties and occupancy. The most fundamental segmentation is differentiating between domestic and nondomestic. The archetypes developed here will draw upon the work of a combination of previous studies. The open-source datasets drawn upon for this work are presented in Table 2.1.

2.3.1 Domestic archetype segmentation

Most domestic archetyping studies in England have drawn extensively on the English Housing Survey (MHCLG, 2016). As the largest component of Great Britain, this study also utilises it. The EHS splits domestic buildings into seven archetypes:

1. End and mid terrace
2. Semi-detached
3. Detached
4. Bungalow
5. Converted flat
6. Purpose built flat

The ONS archetypes per LSOA do not directly correspond to all the EHS ones. They report on dwelling types as:

1. Detached
2. Semi-detached
3. Terraced
4. Purpose built flat
5. Converted flat
6. Others such as bungalow, caravan, etc.

This study combines end terrace and mid terrace to correspond to the ONS data. While the ONS reports on purpose built and converted flats. Converted flats have wide variety in form and the construction information in the available literature is largely for purpose-built flats. Therefore, all flat varieties will be treated as purpose-built flats. The same archetype segmentation has also been used in previous studies (Oikonomou et al., 2012; Stamp, 2016). The observed distribution of the dwelling types used is shown in Figure 2.1.

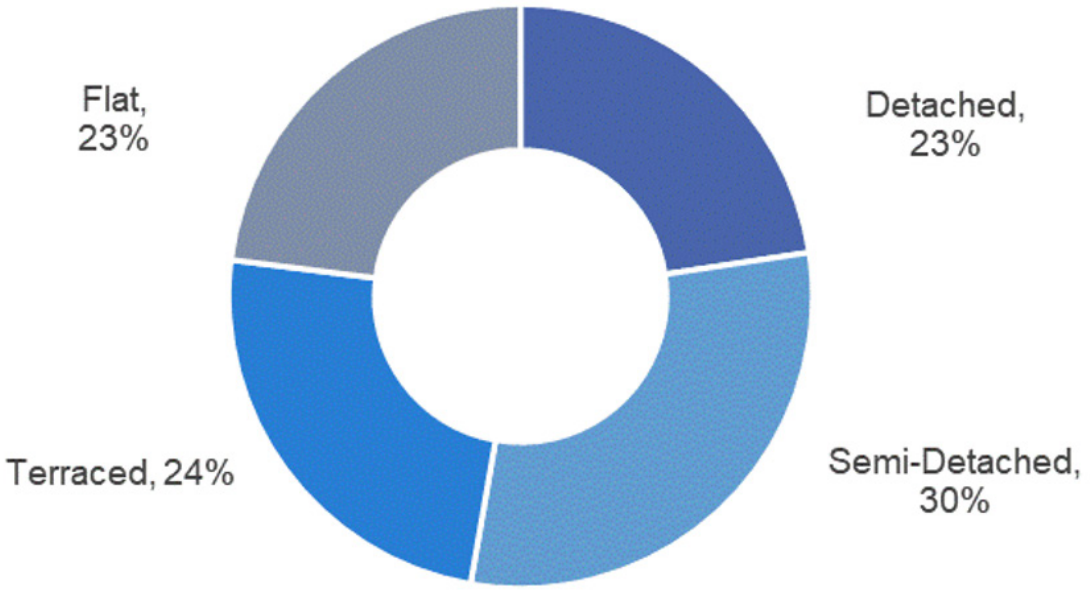

Figure 2.1 Dwelling types in the UK housing stock

Each dwelling category is further split according to construction period. The VOA reports dwelling age in 12 build periods, from pre-1900 to post-2010, corresponding roughly to a decade in length while the EHS splits this into five build periods from pre-1919 to post-1990. The proportion of dwellings per age range has been applied to each dwelling type present in the LSOA. While it is likely that different dwelling types are built in different periods, the age variation per dwelling type is estimated from the overall distribution per LSOA as the data is provided per LSOA without further breakdown of age per dwelling type. This may be an issue with LSOA's that have a diverse range of dwelling types and construction periods but in many LSOA's the construction type and age fall within a narrow range (Boswarva, 2017). The distribution of dwelling build-period is shown in Figure 2.2 adapted from Piddington et al. (2020).

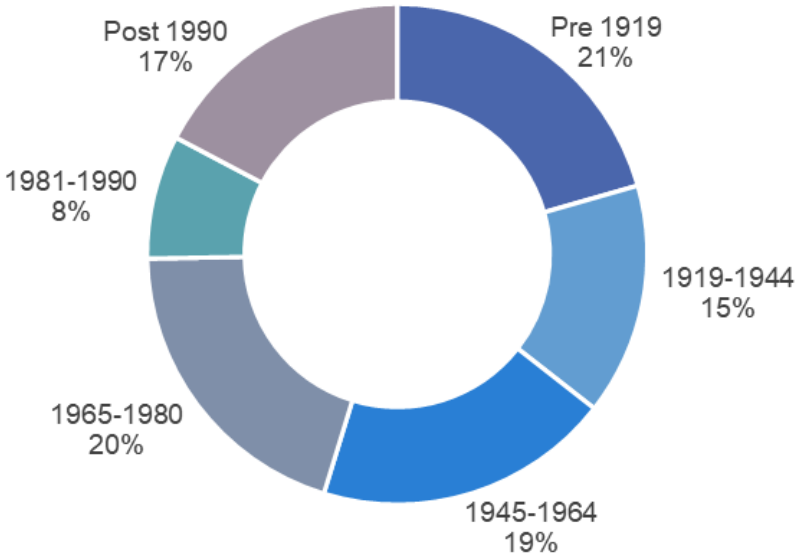

Figure 2.2 Dwelling built period in the UK housing stock

The SAP assessment has 11 age bands that are often combined. Oikonomou et al. (2012) use five age bands with multiple variations, reducing these to the 15 most commonly found in their modelled area. Mata et al. (2014) combine six dwelling types with eight narrow and recent age bands, Cheng and Steemers (2011) use ten age bands that become progressively narrower while Buttita et al. (2019) use the EHS age bands but combine two of the periods.

Table 2.2 Archetypes used in comparative studies

Source	Dwelling Types	Age Categories	Geographic zones
Mata et al. (2014)	6 Dom 3 Nondom	8 pre-1985 to post-2010	4 – major cities
Cheng and Steemers (2011)	5	10 pre-1900 to post-2000	1 – using 30 year mean data
Buttita et al. (2019)	5 with multiple variations	5 pre-1918 to post-1991	4 – major cities
Oikonomou et al. (2012)	5 with multiple variations	6	1 – 52 sites in London
Stamp (2016)	4	4 construction styles	3 weather files
HeLoM	4	5	11 - GB regions

2.3.2 Domestic archetype characterisation

The form and fabric data for each archetype is used to estimate a specific heat loss (SHL) and thermal mass (ThM) from construction and fabric assumption per archetype. Dwelling archetype geometry will be taken directly from the English Housing Survey (MHCLG, 2018). The specific heat loss will largely be derived from construction data from BRE's SAP 2016 from which glazing ratio and performance data are also taken (BRE, 2016). The thermal mass represents the heat capacity of a building or its ability to store heat. Construction and fabric play a large role in the thermal mass as do the internals of a dwelling. SAP gives thermal mass with a thermal mass parameter (TMP) per unit floor area. It has three categories of light, medium and heavy construction ranging from 100 to 450 kJ/m^{2}K. The TMP used are adapted from Stamp (2016) who provides estimates for the building archetypes used here and shows that older constructions tend to be heavier while newer constructions utilise modern lightweight construction methods and so have a lower TMP. Table B-1 in Appendix B contains all the estimates and parameters used for domestic archetype characterisation.

Table 2.3 Domestic archetype data sources

Parameter	Source
Dwelling Geometry	English Housing Survey (MHCLG, 2018)
Construction U-values	SAP 2016 (BRE, 2016)
Thermal Mass Parameter	Stamp (2016)
Boiler/Heating system size	CE54 (Energy Saving Trust, 2010)
Glazing transmittance	SAP 2016 (BRE, 2016)

The power rating and efficiency of the heating system varies greatly between dwellings, and the power capacity determines to a large extent how it is operated. For the purposes of calibrating the heat load with gas consumption data, it is assumed that all buildings have a gas boiler with an average efficiency of 85% for heating and 75% for hot water (BRE, 2016; Palmer and Cooper, 2013). The power ratings of the heating system per archetype are assumed from a conservative calculation of gas boiler power ratings using the domestic heating sizing method CE54 (Energy Saving Trust, 2010).

2.3.3 Domestic occupancy

Mean occupancy has been adapted from the SAP methodology based on floor area (BRE, 2016). Measured hourly gas consumption profiles have been used as a proxy for active occupancy profile and heating system operation for all dwelling archetypes. Average domestic heat load profiles in UK households exhibit a double peak pattern, with morning and evening peaks. From surveys on how dwellings are heated with various heating systems including gas boilers and heat pumps, it appears that dwellings are predominantly heating this way regardless of heating system and mixed work patterns (Hanmer et al., 2019; Love et al., 2017; Watson et al., 2019). Yao and Steemers (2005) showed that the load profile is same across dwelling types, with the magnitude of peaks corresponding to the size of dwelling archetype. A normalised domestic load profile has been adapted from Wang et al. (2020) to represent the probability of active occupancy and operation of heating as shown in Figure 2.3.

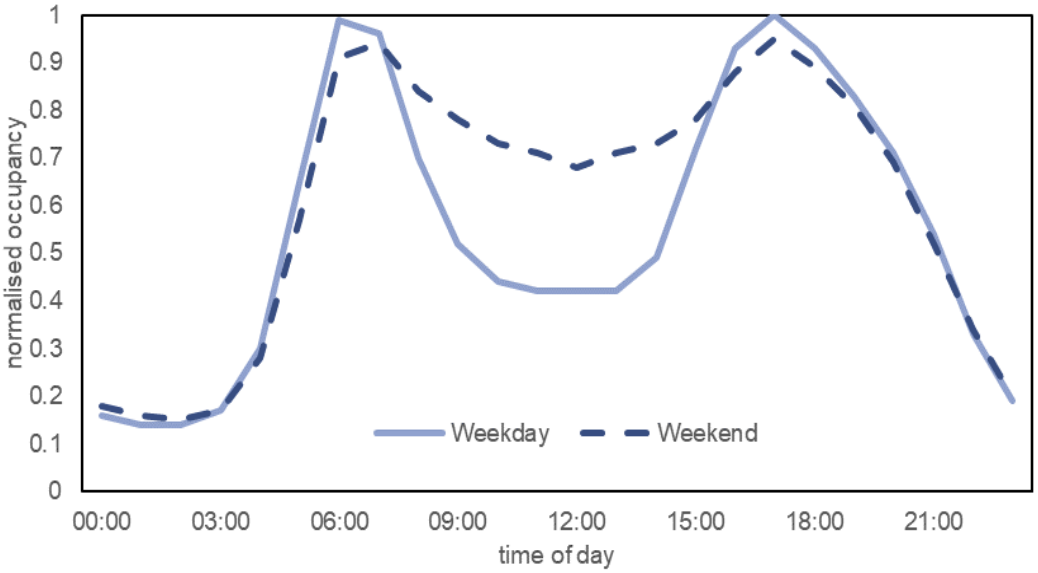

Figure 2.3 Normalised domestic occupancy profiles

2.3.4 Nondomestic archetype segmentation

The nondomestic archetypes are based on the CaRB2 activity classifications which expand on the four VOA bulk classes: retail, office, industry, warehouse (Evans et al., 2017; Valuation Office Agency, 2020). The primary source of data for nondomestic counts and floorspace as previously discussed is the VOA taxation database. The available data from CaRB2 contains activity classification and aggregated floor area per postcode which were combined to LSOA level by matching postcodes to output area. This did not include detail on activity type (due to data sensitivity). While floor area has made available, this data has been deemed inaccurate due to the method of taxation data collection where some classes (such as schools, hotels and hospitals) do not have floor area records (Liddiard, 2020). The CaRB2 activity classifications, count and floor areas are shown in Figure 2.4.

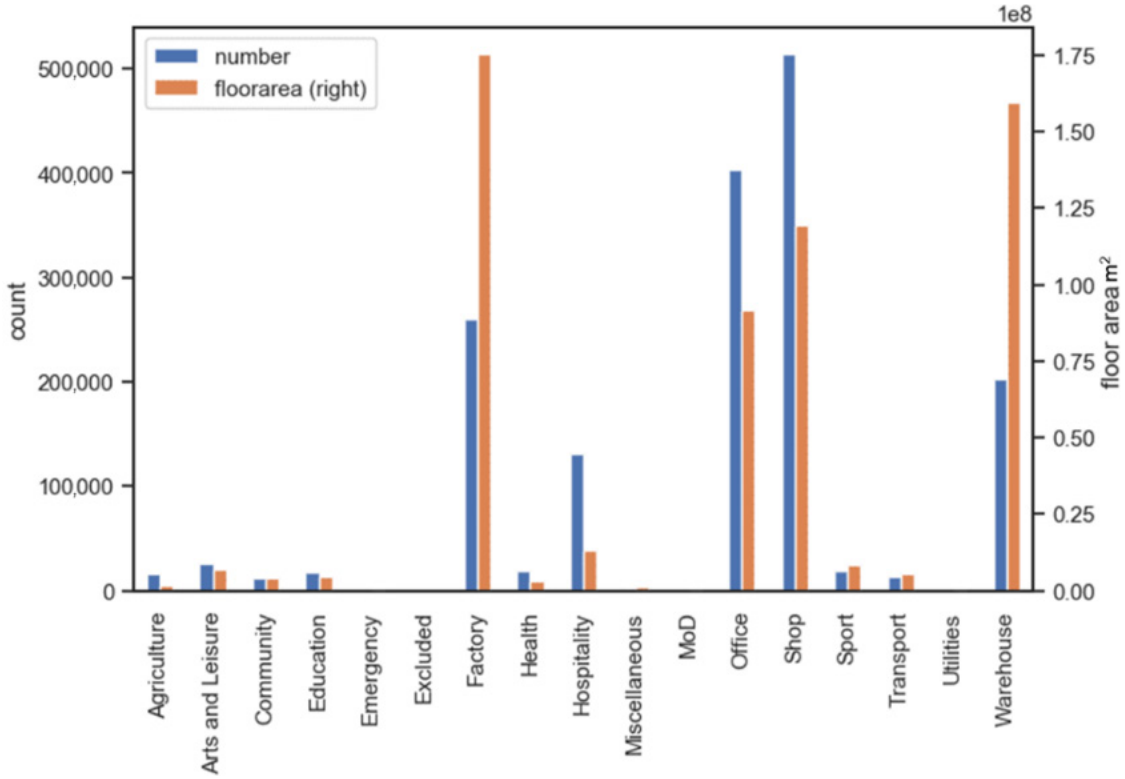

Figure 2.4 Count and floor area per activity classification in the CaRB2 database

For the purpose of urban load modelling, the five most important categories are office and shops (retail), followed by factories, warehouse, and hospitality. It was not possible to obtain localised Scottish nondomestic figures as the CaRB2 data covered only England and Wales. Instead the overall count of each archetype in Scotland was scaled to each MSOA using annual gas consumption data, the share of each classification is shown in Figure 2.5 (Scottish Government, 2018). After filtering for only those in urban area, several categories were omitted or combined. These categories and relative proportions in modelled urban areas are shown in Figure 2.6.

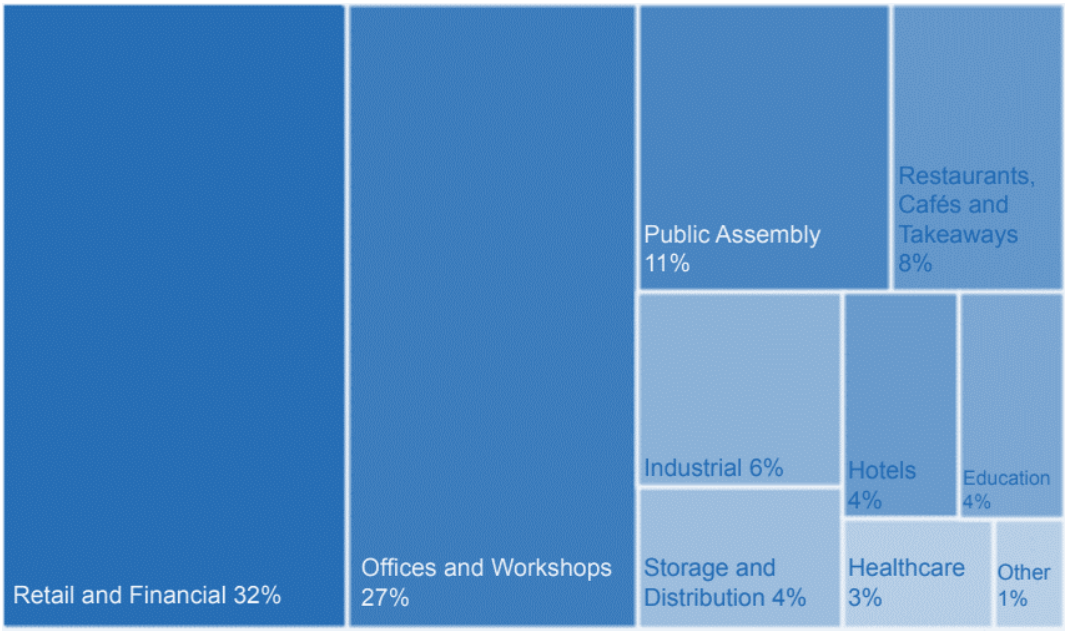

Figure 2.5 Nondomestic classification share in Scotland (Scottish Government, 2018)

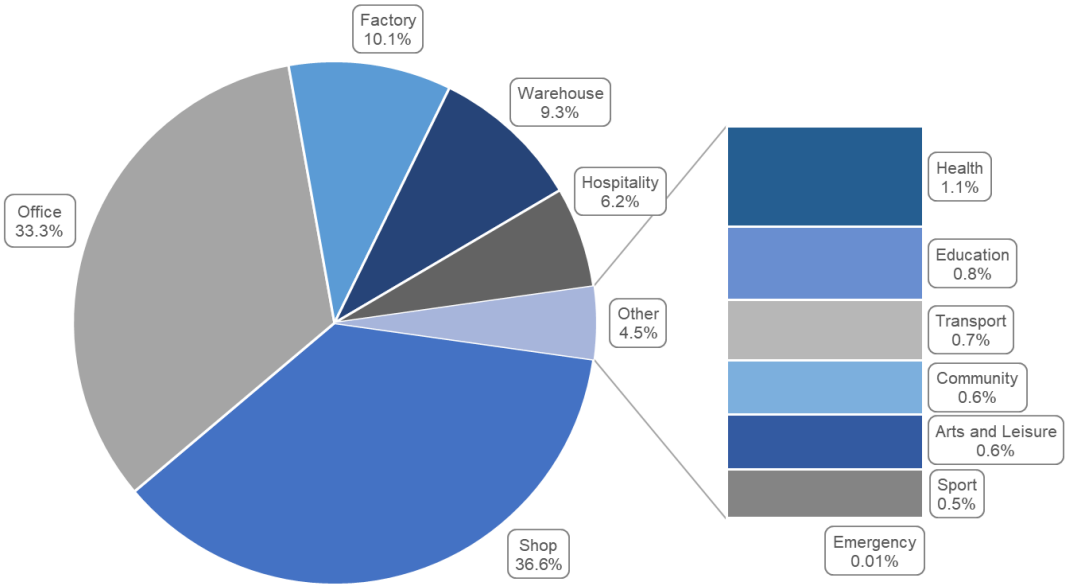

Figure 2.6 Proportion of nondomestic archetypes in modelled urban areas

2.3.5 Nondomestic archetype characterisation

The occupancy and use of nondomestic buildings exhibit a large variation. There can be many different sizes, and floor plans, even within the same classification (DCLG, 2011). For example, while classifications such as “offices” or “education” are generally occupied during normal working hours, the occupancy and usage times can often vary, with occupancy in the evenings and weekends not uncommon in these classifications.

The archetypes were adapted from analysis of the CaRB2 data by Barrett (2020). The mean floor areas for each category were calculated from the total gross internal area and archetype form was inferred from prior surveys of the nondomestic building stock (Gakovic, 2000; Steadman et al., 2009, 2000). A medium-weight construction TMP of 250 kJ/m^{2}K was applied to all archetypes to derive a thermal mass. Benchmark guidelines were followed for the sizing of the heating system and determining internal heat gains in the various archetype activity classifications (BSRIA, 2011; CIBSE, 2015a). Where data and benchmarks for the archetype were not found, the figures were estimated from other archetypes.

Nondomestic internal gains are estimated using benchmark figures from CIBSE (2015a) Guide A. Offices and schools are well represented in other literature (Korolija et al., 2013; Tian and Choudhary, 2012). Where the archetype data is unavailable, such as the case for industrial buildings, this has been estimated based on CIBSE Guide A. A summary of the nondomestic archetype parameters is shown in Table B-2 in Appendix B.

2.3.6 Nondomestic occupancy

Building occupancy and use was determined mainly from analysis of hourly gas consumption data for 37 buildings provided by Sustainable Energy Limited (Challans, 2018). An overview of the provided data is shown in Table B-3. Normalised profiles were extracted for each activity class available in the dataset. These can be found in Figure B-1 and Figure B-2. This was further supplemented through secondary studies on occupancy in offices, shops, health and educational buildings but for non UK based buildings (Duarte et al., 2013; Lindberg et al., 2019). There are three categories where there is a lack of available data on occupancy: factory, warehouse, and transport. Factories and warehouses constitute 19% of the modelled stock and both are very diverse in their activity types. The factory classification can range from a food processing factory to newspaper print works, while it is unclear to what extent warehouses are heated due to the large floor area they occupy. Transport buildings are similarly diverse, from a train station to a petrol station. A 24-hour occupancy with higher daytime usage has been estimated for these categories as shown in Figure B-3 and Table B-4.

2.3.7 Spatial disaggregation

The highest level of spatial disaggregation analysed is the LSOA level. All the GB domestic stock has been mapped to this spatial resolution as shown in in Figure 2.7. The nondomestic activity classifications in the CaRB2 database were available per postcode in England and Wales, but these were mapped to the LSOA level. In Scotland, nondomestic stock counts were only available at the national aggregated scale, these were distributed per MSOA, weighted by MSOA nondomestic gas consumption. A summary per region is given in Table 2.4

Due to computing capacity and storage limitations, only selected MSOAs have been modelled. The gas demand per square kilometre has been estimated per MSOA using Standard Area Measurements, then ranked by gas consumption density. The top 20% cumulatively were chosen as representative of urban heat demand. A further 10% of largest absolute gas consumption were included to comprise a more representative consumption profile to scale to national level. The results for each LSOA and MSOA are stored in table form within an SQL database. Each hour or row of data contains roughly 1600 bytes of data. Six years of results for 10,226 individual LSOAs and MSOAs results in just over 40 GB of data.

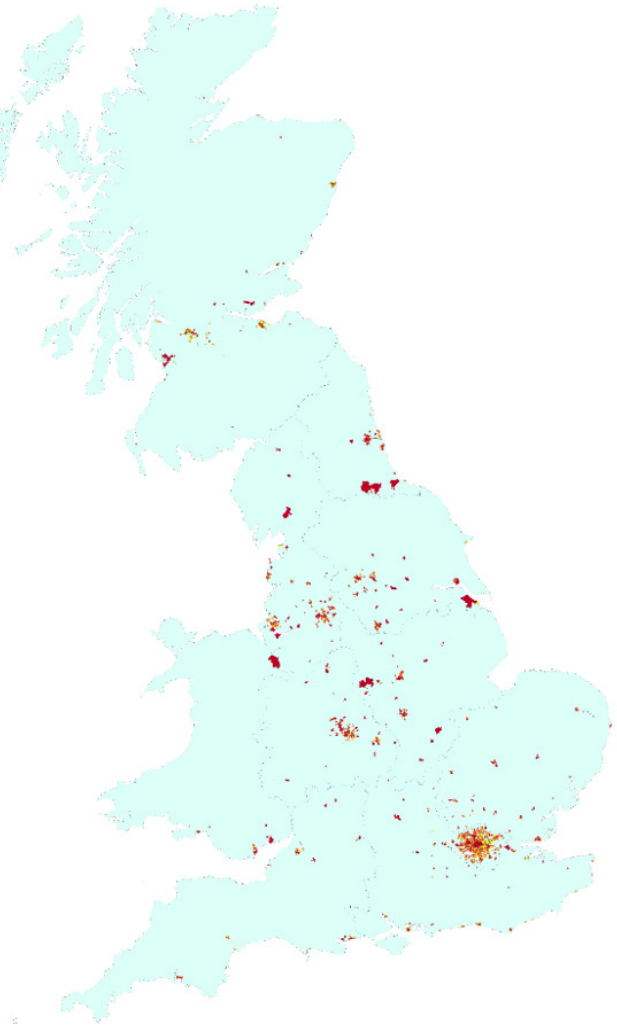

Figure 2.7 Modelled GB MSOA locations

Table 2.4 Summary of modelled regions

Region	LSOAs modelled / total LSOAs	Modelled % of GB Gas consumption	Modelled % of Dom Gas consumption	Modelled % of nondom gas consumption	Modelled % of GB Population
London	3443 / 4835	9.7	9.3	10.3	10.3
South East	906 / 5382	1.8	1.4	2.3	1.6
South West	353 / 3281	0.9	0.8	1.1	1.0
East of England	405 / 3614	1.7	0.9	2.9	1.0
East Midlands	449 / 3614	1.5	0.9	2.5	2.5
West Midlands	919 / 3487	2.4	1.8	3.5	1.0
North West	1002 / 4497	3.8	2.4	5.8	2.0
Yorkshire and the Humber	723 / 3317	3.2	1.7	5.8	1.8
North East	357 / 1657	1.4	1.0	2.2	0.9
Wales	181 / 1909	0.9	0.3	1.3	1.6
Scotland	1051 / 6976	2.7	1.8	4.2	6.7
Total	9789 / 41792	30.0	22.4	41.9	23.8

2.3.8 Weather data

Weather data is divided into GB regions (the highest tier of sub-national division). Weather stations were selected per region based on proximity to population centres and completeness of data, covering at least the period 2010-2016. Met office data was compiled ensuring that each station has been active since at least the beginning of 2010. Missing temperature (wet bulb) values were linearly interpolated unless large gaps of more than 12 hours were found. Missing wind speeds were forward filled for a maximum of 2 hours, otherwise they were interpolated to the next available wind value unless large gaps of more than 12 hours were found. Missing solar observation data was first linearly interpolated if less than three consecutive hours were missing, otherwise values were shifted from the previous 24 hours unless large gaps of more than 24 hours were found. In cases where large sections of data were missing, these were filled using data from the closest available weather station. Details on each regional station used for UK hourly weather observations is shown in Table 2.5 and the geographic distribution of each station is mapped in Figure 2.8.

2.4 Thermal Model Development

Thermal simulations of the building stock are conducted on a per LSOA basis. The compiled data on the numbers of each domestic and nondomestic archetype is applied to the LSOA. Each building is assigned a demand set-point temperature, T_{set}, which is normally distributed about a mean of 20 °C with limits of 15–25 °C. This is based on reported domestic set-point temperatures (Shipworth et al., 2010). There is also evidence that nondomestic archetypes such as offices and schools fall within this range albeit skewed to the higher limit (Korolija et al., 2013; Tian and Choudhary, 2012).

The simulation procedure calculates the temperature change of the building thermal mass per hourly time step. The thermal model simplifies the representation of the buildings as cuboids with heat transfer through four walls. It assumes the temperature of the building thermal mass and internal wall surface to be same as the internal air temperature, T_{int}. The net heat flows from the buildings are the sum of gains and losses and calculated dynamically to update the temperature of the thermal mass.

The ambient temperature, T_{amb}, is given by the hourly weather data. The first step is to estimate the external wall temperature from convective heat transfer to the air to calculate conduction through the wall. Calculating wind induced convection is complicated due to geometry, orientation, and other factors such as roughness and protection from surroundings such as trees or larger buildings. Heat transfer theory suggests a power law model for heat loss from an object but a linear form has been found to fit the data well in the ranges often experienced by dwellings (although this may not hold for very tall tower blocks) (Palyvos, 2008). A linear form equation to estimate the wind convection coefficient for each surface, $h_{c,s}$, with wind speed, v_w, has been suggested (CIBSE, 2007). With the assumption that wind forced convection acts on one side only, the convection transfer is given by (2.2), setting $v_w = 0$ in (2.1) for the remaining surfaces:

$$h_{c,s} = 5.8 + 4.1 v_w \tag{2.1}$$

$$Q_{conv,s} = h_{c,s} A_s (T_{ext,s} - T_{amb}) \tag{2.2}$$

Conduction heat transfer through each surface, $Q_{cond,s}$, can be calculated from:

$$Q_{cond,s} = U A_s (T_{ext,s} - T_{int}) \tag{2.3}$$

Under the assumption of steady-state, conduction through each wall is equal to the convection from the wall, $Q_{conv,s} = Q_{cond,s}$. Using (2.2) and (2.3) we can estimate T_{ext} for each wall and from this, $Q_{cond,s}$ through each wall.

Figure 2.8 Locations of regional weather stations used

Table 2.5 UK hourly weather observations - Regional stations

Region	Station ID	Station Name
London	708	Heathrow
South East	795/862	Shorham Airport/Hampshire (solar)
South West	676	Filton
East of England	461	Bedford
East Midlands	554	Sutton Bonington
West Midlands	19187	Coleshill
North West	1119/1083	Stonyhurst/Shap (solar)
Yorkshire and the Humber	534/370	Bramham/ Leconfield (Solar)
North East	326	Durham
Wales	19206	St Athan
Scotland	24125	Glasgow Bishopton

Solar gains are dependent on the building envelope's window area, A_w, the glazing transmittance, G_t, and irradiance. As windows are vertical, the incident irradiance, I_r, can be calculated from the horizontal irradiance using the Earth's axial tilt angle on a given day and latitude of a given location. The building solar gains, Q_{sol}, can then be estimated by:

$$Q_{sol} = A_w G_t I_r \tag{2.4}$$

Building infiltration is impacted by factors such as wind speeds and the ambient temperature which drives the stack effect (particularly in taller buildings). However, factors such as the opening of windows have a large impact on the ventilation and infiltration rate. The Infiltration loss is simplified to just the air changes per hour, ach, and building volume, V_b, of the archetype:

$$Q_{inf} = 1/3 \text{ ach} \times V_b(T_{amb} - T_{int}) \tag{2.5}$$

Domestic internal gains, Q_{gain}, are estimated from the mean hourly occupancy, P_h, and floor area, A_f assuming 54 W per person, 0.1 W/m^2 for lighting and small appliances, 105 W per dwelling for large appliances (such as refrigerators) (Grant and Clarke, 2014).

$$Q_{gain} = 54P_h + 0.1A_f + 105 \tag{2.6}$$

Nondomestic internal gains are calculated from the intensity factors in Table B-2 multiplied by normalised occupancy from Figure B-1, Figure B-2 and Figure B-3. The sum of the heat transfers, Q_{tot}, can now be calculated from:

$$Q_{tot} = \sum Q_{cond,s} + Q_{inf} - Q_{gain} \tag{2.7}$$

The internal temperature change, ΔT_{int}, is then updated by:

$$\Delta T_{int} = Q_{tot} / M_{th} \tag{2.8}$$

For a large set of buildings, the CIBSE (2015b) code of practice for heat networks suggests the use of an 80% diversity factor for peak space heat load. This diversity factor is multiplied by the normalised occupancy profile value to give the hourly probability of heating system operation and determined randomly for each building.

If internal temperature is lower than setpoint temperature and the building is actively occupied, then the heat demand is the heat required to raise the temperature of the thermal mass to the setpoint temperature up to the power capacity of the heating system. If heat is supplied to the building, then internal temperature is updated using (2.8).

$$Q_{dem} = M_{th}(T_{set} - T_{int}) \tag{2.9}$$

Box 2.2 Diversity factors and peak demand

Although we cannot accurately predict energy demand of a single building or active occupants, many aggregated buildings can be well approximated. We are concerned with the local aggregation of buildings not a single dwelling. Diversity assumes that not all peak demand occurs at the same time and is important when sizing a power/heat plant that serves multiple customers. The capacity would not be the sum of the maximum demand from each, but a lower value as the maximum demands will occur at different times. The diversity factor then indicated the peak aggregated load as a percentage of the sum of the individual loads.

2.4.1 Hot water demand

There have been a range of models produced to calculate hot water demand, mostly for domestic buildings (Fuentes et al., 2018). These have generally been compiled from high resolution sampling of water consumption and are suitable to apply in an individual building

analysis such as the BREDEM estimation of hot water. The building model presented here does not have sufficient detail to calculate high resolution hot water demand per building. As we are not concerned with the heat performance of an individual building but a demand at an aggregated level, it is thus appropriate to simplify the approach to hot water demand.

The average hot water consumption in UK dwellings is reported between 3-5 kWh per day (EST, 2008; Knight et al., 2007). The heat network code of practice (CIBSE, 2015b) states that the Danish standard DS439 for peak domestic hot water demand is widely used in the design of DH in the UK. The peak hot water value (kW) for N number of domestic buildings has been estimated from the Danish standard DS439.

$$Q_{hw,max} = 17.6 + 1.19N_b + 18.8N_b^{0.5} \quad (2.10)$$

The peak heat load is then applied to a daily load profile. The daily domestic water load profiles have been adapted from a study for DEFRA (EST, 2008) and a design guide for hot water in DH networks (Robinson, 2018). From the literature, a weekday, Saturday and Sunday load profile are given as well as a weekday/weekend variation factor. There were minor differences between the Saturday and Sunday load profile but an average of the two is used as a weekend load profile and the adjustment factor was applied to the weekend profile. A further adjustment, f_m for the monthly or seasonal variation is applied as per Burzynski et al. (2012a) which is based on BREDEM. Aggregated hourly domestic hot water demand can then be estimated from (2.10).

Table 2.6 Monthly factor for domestic hot water variation

	Jan	Feb	Mar	Apr	May	Jun	Jul	Aug	Sep	Oct	Nov	Dec
fm	1.10	1.06	1.02	0.98	0.94	0.90	0.90	0.94	0.98	1.02	1.06	1.10

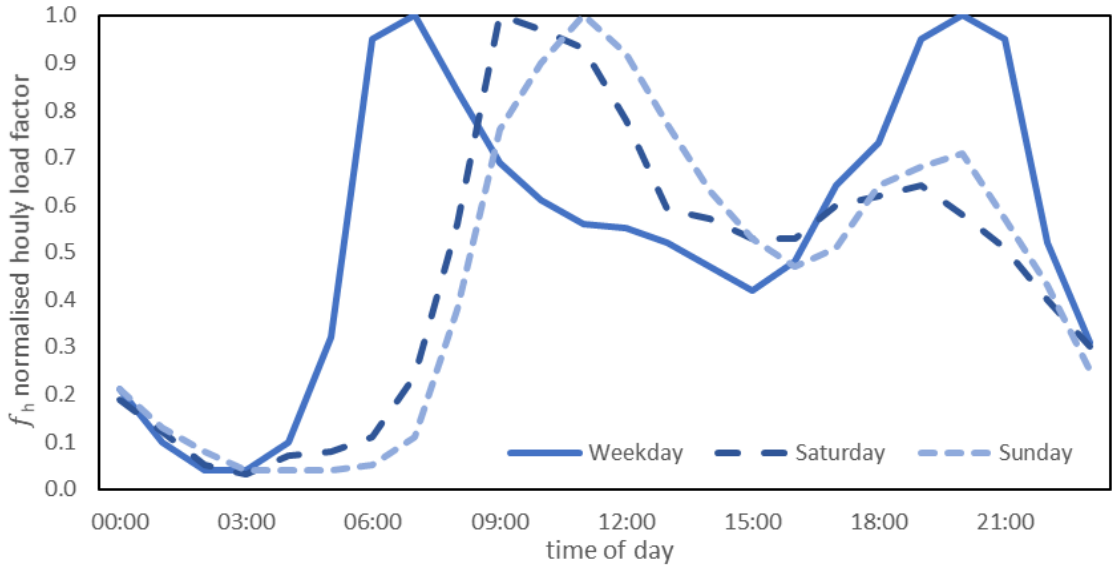

Figure 2.9 Normalised daily load profiles for domestic hot water

$$Q_{hw} = f_m f_h Q_{hw,max} \quad (2.11)$$

Nondomestic hot water (and other low temperature heat) demand is more challenging, especially given the lack of absolute consumption and measured demand profiles. Fuentes et al. (2018) reviewed hot water load profiles in various building uses which showed a pattern that largely corresponded to occupancy.

BEIS (2018a) has published estimates of nondomestic hot water energy consumption based on their Building Energy Efficiency Survey (BEIS, 2016d). The nondomestic hot water energy consumption in the UK was estimated to be around 14,900 GWh in 2015 and comprises 8% of the national nondomestic gas consumption. Given that hot water demand accounts for 10% of

nondomestic heat demand and around 3% of overall space and hot water heat demand in the UK and compared to heating, hot water consumption has less variation between years, the 2015 numbers were assumed to be representative of all years. Further, it is unclear how each of the activity classifications produce hot water. In the case of larger hospitality buildings for example, it is possible that hot water is constantly produced and used in short term storage tanks. Given this, a simplified approach of assuming 8% of nondomestic gas consumption is for hot water, produced by gas boilers (at 75% efficiency) distributed evenly over all hours was assumed. The use of nondomestic gas consumption has its own issues concerning the number of nondomestic gas connections (see section 2.4.2), but it is assumed that large hot water production has been from gas.

2.4.2 Model calibration

The annual domestic heat demand is then compared and calibrated with domestic LSOA gas consumption from 2016 for LSOAs that had at least 50% of dwellings connected to the gas grid using an average boiler efficiency of 85% (Palmer and Cooper, 2013). An assumption is made that the dwellings connected to the gas grid are evenly distributed per dwelling type. This may not necessarily hold true in all areas, for example, all flats in a particular LSOA could be disconnected from the gas grid while all other dwelling have a connection, but this level of detail is currently unobtainable. For areas that had a lower percentage of gas connection, the average regional adjustment was applied across all years.

Table 2.7 Average calibration factors per region

Region	LSOAs modelled	Modelled LSOAs with above 50% domestic gas connection	Mean calibration factor (modelled/measured)
London	3443	2047	0.92
South East	906	654	1.01
South West	353	215	0.99
East of England	405	337	1.10
East Midlands	449	389	1.09
West Midlands	919	829	1.15
North West	1002	856	1.13
Yorkshire and the Humber	723	646	1.09
North East	357	324	1.11
Wales	181	146	1.07
Scotland	1051	764	0.94
Total	9789	7207	1.03

Nondomestic modelled heat loads have been adjusted using the mean regional domestic adjustment factor. The number of nondomestic gas connections do not correspond to nondomestic premise count from CaRB2 as shown in Figure 2.10. Neither is there a dataset on the number of 'non-gas' nondomestic premises as exists for domestic buildings. In the nondomestic sector, multiple premises can share a single gas meter in one building, or across multiple buildings or may have an unconnected supply point. Analysis of the nondomestic gas consumption data shows that around 6% of this fall into the unallocated category. Also, the designation of a nondomestic gas meter is arbitrary and based on a 73,200 kWh cut-off applied by BEIS (2020c), therefore some smaller nondomestic premises fall incorrectly into domestic consumption and vice versa. In addition, it is possible that some industrial gas use may also be

present and it is not possible to easily subtract this demand. However, it is assumed that industrial demand will be small percentage in urban areas with high heat demand density (but may be higher in the modelled MSOAs with highest gas demand in Figure 2.7).

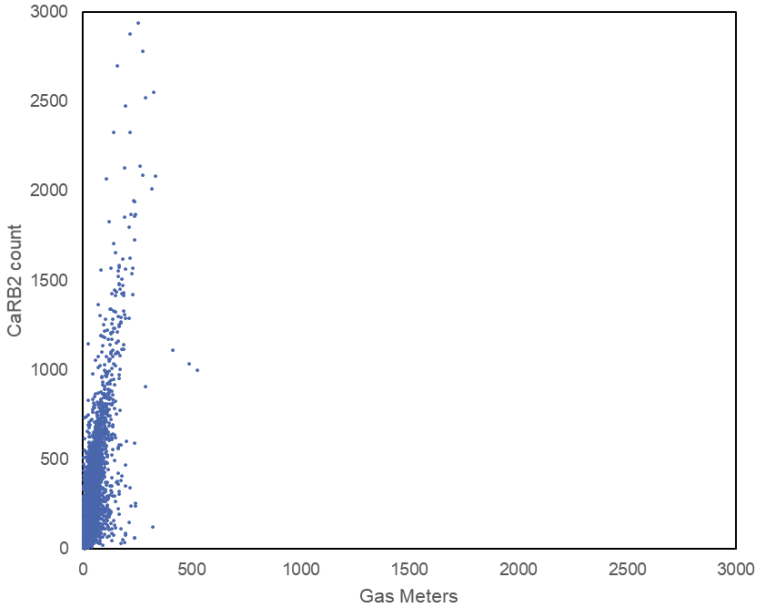

Figure 2.10 Comparison between CaRB2 count and nondomestic gas meters per MSOA

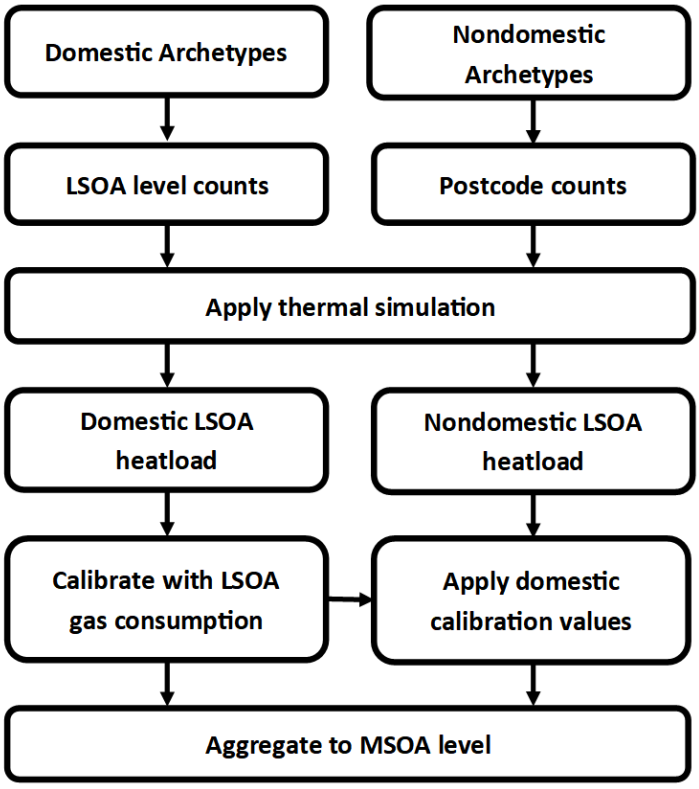

Figure 2.11 Modelling steps for aggregating domestic and nondomestic demand

2.4.3 Parameter sensitivity

The sensitivity of the input parameters to the thermal model was tested. Each parameter in Figure 2.12 was tested one at a time by scaling the parameter and observing the percentage change in total heat load for the entire six-year period. The sensitivity was conducted on 1000 domestic buildings, comprising of each domestic archetype in the ratios given in Figure 2.1 using London meteorology data.

The most sensitive parameters observed in advanced building simulation models are the wall U-values, ventilation rate and setpoint temperature (Imam et al., 2017). Linear responses to the inputs are observed with window thermal transmittance and SHL. Increasing the transmissibility value results in larger thermal gains and thus reduced heat load. The SHL values encompasses both fabric U-values and air change losses. The most sensitive input parameter to the model is the internal setpoint temperature. Reducing the setpoint causes a rapid reduction in heat load, but a rapid increase is not observed with increasing setpoint. A limitation of this model is with the method in which the model infers occupancy and the power capacity of the heating system which both limit the maximum heat demand of a simulated building. As heating systems are normally sized according to the heat load requirements of a building, a constantly occupied and unlimited power heat source should result in larger response in heat load, mirroring the observation with decreasing SHL.

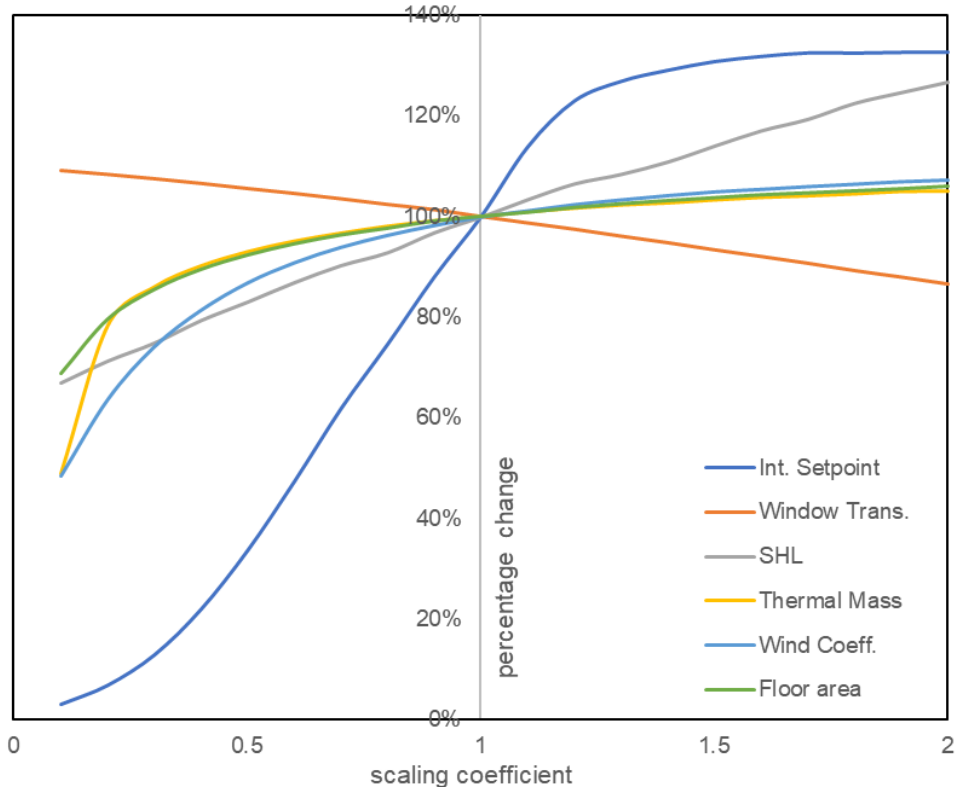

Figure 2.12 Sensitivity of thermal model parameters

2.5 Results

The total domestic and nondomestic modelled areas represent 22% and 42% of the total national (GB) value. These were extrapolated to represent 100% of national demand. These values can be adjusted and extrapolated to future demand estimates specified as a percentage change from current heat demand, for example if the domestic stock were to grow by 10% then the domestic demand figure is scaled accordingly. The 2010 heat load profile is shown in Figure 2.13. The results for 2010 weather data are presented as a comparison with previous estimates of 2010 GB heat demand in Table 2.8 and government estimates (DECC, 2015a) in Table 2.9. The modelled loads correspond well to the annual demand presented in other studies while the peak load has close agreement with Watson et al. (2019) estimate. Quiggin and Buswell (2016) used a restricted and unrestricted profile giving two peak values and the domestic annual figure was imputed from heating efficiency assumptions. Nondomestic annual consumption has been estimated at 124 TWh while the other studies estimated 144 and 105 respectively. The nondomestic peak (which does not coincide with the domestic) is substantially lower than Sansom's. However, Watson et al. (2019) suggests that Sansom overestimated their peaks and their estimate is more robust due to their use of multiple load profiles.

Table 2.8 Comparison of 2010 heat demand with previous estimates

Model	Domestic Annual TWh	Domestic Peak GW_{th}	ND Annual TWh	Total Peak GW_{th}
HeLoM	362	172	124	219
Watson et al. (2019)	391	170	-	-
Sansom (2014)	398	277	144	358
Quiggin and Buswell (2016)	358	262/117	105	-

Table 2.9 ECUK 2010 heating consumption estimates

2010	Domestic TWh	Industrial TWh	Service TWh	Total Nondom TWh	Total TWh
Space Heating	392	35	114	149	550
Hot Water	82	-	22	22	104
Total	483	35	136	171	654

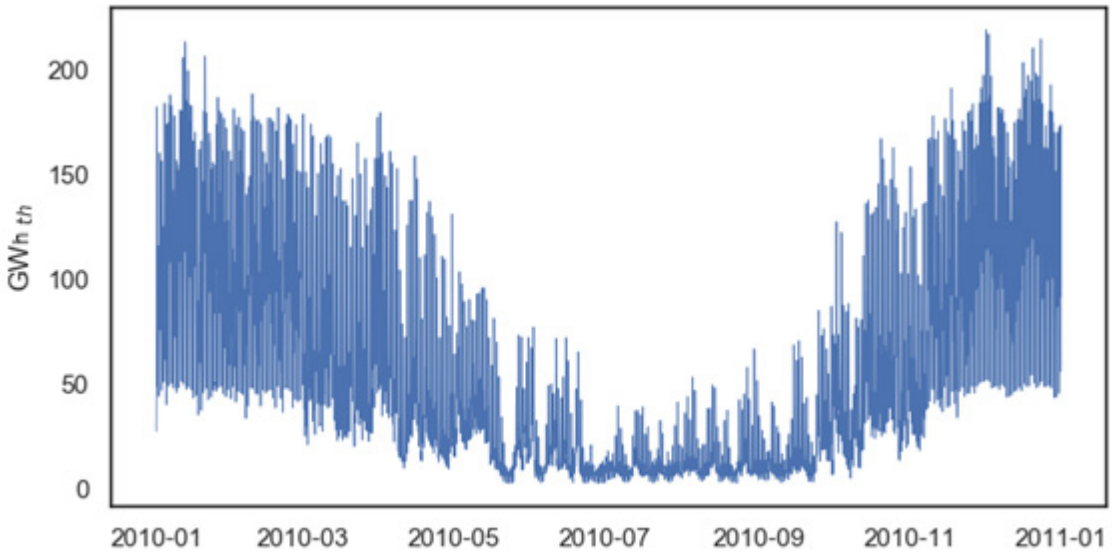

Figure 2.13 Modelled national hourly heat demand for 2010

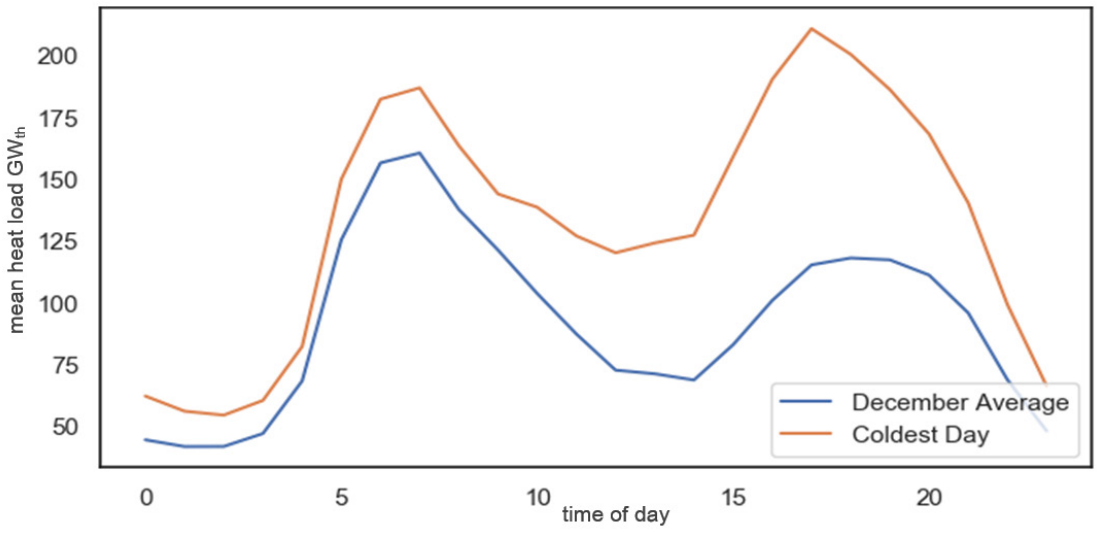

Figure 2.14 Comparison of national coldest day and mean December demand profile

A comparison of the GB load profile for the December average and the peak demand day as modelled in HeLoM are shown in Figure 2.14. The average shows that morning peak is typically larger than the evening peak. However, the peak day has a larger evening peak occurring between 1700 and 1800. The peak to trough ratio is larger than that found by Watson et al. who have a flatter demand curve on the peak day, but it is less than Sansom's. The load profile used in Watson et al. reflects the heating pattern of a heat pump while Sansom's load is based on the equivalent gas consumption. If this is the case, the implications of a high peak for the operation of domestic heat pumps may have profound consequences for the electricity network. To prevent surges in demand, the consumption pattern would need to be altered to flatten the demand profile or some form of demand side flexibility may be required such as TES.

The annual demand duration curve in Figure 2.15 shows that the nondomestic demand is generally consistent throughout the year. Both the domestic and nondomestic showing a steep increase of relatively few hours at peak load with those few hours combining to increase the peak load by around 35 GW_{th}. The hourly national heat load results for all modelled years is shown in Figure 2.16. The heating season can be clearly observed in the darker areas as are the milder periods which punctuate periods of high demand mid-winter.

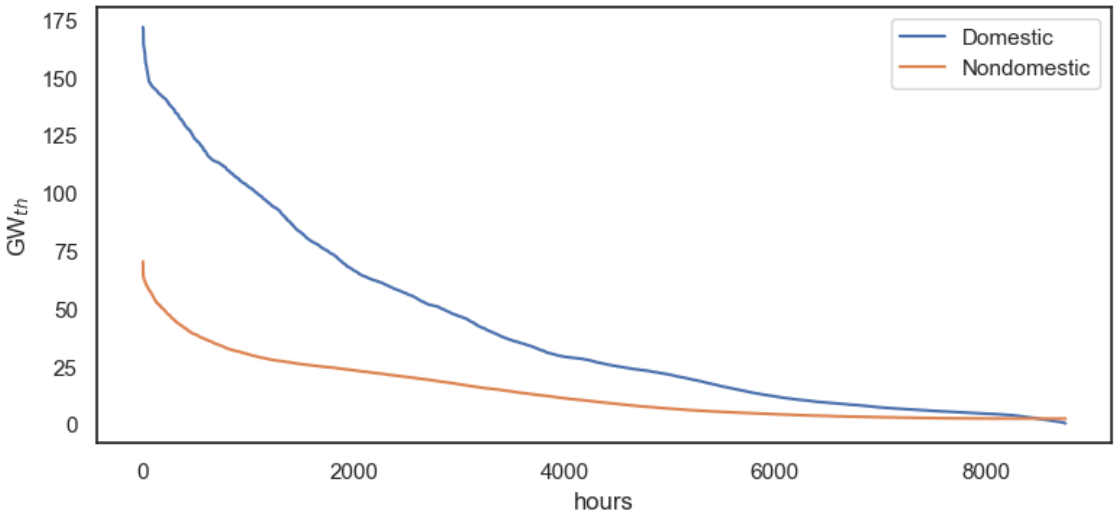

Figure 2.15 Domestic and nondomestic national heat demand duration curves for 2010

2.5.1 Urban heat load

The distinction between overall GB heat load and the urban heat load is made as DH would likely be constructed in urban areas owing to the favourable economics. The ratio of domestic to nondomestic heat loads will make a difference to the daily load profile as will the proportion of each archetype, with urban areas having a higher share of flats for example.

The heat demand from the top 5% of HDD MSOAs has been used as a proxy for urban heat load. Figure 2.17 shows the heat demand duration as a proportion of peak for the GB demand compared to the urban demand. The demands were first normalised such that the annual demands were equivalent and the area below each curve is the same.

The figure shows that the urban base load as a percentage of peak is higher than the overall GB load and remains higher for half the time. The GB load curve then begins to rise sharply, overtaking the urban demand with both curves exhibiting a sharp peak as in Figure 2.15. Figure 2.18 shows that the average urban winter load profile has lower peaks and lower peak to trough ratio compared to the average GB load profile. It also has a much more pronounced morning peak and a quicker drop-off while the daytime loads from nondomestic building prolong the drop-off to the mid-day trough.

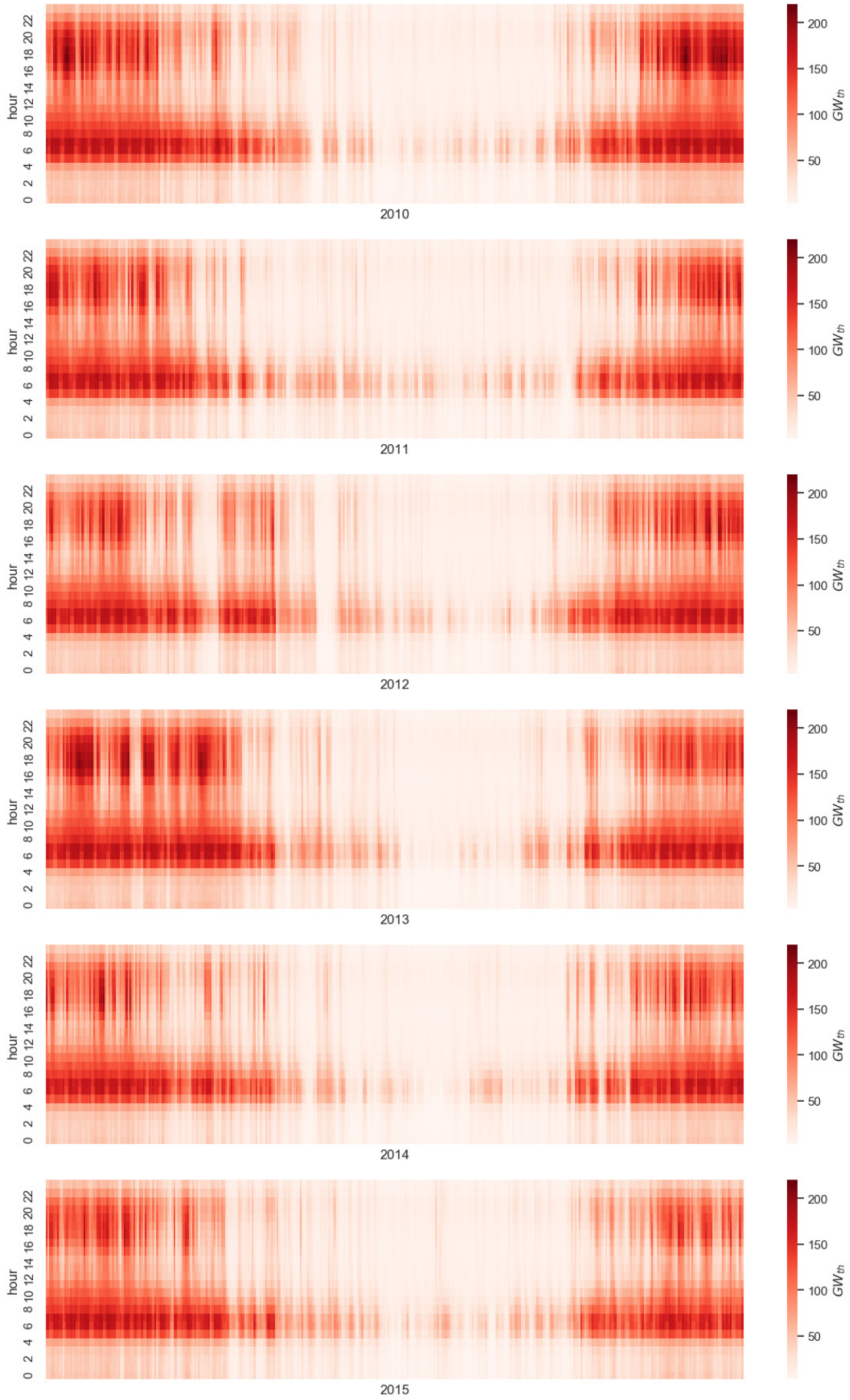

Figure 2.16 Modelled national hourly heat load 2010-2015 from HeLoM

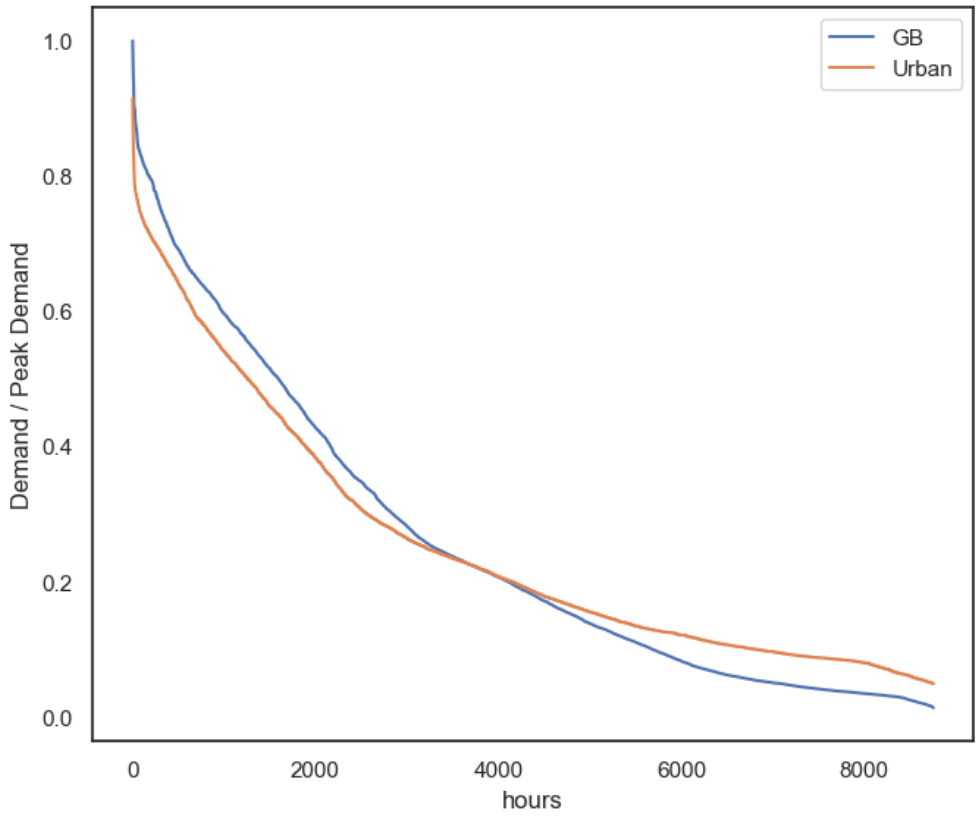

Figure 2.17 Comparison of the national and urban heat demand duration curve for 2010

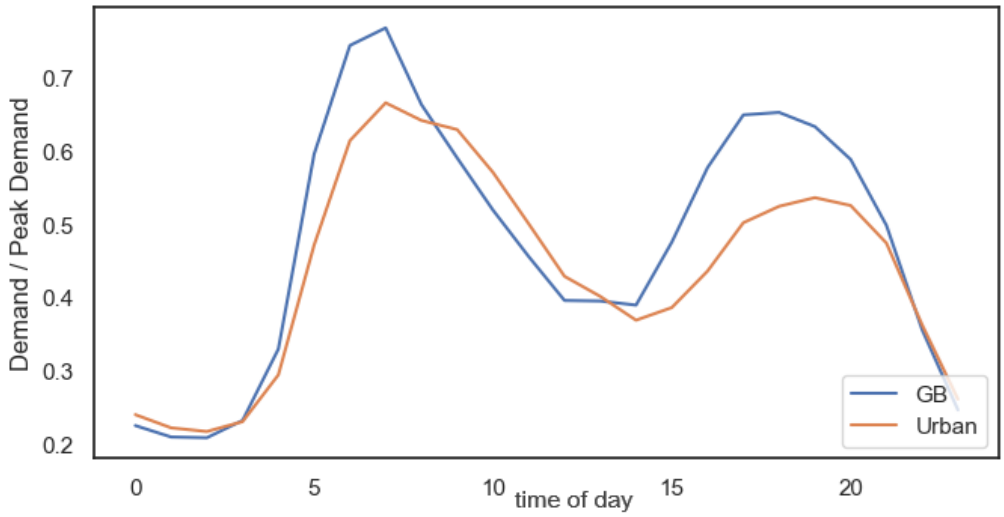

Figure 2.18 Average winter load profile comparison

The spatiotemporal load at the LSOA level is shown in Figure 2.19 (with MSOA boundaries marked in black) at four times (9 am to 6 pm). The annual values of domestic LSOA load have been calibrated to consumption data, but the intraday profile and nondomestic load at this level are estimated model outputs. Such a tool has potential for use by urban planners who may want to identify areas of synergy such as whether a residential area with morning and evening peaks is beside a commercial area with day-time load.

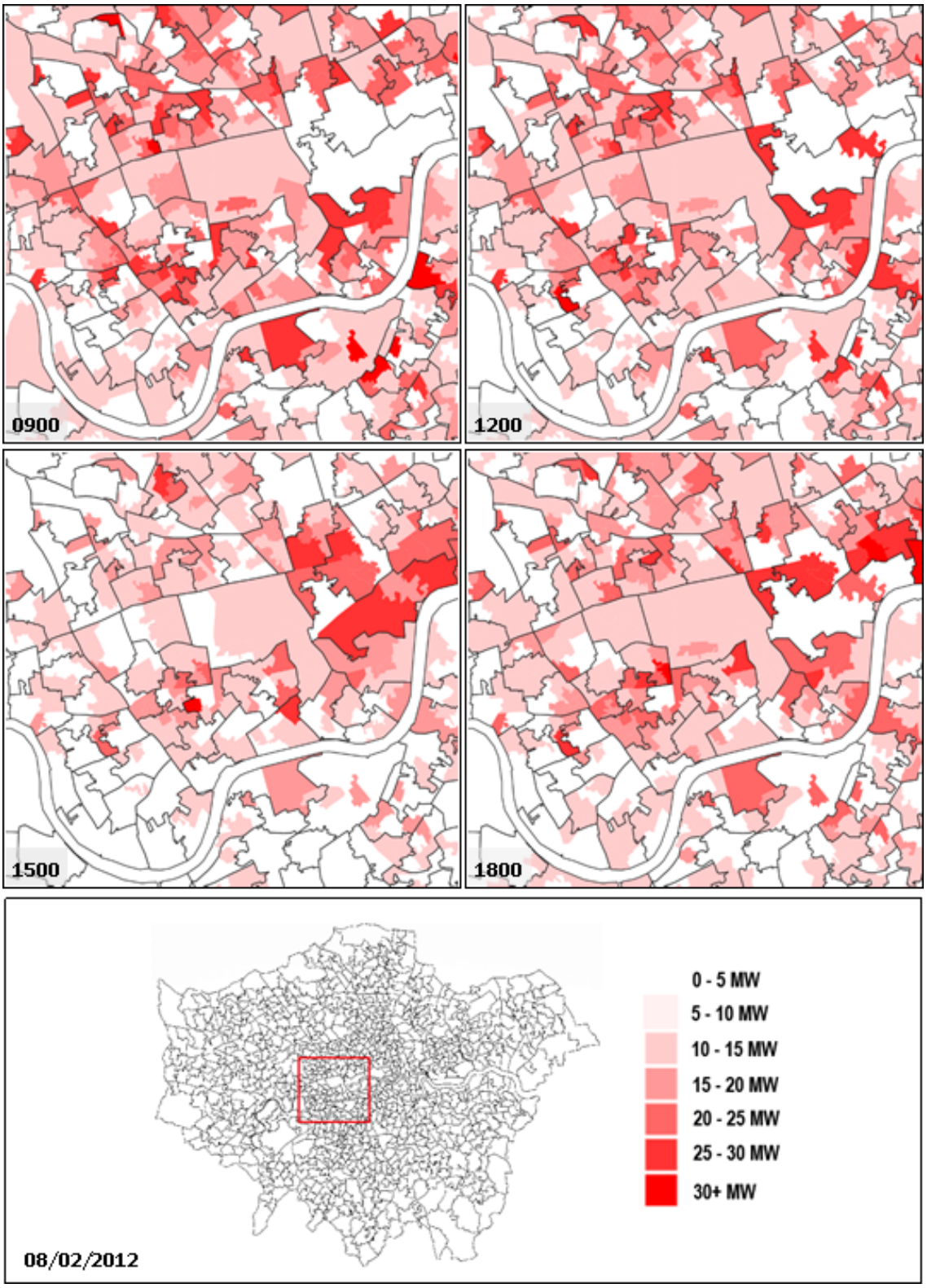

Figure 2.19 Spatiotemporal variation of modelled heat load for an area of London at various times of day

2.6 Discussion

HeLoM has been developed to generate estimates of heat load for both urban sub-city areas and the national level. Previous studies using similar methods have provided an exploration of domestic loads. However, any future large-scale DH development is likely to include nondomestic buildings as well. This model builds on previous work in the segmentation and characterisation of archetypes. A thermal model using regional weather data has been developed to provide hourly heat loads. It too builds on previous work and can be used to test the efficacy of efficiency interventions in future work.

Knowledge of localised peak loads is necessary when planning electricity infrastructure such as in the event of large-scale consumer HP uptake. It also has an impact on the design of DH such as pipe sizing and for energy centres which need to be adequately sized to meet peak loads. The results of the highest HDD areas have been aggregated here as a substitute for total DH load. The results show that there is a discernible difference in the average heat load profile between the national load profile and the urban subset which demonstrates the need to disaggregate the urban load. On the national scale, the impact of peak winter heating loads on the electrical system has been the subject of several other studies. This model suggests that the peak may be more likely to occur around the evening peak with the cumulative contribution of domestic and nondomestic loads.

2.6.1 Development challenges

This work draws on established building stock modelling methods and building thermal modelling such as BREDEM. The thermal model contains many simplifications. It is not suitable for a more detailed single building analysis where more information on the construction, orientation and occupancy would be available. The nondomestic archetypes used here were limited to 12 activity classes but could have benefited from data on activity types as well accurate floor area estimates and more monitored occupancy data. The novelty of the study in this chapter emerges from the synthesis of the methods and data sources used. It has produced high spatiotemporal resolution output using historic meteorological data as the main driver of demand.

Modelling demand at high resolution necessitates high computing and data storage requirements. This is especially the case as the spatiotemporal resolution increases as more detail needs to be captured. The study has relied on historical consumptions data. A central challenge remains in the validation or calibration of results in the absence of reliable benchmarking data on building energy performance (Oreszczyn and Lowe, 2010). Calibration of the output has been done at an aggregated level against total and peak heat load. Using this method, the accuracy of calibration decreases with increasing spatial resolution. At higher resolutions, the impact of any outlier or anomalous building has a larger impact on the total heat load. This may become less of a challenge in future with smart meter monitoring.

The translation of the modelled heat loads to HP electricity load profiles (see section 3.7.3) may also be dubious. HPs are unlikely to be operated as gas boilers are. Adapting these heat loads to HP electrical load profile may be inaccurate. A similar argument could be applied to the use of low temperature DH demand which is likely to have a flatter load profile.

Such a tool however, has potential for use by urban planners. It can be used to identify areas of temporal synergy such as whether a residential area with morning and evening peaks is beside a commercial area with daytime load. The results cannot be used for local DH design. DH design typically requires a more localised analysis of heat loads, identifying large heat loads, heat sinks and the loads that differ from the standard occupancies modelled here.

2.6.2 Uncertainties in demand

A central assumption underlying the modelling here is that any future DH expansion will occur in areas of high HDD. The spatial distribution of heat loads is unlikely to differ much. However, there are large uncertainties in future demands from factors such as population growth, efficiency improvements and climate change effects. While population growth and efficiency improvements can be accounted for in the presented modelling, climate change may have the biggest impact. The Met Office UK climate projections envisage a range of 0.7 - 4.2˚C warmer winters by 2070 (Lowe et al., 2018). Additionally, there may be more erratic weather patterns whose impacts cannot be easily measured or recreated using past weather data. Building efficiency improvements may counteract increases in population growth but more recently we have experienced an upheaval in working patterns and building occupancy. How this might affect absolute demand, day to day temporal variations from weather patterns and seasonal variation from climate change is still unclear. These uncertainties do not invalidate any such analysis. Combined with the many other uncertainties, the modelling will provide an understanding of the causalities in the system and enable better system design.

3 ELECTRICITY COST MODEL

Chapter Summary

This chapter details the development of the Electricity Cost Model (ElCoM). To accommodate the variability of renewable generation, flexibility in the network is vital. A primary flexibility option is grid scale electricity storage. The goal of ElCoM is to model the effect of storage on electricity costs for highly renewable scenarios. A simulation is made of the electricity system using capacity factors based on measured meteorology to drive renewable output and the consequent operation of grid storage to balance differences between demand and generation. A marginal costing method is devised to calculate the operational costs incurred in each hour. These cost structures can form a transparent economic base for informing market design and setting prices for use in energy system models. After validating the output against historic data, ElCoM is then applied to a modified net-zero scenario. The scenario is high-renewable and highly electrified, utilising the heat demand modelled in chapter 2. Results show that while costs for renewable generation are relatively low, reliance on battery storage for backup particularly during peak periods can result in high electricity supply costs. The variability and long runs of low-cost electricity favours the use of storage. Thermal energy storage in district heating is a low-cost option that can take advantage of this variation. The output from ElCoM provides the basis to compare storage options, analyse the impact of electrified heating and to develop the operational control strategy for district heating.

3.1 Renewable Energy and Grid Balancing

The UK already has a large amount of variable renewable energy (VRE) on the electricity grid. With the predicted mass electrification of other sectors such as heating and transport, the demand on the grid is also projected to grow. Managing this demand with VRE will require a change in the way in which the grid is operated, possibly requiring significant amounts of electricity and other storage operated in a smart energy system.

The increase in VRE on the grid is creating challenges with grid balancing and meeting peak electricity demand. This issue is currently solved largely through the use of dispatchable, fossil fuel operated plants such as gas turbines. Grid electricity storage such as batteries is an option to provide flexibility and reduce curtailment of renewable resources. A secondary objective of this work is to provide an analysis of their economic viability and impact on electricity prices.

Historically, electricity prices have followed a predictable pattern of daily cycles of peak and off-peak prices with seasonal variability and a strong link with fluctuations in fuel prices (Grubb and

Drummond, 2018). This predictability enables planning of smart grid infrastructure requirements as well as the electrification of other sectors by making informed investment decisions. However, with VRE composing a larger share of the electricity system's generating capacity, electricity prices are becoming less predictable as exemplified by a recent record run of negative prices following by a sharp spike in balancing costs on the grid (Elexon, 2019; Ofgem, 2018).

As VRE increases, imbalances between supply and demand at daily, seasonal and annual timescales are expected to increase (Joos and Staffell, 2018). To avoid curtailment of VRE and to ensure that low carbon electricity is supplied during periods of low VRE, some forms of electricity storage will be required on the grid. With capital costs declining, lithium-ion batteries are experiencing a rapid uptake at the utility scale. As recently as 2016 a deployment of 15 GWh of battery storage by 2030 was considered ambitious (Strbac et al., 2016). More recent studies have revised this figure to over 100 GWh by 2035 to achieve a high renewable deployment (Aunedi et al., 2021).

The present system has a low but growing VRE penetration with thermal fossil fuel plants composing the largest share of generation. Flexibility is largely achieved by dispatchable plant using stored fuels such as fossil and biomass. These fuels provide a large provision of the balancing requirements in the current system and complemented by storage such as pumped hydro. VRE generators have been rapidly reducing in capital costs and have very low operational costs (BEIS, 2016e). But they are inflexible, and the subsequent costs of integrating VRE must then be considered. As the penetration of VRE on the system increases, the flexibility costs associated with them are projected to rise (Strbac et al., 2015). The impact a larger storage capacity will have on electricity cost patterns is uncertain. This is compounded by the uncertainty surrounding future demand and supply profiles. While studies show that VRE could reduce costs, there has been less analysis on the impact of the cost of energy storage on electricity supply costs.

This chapter develops a methodology used to derive a time-series of electricity generation costs for scenarios with high renewable deployment and with large capacities of grid storage. This is followed by the development of a net-zero scenario, with the translation of generation costs to electricity prices for the scenario.

Box 3.1 Definitions of Cost and Price in context

The definitions of cost and price were discussed in Box 1.1. A cost refers to the value of inputs to an enterprise and marginal costs represents the value of adding a unit of production to a system while price is the value paid for an output of an enterprise and is in theory, equal to the marginal cost for an efficient market.

ElCoM calculates the hourly marginal cost of generating electricity for the grid. It then adds on to this, transmission and distribution costs which equals the total cost of producing and supplying electricity to end users. Assuming an efficient market, this is then the hourly electricity price to consumers of grid supplied electricity.

The electricity price then forms part of the cost of supplying heat for a DH network in the subsequent chapter. The other costs incurred by DH network operators include the capital, operating and maintenance costs. This will be explored further in Chapter 4. Extending this, (although not discussed in this thesis), the cost of heat supply (and the DH operator's profit margin) then forms (among other factors) the price of heat to consumers.

3.2 Review of Renewable Electricity Price Variance

Forecasting of electricity prices has been well explored. Various approaches such as econometric, statistical, or multi-agent models are used to assist in estimating spot prices over various time horizons. Weron has provided a detailed review on the state of the art in electricity price forecasting techniques (Weron, 2014).

There have been numerous studies analysing the effect of VRE on spot prices. Many of these show a rise in volatility of prices. Much of this analysis has been performed on historical data of northern European electricity markets.

Dong et al. (2019) showed using historic data on the Nordpool market that price volatility increases with a higher penetration of renewables. This increase in volatility is more pronounced in regions where wind generation was dominant. Wozabal et al. (2016) performed a statistical analysis of spot price variance in Germany, challenging the assumption that higher VRE increases price variance. They found that small fractions of VRE actually decreased price volatility, but higher fractions resulted in larger increases in price variance. They highlight the importance of price variance as a revenue stream for smart grid infrastructure such as storage. Dillig et al. (2016) use historic spot prices in Germany to create counterfactual prices in the absence of VRE. They found increased hourly volatility in prices and show that prices in a higher VRE system are lower on average than a system without VRE. They also find that increasing VRE in the system results in a higher cost of dispatchable generation, potentially due to lower capacity factors. Comparing the German system with high solar capacity and the Danish system with high wind over various timescales, Rintamaki et al. (2017) studied volatility of prices during high VRE periods. They observed that daily volatility of prices in the wind dominated system is reduced in high wind areas. This is attributed to stable wind speeds over daily timescales. They also found that volatility increased in a high solar system due to the daily fluctuation in solar power. Price volatility on a weekly scale was shown to increases in both cases. This is supported by Wozabal et al. who found that small fractions of wind power leads to a reduction in price volatility.

There have recently been some attempts to quantify the effects of largescale VRE in future scenarios in various markets. Pikk and Viiding (2013) analyse the Nordpool market spot price and predict a higher volatility in a high VRE scenarios. Similarly in Germany, Ketterer found that an increase in wind generation capacity will lead to a more volatile spot price but with reduced average prices (Ketterer, 2014). Sorknæs et al. (2019) Investigated the effect of VRE on wholesale prices using a market economic simulation in EnergyPLAN. They calibrated their economic model with 2015 Nordpool spot prices then simulated future VRE capacity effects on prices. The authors determined that any increase in VRE generation reduces wholesale prices.

Badyda and Dylik (2017) studied historical market and renewable generation data for several European countries. Extrapolating their observations, they predict a pronounced seasonality in the price variance with up to three times higher average prices in high demand periods. Maxwell et al. (2015) used a similar method to investigate the role of renewable subsidies in Denmark. They state that future work would benefit from a better understanding of how VRE effects electricity prices.

3.2.1 Marginal cost methods

The previous authors have studied price variance using statistical or econometric analysis to model and describe prices in high VRE scenarios. Another class of models described by Weron (2014) falls into the “fundamental model” category, so called as it attempts to describe the important physical and economic factors that give rise to generation costs. The use of marginal generating costs falls into this latter class. These models typically use defined marginal cost curves for generators and determine cost by the point at which it intersects with demand curves.

The use of marginal costs in predicting electricity prices is a standard method to predict system prices and is a useful price estimator (Müsgens, 2006). Electricity markets consist of many

generators bidding to supply electricity, each with differing costs. Economic theory predicts that in a market with perfect competition and sufficient capacity, the market auction price should clear at the cost of supplying a marginal increase of demand in the system. Further, the price of electricity should be equal to the marginal cost of the most expensive generator active on the system. Even though cheaper generators may be active on the system, market price is set at the highest auction clearing price and all electricity generators obtain the same remuneration.

However, the actual wholesale price of electricity is rarely at the marginal cost due to market imperfections and secondary costs. Marginal costs can provide a reference point about which wholesale prices deviate. Marginal costs have been shown to be the largest component of day-ahead wholesale electricity prices in the UK. This includes the added costs of transmission, distribution and mark-ups from utility companies, composing about 40% of end electricity prices (Gissey et al., 2018).

Haas et al. (2013) study the impact of solar power in European electricity markets using a marginal cost method. Like other studies, they predict higher volatility at both hourly and daily timescales which will in turn result in higher operating costs for dispatchable generators in the long term. They highlight the growing importance of balancing markets going forward in Europe. Morales et al. (2011) used locational marginal costs to study the impact of regional wind power generation on a simulated electricity market to obtain statistical characterisation of wind prices with wind power and Müsgens (2006) has used marginal costs with a dispatch model to study market power in Germany and the effect of integration with other markets. A study of the merit order effect due to the cost of wind generation found depressed electricity prices and lower returns to other generators in the Spanish market (Figueiredo and da Silva Pereira, 2017). The authors used this to highlight the inadequacy of the Iberian power market to incentivise further investment.

Marginal costs have been used by Lamont to assess the system value of VRE and to optimise generator capacity on the GB system (Lamont, 2008). They use a simplified dispatch model of ‘always-on’ baseload, then a selection of VRE or dispatchable plant based on marginal costs. They assumed that the cost of constraining wind power is at the price set by the renewable obligation certificate rather than marginal run costs. Green and Vasilakos (2011, 2010) used a market equilibrium model with marginal generator costs to study market behaviour and the impact of wind power on long-term prices. They find that yearly variations of wind output can affect intra-year revenue for wind generators by up to 20%, but this is lower than the present impact of fluctuating fuel costs. In addition, they find that that the revenue wind generators receive for constraining output has significant consequences on the resulting capacity mix. Seel et al. (2018) have used marginal costs to analyse wholesale price patterns in the four grid regions of the USA. Using a capacity expansion model to derive high VRE scenarios, they found a reduction in average annual prices throughout but differing average price patterns based on VRE mix and region.

Notably, in the literature presented, there has been a lack of analysis on the effect of large-scale grid storage on electricity supply costs. The method presented in the following sections presents a contribution to this literature.

3.3 Modelling Methodology

This section first develops a simplified representation of the electricity system with large fractions of VRE and grid storage. It is a simplified representation where each generator type is treated as an aggregate, while spatial and transmission constraints are not explicitly modelled. Generation capacity is split into flexible and inflexible generation. Flexible generators are assumed to be Combined Cycle Gas Turbines (CCGT) that are able to adjust output to follow demand. VRE output varies uncontrollably with the wind resource but can be spilled or constrained. Baseload is assumed to be nuclear generation with constant output but could equally be a thermal generator with carbon capture and storage (CCS). The approach assumes

flexibility is first achieved with grid storage, then via dispatchable CCGT. The supply of electricity from storage is essentially treated as another generator

Note that the costs initially calculated are at the point where generator and storage supply electricity to the high voltage grid, and do not include transmission and distribution losses. These costs might be simple constant additional costs per kWh, or more complex reflecting hourly demand variations which determine network capacity and losses. These additional costs will be smaller for high voltage supply, such as to industrial or DH HPs for example, compared to the majority of consumers on the distribution grid.

3.4 Dispatch Model

Renewable generation is defined via hourly capacity factors (the percentage of installed capacity generating power), from historical meteorological data and projected installed capacity. Dispatchable generation capacity is assumed to be sufficient to meet any residual deficit in demand. The maximum required dispatchable generation occurring in a year is then one input to the capital cost of the system used in the calculation of marginal costs.

Demand data is an exogenous input to the model and assumed inelastic i.e., demand is always met regardless of the cost of electricity. Hourly demand is scaled for each scenario from a historical demand timeseries such that it corresponds to the same time period to maintain the weather linkage. This initial scaling assumes that historic demand profiles are preserved in future scenarios and will be revisited later.

The capacity factor or Availability, A, for each renewable generator (onshore wind - ONS, offshore wind - OFS, solar – SOL) is multiplied by the installed capacity, C, to obtain hourly renewable generation. This is added onto a baseload generation capacity, C_{BSL}, defined in the scenario. Baseload generation is assumed constant throughout the simulated period and is always less than or equal to the minimum demand. Consequently, the baseload never sets the marginal price in this model.

Total low carbon electricity generation, G_{LCB}, for each hour, i, is then the sum of baseload and all VRE generators:

$$G_{LCB,i} = C_{BSL} + C_{ONS}A_{ONS,i} + C_{OFS}A_{OFS,i} + C_{SOL}A_{SOL,i} \quad (3.1)$$

If there is a surplus of electricity generation over demand D_i, $G_{LCB,i} - D_i > 0$, then $G_{LCB,i} - D_i$ is allocated to the available storage if charge capacity is available otherwise the renewable power is constrained. If the demand exceeds the available generation $G_{LCB,i} - D_i < 0$, then the electricity storage is discharged by the amount $D_i - G_{LCB,i}$. If the discharge is insufficient, the dispatchable power generators, CCGT is then activated and the dispatchable generation is $G_{DSP} = D_i - G_{LCB,i} - G_{DCH,i}$.

Here it is assumed that storage operates in coordination with VRE to meet residual demand deficit or absorb the residual surplus. An implicit assumption in the modelling is that all stores charge and discharge simultaneously by the same fraction of their capacity. High carbon dispatchable generation is treated as a last resort in order to minimise the associated emissions. The choice is made to contrast with a conventional market in which generators bid to supply electricity. The aim of the smart grid infrastructure is to prioritise emissions reductions. This may well arise in a conventional market structure with the inclusion of carbon costs. Initially, no constraints are placed on the charging and discharging power of storage. This assumption becomes reasonable as the number of individual stores increases but will be verified in the results.

3.5 Marginal Cost Method Development

Upon completing a simulation of the electricity system, each hour is classified as one of four basic hour types, some of which have further subdivisions. For each hour type there is a different algebraic expression used to calculate the marginal electricity generation cost, MC.

- Type 1 SRP: Hours with surplus renewable generation, "Surplus Generation hours". These are hours where supply exceeds demand and remaining storage capacity.
- Type 2 CHR: Hours in which electricity storage is charged "Charge hours"
- Type 3 DCH: Hours in which electricity storage is discharged "Discharge hours" subdivided into:
  - Full cycle discharge (DCHf) hours where storage capacity is full prior to discharging
  - Part cycle discharge (DCHp) hours in which storage is partly charged prior to discharging
- Type 4 DSP: Hours in which backup dispatchable generation is required "Dispatch hours" subdivided into:
  - Peak dispatchable hours DSPp where the difference between electricity demand and low carbon generation is at its highest which determines its capacity (GW)
  - Off-peak dispatchable hour DSPo which are all other dispatchable hours

The procedure must be carried out in a particular order. After simulating the electricity system for a period of a year (or number of years), the marginal costs for Surplus hours, C_{SRP}, are calculated followed by the cost for Dispatch hours, C_{DSP}, both peak and off-peak. Charge hours costs, C_{CHR}, are then calculated which finally enable the Discharge hour costs C_{DCH}, to be calculated.

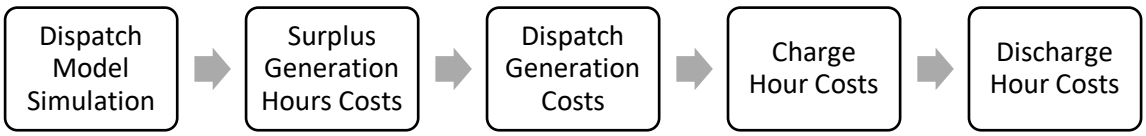

Figure 3.1: Order of operation to calculate marginal costs for each hour type

3.5.1 Surplus generation hours

When baseload and renewable generation exceeds demand and electricity storage charging capacity, curtailment of renewable generation will be required. It would be economic to curtail the renewable technology with the highest variable cost (however these are small for renewable generators). This is analogous to creating a merit order of net variable cost and identifying where Demand intersects the resulting merit-order stack. This indicates the particular renewable technology that sets the market price during that hour and may vary hour by hour. This technology is the "marginal technology," denoted by the subscript m.

The marginal costs for Surplus Generation hours, MC_{SRP}, is then given by the variable costs of the marginal generator, V_m, minus the cost of constraining output from the marginal generator, M_m:

$$MC_{SRP,i} = V_{m,i} - M_{m,i} \tag{3.2}$$

3.5.2 Off-peak dispatch hours

When electricity demand exceeds the available low-carbon power including stored electricity, demand must be met by dispatchable plant, this is assumed to be CCGT but could be one of several plant types. To minimise carbon emissions, it is assumed that this plant only operates

during the hours required to make up the generation shortfall. Therefore, all the year-on-year costs of the dispatchable plant must be met by this operation; but it is assumed these are legacy plant with sunk costs, so they do not incur capital costs. Hence, for off-peak dispatchable hours, the marginal generation costs, MC_{DSPo}, in £/MWh is given by the variable operating costs of the dispatchable plant:

$$MC_{DSPo,i} = V_c \tag{3.3}$$

The variable operating costs include fuel and carbon costs, and variable O&M costs. The O&M costs in this case will need to be a conservative estimate due to the impact on efficiency and O&M of frequent ramping, part load and cold start.

3.5.3 Peak dispatch hours

The annual fixed operating costs of the dispatchable plant are recovered during the peak dispatch hours. These costs are often called Fixed Other-Works Costs (FOWC) which are a close approximation of the Net Avoidable Cost (NAC), the net cost of keeping the plant open for another year.

In a system with VRE, there is uncertainty over the operation of dispatchable capacity and therefore of the revenue it will obtain from the hourly market. Therefore, the UK has had a Capacity Market auction whereby the generator or store receives a guaranteed annual payment regardless of the amount generated. This market is currently under investigation but is assumed to apply in the costing methodology (Carbon Brief, 2018). Battery storage was permitted to participate in the capacity market; however, the costs of providing peak demand from storage remains high. The National Grid recovers the cost of the capacity market auctions during peak weekday demand periods, November-February 4-7pm or around 240 hours or 2.7% of hours in the year (though this means of allocation is somewhat arbitrary) (Inenco Energy, 2016).

Following this means of recouping marginal capacity costs, 2.7% of the Dispatch hours with the highest difference between Demand and Low Carbon Generation, $D_i - G_{LCB,i}$, are allocated as Peak Dispatch hours. The marginal cost for peak dispatch hours, $MC_{DSPp,i}$, is then calculated by the product of annual fixed costs of the dispatchable generator F_D, and the peak dispatchable generation, $G_{D,i}$, divided by the the forced outage rate of dispatchable plant, R_{CD}, and total dispatchable generation in all peak dispatch hours, plus the variable costs:

$$MC_{DSPp,i} = \frac{F_D \underset{DSH}{max}(G_{D,i})}{\left(1 - \frac{R_D}{100}\right)\sum_{DSHp}(G_{D,i})} + V_D \tag{3.4}$$

3.5.4 Charge hours

A projection of the incremental renewable generator is made which is the renewable generator that sets the cost of charging storage. The incremental technology in the UK would likely be offshore wind. This is based on the constraints on the building of further onshore wind, its higher output in winter when demand is high and the higher cost of solar generators. The incremental technology is distinct from the marginal generator which can be any VRE (including incremental), storage or dispatchable, during an hour.

The marginal generation cost during charge hours is set by the incremental technology, denoted by subscript n, for a given scenario. The variable cost of the incremental technology, V_n, during surplus hours in which it is less than that of the marginal technology must also be recovered. These 'energy credits' can be calculated by the difference in variable costs minus the cost of constraining output between the marginal and incremental generator:

$$\sum_{SRP} G_{n,i}\left[\left(V_{m,i} - M_{m,i}\right) - \left(V_n - M_n\right)\right] \tag{3.5}$$

The fixed costs of the incremental renewable generator, F_n, across the year (or the chosen time period for calculation) must be recovered. This fixed cost is given by the expression:

$$\begin{aligned} F_n = &\sum_{CHR}\left(A_{n,i}MC_{CHR,i}\right) + \sum_{DCH}\left(A_{n,i}MC_{DCH,i}\right) + \sum_{DSP}\left(A_{n,i}MC_{DSP,i}\right) \\ &- \sum_{CDD} A_{n,i}\left(V_n - M_n\right) \\ &+ \frac{1}{C_{n,i}}\sum_{SRP} G_{n,i}\left[\left(V_{m,i} - M_{m,i}\right) - \left(V_n - M_n\right)\right] \end{aligned} \tag{3.6}$$

Substituting for MC_{DCH} (3.12) and using the following approximation:

$$\begin{aligned} &\sum_{DCH}\left(A_{n,i}\left[\sum_{CHRc}\left(A_{n,i}MC_i\right) \Big/ \sum_{CHRc}\left(A_{n,i}\right)\right]\right) \\ &\qquad \approx \left(\sum_{DCH} A_{n,i}\right)\left(\sum_{CHR}\left(A_{n,i}MC_i\right) \Big/ \sum_{CHR}\left(A_{n,i}\right)\right) \end{aligned} \tag{3.7}$$

The marginal cost during charge hours is given, from (3.6), (3.7) and from (3.12) below, by:

$$\begin{aligned} &MC_{CHR,i} \\ &= \frac{F_n - \frac{1}{E_s}\sum_{DCH} K_{DCH,i}A_{n,i} - \sum_{DSP}\left(A_{n,i}MC_{DSP,i}\right) - \frac{1}{C_n}\sum_{SRP} G_{n,i}\left(V_m - M_m\right)}{N_{CHR}A_{n,i}\left(1 + \frac{1}{E_s}\frac{\sum_{DCH} A_{n,i}}{\sum_{CHR} A_{n,i}}\right)} \\ &+ \frac{\left(\frac{1}{C_n}\sum_{SRP} G_{n,i} + \sum_{CDD} A_{n,i}\right)\left(V_n - M_n\right)}{\frac{1}{E_s}\sum_{DCH} A_{n,i} + \sum_{CHR} A_{n,i}} \end{aligned} \tag{3.8}$$

3.5.5 Discharge hours

Assuming the storage has a constant efficiency E_s with no standing loss assumed then for every unit of power discharged, $1/E_s$ units of power must be charged. The cost of charging the storage must be recouped from discharging. The assumption is made that all the individual batteries are charged and discharged evenly across each individual unit in the capacity as if one single aggregate battery. The cost incurred from this charging is dependent on the cumulative charge hour costs preceding the discharge, back to when the store was last empty, denoted with CHRc. The average cost of charging during charge hours in the period preceding the discharge, weighted by the availability of the incremental renewable generator is given by:

$$\sum_{CHRc}\left(A_{n,i}MC_i\right) \Big/ \sum_{CHRc}\left(A_{n,i}\right) \tag{3.9}$$

The fixed cost of storage capacity must also be recovered during discharging. Here it is assumed that the marginal cost of supplying power from discharging storage is driven by the incremental storage cost to meet incremental demand and the cost of charging the storage from renewable generators.

The recovery of the fixed cost of storage during discharge hours in this method is recovered through full charge-discharge cycles. A full discharge cycle is defined as each time the storage

capacity is full preceding the discharging cycle which can run for multiple hours. Part discharging cycle are other hours when storage is not full prior to the discharge cycle. The cost of grid storage during part and full discharge hours K_{DCH}, is defined by the storage capacity, C_s, the fixed and variable running costs of storage, F_s and V_s, the storage efficiency (defined as effective energy output per input), E_s, and the discharged amount Q_{DCH}:

$$K_{DCHp,i} = V_s \tag{3.10}$$

$$K_{DCHf,i} = \frac{F_s C_s}{\sum_{DCHf} Q_{DCH,i}} + V_s \tag{3.11}$$

The marginal cost during a discharge hour is then given by:

$$MC_{DCH,i} = K_{DCH,i} + \frac{\sum_{CHRc}(A_{n,i} MC_i)}{E_s \sum_{CHRc}(A_{n,i})} \tag{3.12}$$

3.5.6 Data sources

The capacity factor data to construct hourly renewable generation profiles have been obtained from the work of Pfenninger and Staffell (2016) published on the 'Renewables Ninja' website. The capacity factors are derived from a combination of historical meteorological data and known or planned renewable generator locations.

Electricity demand data is obtained from the National Grid's historic demand data archive which contains the demand on the transmission network and a breakdown of each power source meeting the demand per half hour (National Grid ESO, 2019). Hourly demand is calculated from the sum of two half hourly periods. This data however is not fully representative of the true GB electricity demand as it does not include any power generation embedded in the distribution network.

Cost assumptions where possible were obtained from government projections. The cost of dispatchable generation (CCGT) was obtained from Leigh Fisher and Jacobs (2016) report commissioned for DECC. Similarly, the cost of renewable generation was taken from a review undertaken by ARUP (2016) for DECC. Other assumptions were sourced from the Department for Business, Energy and Industrial Strategy Electricity Generation Costs report (BEIS, 2016e). An electricity storage cost review by IRENA (2017) was used for battery storage (Li-ion) assumptions supplemented by Lazard's (2019) levelised cost of storage analysis. Where applicable, all costs in this thesis have been adjusted for inflation to 2020 figures. An overview of these can be found in Table C-1 of Appendix C.

3.6 Model Validation

The model output is first compared to historic generation data for the year 2016 before the results from two high VRE scenarios are presented. These scenarios are adapted from the National Grid's Future Energy Scenarios (2017a), using the projected generation capacity mix from the two scenarios that conform to the 2050 decarbonisation targets.

3.6.1 Dispatch model

The model output using 2016 renewable capacities is compared to historic generation data for the year in Table 3.1 (BEIS, 2017b). This method is designed for a renewable and storage dominated system thus an exact match for electricity generation and prices with a present-day system should not be expected. However, it is useful to compare the low carbon generation output from the model with the data. In the model, all other generation is assumed to be dispatchable whereas this is not the case in the present-day system.

Baseload nuclear generation is overestimated as the model assumes a 100% availability. The data shows an 83% annual capacity factor for nuclear generators which would be due to maintenance or faults affecting availability. Comparison for the output of the renewable generation data from Stafell and Pfenninger (2016) shows that it has been calibrated accurately. Solar PV and offshore wind outputs are very close to historic output data while onshore wind has been slightly overestimated.

Table 3.1 Comparison of 2016 low carbon generation with modelled generation

	Onshore Wind TWh	Offshore Wind TWh	Solar PV TWh	Nuclear TWh
2016 Data	21.1	16.4	10.3	65
Modelled	24.3	16.0	10.7	78

3.6.2 Scenario Analysis

The scenarios "Two degrees" and "Community Renewables" from the National Grid's Future Energy Scenarios 2017 are designated here as 'Scenario A' and 'Scenario B.' The details of these scenarios are presented in Table 3.2. The renewable generation and grid storage capacity from the two scenarios was used as input for the scenario analysis and 5% interest on all capital costs has been applied for initial analysis.

Table 3.2 National Grid FES Scenarios comparison

Scenario Name	Demand (relative to 2017)	Offshore Wind GW	Onshore Wind GW	Solar PV GW	Nuclear GW	Total Capacity GW	Grid Storage GWh
A (Two Degrees)	+25%	43.4	22.3	43.7	20.0	224.3	17.3
B (Community Renewables)	+48%	32.5	50.7	66.2	18.6	267.6	29.0

A comparison of the modelled marginal electricity generation costs for each scenario with wholesale prices from 2016 in Table 3.3 shows that the average daily cost of electricity generation is lower than the 2016 average price in both high VRE scenarios modelled here. The maximum average daily cost is higher however due to the fixed annual costs of dispatchable generation (assumed here as CCGT) being recouped over fewer hours of the year. Additionally, these would also be the days that have the highest difference (residual) between electricity demand and renewable generation, requiring dispatchable plant to fulfil the remaining demand.

Table 3.3 Cost comparison with renewable capacity and storage

Scenario	Renewable Capacity GW	Wind Share of total capacity	Solar Share of total capacity	Average £/MWh
A (Two Degrees)	109.4	29%	19%	34.1
B (Community Renewables)	149.4	31%	25%	35.1
2016 actual	26.79	16%	11%	41.12

The scenarios were modelled using demand and renewable data from 2006-2016. The results for individual years can be found in Appendix. A. detailed look at Scenario A in Figure 3.2 shows a winter month period in 2016 with the residual renewable generation (above) and storage levels and electricity costs (below). It shows that costs frequently spike corresponding to cycling of electricity storage levels in the system. When storage levels are full, surplus generation hours result in low costs. However, as a result of renewable fluctuation the storage level varies rapidly requiring discharge then dispatch periods, which result in higher costs. Two peak dispatch hour are observable near the beginning of December when residual generation is most negative. It

suggests that the storage capacity in Scenario A is insufficient for the renewable capacity in the absence of other flexibility options.

Explicit constraints on charging and discharging rates have not been applied. However, the peak power to energy ratio in the simulations of the scenarios was 0.66 MW/MWh. This is within the limits of grid scale lithium-ion storage where typical power to energy ratios are 1.0 (Hesse et al., 2017).

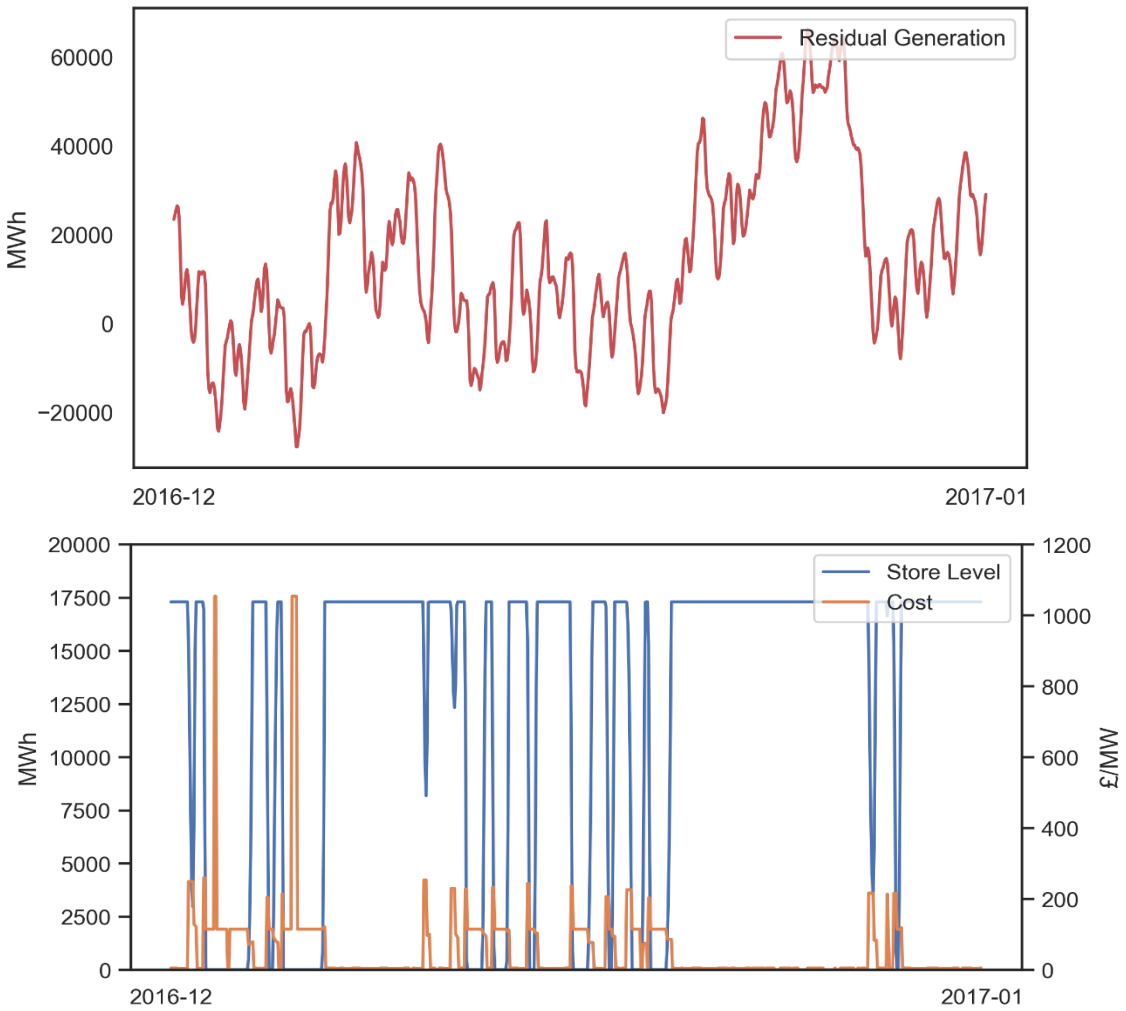

Figure 3.2: Residual renewable generation (above) and resulting cycling of storage and costs (below) for Scenario A 2016

Off-peak dispatch hours are cheaper than discharge hours under the current cost projections used. This is the case with the current assumptions of short run variable costs of dispatchable hours being less than that of discharge (fuel £35/MWh, carbon £70/MWh, O&M £1.5/MWh). For the storage capacity defined in Scenario A, a total short run variable cost for dispatchable generation would need to be at least that of the highest discharge cost, £251/MWh. From the perspective of limiting carbon emissions, it would be desirable to have DSP hours cost higher than DCH hours. Adjusting DSP hour costs to be higher than DCH hours meant that the average in Scenario A increased from £36.34 to £49.83, almost a 40% increase in average annual costs.

Within the current market framework, unless fuel or carbon costs increase above projected values, dispatchable/thermal generation would be higher in the merit order than less carbon intensive electricity from discharging electrical storage, owing to their lower marginal costs, Figure 3.3. Figure 3.4 shows adjusted dispatch hour costs to reflect an ideal scenario where dispatch costs are higher than discharge costs.

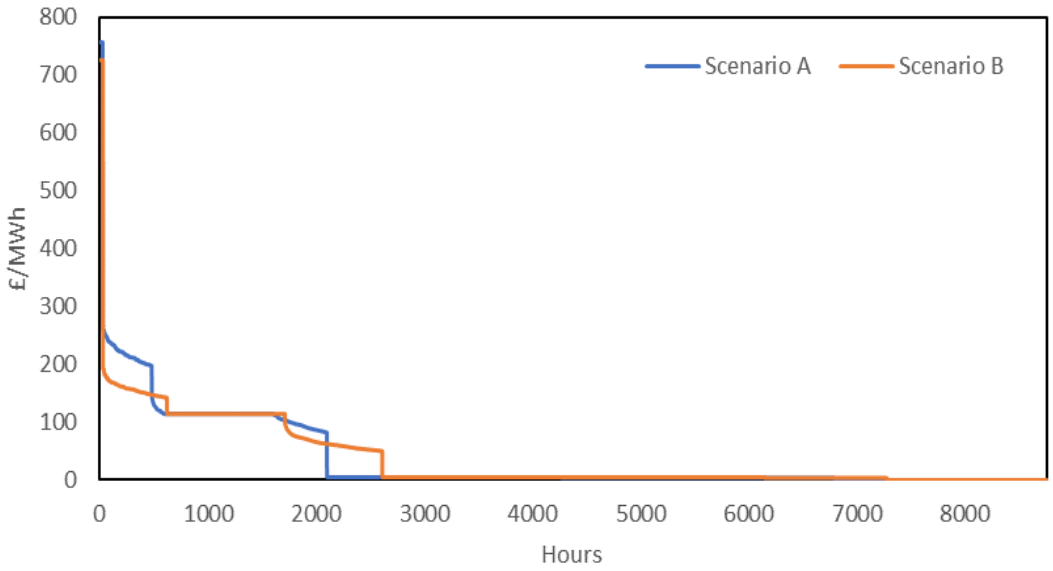

Figure 3.3: Scenario A and B cost duration curves 2013

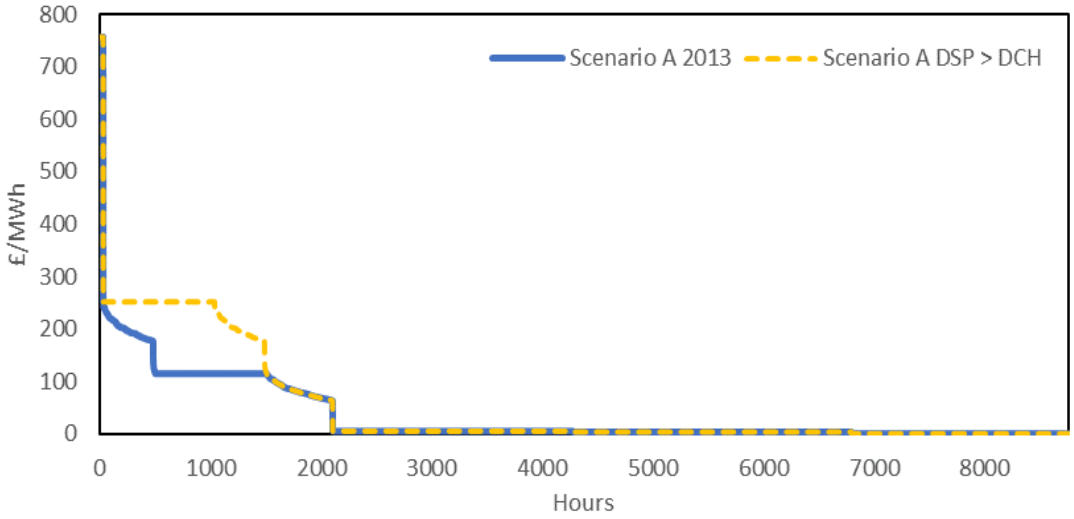

Figure 3.4: Scenario A 2013 price duration curve with adjusted DSP hour costs

For both scenarios, the positive residual generation from renewables is far higher than the negative residual, Figure 3.5, which suggests an overcapacity of renewables in both scenarios. Analysis of the residual duration curves as well as the absolute maximum of negative residual generation can allow better estimates of storage requirements and the corresponding effect on prices, but an optimisation of scenario storage levels is beyond the scope of this study.

Figure 3.6 shows a 24-hour rolling average of the mean modelled generation costs for scenario A from the 2006-2016 data, scenario B exhibited a very similar distribution. A clear seasonality can be observed in the costs, with higher cost periods being concentrated in the winter where despite wind generation in these scenarios being higher, there are periods of low generation coinciding with high demand often leading to higher costs.

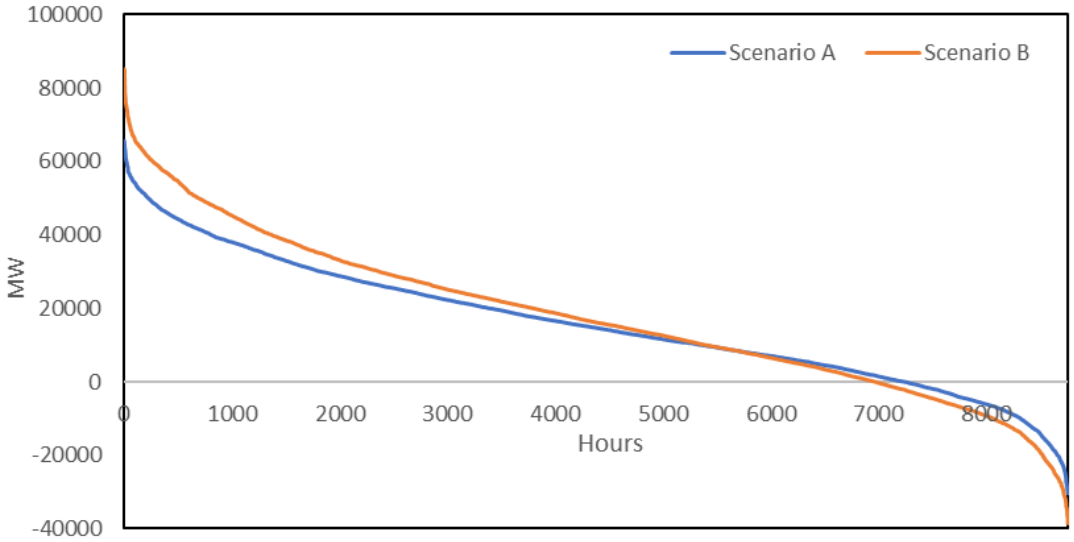

Figure 3.5: Residual renewable generation for scenario A and B 2013

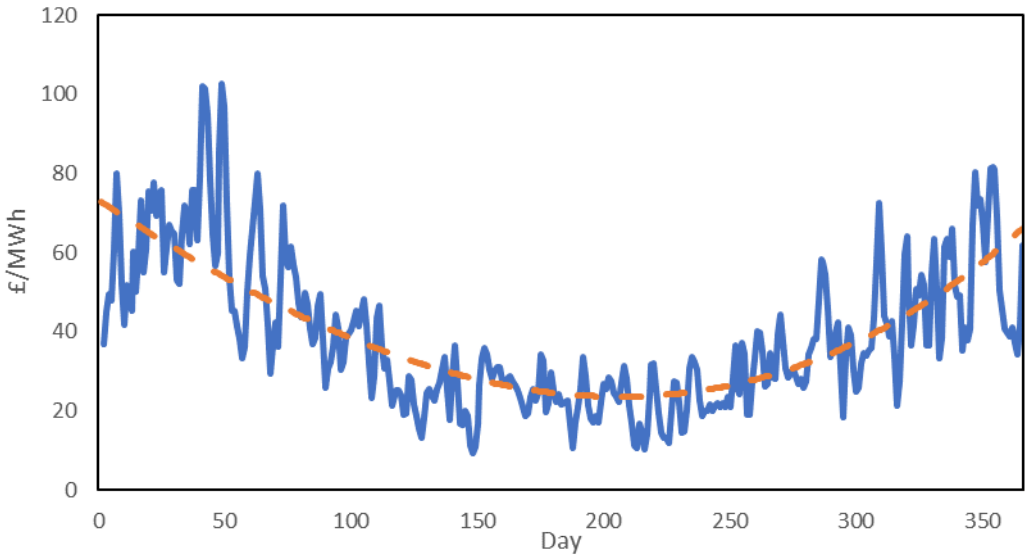

Figure 3.6: Scenario A 24-hour rolling average of modelled costs and trendline 2006-2016

Another observation is that an increase in the share of renewables does not directly lead to lower average electricity generation costs. This can be seen in the average cost difference between scenario A and B. These are similar despite B having a significantly higher renewable capacity to meet a significant difference in demand. Scenario A has higher average costs in some year compared to B.

The fewer dispatch hours that occur within a year, the higher the maximum costs become as there are fewer hours where dispatchable plant operates. The fixed annual costs of the dispatchable plant per MWh of electricity grows as there are fewer peak dispatch hours against which to recover fixed costs of the capacity. The cost of electricity from peak dispatch hours would decline if dispatchable plant capacity decreased, in other words, if the highest negative residual decreases.

This peaking function at high demand times is normally performed by open cycle gas turbines (OCGT) that are able to ramp output, consequently they have high O&M and variable costs but low fixed costs. Cost for DSP hours are based on CCGT due to their higher efficiency and predicted improvement in technology and ramping ability. Also, as renewable generation grows, dispatchable generation will be gradually retired; by about 2050, the remaining dispatchable plant may likely be already-existing CCGTs.

3.6.3 Sensitivity Analysis

Scenario B is presented alongside high and low-cost projections to display the sensitivity of prices to capital cost projections. In this case, the interest rate on capital costs for renewables and storage has been adjusted from the base case of 5% to a low case of 2.5% and high case of 10%. The variable operational costs of dispatchable generation have been adjusted to ±20%.

It is observable in Figure 3.7 that surplus hours are the same for each case as these are only dependent on the variable operating costs of renewables. Peak DSP hours (not shown) are affected in the same way as off-peak DSP hours as it is assumed that no new dispatchable plant is built and thus no new capital is required. DCH hours are affected as expected due to the changed annuitised capital costs of storage capacity. In this particular scenario, the costs for charge hours in the high costs case is below the base case (Table 3.4). This is due the increased revenue to the incremental renewable from higher costs in both DSP hours and DCH hours. If dispatchable generation costs were left unchanged, then it is expected that CHR hour costs would be changed in line with the change in annuitised capital costs of the incremental renewable generator.

Table 3.4 Average price comparison for high and low-cost cases

	£/MWh		
	Scenario B	**Scenario B High**	**Scenario B Low**
Average Annual Price	36.40	40.51	31.05
Average Discharge Price	156.97	181.65	134.95
Average Charge Price	62.88	58.02	53.79

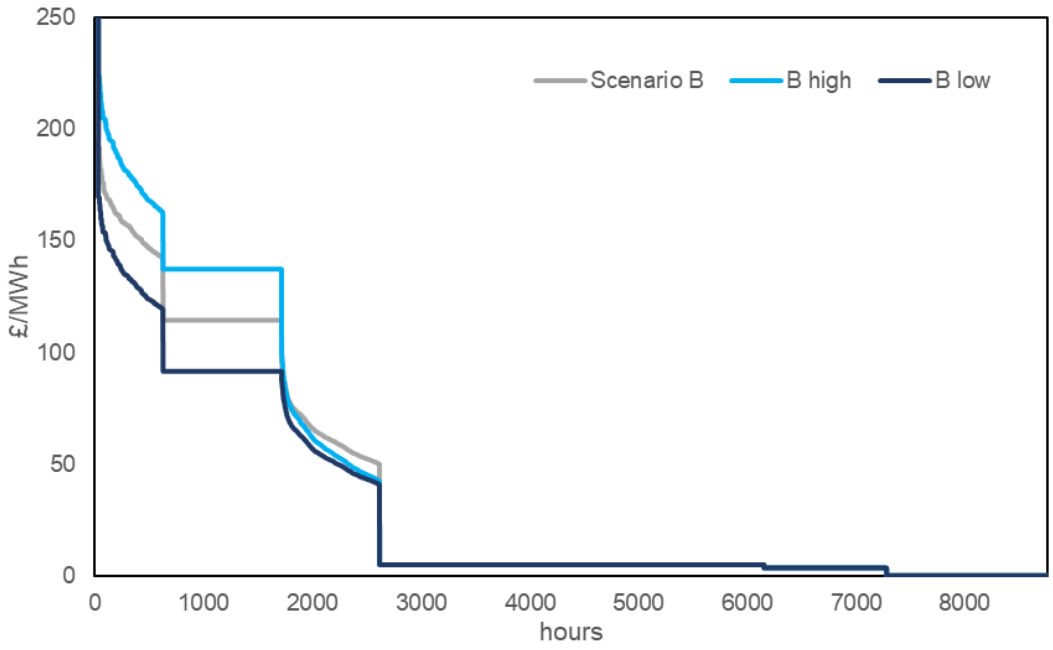

Figure 3.7: Scenario B with high and low-cost projections (clipped for detail)

3.7 Scenario Development

The scenarios presented thus far from FES 2017 have since been superseded. UK policy makers have since introduced more ambitious net zero targets (BEIS, 2020a; Committee on Climate Change, 2019). A scenario from the revised FES (2020) is adapted for use in the following chapters.

An overview of these scenarios adapted from the FES 2020 data tables is given in Table C-2 and Table C-3. The revised scenarios all have ambitious renewable generation targets. Of these

'Consumer Transformation' (CT) and 'Leading the Way' have a high battery storage capacity, with most of the other storage capacity comprised of short term pumped hydro. The CT has a larger baseload, comprised of Nuclear and thermal generators with CCS, higher annual demand, and lower fossil fuel capacity. It also has the largest electrified heating projections of all the scenarios with the most ambitious district heating development targets. This makes it a suitable Net Zero (NZ) scenario to adapt for this study which will be used for analysis of electrified DH.

3.7.1 Electricity demand

Electricity demand is composed of the existing demand data as per the previous scenarios but with the addition of electric vehicle (EV) demand and HP demand. The largest departures from the CT scenario will be the assumption of 100% electric heating as opposed to around 70% in the original scenario. The increased fraction of electric heat demand increases the total annual demand in this scenario to 520 TWh. Hourly electricity demand is composed of scaled historical electricity demand profile (as described in section 3.4) and new HP and EV demand.

3.7.2 Electric vehicles demand

The daily EV charging load profile shown in Figure 3.8 was derived from the inverse of daily traffic flow statistics (Barrett, 2020). The profile is then multiplied such that the annual demand is consistent with the scenario demand of 87 TWh in Table C-2. This results in the same daily EV load whereas in reality there are variations across the week and year. There are further complexities such as EVs contributing to ancillary services and balancing (vehicle to grid), which have not been modelled.

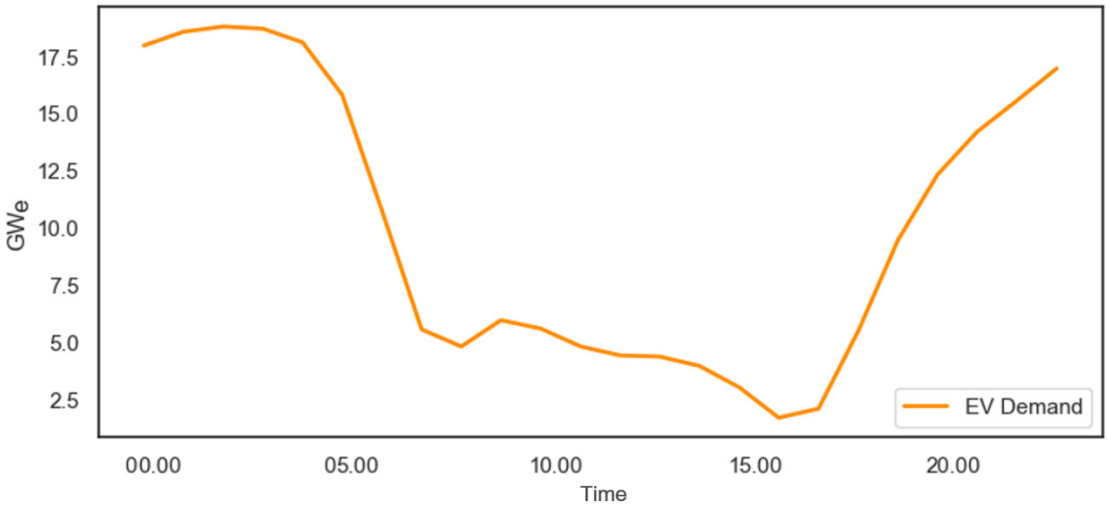

Figure 3.8 Daily Electric Vehicle demand profile for the NZ scenario

3.7.3 Heat pump demand

The national GB heat demand, D_H, from the HeLoM model are used to estimate the demand for electric heating from HPs, $D_{E,HP}$. The FES 2020 CT scenario has around 70% electrical heat with the remainder from hydrogen and biofuels. For the NZ scenario we assume 100% of the heat demand is met by HPs, increasing the electric heat load by 30%. The annual electricity demand then increases from 450 TWh to 520 TWh. Using the ambient temperature, T_{amb}, a separate COP is calculated for domestic heat pumps using a Carnot efficiency based on absolute temperatures in K, E_{CAR}, of 0.4 and 0.45 for nondomestic heat pumps according to (3.13) assuming an output

temperature of 50°C (323 K). The heat demand can then be converted to a heat pump electrical demand from (3.14).

$$COP_{HP} = \frac{E_{CAR}(273 + 50)}{273 + 50 - T_{amb}} \quad (3.13)$$

$$D_{E,HP} = \frac{D_H}{COP_{HP}} \quad (3.14)$$

Most of these heat pumps are likely to be connected to the local electrical distribution network so appropriate distribution losses must be applied. UK Power Networks estimate that overall distribution losses across the country are in the region of 6% (Strbac et al., 2018a). Distribution losses, L_{DST}, are first estimated from (3.15) with a constant loss factor and variable power law losses, and factors z_0 and z_1 from (Barrett, 2014). In contrast to applying a constant loss factor, this results in larger losses when HP demand, $D_{i,HP}$, on the distribution network is high.

$$L_{DST} = z_0 + z_1 D_{i,HP}^2 \quad (3.15)$$

This provides the hourly variation of losses in accordance with the demand level. National Grid (2017b) published seasonal average transmission system losses for the London region as: Spring 1.3%, Summer 1.3%, Autumn 2.1%, Winter 2.9%. Assuming distribution losses follow the same seasonal pattern as transmission losses, seasonally losses are then: Spring 5.0%, Summer 5.0%, Autumn 8.1%, Winter 11.1%. Distribution losses are then normalised seasonally to these percentages and the heat pump demand, $D_{i,HP}$, is suitable inflated.

The reference load consists of all existing time varying demands from historic demand data but suitably scaled as per the demand in the CT scenario. The historic demand is scaled such that the total CT scenario demand in Table C-2 is the sum of electric heating demand, EV demand and the scaled historic demand. The modelled daily demand from 2012 for the NZ scenario is shown in Figure 3.9.

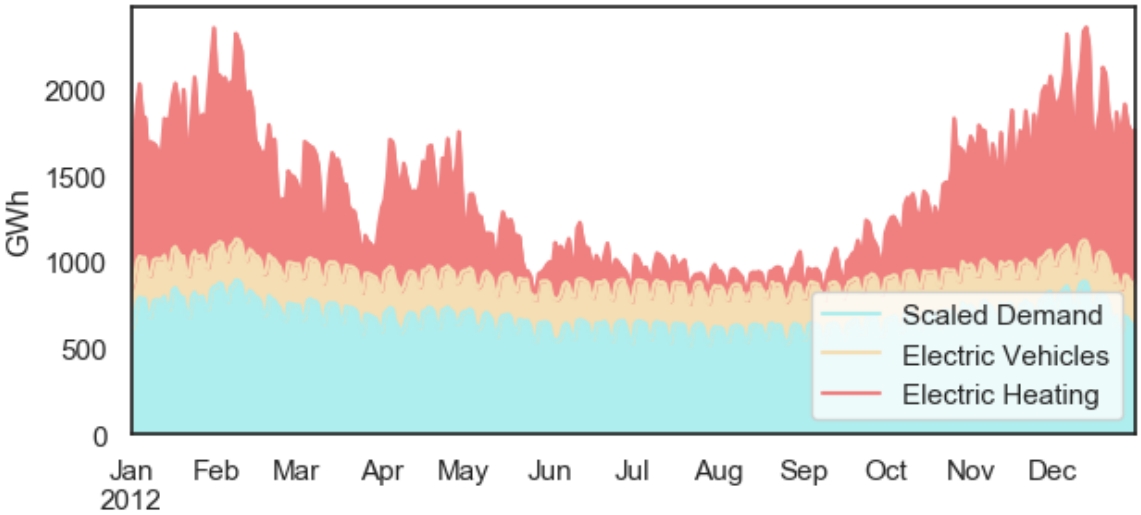

Figure 3.9 Modelled 2012 daily Electricity Demand for the NZ Scenario

3.7.4 Electricity generation

As described in the dispatch methodology, electricity generation comprises renewable generators – composed of onshore wind, offshore wind, and solar PV, dispatchable generators and grid storage (batteries). However, several further adjustments and assumptions are made for the NZ scenario. Firstly, offshore wind technology has improved in recent years and average capacity factors are projected to increase. Second, the increase in demand for the adapted NZ scenario necessitates an increase in generation and storage capacities.

The baseload generation as described in section 3.4 is assumed constant throughout the simulated periods and is set less than the minimum demand. As it is always less than the demand, consequently it never sets the marginal cost of electricity generation and its composition is not an important factor in this study. However, it is assumed to be nuclear generation with constant hourly output but could equally be a thermal generator with carbon capture and storage (CCS).

3.7.5 Offshore wind turbine technology

The projected wind capacity factors from the Renewable Ninja dataset have an average below 40%. This is in line with UK aggregate offshore capacity factors which have increased from 30% to 40% (IRENA, 2019; The Crown Estate, 2019). In 2020 the average offshore UK installed wind turbine is around 3-5 MW capacity, however the largest wind turbines being installed in the North Sea in 2020 have a 12 MW capacity for which the capacity factor is projected to be 63% annually (GE, 2018). A report commissioned by BEIS projects aggregate offshore capacity factors to rise by up to 60% by 2035 (BEIS and DNV GL, 2019) and design for offshore turbines of up to 50 MW are currently under development (Gerdes, 2018) which may make capacity factors higher than 60% feasible. Offshore capacity factors are transformed for the NZ scenario by raising the original factor to a power of 0.565 to produce a mean capacity factor of 55%. The transformed capacity factors are shown in Figure 3.10 where the factors are more evenly distributed whereas the original factors had a large concentration in the lower quartile (before transformation; μ =0.38, σ^2 =0.042 and after; μ =0.55, σ^2 =0.048). Higher capacity factors may reduce storage requirements, but this also depends on how the generation is distributed across the year relative to demands.

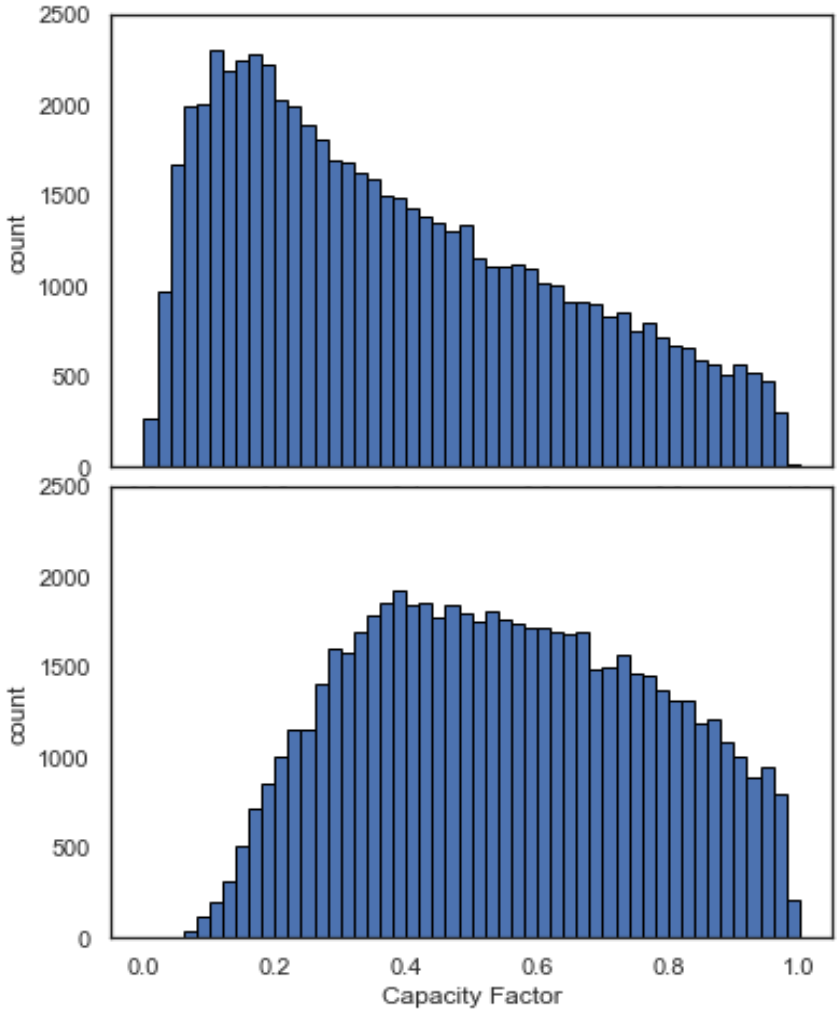

Figure 3.10 Offshore capacity factors before (top) and after (bottom) transformation

3.7.6 Generation and storage capacity

The Consumer Transformation scenario is simplified to create an all-renewable scenario. Core aspects of the electricity system are retained from the CT scenario while sufficiently simplifying it to work with ElCoM. Other capacity such as hydrogen, other renewables, as well as flexibility aspects such as interconnectors are omitted, this needs to be compensated for by increasing the renewable generators.

As minimum demand has increased in the NZ scenario, the baseload generation is raised from 17 to 25 GW, the new minimum system demand. The renewable and storage capacities are also scaled up, maintaining the relativity between the renewable generators and with storage. The 2010 weather year was used as the design year, representing a stress test with the highest electricity costs and most DSP hours from all the simulated years.

An acceptable level of dispatchable generation, which we assume as the security of supply for the scenario, was designated as 2% of annual demand. As per Figure 3.11, it was found that a scenario multiplier of 1.25 is sufficient to reduce dispatchable generation to 2% of annual demand without significantly altering DSP and DCH prices. The resulting NZ scenario generation and storage capacities are shown in Table 3.5 and the modelled total daily demand and generation for 2010 is shown in Figure 3.13. There was a substantial difference between storage requirements to attain this security of supply in 2010 compared to other years.

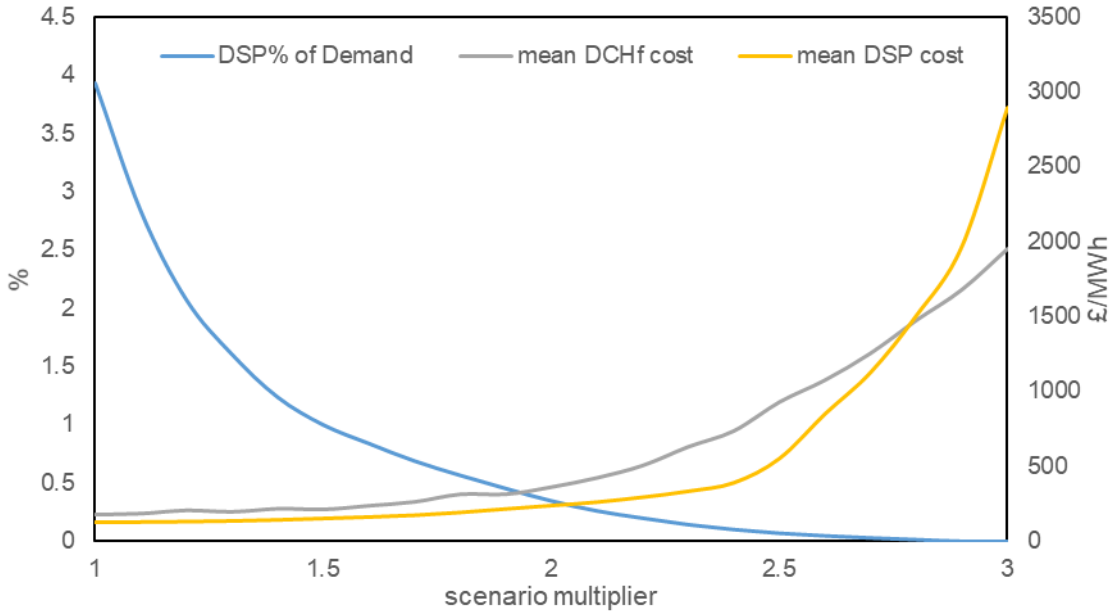

Figure 3.11 Base scenario adjustment factors experimentation

The remaining 2% of dispatchable generation (less than 1% of hours in a year) is assumed to be entirely covered by system flexibility which includes industrial demand side response and interconnectors. To compensate for the omission of dispatchable generation in the NZ scenario, DSP hour costs are instead assumed to replaced by a 'flexibility cost' a value equal to the highest DCHf cost. As the costs of DSP hours have reduced, the cost model is re-run for CHR and DCH hours to ensure that the revenue earned by the incremental renewable generator (i.e. offshore wind) is adjusted and consistent with the new DSP costs. This results in a small reduction (£2/MW_e) in CHR and hence DCH costs as there are very few DSP hours in the year and account for a small amount of revenue to the incremental generator.

Table 3.5 CT base scenario and adjusted NZ generation and storage capacity

	CT	NZ
Solar GW	75.36	94.20
Offshore wind GW	82.72	103.4
Onshore wind GW	47.74	59.67
Baseload GW	17.92	25.41
Total Storage GWh	194.1	242.62

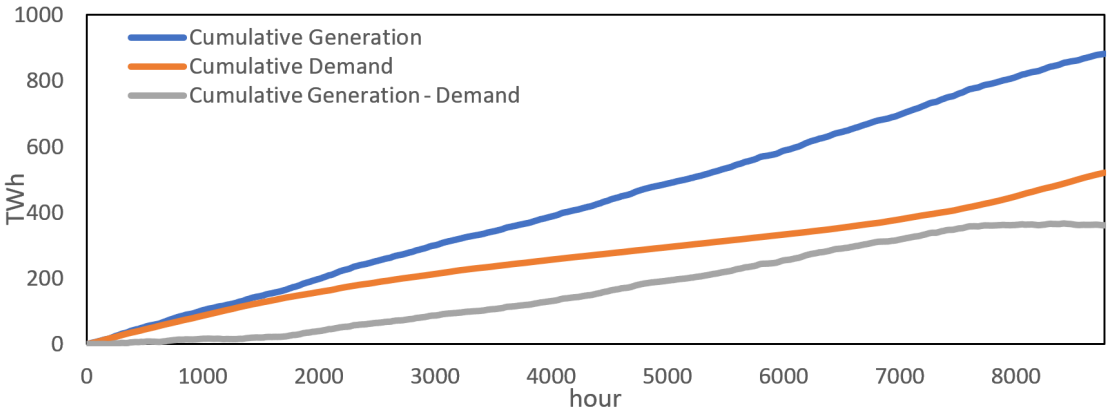

Figure 3.12 Cumulative Demand and Generation for NZ 2010

Figure 3.12 shows the cumulative demand and generation for 2010 with the NZ scenario. Cumulative generation is always higher than cumulative demand creating a large surplus. However, the fraction that can be stored depends on storage power and energy capacities. The cumulative generation minus demand line shows the surplus generation that can be absorbed by storage. This is not the same as the actual operation generation minus demand curve which becomes negative when demand is higher than generation.

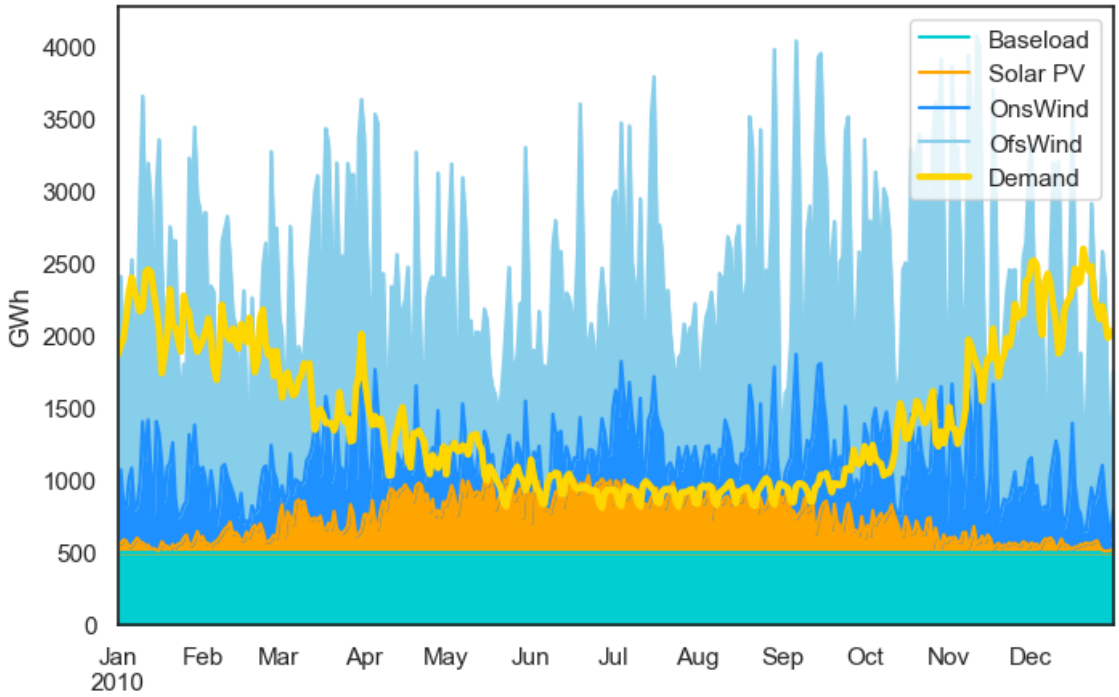

Figure 3.13 Daily total Demand and Generation for NZ 2010

3.7.7 Electricity consumer price

DH HPs are assumed to be connected to the high voltage (HV) transmission and measured half-hourly for industrial consumers. The final price is also inclusive of transmission (TNUoS) and distribution (DUoS) charges. Transmission losses are included as per the method with consumer HP demand, but low voltage (LV) distribution losses do not apply to HV industrial HPs.

Transmission charges are calculated based on the average power demand over three Triad half-hours in the year (National Grid, 2017b). These are the half-hours of highest demand on the system. These charges are normally very high with National Grid forecasting that for London the charge will reach £60 per kW by 2025. The Triad half-hours are not known in advance but are only identified at the end of the year. However, National Grid do provide warnings in advance of half-hours which run the risk of being Triad half-hours. To deal with this, the ten hours of highest electricity demand are identified and set to the maximum cost in that year if they already aren't the most expensive.

Distribution charges for half-hourly metered HV customer according to UK Power Networks (2020) consist of a unit charge of 2.403 p/kWh, which applies between 11:00 and 14:00, and between 16:00 and 19:00, on Mondays to Fridays across the whole year. A capacity charge of 7.79p per kW for every day of the year, and a fixed fee of 75p for every day of the year.

The cost of electricity supply for the NZ scenario in 2010 is shown in Figure 3.14 inclusive of the extra charges. While we assume that this would be the price paid by consumers in a perfect market, there are many factors that influence the price such as environmental and social obligations, supplier operating costs and margin, and VAT where applicable. Further, different consumers will have different tariffs and it is unlikely that domestic consumers will be exposed to the modelled costs spikes. Tariff design is important for energy companies so that they are able to absorb these high-cost periods and provide competitive prices for consumers.

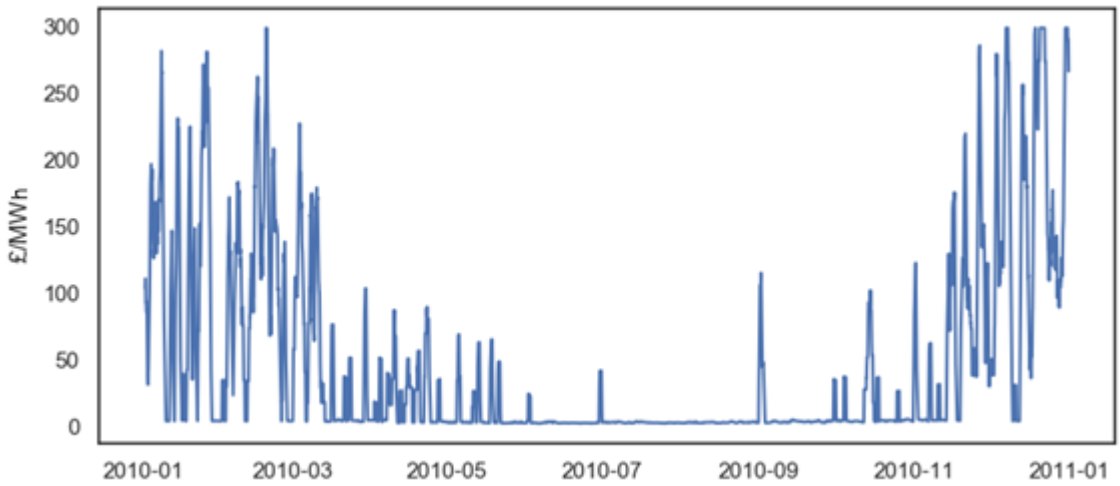

Figure 3.14 NZ Scenario daily mean electricity costs

There are a further cost of supply and supply margin that industrial half-hourly customers experience such as supplier costs and profits, and system balancing costs (Grubb and Drummond, 2018). These costs are estimated to increase the final price by £10.26 per MWh. Assuming an efficient market, the final charges to an industrial consumer compared to the cost of generation for 2010 weather data are shown in Figure 3.15. These costs and prices are assumed to apply in the future.

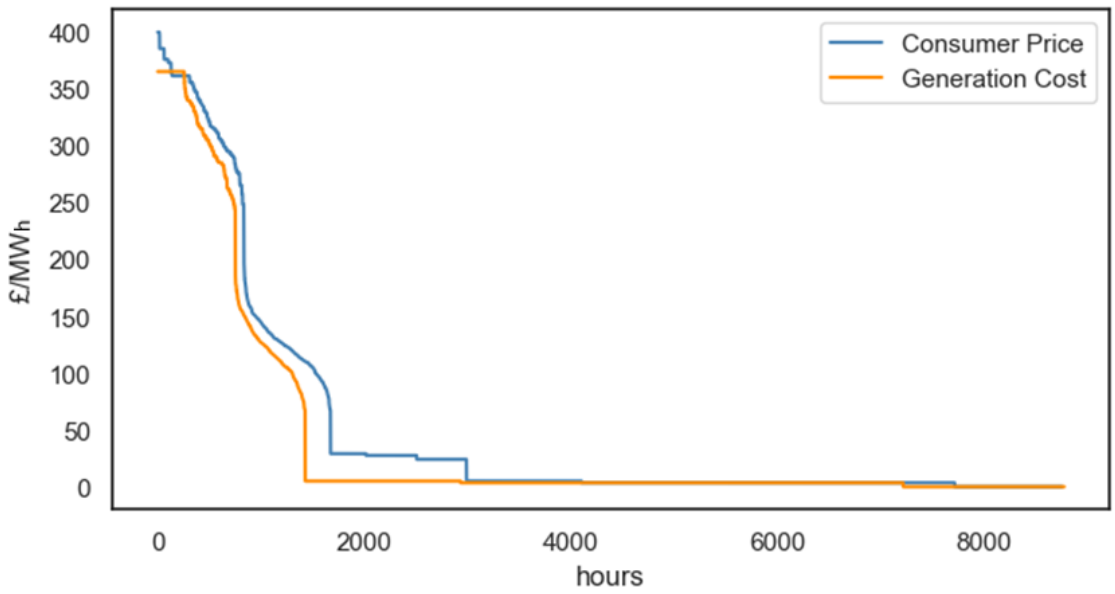

Figure 3.15 Duration curve of electricity prices and generation costs for NZ 2010

3.8 Discussion

A simplified electricity dispatch model has been described along with the details of a marginal cost-based pricing method. This has produced a time-series of generation costs corresponding to high VRE and storage scenarios. Forecasting precise electricity prices is infeasible. Rather, the method presented here allows an exploration of future cost patterns and magnitudes that can provide some insight into how electricity purchasing and pricing decisions can be made. The output can then be used in energy system models to assess options such as DH storage, and to help define markets for investment and dynamic operation.

Higher VRE capacities in the future will increase the need for investment in flexibility options. The GB system currently has a lot of flexible dispatchable generation using stored fossil fuels. To reduce carbon emissions from power generation, the reliance on fossil fuel dispatchable generation will need to be virtually eliminated. Flexibility can be provided with electricity storage of some form, but also by storage such as with DH heat (as explored later), bioenergy or synthetic fuels such as hydrogen. Transmission links with other countries can aid in balancing and thereby reduce storage needs.

VRE, particularly wind, has rapidly reduced total generation cost and low marginal short run avoidable costs but requires other technologies to balance demand and supply. The cost patterns of future electricity generation will become more uncertain and unpredictable, which translates to uncertainty in wholesale electricity spot prices. Better knowledge of these price patterns enables better decision making and encourages investment in smart grid infrastructure and electrification of other sectors as well as being important for electricity utility and industrial consumers.

3.8.1 The impact of costs

Previous studies that have quantified the distribution and variance of future electricity generation prices have been based on detailed simulations of the electricity market. These are difficult to replicate without access to custom tools or software. Most have also lacked an analysis of the effect of integrating electricity storage into a system with renewables.

Electricity prices arising from markets should reflect the costs of building and operating electricity assets. This includes storage, such that economic optimality arises to the degree possible given market imperfections. Markets should be sufficiently competitive regardless of who owns and controls storage operation: The operational market might be managed by, for

example, National Grid, even if owning no storage. The costing method presented here can inform the design of efficient, cost reflective markets that also meet other criteria such as the avoidance of penalising the poorer consumers with extreme price spikes.

The modelling here assumes perfect foresight. In practice, real-time indicative marginal costs could be estimated ex-ante using forecasts of social activity and weather, and hence demand, and wind and solar generation. Using modelling taken forward as the rolling year develops, it can take advantage of past data and forecasts of demand as well as of generation availability. At the end of the accounting year, adjustments could be made to settlements so that they conform to accurate marginal costs calculated ex-post.

The method has made several key assumptions, one of which is that the carbon intensity of electricity generation should take precedence in the merit order of supply. The analysis of two high VRE and storage scenarios shows that that the capacity cost of storage results in the cost of battery discharge being higher than the marginal costs of dispatchable plant. The merit order would be the same as a cost-based order if the short run cost of dispatchable generation was more expensive than electricity discharged from storage. This would however require carbon or fuel costs to be significantly higher than is assumed.

The high VRE scenarios show prolonged low marginal cost periods that last for several days followed by spikes usually occurring at high demand periods where peaking plants are required. This confirms the observation from previous work that short term variability of costs is reduced in high wind scenarios, but intra-day variance is increased. These spikes may be predictable in advance through projections of demand and advanced forecasts of VRE generation. Another trend observed from these high wind scenarios is the seasonality in mean prices that are observed in both scenarios for each modelled year. That is, the frequency of prices from discharge and dispatch hours is higher in winter periods and suggests that there might be a role for seasonal energy storage to reduce this seasonality effect.

3.8.2 The net zero scenario and district heating

Scenario development was not a primary aim of this study. The generation and storage capacities presented in the NZ scenario are large and echo the messages coming from other studies. A recent study into the lowest cost generation mix required to achieve net-zero found that the required offshore wind capacity is more than double the existing 2030 targets at over 100 GW. Additionally, the study finds that a large expansion in the current energy storage capacity is needed to accommodate renewable generation at between 187-312 GWh (Aunedi et al., 2021). This goes to highlight the scale of transformation required to achieve net-zero for the electricity sector.

The NZ Scenario is a modification of an existing National Grid scenario which is in line with the UK's net zero targets for the electricity sector. The scenario is modified such that heating is fully electric with consumer heat pumps replacing the fractions of hydrogen and biofuel-based heating prescribed in the original CT scenario. The heat pump demand is taken from the HeLoM model with the addition of variable distribution and transmission losses. The increase in electricity demand necessitated a larger grid generation and storage capacity such that the relativity between total and peak demand is retained in the NZ scenario. The remaining fraction of DSP hours were eliminated by assuming they can be covered by other flexibility measures such as demand side response.

Once costs are generated by ElCoM, various network charges are added to convert these into final electricity prices. These prices are intended to represent the variability that would be experienced by a DH operator in such a scenario. The magnitude of prices is expected to provide an estimate for the operating costs of DH in the subsequent chapter. Electrified DH systems will need to be designed to the patterns of a future electrical grid to achieve net-zero. The flexibility they provide through TES capacity will in-part be dependent on these price patterns.

4 DISTRICT HEATING MODEL

Chapter Summary

This chapter details the development of the District Heating Model (DiHeM). Academic and commercial modelling of district heating is a developed field. However, the impact of electrification and the consequences of a highly renewable grid on district heating are less well explored. The operating strategy for cost minimising in district heating system models is dependent on the size of thermal plant and storage capacity as well as its operational conditions. Physics-based representations of a district heating network and thermal energy storage are developed. DiHeM assumes a 70°C flow and variable return temperature modelling dynamic COPs and thermal losses. Using the urban heat load from chapter 2 and hourly electricity prices from Chapter 3 as a basis for operation, heuristic control strategies are first explored. A model predictive control optimisation is then applied to DiHeM to find low-cost combinations of heat pump and thermal energy storage sizes. The minimum electricity operating costs were found to vary by year, dependent on annual conditions. Results show that thermal energy storage equivalent to around 1% of annual demand is sufficient to minimise operating costs and enables operational flexibility beyond 4 days. Access to this extra storage capacity could provide benefits for the electricity system. The cost of delivered heat is found to be financially competitive with other options, at around £88 per MWh_{th} but this is largely dependent on the capital costs of the network.

4.1 Review of District Heating Modelling

Many tools and models have been developed to analyse and simulate DH. The modelling of DH overlaps with the field of urban energy modelling, often including local electricity systems due to the prevalence of Combined Heat and Power (CHP) based DH. There are several ways to segment these models; based on purpose, such as simulation, optimisation, analysis type; or the modelling methods used and approach of the model.

Modelling methods in the literature are split as physical models and black box or energy models (Guelpa, 2020; Talebi et al., 2016). Physical models, sometimes also referred to as network models as they explicitly model the network features, include the primary network, plant layouts and configuration of the network. Energy models, so called because they omit direct representation of many network features, are normally simplified representations that model the energy transfers in the system via relationships between components. The calculations in these can also be categorised as steady state or dynamic. DH networks are inherently transient systems that are in constant imbalance, and steady state is rarely achieved. Most models employ

steady state calculations for the hydraulic network components as dynamic fluid simulations are computationally demanding and requires a large amount of input data. For example, a branch of piping is rarely ever at a single temperature, rather temperatures propagate and details of the losses change depending on what part of the flow is being analysed. Steady state simplifies this to a single temperature and loss in the branch. There are cases when a detailed simulation of the inner workings is needed; such as when measuring pressure waves which can propagate faster than temperatures in the system (Kallio, 2020). These details are generally not required in many forms of analysis. This review segments the literature as network design aids, simulation models and energy models.

4.1.1 Design aid models

Design aid models are normally network models and typically aim to refine and optimise aspects of the system including pipe size and routing; flow characteristics such flow temperature and flow rates; and plant configuration and capacity. The network topology and pipeline modelling can have a substantial impact on results (Guelpa, 2020). Fluid flow modelling in pipes is computationally expensive. This is usually simplified to characteristics of flow and estimated pressure losses for each branch between 'nodes' of a network. The pipe types and diameters can then be selected based on required flow rates and modelled heat losses.

Ahmed and Mancarella (2014) developed such a model to assess the performance and economics of DH designs. It intended to give strategic overview on the feasibility of DH given specific inputs parameters. The model sized pipes based on flow characteristics and used exogenous heat loads which they calculated via building simulation software (EnergyPlus). They tested several configurations, finding that the network cost of pipework installation is the most influential factor. The authors cite the lack of tools to evaluate techno-economic performance of DH systems as their motivation. Barone et al. (2020) built a dynamic model to compare DH and cooling networks to both asses feasibility and optimisation. Using an implementation in Matlab, they calculate heat loads for every branch of the network. The model optimises flow parameters and selects standard pipe sizes given inputs such as load topology and weather data to calculate losses. Dominković et al. (2017) used similar methods to assess the interconnection of several DH grids and optimise the connection points. Thermal characteristics of different network layouts were compared by Kuosa et al. (2013). They used a static analysis built with excel-visual basic that compared flow conditions and losses. They demonstrated a method that allows adjustment of heat demand at the building level.

Modelica is a widely used language for dynamic DH modelling. It has been used to assess the coupling of DH with distributed energy generation (Leitner et al., 2019; Simonsson et al., 2021). Leitner et al. model the flow with a 1D wave equation, capturing the thermal inertia within the pipe network. The authors have made their modelling library opensource. Another Modelica based dynamic model used a combination of topology input in the form of CAD drawing and data pre-processing in Matlab to simulate heat propagation in pipes (Hermansson et al., 2018). Like many other studies, the model has been validated with data from an operational DH system.

4.1.2 Simulation and digital twins

Simulations of DH systems are usually 'digital twin' physical models created as an operational aid and to assess improvements. This means that there is no clear distinction between simulation or design tools. These models contain high temporal resolution dynamic simulations, fully capturing the hydraulic network. One of the prominently used commercial simulation tools is Netsim (2017). Netsim allows the detailed reconstruction of a DH including pipes details and locations of loads. It can perform both static and dynamic calculations. Network layout is modelled as a set of interconnected nodes and the level of detail can be adjusted to include only primary pipelines or the entire secondary pipework. The flexibility of the software makes it useful for analysing changes in the network. For example, Brandt et al. (2014) used Netsim to

analyse distributed generation to conclude that differential temperature fronts lead to pipe fatigue. Termis is another simulation tool modelling the hydraulic network and can use live data to improve operational efficiency (Aveva, 2018). Other advanced features available in Termis include the addition of forecast data and maintenance scheduling via analysis of flow conditions. Other full simulations of DH network and plant include PSS Sincal which also allows testing of operating strategies (Pirouti et al., 2013).

In simulation models, accurate pipe simulation allows for the estimation of pressure drops and thermal losses in the network. The topology of the network is also vital to the simulation, and the tools have various ways of inputting and modelling the network. Ancona et al. (2014) use a graphical user interface to input network layout. The geometry is input as a series of nodes with components attached such as heat exchangers. They validate their model against Termis.

The commercial tool Apros (2021) is used for the simulation of DH systems. It can model both the thermal plant and the hydraulic network. Kallio (2020) created a digital twin of an entire network down to substation components. Despite validation with historic data, errors were still present in the simulation with the author citing the difficulty of simulating a high level of detail. This was also the issue with needing to refine the calculation of pressure drops across junctions.

The spHeat tool was developed for simulation and used to assess operational strategies (Ben Hassine and Eicker, 2013). SpHeat simulates dynamically in Matlab and includes features such as the impact of spatial heat load distribution. The authors determined that network efficiency can be improved by 10% if large loads were located closer to the thermal plant.

Jing et al. (2014) use a bespoke energy simulation in Matlab for a DH and cooling system with renewable generation. They statistically optimised plant components to devise a control strategy to minimise fuel consumption. Simulink is a graphical environment for Matlab and is widely used for simulation and control modelling. Li et al. (2016) use it to simulate the primary network components and connections to improve flow characteristics and selection of appropriate pipe dimensions.

4.1.3 Energy models and system analysis

Energy models omit a direct representation of the distribution network and only model the energy flows from the central plant. Commercial models that aid in the design and selection of energy centre plant such as EnergyPro are available, this form of analysis in the literature has frequently used bespoke modelling tools. Typical applications of these models look to configure plant size or analyse the operation of the DH plant in the context of a wider system. One such model, EnergyPLAN is used for planning of national and local energy systems (Lund et al., 2015). Given the prominence of DH in Scandinavia, the simulation of DH and its interaction with the wider energy system, particularly with variable renewable energy is a main feature of the model. It has been widely used in academic research to study to study the impact of DH on national energy systems and has localised input files for many regions and countries including the UK.

Saletti et al. (2020) simulated the energy transfers from plant to substation to optimise layout for conditions where extensive network data is not available. Noussan et al. (2014) analysed the upgrade of the thermal plant of an existing DH system. They used an energy modelling method with ten years of high resolution (360 seconds) heat load data from the central plant. The analysed various configurations for the central plant to find optimal TES levels.

Nuytenn et al. (2013) developed an energy model to analyse operational flexibility of a CHP with either centralised or distributed TES. They simulate heat loads and generation as energy fluxes using historic demand data to test various operational strategies and find that centralised TES offers superior flexibility. Noussan et al. (2014) perform a similar analysis with a combination of biomass boilers, CHP and TES, using high resolution demand data. They determined that TES improves their system's efficiency by 8.6%.

A study with similar goals as this project used an energy model with operational optimisation to analyse the performance of a DH energy centre (Reynolds et al., 2018). They used an hourly demand as input with operational optimisation of a CHP and boiler in conjunction with TES. Similar methods have been used by Verilli et al. (2017) and Gambino et al. (2016) who study flexible loads as do Wang et al. (2015) who simulate a thermal plant with the addition of solar thermal generation and Wernstedt et al. (2003) who use this approach with operational optimisation to evaluate control strategies with various plant configurations.

4.1.4 Control and optimisation methods

Models of DH systems require a method to dispatch heating and control the use of TES. The operating strategy chosen can have a profound impact on the outcome. Operational control and management is important for DH systems in practical use. Operational management of a DH system focuses on improving the efficiency of the system and minimising operational costs or maximising revenue such as with the generation of electricity from a CHP. Much of the literature on operation and control has focused on the optimisation of CHP in DH, often in conjunction with TES. This is as CHP-DH systems are the most predominantly installed DH systems. There is a comparative lack of analysis on the operation of HPs in DH, particularly for future scenarios, despite CHP being more complex than HP based DH. The implementation would require an energy model. Common inputs would include constraints, demand and prices with the operational objective typically being cost, efficiency or emissions optimisation.

Operation control often employs model predictive control (MPC) algorithms with dynamic process models, optimising over a finite time horizon. MPC are a set of techniques that computes the current optimal control sequence based on information of future conditions, implementing the first step of this sequence, and progressing forward in time recalculating for the evolved systems. It can therefore be applied to real time operation with the use of feedback loops to adjust processes and predict how a system is likely to respond.

MPC is suitable for processes with continuous variables such as the control of flow rates and temperatures. MPC differs from other control methods such as proportional–integral–derivative (PID) control in that it utilises data on future operating conditions to predict the behaviour of the system. MPC employs an algorithmic optimisation and may use linear programming, mixed integer linear programming (MILP), mixed integer nonlinear programming (MINLP), genetic algorithms and dynamic programming (DP) and typically computed with commercially available solvers such as GAMS and CPLEX.

The choice of algorithm depends on the system functions and processes being modelled as these can often be nonlinear. While nonlinear algorithms allow complex interactions to be modelled, linear algorithms are often faster and scale better. But they can be limited in applications and care must be used with the formulation as global optimum solutions are not always attainable or indeed known. Nonlinear processes and constraints can be linearised or approximated when used with linear algorithms. This can however, adversely impact the accuracy of results (Atabay et al., 2018). These methods normally require high computational effort which is made worse with larger network sizes and more variables (Vandermeulen et al., 2018). The alternative is to use deterministic or heuristic methods that employ ‘rule of thumb’ decision trees or function gradients, thus avoiding the higher computational effort. These algorithms can perform well when applied to a narrow operating range (Sarbu, 2021).

Comprehensive reviews on the use of MPC for DH modelling have been covered by Sameti and Haghighat (2017) and Vandermeulen et al. (2018). The literature features many examples of single objective MILP optimisation for a variety of configurations. It has been applied to the scheduling of CHP with TES and boilers by Verrilli et al. (2017). The authors account for the quality of forecast and included constraints such as plant layout in their formulation. Similarly Gambino et al. (2016) present a control strategy that minimised costs of heat production with boilers and TES, with a particular focus on the physical modelling of boiler operating constraints.

The use of TES was compared to the thermal inertia of the DHN and building using CHP with the objective of minimising costs. The formulation involved an iterative approach to approximate nonlinear interaction (Leśko et al., 2018). Moustakidis et al. (2019) propose an innovative multi-level MPC formulation. Each level computed over different time scales, from long-term forecasts for strategic decisions to immediate operating conditions enabling fast response for hydraulic control and refinement. The long-term forecasts are supported by machine learning from weather data and smart meter monitoring. The authors applied their optimisation to a simulation of a real network to minimise operating costs. They found that the optimal control strategy regularly keeps TES levels low during periods of low demand. The use of TES with CHP and solar power was simulated with a monthly forecasting horizon to minimise global costs (Wang et al., 2015). They found that TES is used frequently, and CHP output fluctuates more. Other formulations have looked at CHP-TES in different configuration to maximise electricity export revenue. The price volatility of a future spot market could encourage the use of CHP to generate revenue (Romanchenko et al., 2017; Vanhoudt et al., 2018).

Comparatively few studies have used nonlinear programming (NLP) methods to control operation. The thermal inertia of a DH system and buildings was used in conjunction with CHP to improve the utilisation of renewable electricity and to minimise operational costs using a MINLP (Gu et al., 2017). Powell et al. (2016) present a MINLP to find optimal charge rates for TES with the objective of minimising costs when participating in the wholesale electricity market over a 24-hr time horizon. Other NLP formulations have considered thermal comfort in building while minimising operating costs in the DH system (Fanti et al., 2015).

Genetic algorithms have been used by Pirkandi et al. (2016) with a multi-objective optimisation of a CHP paired with gas turbine. Evins (2016) employs multi-objective optimisations to optimise CHP plant layout and control. Other novel techniques have been employed by Hohmann et al. (2019) who achieved the simultaneous control of flow rate and temperature via a two-stage stochastic optimisation and Claessens et al. (2017) who optimised the control of DH power production using learning algorithms.

Despite the design problem being similar, there has been little analysis of HPs in a DH context, with control studies focusing on building systems (Fischer and Madani, 2017). The use of MPC with HPs in tandem with batteries has been considered , with a focus on dynamic pricing and grid ancillary services (Fischer, 2017; Fischer et al., 2014; Georges et al., 2017; Nielsen et al., 2013). The optimal operation of a HP with TES and batteries under variable electricity prices was studied, achieving a 25% reduction in annual costs using DP (Salpakari and Lund, 2016).

Despite DiHeM not including detailed modelling of the hydraulic network, an appropriate formulation with MPC and LP could control flow rates. However, the goal with this analysis is to control the use of HP and TES, controls that are essentially binary decision variables and suited to the use of a Dynamic Programming (DP) algorithm. Moreover, the operating conditions have highly intermittent signals from the supply costs and LP formulations have been shown to not be good at responding to these. DP is a method that allows a high degree of expression with the system formulation and has been shown to perform better than other NLP and LP when applied to an energy storage system with variable electricity costs (Atabay et al., 2018).

Box 4.1 Dynamic Programming - DP

The Python optimisation library Prodyn uses an MPC optimisation method known as dynamic programming (DP) and has been applied to the operation of energy storage with dynamic pricing (Atabay et al., 2018). It is based on Bellman's principle of optimality (Bellman, 1952).

The method is suitable for multistage decision problems where each step is dependent on previous steps. It breaks the problem into a finite number of subproblems and drops paths that are not possible. The algorithm can be applied backwards or forwards in time. The forward implementation requires a starting state to be selecting, from which the optimal control route to each possible endstate is given.

The method allows a high degree of freedom of expression when defining the model function. It can permit complex interaction between variables but the need to discretise continuous variables can lead to suboptimal solutions and the degree of discretisation can lead to scaling issues leading to high computational costs. This can be time consuming as the computational requirements scale with the number of possible state values, control decisions and timesteps. A full overview of the theory and implementation of dynamic programming is given in Bertsekas (1995).

4.1.5 Summary of review

The review of DH modelling has provided an overview of the types of models and tools for DH in contemporary use. The energy model approach, where the simulation of DH requires only details of the energy transfers in the system, is widely used in the literature and is a suitable means of analysing the HP-TES energy centre. The method of controlling heat dispatch and allocation of TES heat is an essential feature of dynamic DH modelling. There are a variety of control and optimisation techniques ranging from heuristic based control to MPC methods. The use of a MPC utilising DP has been selected as a suitable method for application in this project.

4.2 Modelling Methodology

The objective of DiHeM is to simulate the operation of DH with an exogenous input of heat loads and a series of electricity prices. This will be used to explore configurations of the DH system and how this in turn influences the operation of the system. HP and TES capacities are defined as input parameters and amongst the outputs are the electrical input E, to the HP and the cost of this power.

The TES is considered as a pressure connected, stratified water tank. The tank hot water temperature, T_h, is assumed the same as the flow temperature and stratified into two layers, with the cold layer temperature, T_c, variable depending on the DH return temperature. In reality T_h is often slightly higher than T_f to compensate for losses and dilution upon discharge (Sarwar, 2020). We assume pressure connection as opposed to hydraulic separation. Separation is achieved via heat exchangers and is beneficial in several circumstances such as for systems that have high pressure variation due to terrain or if the quality of return water cannot be trusted. This is sometimes the case if heat interface units (HIU) are not used in the primary circuit. The advantages of pressure connection are that temperature differentials across the heat exchanger are eliminated as this would require a higher T_h and thus higher HP output temperatures resulting in a lower coefficient of performance (COP).

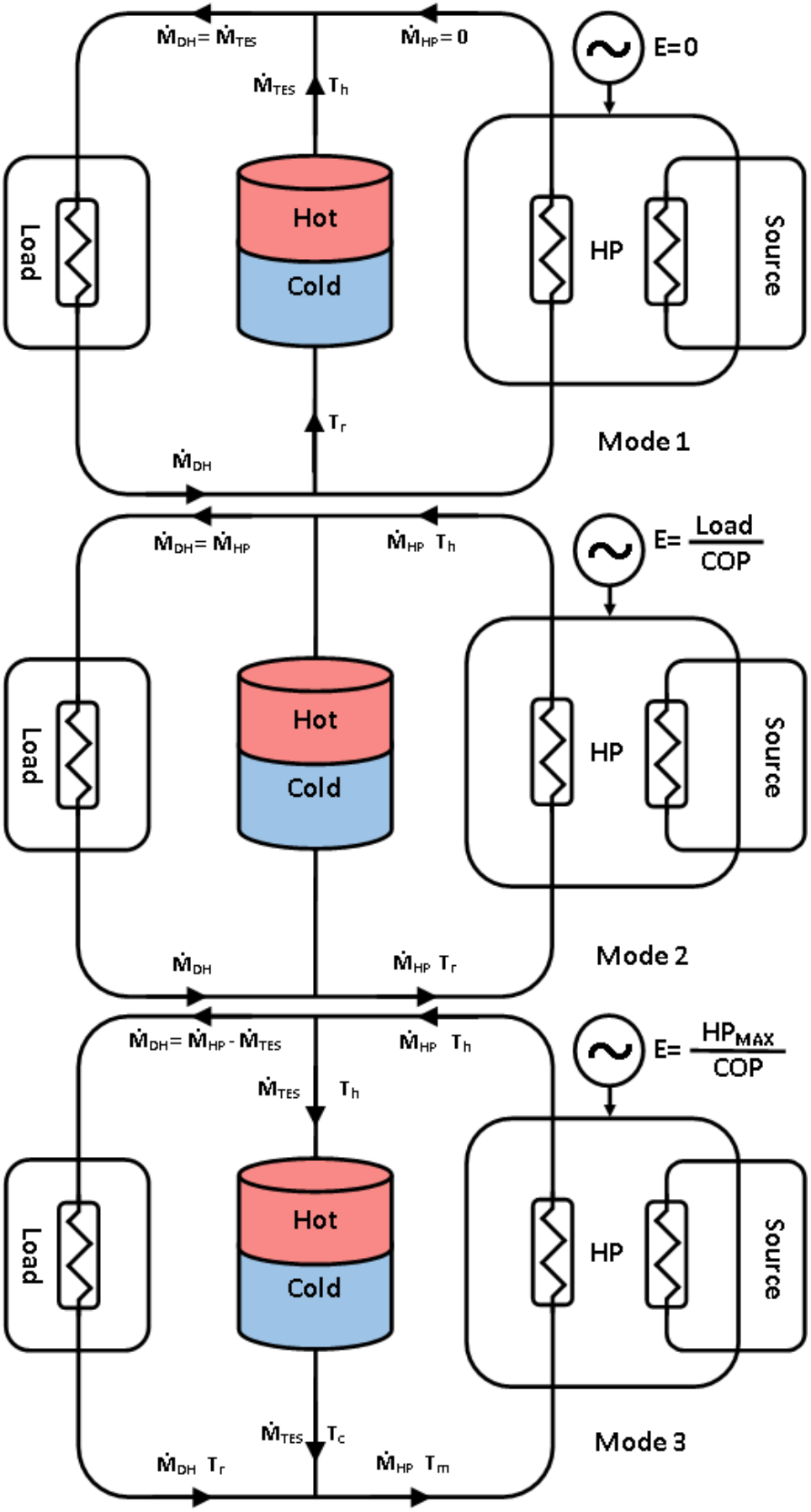

Figure 4.1 Modelling of DH network operating modes

The distribution network transports hot water from the energy centre to buildings and returns cooler water. It is to be modelled as a closed loop network where the return flow is reheated to the desired flow temperature. Typical UK DH systems are designed at a flow and return temperature of 80/60°C, but rarely achieve this temperature difference due to inadequate design and commissioning (Crane, 2016). Surveys of operating schemes in the UK has found an average flow temperature of 88°C while the corresponding survey numbers in Denmark are 78/43°C (Averfalk and Werner, 2017; DECC, 2015b). The move towards the fourth generation of DH systems envisions flow temperatures of 70°C and below with average return temperatures circa 20°C (Lund et al., 2014).

Acceptable flow temperatures are limited by the sizing of the heating systems installed in buildings. This puts a constraint on the flow and return temperatures. It has been shown that with efficiently designed buildings and heating systems, supply temperatures can be as low as 45°C. Low-temperature DH systems been demonstrated in small scale test cases in the UK and abroad (Burzynski et al., 2012b; Celsius, 2020; Lund et al., 2018). While the modern DH paradigm aims for lower supply and return temperatures, the housing stock in the UK may be a limiting factor in what flow temperatures can be achieved in future DH systems (Millar et al., 2019). If future DH development is limited to purpose-built buildings, then those systems could quite possibly achieve low flow temperatures. However, a large-scale uptake of DH would likely include many existing buildings and the UK historically has a low replacement rate.

This model assumes a flow-supply temperature, T_f, of 70°C, which is considered on the upper limit of what can be considered 'low temperature DH' (Best, 2018). A peak return temperature of 50°C is set, giving a minimum temperature differential of 20°C.

4.2.1 Operating modes

The possible operating state of the DHN's components over an hour is defined as one of three discrete modes:

1. The HP is off, there is no electrical input, and the heat load is met entirely by discharge from the TES. This can only occur when there is sufficient hot water in the TES.
2. The HP is on and covers the entire heat load (or its maximum capacity). The electrical input to the heat pump corresponds to the contemporaneous COP.
3. The HP is at full capacity and covers the entire heat load using the residual spare capacity to charge the TES.

A combination of modes in the same hour may also be possible. Such as in the case of an undersized HP and insufficient TES which is unable to cover the heat load. In that case the HP provides its full capacity followed by a discharge from the TES, mode 1 followed by mode 2. A schematic of the operating modes is shown in Figure 4.1.

4.2.2 Distribution network

Return temperature should decrease at part heat load to reduce pumping costs and heat losses. The relationship between return temperature and heat load is complex, depending on the heat interface units (HIU), characteristics of the space-heating emitters and of the hot water service heat exchangers as well as many other case specific factors. Achieving low return temperatures, T_r, is generally a good indicator of DH efficiency and allows smaller pipes and pumps. This reduces thermal losses and enables more energy storage in the TES due to a larger temperature difference (Crane, 2016). Historically, some DH systems were designed with fixed flow rates using bypasses around the heat emitters/exchangers. This results in higher than necessary flow rates and high return temperatures leading to inflated pumping costs and heat losses. For these reasons, variable volume-fixed flow temperature schemes are now the standard with all modern DH systems.

As a simplified approximation, a linear relationship with the DH load is used. Starting from a maximum of 50°C at times of peak heat load, as the heat load tends towards zero, so will the flow rate. The return temperature therefore tends towards the ambient temperatures for space-heating, around 15°C.

Return temperature at timestep i is given by (4.2), where L is load:

$$\mathrm{T}_{r,i} = 15 + 35(L_i/L_{peak}) \tag{4.1}$$

The mass flow rate, $\dot{M}_{DH}$, in the DH system can then be calculated using the return temperature from (4.2), by the specific heat of water c_w:

$$\dot{M}_{DH,i} = L_i/c_w(T_f - T_{r,i}) \tag{4.2}$$

In mode 1, there will be no electrical input to the HP and mass flow rate of discharge from the TES is equal to the mass flow rate of the DH. In mode 2, there is no mass flow through the TES and the mass flow rate from the HP is the same as the DH mass flow rate. Mode 3 is more complex due to the flows through the TES. We assume that the HP heat output Q_{HP}, is at the maximum HP capacity. The mass flow rate through the TES, $\dot{M}_{TES}$, is taken in the negative direction, with inflow charging the TES. $\dot{M}_{HP}$, is the mass flow rate through the HP's output heat exchanger and T_m is the temperature of the mixture of the return flow and TES cold discharge at temperature T_c. The state of the DH system can then be calculated from the following equations (4.3)-(4.6):

$$\dot{M}_{TES,i} = \dot{M}_{HP,i} - \dot{M}_{DH,i} \tag{4.3}$$

$$Q_{HP,i} = \dot{M}_{HP,i} c_w (T_f - T_{m,i}) \tag{4.4}$$

$$T_{m,i} = \frac{(\dot{M}_{DH,i} T_{r,i}) + (\dot{M}_{TES,i} T_{r,i})}{\dot{M}_{HP,i}} \tag{4.5}$$

$$M_{TES,i} = \frac{\frac{Q_{HP,i}}{c_w} + \dot{M}_{DH,i}(T_f - T_{r,i})}{(T_f - T_{c,i})} \tag{4.6}$$

4.2.3 Distribution losses

Reported distribution losses among current schemes vary greatly and losses above 40% for older DH schemes are not uncommon. Modelling distribution losses is complex even when a DH with a known topology is simulated. An inexhaustive list of factors that contribute towards these losses include piping length, material and insulation level as well as trench depth, ground temperatures, connection into buildings etc. as well as of course, flow temperatures (Vesterlund et al., 2013). Without explicitly including pipe sizes and making assumptions on insulation levels, distribution losses cannot be directly calculated. A reasonable assumption here would be to assume distribution losses in line with projections for 4GDH systems and current best cases.

Making comparisons between losses is complicated by the fact that there is no standard method of measuring or reporting losses (Masatin et al., 2016). A Nordic Council report estimates that distribution losses accounted for 10%, 11% and 12% of total energy produces in Finland, Norway and Sweden respectively with no indication of methodology (Patronen et al., 2017). Surveys in the UK have found average distribution losses for bulk schemes where the operator delivers heat to distribution points at 6% and non-bulk schemes where the operator delivers directly to

end customers at 28% (DECC, 2015b). It can be inferred from this that a large amount of losses are incurred at the connection points into buildings and internal distribution pipework. The DECC study also reported parasitic electrical losses of 1-4%.

A reasonable assumption to make is that future DH systems, with lower operating temperatures and flow rates appropriately designed and commissioned with optimal routing algorithms, and with a milder climate in general, would have losses in line with the best Scandinavian systems. This model will then apply a constant 12% distribution loss factor.

4.2.4 Thermal energy storage

Thermal Energy Storage has been a main component in DH systems for many decades. It has primarily been used as a short term/diurnal storage device in conjunction with CHP based heat generation. The construction and modelling concepts for TES as a mature technology are well established.

Tank TES (TTES) are normally insulated steel cylindrical constructions. They achieve stratification of water temperatures through the use of diffusers to avoid mixing of the layers with a small transition zone between them. Hot water can then be siphoned from the top, with a cold-water connection at the bottom of tank. Stratification makes calculating heat losses from the TES more complicated and CFD based simulations are often employed to model the losses (Kong et al., 2016; Ochs et al., 2021). The tanks maintain a constant mass of water with cold water being discharged simultaneously as hot water is delivered to the tank and vice-versa (Thomsen and Overbye, 2016).

Smaller tanks are typically constructed with a height/diameter (h/d) ratio of higher than one to increase stratification in the store. Larger stores however, tend to have larger diameters with a h/d ratio between 0.4 and 0.7. This is largely due to the engineering limits of the steel construction to limit the stresses from water pressure. The extra cost of construction and maintenance for thicker tank walls effectively limits the practical sizes of TTES. While the tanks are normally clad in a layer of insulation, heat losses also benefit from an economy of scale due to the geometry of a tank. Doubling tank diameter increases volume by a factor of 8 and surface area by a factor of 4 which effectively halves the percentage heat loss.

Estimates for the cost of TTES also show economies of scale. As the energy capacity depends on the temperature range with which the store is operated, numbers are generally presented as a cost per unit volume. Eames et al. (2014) show that smaller stores can cost upward of £390/m^3 while the DECC (2015b) evidence gathering on TES report suggests that this can fall to less than £100/m^3. The Danish Energy Agency (2018) shows that the upper limit for these economies of scales with TTES takes effect in the 10,000 – 15,000 m^3 range, beyond which it is more efficient to use alternative forms of large scale TES such as pit TES (PTES). They recommend the use of a power-law relationship with the volume, V_{TES}, to estimate capital costs where the cost per m^3 is $6705V_{TES}^{-0.47}$, as shown in Figure 4.2, but add that this is highly sensitive to the cost of steel which may also fluctuate with energy prices.

With the increased use of renewable sources for heat production, larger or multiple TES are becoming more common. The larger tanks can be found fully or partially buried or replaced by pit PTES that use similar operation principles (Ochs et al., 2009). Schematics of this are shown in Figure 4.3.

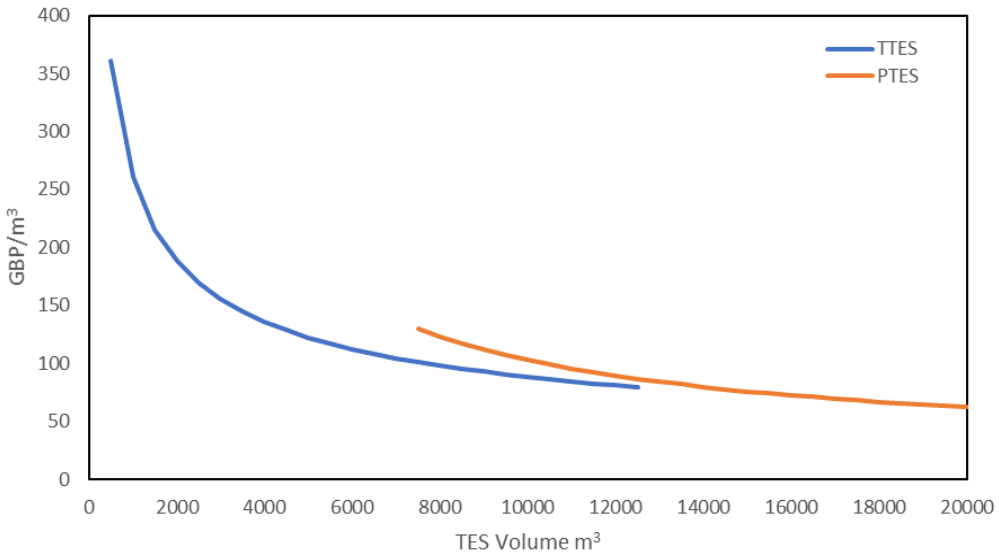

Figure 4.2 Costs per unit volume for TTES and PTES

PTES are essentially plastic lined reservoirs and have been demonstrated in several commercial projects such as the Vojens in Denmark, which at 200,000 m^3, operating at 80°C, holds over 12 GWh of thermal energy. Evidence from these projects shows unit costs of around £25/m^3 or £500,000/GWh_{th} (Danish Energy Agency, 2018; Eames et al., 2014). While PTES thermal losses appear comparable to those of well insulated tanks (Sørensen and Schmidt, 2018), the round trip efficiency is lower at 70% (compared to 98%). This is likely to improve with increased standardisation and commercial development. It should be noted however, that the costs shown in Figure 4.2 do not include the cost of land and 15% of these costs are dependent on local ground conditions. Construction costs per unit volume PTES is cheaper, with the cost per m^3 being $97359V_{TES}^{-0.74}$, and more practical than large scale TTES at larger sizes but the land requirements and ground conditions can be limiting factors and may not always be available near urban areas which can increase costs (Hesaraki et al., 2015).

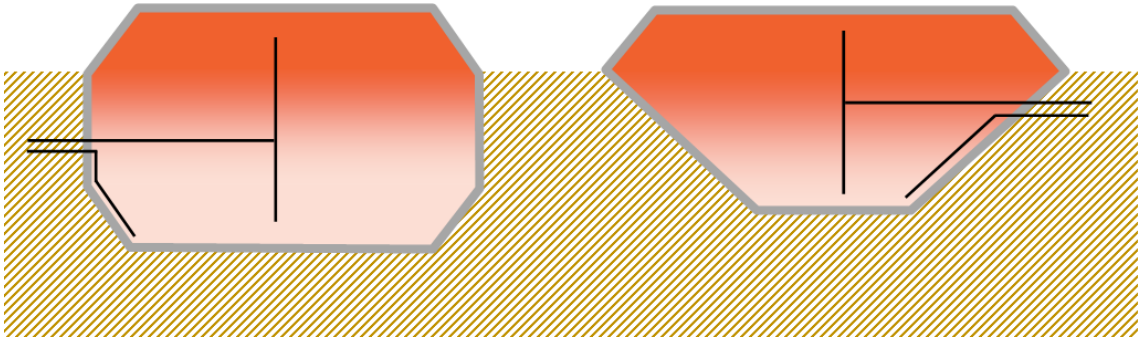

Figure 4.3 Schematics of partially buried TTES (left) and PTES (right) adapted from (Sørensen and Schmidt (2018)

4.2.5 TES implementation

The mass of hot water, $M_{h,i}$, in the tank at any time determines the state of charge and the flow rate, $\dot{M}_{TES,i}$, measured in magnitude and direction, charge or discharge, enables the state of charge to be calculated in the next hour, $M_{h,i+1}$. $T_{c,0}$ is initialised at 32.5°C and updated upon mixing with water at T_r entering the bottom of the TES while discharging during mode one. During mode 3, $\dot{M}_{TES,i}$ is taken in the negative direction and $\Delta M_h = \dot{M}_{TES,i}$ increases accordingly at T_h while $M_{c,i} = -\dot{M}_{TES,i}$.

Thermal losses, Q_{TES}, via conduction are estimated based on a cylindrical steel tank with h_{TES}/d_{TES} ratio of 0.5. Wall thickness, τ_s, is estimated using (4.7) assuming construction from steel (304) commonly used in such applications with a modulus Y_S of 207 MPa and a safety factor, SF, of 1.5

under ambient pressure, P_{amb} (Engineering ToolBox, 2005). The tank walls are clad with 300 mm of insulation, τ_n, (Danish Energy Agency, 2018) with thermal conductivity, k_n, of 0.05 W/mK, using stainless steel's thermal conductivity, k_s, of 20 W/mK. Heat losses are then computed as per (4.8) with conduction across the surface area, A_{TES}, using the mean average water temperature in the thermal store, $\bar{T}_{TES,i}$, as the internal temperature.

$$t_T = \frac{P_{amb} h_{TES} SF}{2Y_S} \tag{4.7}$$

$$Q_{TES,i} = \frac{A_{TES}(\bar{T}_{TES,i} - T_{amb,i})}{\left(\frac{\tau_S}{k_S} + \frac{\tau_n}{k_n}\right)} \tag{4.8}$$

$$\Delta M_{h,i+1} = \frac{Q_{TES,i}}{c_w(T_h - T_c)} \tag{4.9}$$

$$\Delta T_{c,i+1} = \frac{Q_{TES,i}}{c_w M_{c,i}} \tag{4.10}$$

In the absence of a more sophisticated model for the TES, losses are applied to the TES by subtracting the equivalent mass of hot water and increasing the cold-water mass according to (4.9). In the event where there is no hot water remaining, losses are applied by reducing t_c according to (4.10). Losses from the mixing of the hot and cold layers are neglected as this requires a more sophisticated model of the TES and fluid mechanics taking account of effects such as buoyancy.

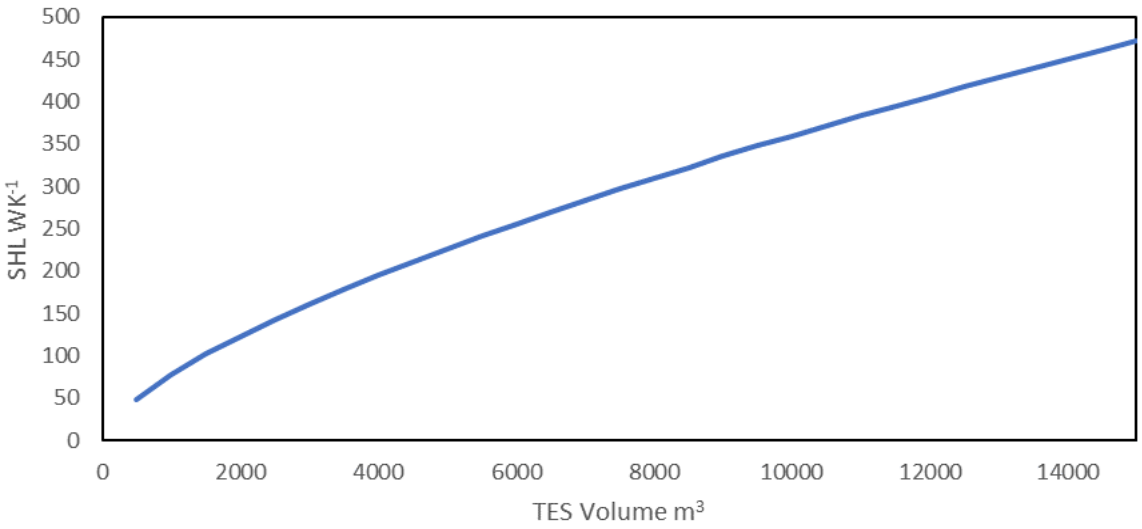

Figure 4.4 Specific heat losses from modelled TES

4.2.6 Heat Pump

The use of large-scale heat pumps in DH is not new but future high renewable scenarios may favour their use due to the decarbonisation of the electrical grid. Vapour compression cycle heat pumps have commonly been used in DH applications. Absorption cycle heat pumps are now becoming popular for use, in part due to their ability to provide cooling (Averfalk et al., 2017). Large heat pump installations often include multiple HPs in parallel that have multi-stage compressors, using a variety of refrigerants and heat sources (EHPA, 2019). Without needing to infer too much about the precise set-up, we assume a single stage HP defined by a maximum heat output capacity and a generic source temperature.

The COP of a HP is dependent on the operating conditions. The difference between the sink and source temperatures limits the maximum theoretical COP, termed the Carnot efficiency. The actual operational COP can then be estimated by applying an efficiency factor, η_{HP}, that accounts for losses from various factors of machine design. This efficiency factor can vary depending on operating temperatures and manufacturers often produce COP curves on a case by case basis for specific operating conditions and setups, applying quadratic regressions to obtain precise HP COPs (Ruhnau et al., 2019). If the operating conditions are relatively constant, then a constant η_{HP} can be applied. A range between 60-70% of the theoretical performance has been suggested as providing realistic HP COPs by an industrial heat pump manufacturer (Eckett, 2020).

4.2.7 HP implementation

Large HP installations can use industrial waste heat or other environmental heat sources. These are however dependent on local availability and may have a large regional variances with individual systems having higher COPs that are not reproduceable at all locations. Alternatively, sources could be some mix of borehole, water (sea/river/sewage) source, air, waste heat etc. but detailing designs for different resources at different locations is beyond the scope of this research.

The choice has been made to model a generic source temperature assuming it is reflected by the seasonal variation in ground temperatures. Ground temperatures provide a reasonable estimate of the seasonally varying input to the HP. Beardsmore and Cull (2001) have given the calculation of temperatures at depth from period surface heating as per (4.11). Source temperatures, T_S, were calculated at an assumed depth of z=3m and thermal properties of soil ε were estimated as per the data in Busby (2015).

$$T_{S,i} = T_0 e^{-\varepsilon z} \sin(2\pi t_i - \varepsilon z) \tag{4.11}$$

We model the COP as a fraction η_{HP} = 65% of the Carnot cycle efficiency. A heat exchanger between the HP condenser and the heat sink (the DH flow) is required to raise its temperature from the HP heat exchanger inlet (either the return or mixture temperature, T_r or T_m) to the flow temperature, T_f. The HP condenser at temperature T_{cond}, must then be higher than T_f to allow for losses across the heat exchanger which we assume is a counterflow heat exchanger. Most common refrigerants used in heat pumps have critical temperatures well above 70°C (and boiling point well below 0°C) therefore 75°C is selected as a constant T_{cond} (Zehnder, 2005). The log-mean temperature, ΔT_{LM}, across the heat exchanger is then used to calculate the COP from (4.12) and (4.13) where $T_r = T_m$ in Mode 3. The electrical input E_i to the HP during hour i required to output heat H_i is then simply $E_i = H_i / COP_i$.

$$\Delta T_{LM,i} = \frac{\left(T_{cond} - T_{r,i}\right) - \left(T_{cond} - T_{f,i}\right)}{\ln\left(\frac{T_{cond} - T_{r,i}}{T_{cond} - T_{f,i}}\right)} \tag{4.12}$$

$$COP_{HP,i} = \eta_{HP} \frac{T_{cond} - \Delta T_{LM,i} + 273}{T_{cond} - \Delta T_{LM,i} - T_{S,i}} \tag{4.13}$$

In reality, there would also be a heat exchanger between the ground and the HP evaporator but as a generic source temperature is being modelled and an appropriate Carnot efficiency is being applied, this may be simplified. Figure 4.5 shows modelled COPs alongside daily mean ambient temperatures and modelled ground temperatures using 2015 weather data. The COPs show seasonal variance as well as hourly variance according to T_r which is determined by DH load. The mean modelled COP across all weather and all years is 4.3 and corresponds to surveyed operational and modelled HPs in this temperature range (David et al., 2017; Pieper et al., 2019; Ruhnau et al., 2019).

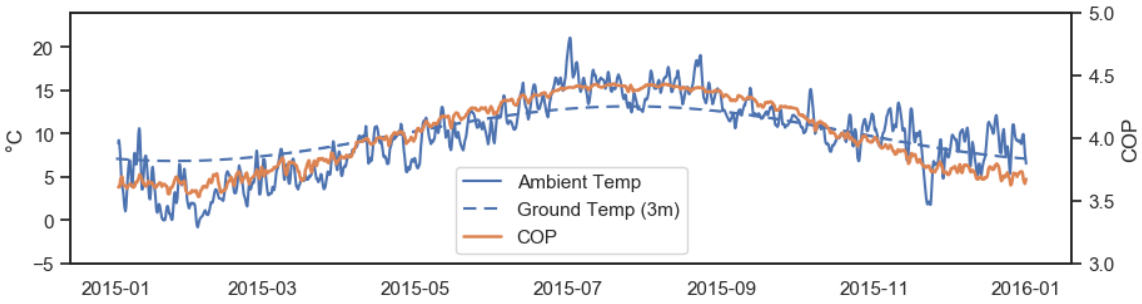

Figure 4.5 Modelled daily mean COPs compared to ambient and ground temperatures 2015

Previous designs of large heat pumps were not suitable for fast load changes and modulation, not least because frequency-controlled heat pumps have a more complex design. Modern industrial heat pumps are able to ramp up at 20% per minute and a minimum output 25% of capacity (Eckett, 2020). Over an hour this is negligible, hence no ramp limits are applied to the output.

4.3 Operating Algorithm Development

To assess the performance of the DH network and TES, it is necessary to evaluate how it will be operated. This section covers the development of operating algorithms that can be used to simulate operation based on the electricity costs from ElCoM and the heat loads from HeLoM. The operating algorithm selects one of the three operating modes to minimise operating costs while meeting the heat load at all times. In the event where heat load is partially met, a penalty cost is applied. This may occur if the HP has insufficient capacity or the TES has insufficient charge. A penalty is applied that is equivalent to the use of electric resistance heaters (i.e. COP = 1). The cost of electricity, C_E, to operate the HP is:

$$C_{E,i} = \left(Q_{HP,i}/COP_{HP,i}\right)P_{E,i} \tag{4.14}$$

DiHeM assumes that the DH operator has knowledge of the heat demand and the electricity cost during each timestep hour. The issue of lookahead and accuracy of forecasts will be addressed later. The costs shown in this section concerned with algorithm development are (unless otherwise stated) derived from the annuitised capital and operating costs of TES and HP (which includes electricity costs). A discount rate of 3.5% is applied to DH infrastructure capex (HM Treasury, 2018). The DH costs used and the sources from which they are derives are shown in Table D-1 in Appendix D. The initial exploration excludes the cost of the network for clarity as this remains unchanged.

4.3.1 Analysis of operating conditions

Electricity costs and heat loads have been modelled for the period 2010-2015. For simulation purposes and data presentation, it is useful to simulate from midyear to midyear to avoid having to begin in midwinter. Ambient temperatures and offshore wind capacity factors are the main drivers of heat demand and electricity costs in the NZ scenario. Thirty years of meteorological data for winter total offshore wind capacity factors (see chapter 2) and average winter ambient temperatures show a large degree of correlation Figure 4.6. Of the modelled years, 2010 has both the lowest total capacity factors and lowest average temperature (only 1985 was lower). The 2014-2015 period is the closest to an ‘average’ year in terms of temperature and capacity factors.

For economic operation, the worst circumstances are a prolonged run of high electricity costs coinciding with a period of high heat demand. For this analysis, the urban heat load (see chapter 2) has been scaled to a load averaging 1 TWh per year.

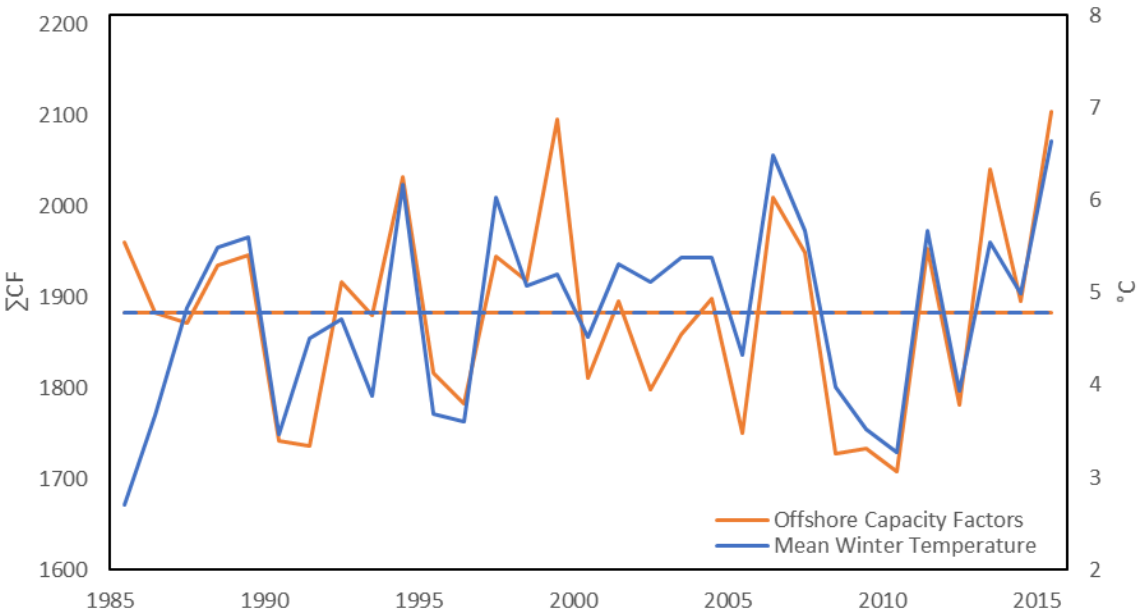

Figure 4.6 Comparison of winter season wind capacity factors and mean temperature

Figure 4.7 shows the five-day rolling average of the electricity costs and heat loads from ElCoM and HeLoM. For the period 2010-2011, the long run of above average heat loads coinciding with high electricity costs suggests this will be a challenging period and the DH must reliably meet the heat load in this time. A large TES and/or a well-designed operational control algorithm will be needed to minimise costs, and this represents the worst-case conditions in the simulated period. In contrast, 2012-2013 which also has high electricity costs and above average heat loads, there are long periods of sustained low costs that can allow TES to recharge for the following high-cost period. The success of such a strategy would again be dependent on the design of the control algorithm. 2013-2014 has both above average winter temperatures and capacity factors with no sustained period of high costs, lower peak costs, and below average heat loads. It represents the best-case year in the modelled periods.

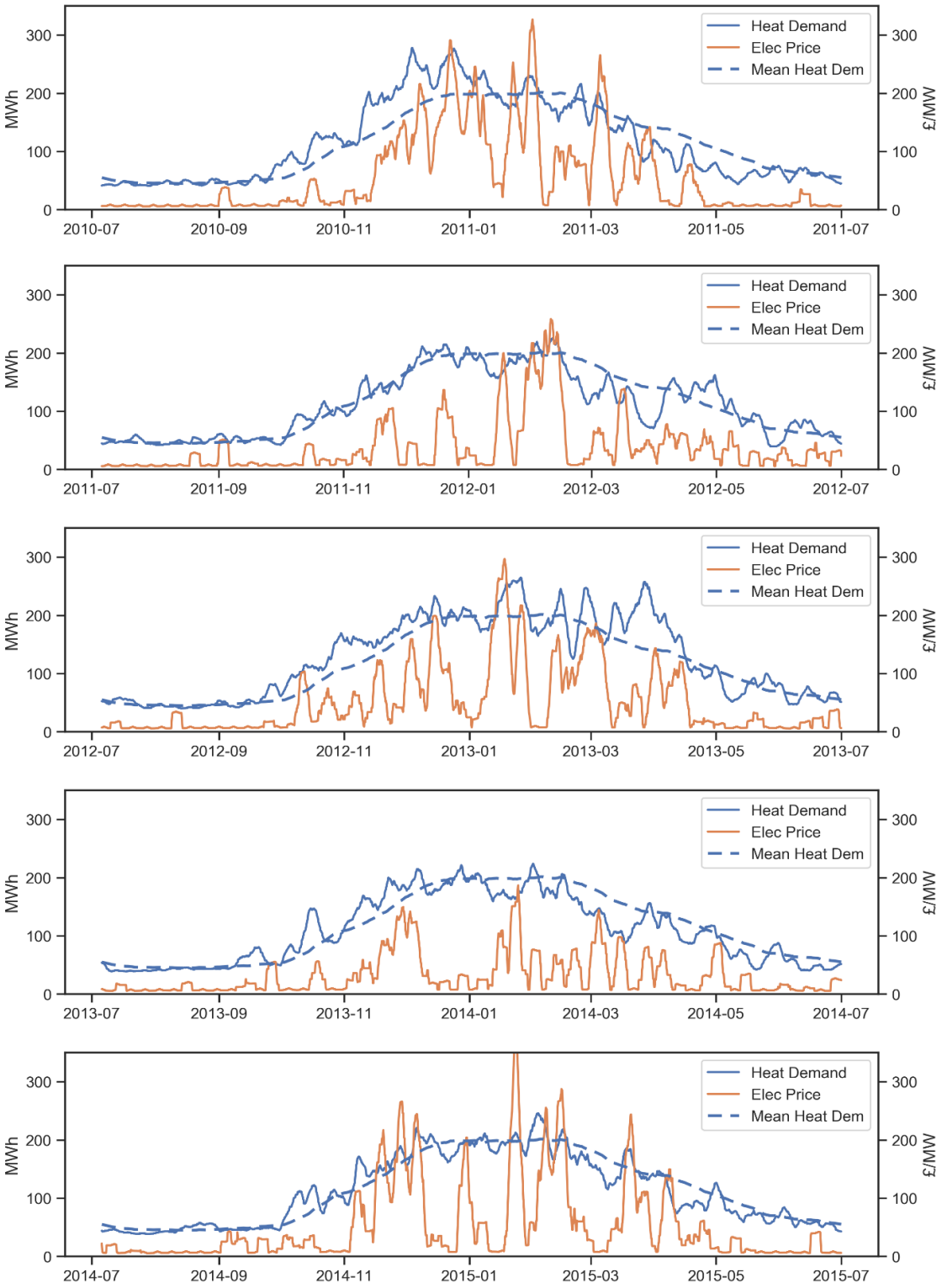

Figure 4.7 Five day rolling average of electricity costs and heat demand

To design an operating strategy, it is useful to consider the main parameters that influence its results. Figure 4.8 shows 12 hour rolling mean costs and demand for selected periods, highlighting the challenge with designing an operating algorithm. It is reasonable at this stage to assume that the operator has knowledge of demand and grid conditions or cost. Charging is most economical during hours with the lowest electricity costs (neglecting losses). A sufficiently sized TES and HP combination should be able to cycle the TES (blue and green arrows) from the beginning of December 2010 until the third discharge period which sees a long run of consistently high prices.

Figure 4.8 12 hour rolling demand and prices for selected periods

Basic algorithm (BSC): The simplest strategy would empty the TES and must then use the HP during expensive hours (red arrow). During the beginning of February 2013, there is a long period of low costs which can only be fully taken advantage of with a sufficiently large store. There are short periods between the peaks which may be enough to recharge the TES given a sufficiently sized HP. Towards the end of the month, there is a long stretch of high prices which would deplete the TES with a basic operating strategy.

Trigger algorithm (TRG): A more advanced strategy would charge and discharge during the local price peaks and troughs (blue and green dashed arrow).

Dynamic optimisation algorithm (DOA): A more complex strategy involves foresight of prices and heat load (see RDOA section 4.3.5) which enables charging at moderate prices to avoid very high prices and unnecessary charging in a later period. The matter is further complicated by TES losses. An optimum operating strategy is then highly dependent on the configuration of HP and TES. This determines both how long heat demand can be met by the TES and how quickly the TES can be recharged.

A look at the correlation between hourly electricity costs and demand in Figure 4.9 shows no clear relationship between the two. This highlights a significant challenge in devising a heuristic based operating strategy that is based on the present operating conditions alone. There is a large concentration of low prices across the range of heat demand but especially at lower demand which corresponds to the large amount of surplus hours in the summer.

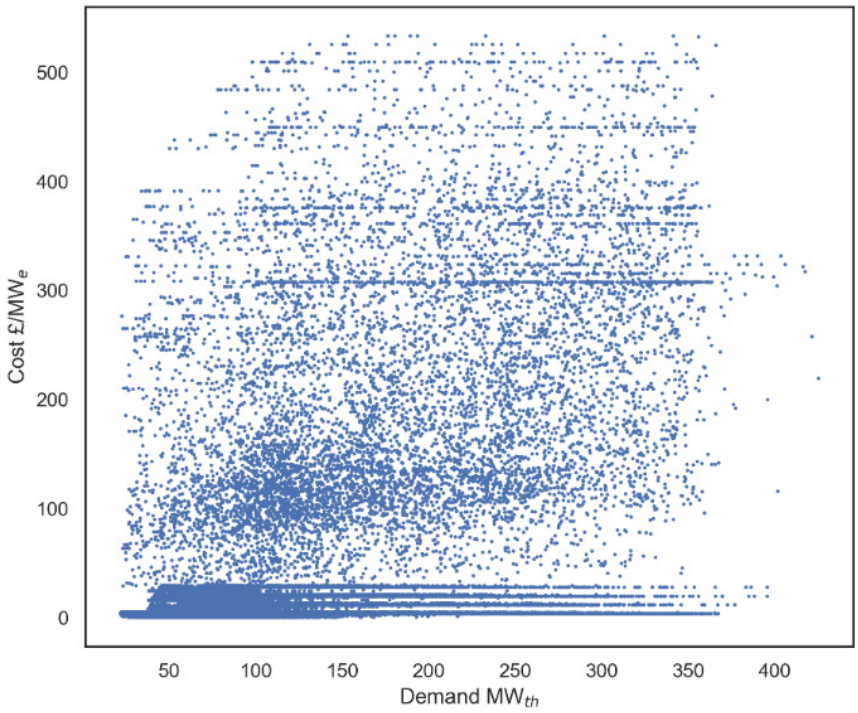

Figure 4.9 Correlation between heat demand and electricity cost

4.3.2 BSC algorithm

The first exploratory approach is the BSC algorithm. The BSC is a heuristic algorithm that operates based on present grid conditions with the assumption that grid can provide signals on the status of the grid: for example, if there is a generation residual surplus or deficit. This would be beneficial from the viewpoint of the electricity system operator encouraging shifting electricity consumption to surplus generation periods.

The BSC uses hour type as the operating decision whether to charge TES. The HP is operated based on unrestricted TES charging limited to surplus hours (up to HP power limit). The use of the HP is avoided during all other hours unless the TES has insufficient capacity to cover the heat demand.

The conversion between TES percentage of annual demand and number of peak hours for this DH heat load is shown in Table 4.1. All analyses from this point on were conducted assuming a network of 50 GWh per annum average demand. Figure 4.10 shows the effect of varying HP and TES using BSC. For the worst-case scenario period 2010-2011 the lowest cost range starts at around 1.5% of annual demand and a HP sized to 100% of peak demand (which occurs in 2010-2011) in comparison to the average period of 2014-2015 where the minimum occurs at a smaller HP.

Table 4.1 TES percentage and peak hours equivalence for modelled DHN

TES % of Annual Demand	TES number of Peak Hours storage
0.1	1
0.2	2
0.5	10
1.0	20
2.0	40

Looking at the hourly operation shows that the TES discharges during non-surplus hours before the higher peak prices are reached. The BSC has limited use and a more sophisticated method that utilises electricity or a lookahead is required.

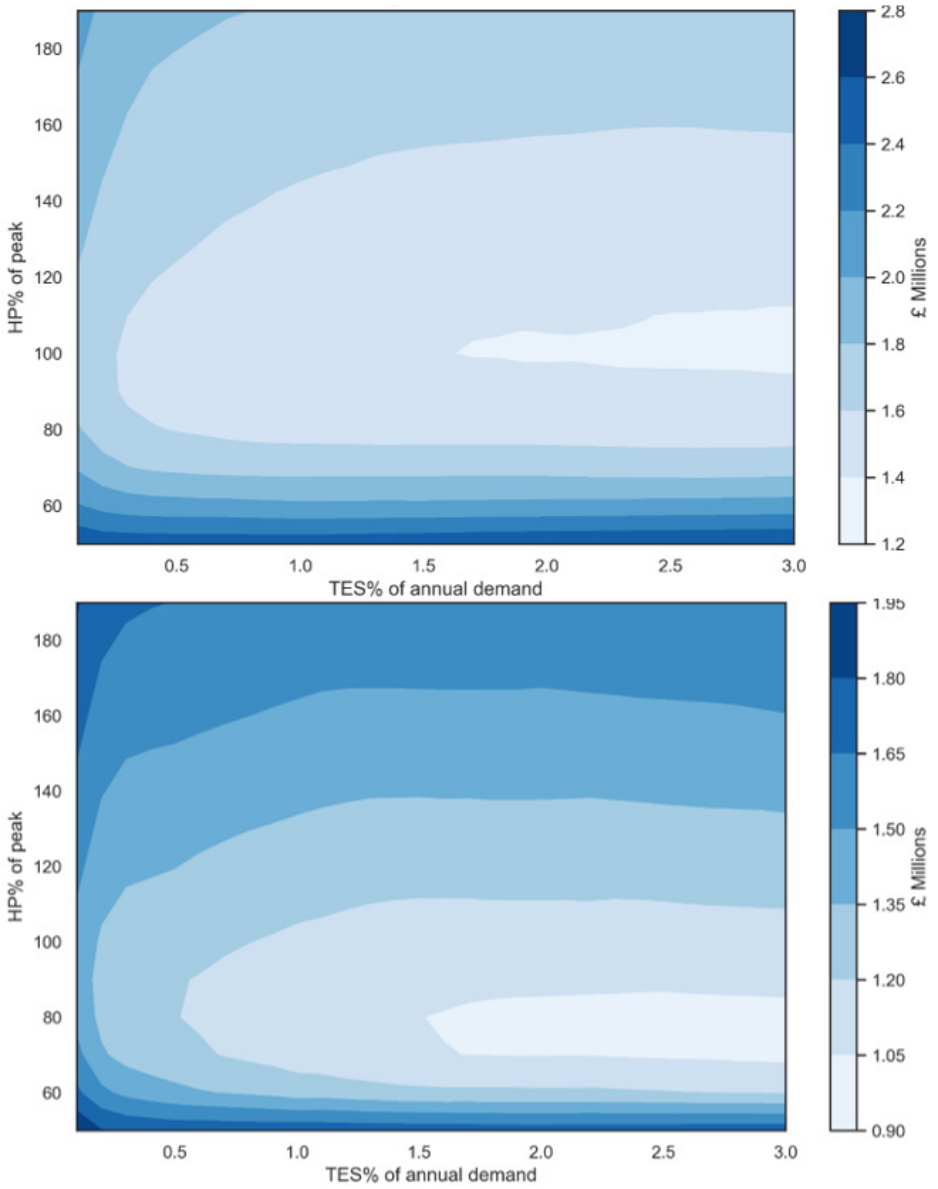

Figure 4.10 The effect of relative TES and HP size on cost (HP+TES annuitised capital) 2010-2011 (top) and 2014-2015 (bottom)

4.3.3 TRG algorithm

The TRG algorithm concept is an extension of the BSC in which it is assumed that the operator has knowledge of the current electricity cost. Another heuristic algorithm, it operates by a set trigger price below which the HP will try to maximise utilisation to charge TES and discharge the TES above this price. Electricity costs and hour type are linked but the trigger price method provides a greater control over when to charge and discharge as an intermediate value of trigger price can be set.

Figure 4.11 shows the effect of varying trigger price on the cost of electricity (a) and the total cost (b) with relative HP and TES sizes at the best trigger price found for each combination. The figure demonstrates that the optimal trigger price varies depending on the combination of HP and TES. Lower trigger prices are found for larger HP and TES as these give access to more hours and hence charging opportunity. The actual optimal trigger price was also found to vary depending on the period and season simulated with the lowest trigger prices found in the summer season. This indicates that the TRG can be extended through an adaptive trigger that can vary, based on operating conditions. Some form of lookahead could also be paired with this method.

These exploratory simulations reveal that larger HP, beyond 100% of peak capacity have little effect on the cost of electricity (Figure 4.11b) and as HPs do not exhibit economies of scale with size, this leads to higher total costs overall (Figure 4.11a). The electricity costs plateaus near a 100% HP size in the average 2014-2015 period. This can also be seen using the BSC where minimum costs are reached at around a 100% HP for the worst-case period and around 75-80% for the best-case period. Despite the cases where an undersized HP is economically beneficial, there is a strong case to use HP sized to peak capacity to ensure security of supply for the DH network. Further, larger HPs may have an adverse effect on the electricity network and may lead to higher connection charges. Therefore, the simulations presented in this chapter will proceed with a HP sized to 100% of peak heat demand.

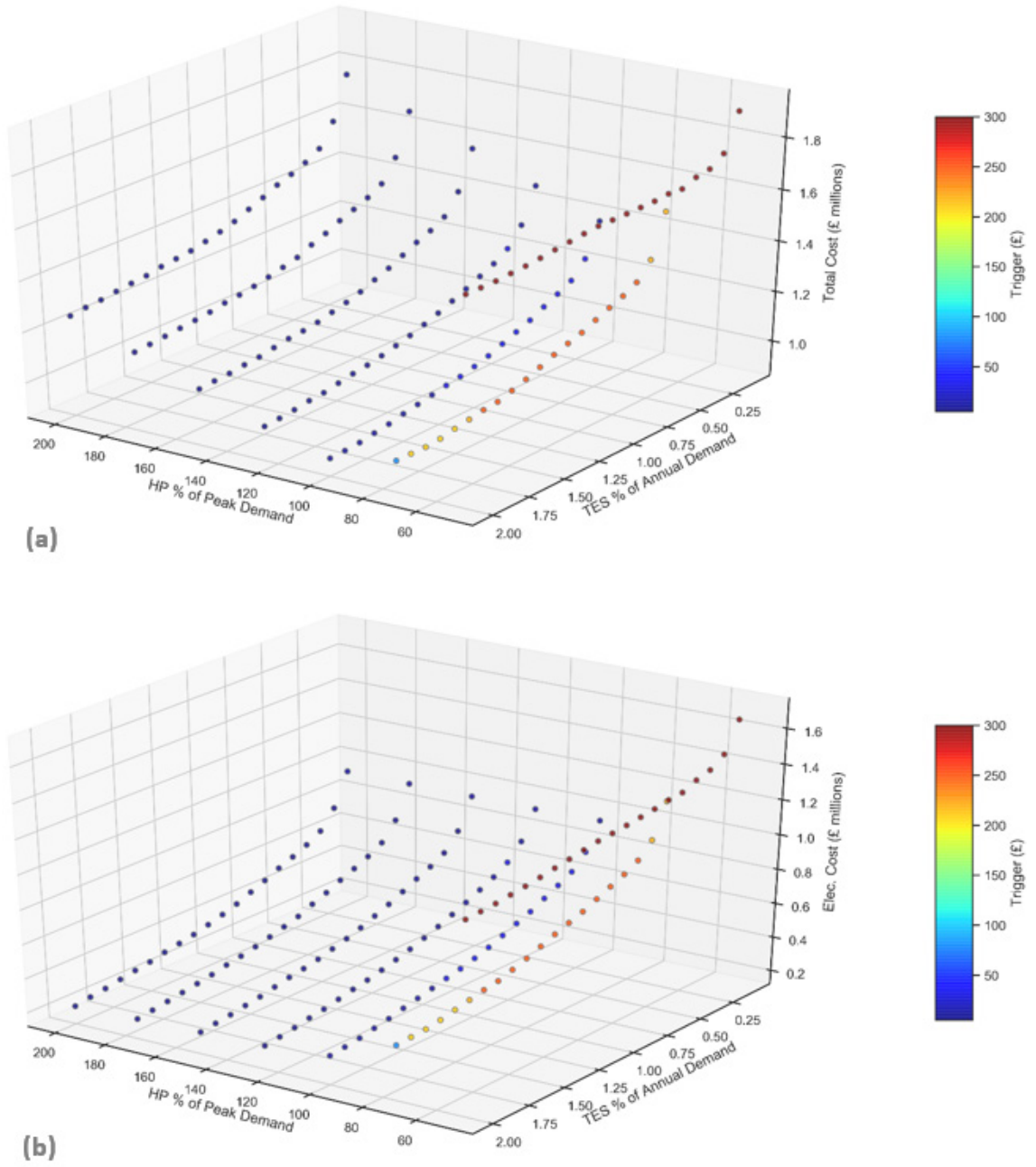

Figure 4.11 The impact of varying HP and TES with optimal Trigger prices on total cost (a) and electricity costs only (b) for the period 2014-2015

4.3.4 Dynamic optimisation algorithm

To assess how well the designed heuristic algorithms (BSC and TRG) work, we compare their results to the theoretical minimum costs using the Dynamic Optimisation Algorithm (DOA). The DOA utilises an open source operational optimisation library called Prodyn (Atabay, 2016) which utilises dynamic programming techniques to determine the optimal sequence of control modes to minimise total cost. The DOA is initially applied with perfect foresight over all defined hours with defined start and end states for a discretised system. Prodyn utilises dynamic programming (DP) techniques to determine the optimal sequence of control modes to minimise total cost. The DOA is applied with perfect foresight of demand and prices over all defined hours (in the year or period simulated), with defined start and end states for a discretised system.

Atabay (2018) explains how a model function such as the DH system must be discretised when using the DOA. The DOA is applied to the DH system model with discrete decision variables, U_i, used in the three operating modes for each time step.

The TES must also be divided into discrete levels, X, and the inputs and outputs to the TES, which are continuous variables, must also be discretised. A compromise must be made between accuracy and speed. Larger step sizes speed up the DOA at the expense of accuracy. The TES is divided into discrete levels, X, of size 1 MWh for all store sizes, so the number of levels depends on the size of TES. To avoid having to select a start and end state for the TES during midwinter, which would impact the operation, the simulations are started and ended midsummer from empty-to-empty charge state ($X_0 = X_N = 0$) as this has the least impact on the final result. The DOA applies the model function, ƒ, to calculate the state of the TES, X_i, at the next timestep.

$$X_{i+1} = f(X_i, U_i) \tag{4.15}$$

The algorithm computes the cost C_i of going from X_i to X_{i+1} when a decision U_i is made at a timestep for each possible decision and TES state (for example only those states that can be attained in a single timestep with the HP combination are computed).

$$C_i = g(X_i, U_i) \tag{4.16}$$

The algorithm then works forward from the defined state X_0, over N timesteps to finds the sequence, ϕ, which minimises total costs, J, over all timestep.

$$J_\phi = \sum_{t=0}^{N} g\left(X_t, U_t^\phi\right) \tag{4.17}$$

A comparison of the hourly operation of the algorithms highlights the simplicity of the heuristic algorithms. Figure 4.12 shows the operation of the algorithms for the same period with a 0.1% TES - this is shorthand for a TES capacity of 0.1% of annual demand (GWh). The DOA regularly cycles on a daily basis, charging during the night and discharging mostly during the daily peaks even during a long run of high prices. This is what would be expected of a diurnally sized TES. In comparison, the BSC and TRG approaches cycle far less often.

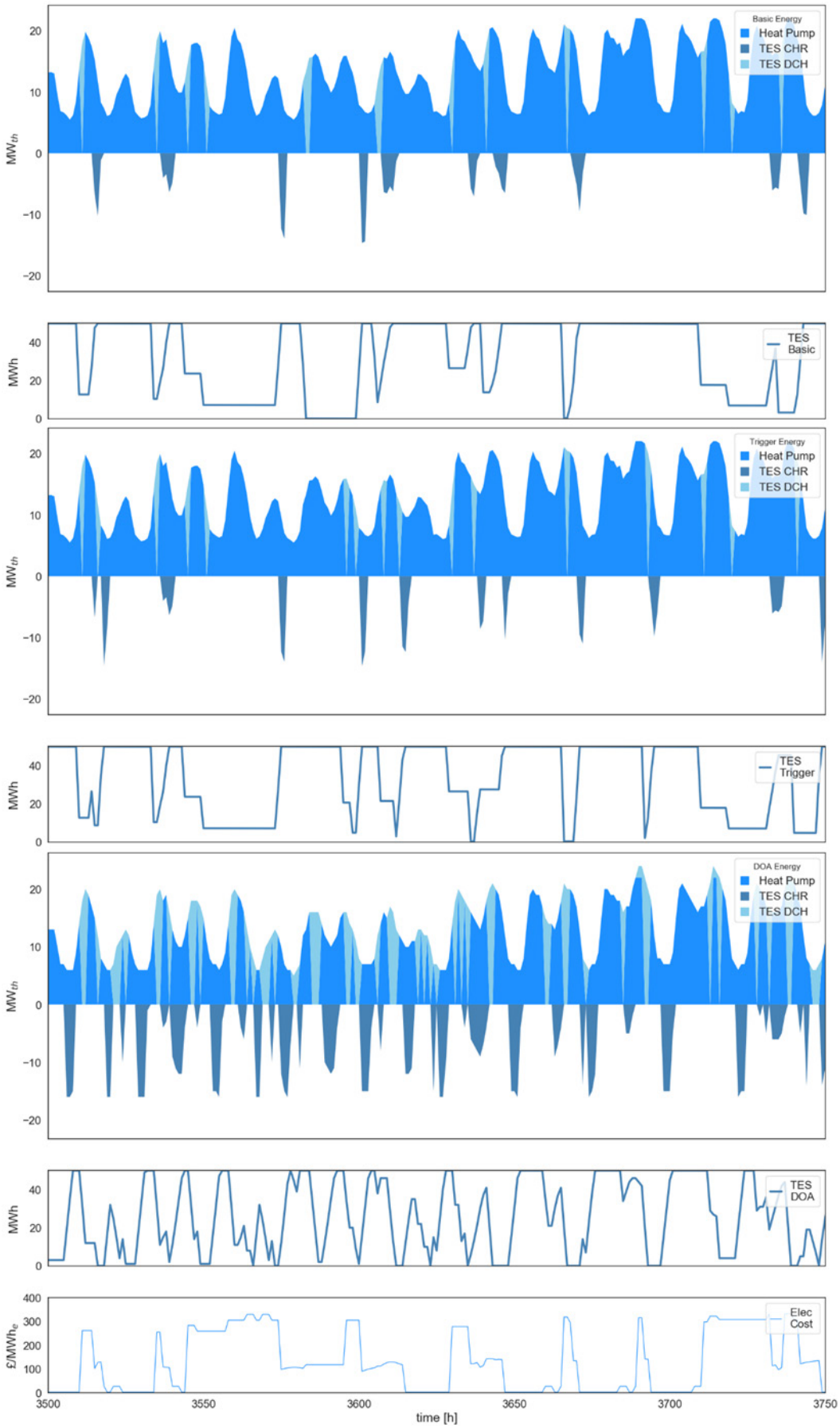

Figure 4.12 Hourly operation of 0.1% TES for BSC (top), TRG (middle), DOA (bottom)

Figure 4.14 shows the hourly operations of the algorithms with a large TES - 1% of annual demand. It is observable that the cycling of TES with the TRG roughly mirrors the DOA. These cycles correspond to the timings between prolonged high price periods which triggers the TRG algorithm. The BSC is less successful in recreating this behaviour. The DOA however, utilises the TES far more in each cycle, charging and discharge small amounts to avoid short-term price spikes. A diversion in the algorithm behaviour is observable from around the 6000 hour point onward. Here the DOA keeps the charge state of the TES low, charging only later in the low-price period while the BSC and TRG both immediately recharge to capacity. This can only be achieved with foresight of conditions while the BSC and TRG only uses present operating conditions. Another factor not considered by these is the hourly variation in COP. The COP varies based on seasonal variation and hourly operating conditions. Higher COPs normally occur during lower demand periods where the return temperatures are lower. This favours charging overnight where not only is demand lower and prices tend to be lower, but the COP is higher.

The effect of using large-scale TES on electricity costs during the best and worst-case periods using the DOA algorithm is shown in Figure 4.13. In the best-case simulated period 2013-2014, 2% TES eliminates all cost spikes and TES larger than this would be redundant in the modelled prices of the assumed high renewable system. But in the 2010-2011 period, 2% TES is unable to flatten the costs and they can only be reduced with larger TES capacities. Although the costs during a given hour aren't eliminated, Figure 4.15 shows how these costs are progressively reduced with increasing TES.

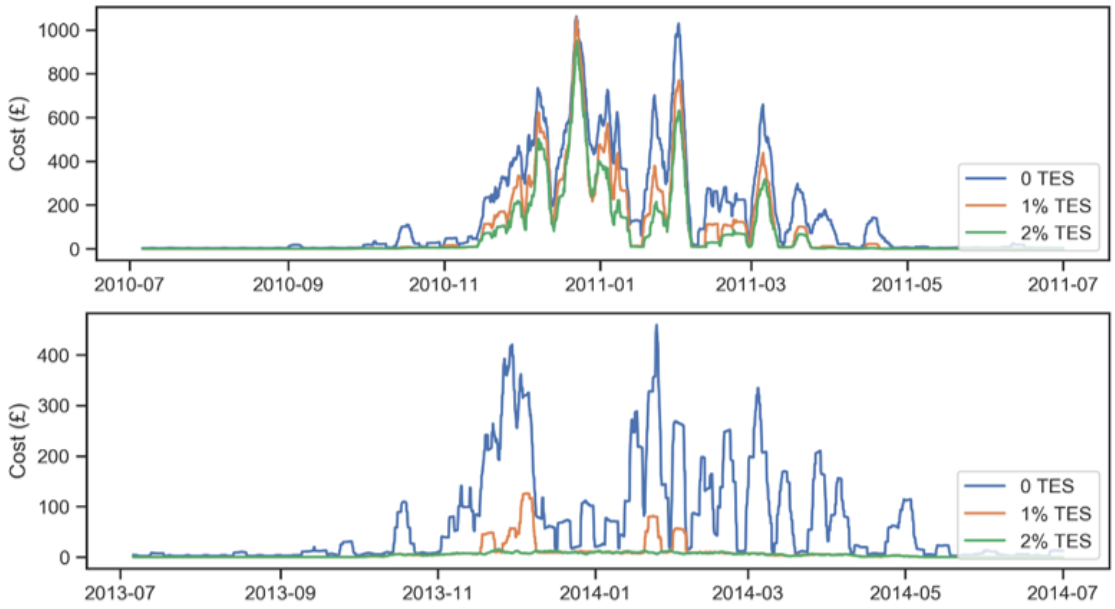

Figure 4.13 Comparison of five-day rolling average of electricity costs with various TES sizes using DOA for 2010-2011 (top) and 2013-2014 (bottom)

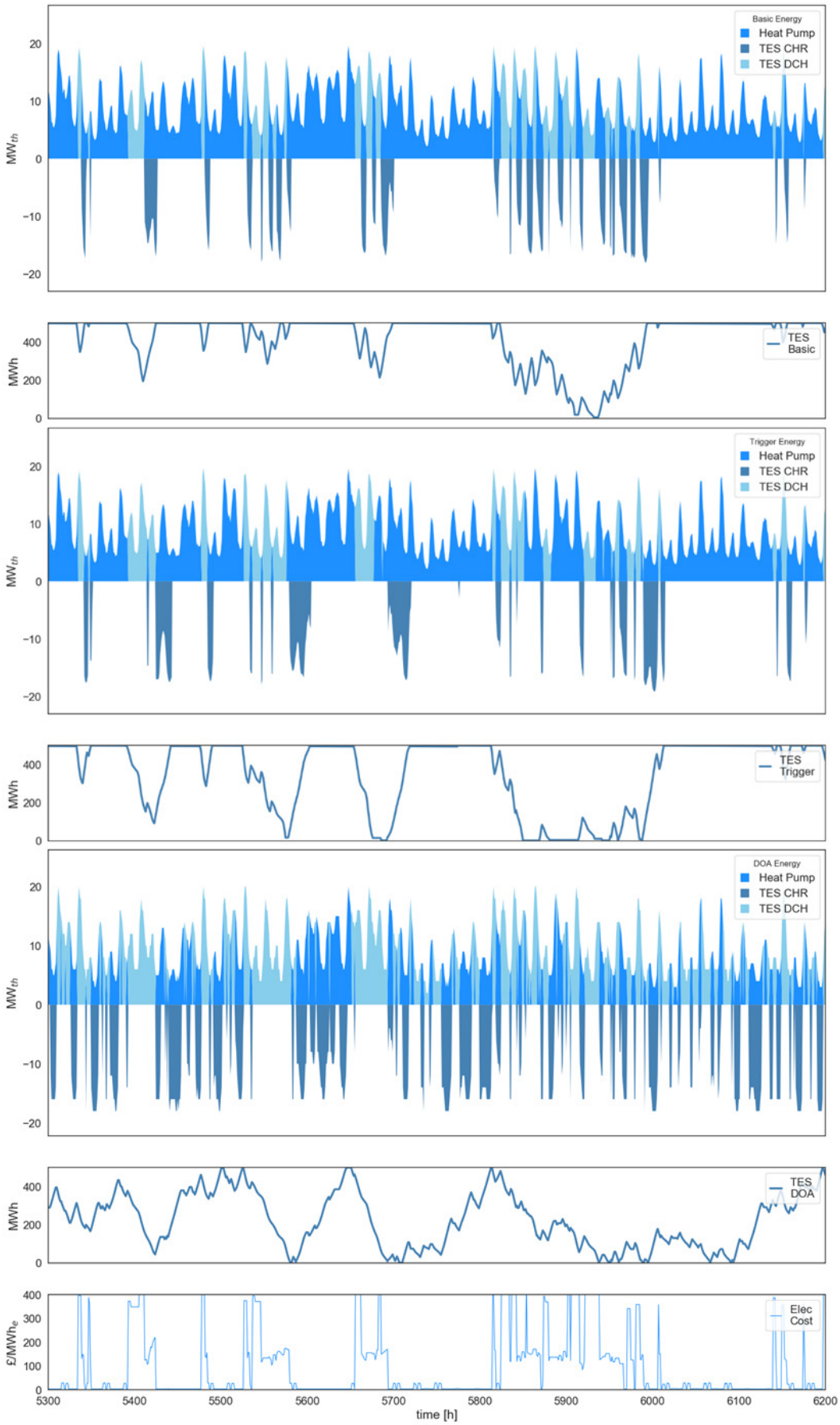

Figure 4.14 Hourly operation of 1% TES for BSC (top), TRG (middle), DOA (bottom)

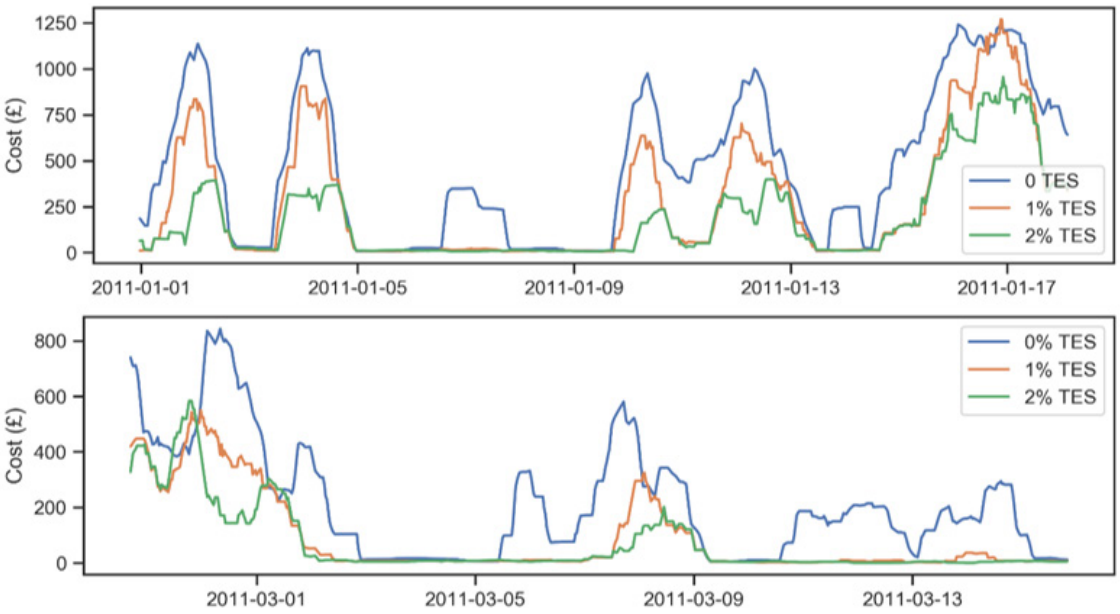

Figure 4.15 Comparison of 24-hour rolling average of electricity costs with various TES sizes using DOA for select periods

The DOA shows the optimum operating procedure for any size TES and operating conditions. It highlights the complexities involved with designing a rule-based heuristic algorithm. The operating rules and concepts differ depending on the size of storage to demand ratio. Development of a heuristic algorithm may have limited practical use except for efficiency of modelling. The practicality would also depend on that future data is actually available to DH operators and techniques such as machine learning could provide powerful tools to refine such heurisitic algorithms. The DOA provides a useful measure as to how well the BSC and TRG algorithms perform compared to a theoretical optimum. The DOA so far has perfect knowledge of the operating conditions, with foresight over all hours and hourly COPs. To ascertain a realistic indication of DH operation in real operating conditions, it is necessary to limit the information available to the DOA.

4.3.5 Rolling Dynamic Optimisation Algorithm

With the DOA, a specific starting and ending charge state must be set. If the ending charge state is left undefined, the algorithm will always empty the storage at the end as the minimal solution. In theory, a DH operator with perfect foresight of operating conditions of the entire year or winter period could perform the optimal combination of operating modes to minimise the annual operating cost. In practice this will never be achieved as beyond the immediate future, the accuracy of forecasts diminishes, and instead seasonal statistics will need to be relied upon. The DOA can be applied on a rolling basis with a limited lookahead time but a final charge state at the end of the optimisation must be defined. Here it is necessary to introduce the concept of lookahead time and forecast accuracy.

The National Grid currently bases their own generation and demand forecasts on Met Office data which they receive 4 times per day at hourly resolution for 14 days ahead (Caplin, 2017). From this data they can project wind and solar generation as well hourly demand from demand forecast models. Electricity cost projections using the method from ElCoM are dependent on supply and demand forecasting. National Grid produces, 2 day ahead and 7 day ahead hourly forecasts as well as 2-52 week ahead weekly peak forecasts. These are published via Elexon and indicative day ahead prices are also available on short term energy trading platforms. The Met Office describes its own forecasts in the 1-2 day range as a “detailed forecast”; 3-5 days as a “general picture”; 6-15 days as a “broad description”; and 16-30 days as an indication of probable weather conditions (e.g. warmer or wetter). They have found a 92% forecast accuracy

in temperatures within ±2°C in their week ahead forecasts and these will generally improve by the time DH would be scaled up (Met Office, 2017).

It is then reasonable to assume that a short term (up to seven day) look ahead is possible with high accuracy to forecast DH load. Beyond this there would be a good indication of relative conditions. Similarly, with the demand and generation forecasts, short term electricity cost projections can be made. The hourly operation over which the DOA lookahead is applied is then be restricted to 5 days (120 hours). Information from 7 day (168 hours) ahead hourly forecasts can be used to inform the endstate (at 120 hours). Beyond 7 days projections will need to be made.

The rolling DOA algorithm (RDOA) is an application of the DOA on a rolling basis with a limited time horizon lookahead period. As demonstrated by the DOA, the operating strategies of a small TES is different to a large TES. With a small TES, that is sized for diurnal demand, the operating strategy is normally to charge overnight during low prices and discharge at peak times or when both demand and prices are higher during the day. In this case knowledge of future operating conditions beyond a few days is of little use. With large TES, projections of conditions a week or further in advance are desirable to optimally utilise the capacity. For the aforementioned reasons above, the time horizon on which the RDOA is operated, lookahead is restricted to a maximum of 120 hours (5 days). Running the RDOA over this full lookahead period for small TES becomes redundant and experimentation has shown that beyond a point it gives the same results at the expense of computation times. The required lookahead duration is estimated based on the HP and TES capacity as well the mean winter DH load. The duration of storage in the TES, D_{TES}, can be estimated from the mean winter load $\bar{L}_{DH}$

$$D_{TES} = \frac{TES_{max}}{\bar{L}_{DH}} \tag{4.18}$$

An endstate for the RDOA lookahead must be defined, a TES level after a given number of hours cannot be more than the HP is able to attain in that time. The average time to recharge the TES from empty during the winter season, D_{CHR}, can be estimated in relation to the HP capacity minus $\bar{L}_{DH}$.

$$D_{CHR} = \frac{TES_{max}}{HP_{max} - \bar{L}_{DH}} \tag{4.19}$$

As the HP size to TES size ratio decreases, D_{CHR} will become larger than D_{TES}. In this case, D_{TES} must be set equal to D_{CHR} with a minimum operation over 24 hours and a maximum of 120 hours. The selection of the rolling final charge state is based on analysis of the DOA operation. We assume that the final charge state must be sufficient to cover demand in a projected period equal to D_{TES} beyond the RDOA lookahead, from all hours where the electricity price is higher than the trigger prices found in section 4.3.3.

Where the projected period is beyond the 7-day horizon of hourly forecasts, then the demand is extrapolated from the demand during the 'known' lookahead period. As this endstate is always in a future horizon it is never reached, but during intermediate time steps, the RDOA may indeed find it optimal to completely charge or discharge the TES. Where the projected period is beyond the 7-day horizon of hourly forecasts, then the demand is extrapolated from the demand during the 'known' lookahead period. After running the RDOA, the optimal control for the lookahead period is returned and applied only to the first 24 hours. The RDOA then moves forward by one day to re-calculate. The RDOA sequence and interaction of Prodyn with HeLoM is shown in Figure 4.16.

The TES levels over the period 2014-2015 for various TES capacities using the RDOA are shown in Figure 4.17. The smallest TES size shown, 0.1% annual demand or 2 peak hours shows constant cycling throughout the year similar to the DOA in Figure 4.12. The regular charge/discharge

frequency is maintained at 1% TES and the full capacity of the TES is regularly utilised in the heating season while the utilisation of full capacity reduces at 2% TES.

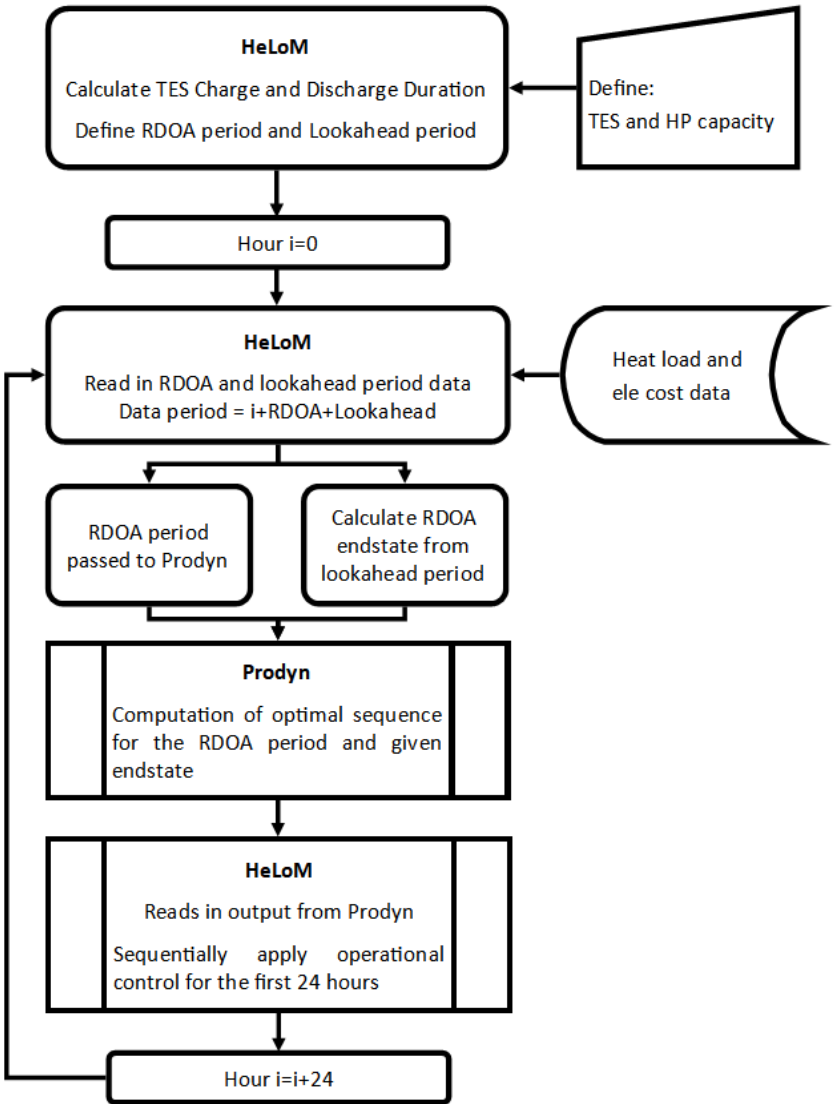

Figure 4.16 Implementation of Prodyn optimisation algorithm with HeLoM

Box 4.2 Challenges of developing the RDOA

Creating the RDOA procedure required much experimentation. This was mainly regarding the length of the period in which to run the DOA, lookahead period and endstate selection. Where possible, it was desirable to reduce the DOA run length to avoid unnecessarily lengthening computation times; though in practice this would not be an issue for DH operators.

The endstate is selected such that it is sufficient to cover the demand in the costlier hours during the lookahead period. The lookahead period must be adjusted based on the size of the TES. A long lookahead period for a small TES may lead to assignment of a constantly full TES and conversely a short lookahead period for a larger TES may underutilise the TES capacity. Another factor to consider was the size of HP. The endstate selected must be attainable with the HP size while also being able to meet demand. Defining the endstate incorrectly could lead to suboptimal operation

Through trialling several methods, the given definitions of charge and discharge duration were settled upon as this was found to give the best results for all HP and TES combinations. Variations of endstate such as a seasonally defined end state were considered, but this loses the strength of the lookahead ability. This was particularly in the case of unseasonal weather. Varying endstate and lookahead based on (the known) projected demand gave best results.

The full charge/discharge cycles of the TES at larger sizes correspond directly to periods of high electricity prices. With a HP capacity equal to peak demand, and a 1% TES, charging of the TES from empty to full takes between 1 and 2 days. With a 2% TES, this increases to 2 to 4 days. The doubling of TES capacity from 1% to 2% has little effect on the broader operating patterns in comparison to the operating pattern at smaller sizes. With a high forecast accuracy in the sub-2-day period, the RDOA operation of a 1% TES can be practically recreated in 'real world' conditions with a high level of confidence.

The TES operation can be split into sub daily cycles and multi day cycles. Figure 4.18 demonstrates the smallest cycle length with a 0.1% TES is a single diurnal cycle. It has a stronger twice daily cycle and less intense shorter cycles on the order of a few hours (lower frequency equates to longer cycle lengths). This shows that the small duration TES never holds a full charge for longer than a day with a small TES, often cycling multiple times per day, in response to daily loads variation. The 1% TES also demonstrates these sub-diurnal cycles, but also has longer multi-day cycles shown in the inset on a logarithmic scale with a 3-day and 7-day cycle showing strong signals.

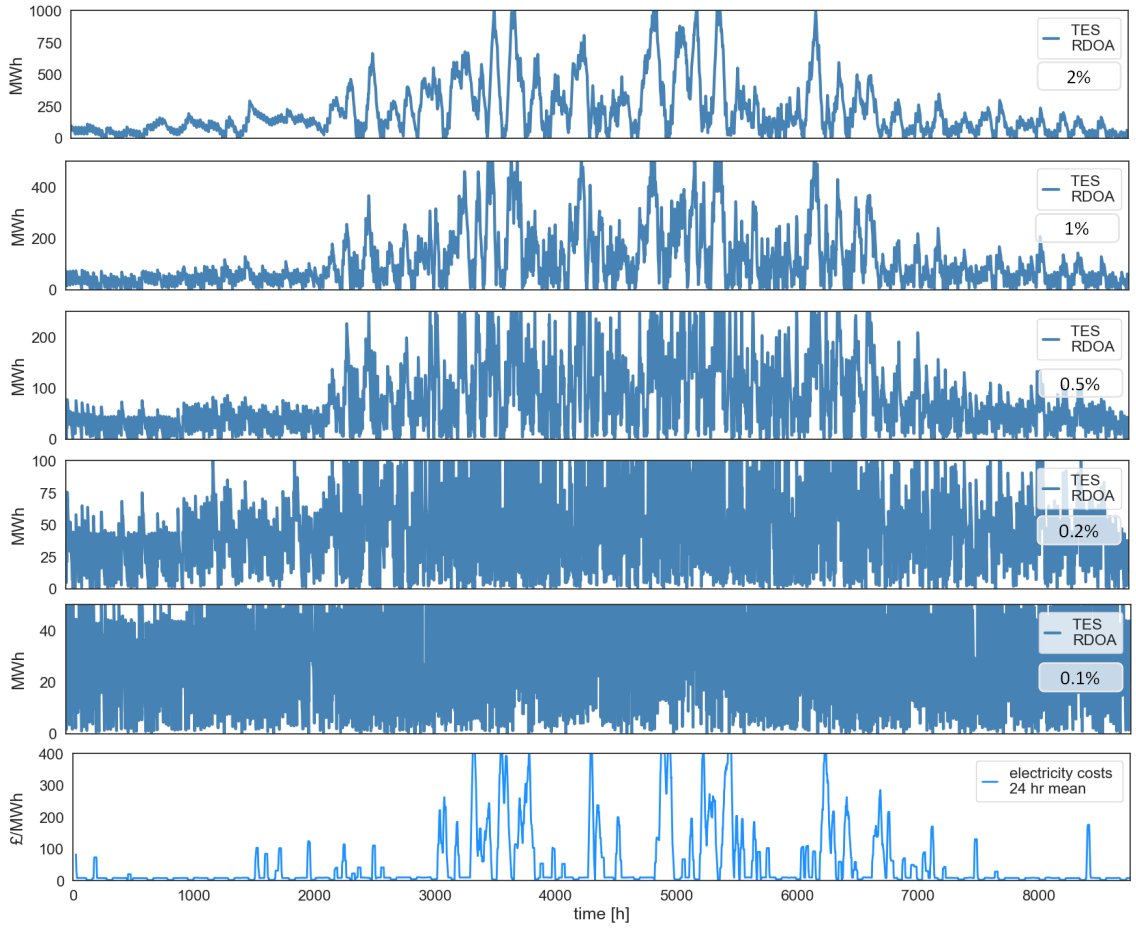

Figure 4.17 TES operation at various TES sizes using the RDOA for the period 2014-2015

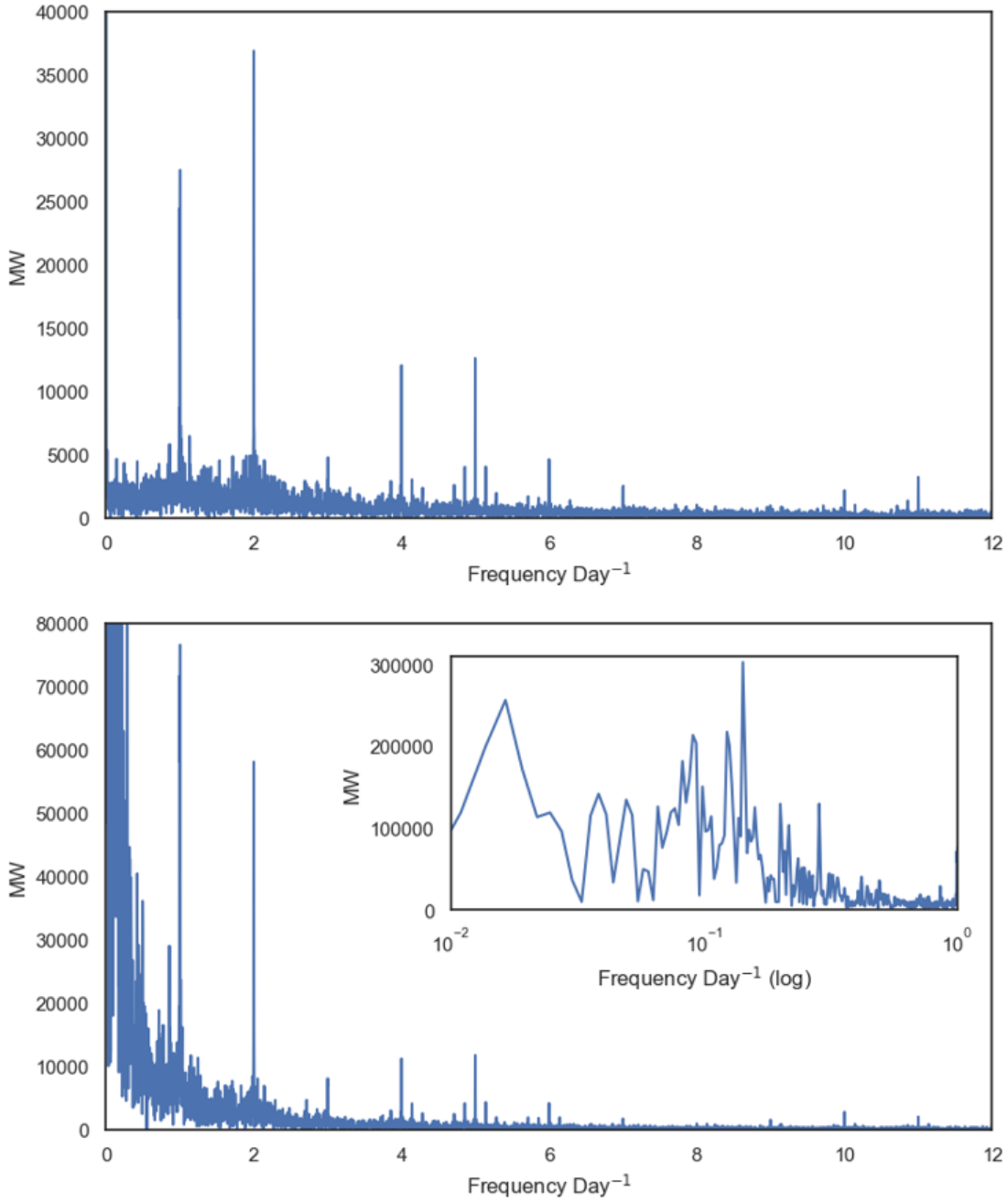

Figure 4.18 Frequency analysis of TES cycles using a 0.1% TES (top) and 1% (bottom) with super-diurnal cycles inset for the 2014-2015 period

4.4 Algorithm Comparison

Comparing the results of each algorithm in Figure 4.19 for the best-case and worst-case periods shows that the RDOA as expected outperforms the other BSC and TRG algorithms. While the trigger price compares well, it requires experimentation to find the appropriate trigger price. However, this shows that the TRG is useful for efficiently exploring DH configurations. It can generate results relatively quickly, with simple heuristics and known performance limits.

The RDOA is 18% higher than the minimum electricity costs given by the DOA. The absolute cost difference between the RDOA and DOA in the worst-case period is almost three times more than the best case. All the algorithms plateau at a level beyond which extra TES capacity provides little benefit except for in the worst-case period where the plateau is not reached with any

algorithm even with 5% TES size. However, there is a gradual rate of reduction and the costs at 1% TES is within 25% of the 2% TES size.

For the 2013-2014 period, the RDOA plateaus at over 80% higher than the DOA value with a difference of around £27,000 compared to 2010-2011 where the RDOA plateaus at just under 20% higher than the DOA value but with a difference of nearly £60,000. This highlights the difference in potential operating costs between a best-case year and worst-case year. Figure 4.20 shows the graph for RDOA in all modelled periods. It demonstrates that costs plateau around 1% TES for all periods except the worst-case period 2010-2011. The RDOA shows that for every measured year, the operating electricity costs for 1% TES were within 1.25 times the costs of a TES of double the size, suggesting that the best TES to annual demand ratio is in the 1 - 2% range.

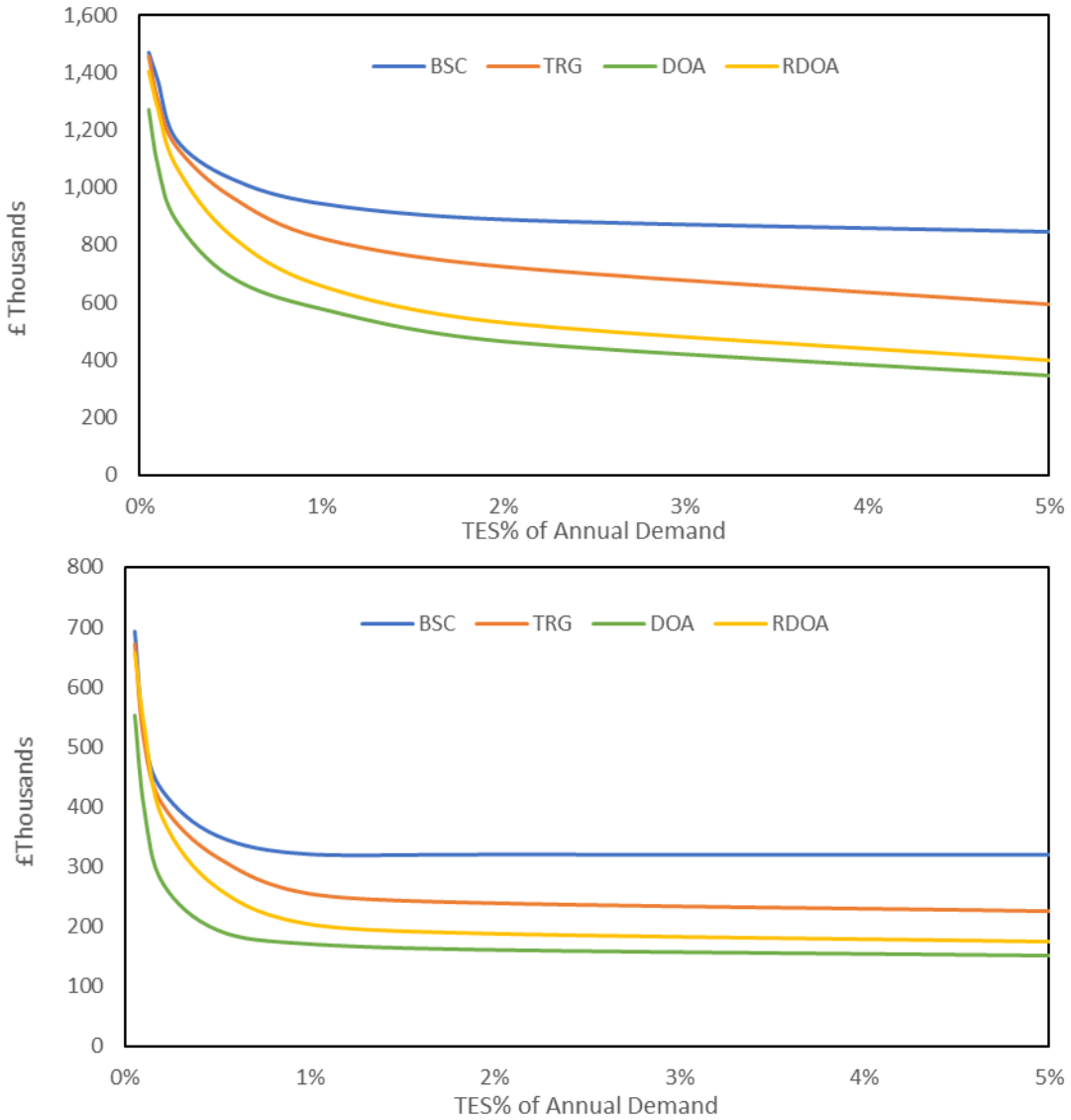

Figure 4.19 Comparison of electricity costs of all algorithm from the periods 2010-2011 (top) and 2013-2014 (bottom)

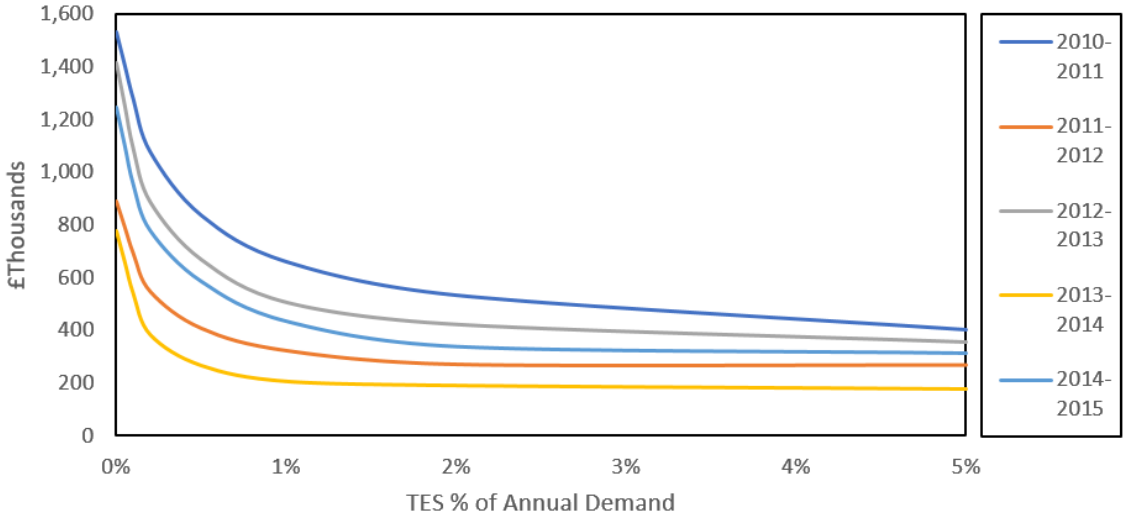

Figure 4.20 Operating electricity costs for each period using the RDOA

4.5 District Heating Network Configuration

The total annual DH operating costs inclusive of annuitised capital network, TES, HP, and electricity costs are shown in Figure 4.21. The medium range costs from Table D-1 have been used assuming a network of 50 GWh per annum average demand and a 22 MW_{th} heat pump sized to peak demand. The TES costs assumes economies of scale for all sizes and the electricity costs are the mean annual electricity operating costs for each TES value from all modelled periods. The minimum operating costs are at a TES value of 1.3% of annual demand. This corresponds to a levelised cost of heat (LCOH) of £88 per MWh_{th} and is around 11% saving in operating costs per year. The low and high-cost ranges were £50 and £128 per MWh_{th} of delivered heat. Using TES costs that are within the economies of scale range, the cost curve will remain the same at larger DH sizes and the LCOH will be preserved.

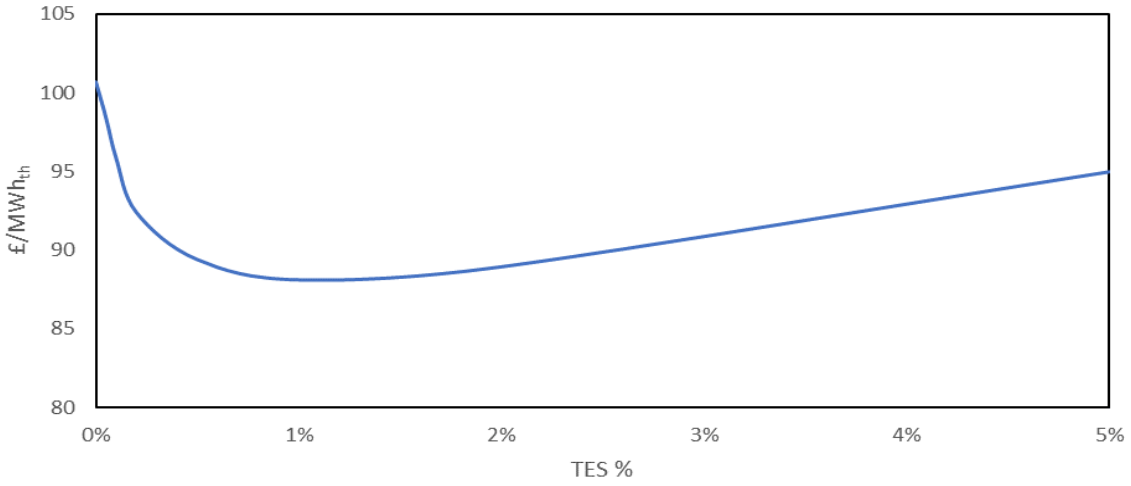

Figure 4.21 Total annuitised capital, O&M, and electricity annual costs per MWh of delivered heat for varying TES capacities

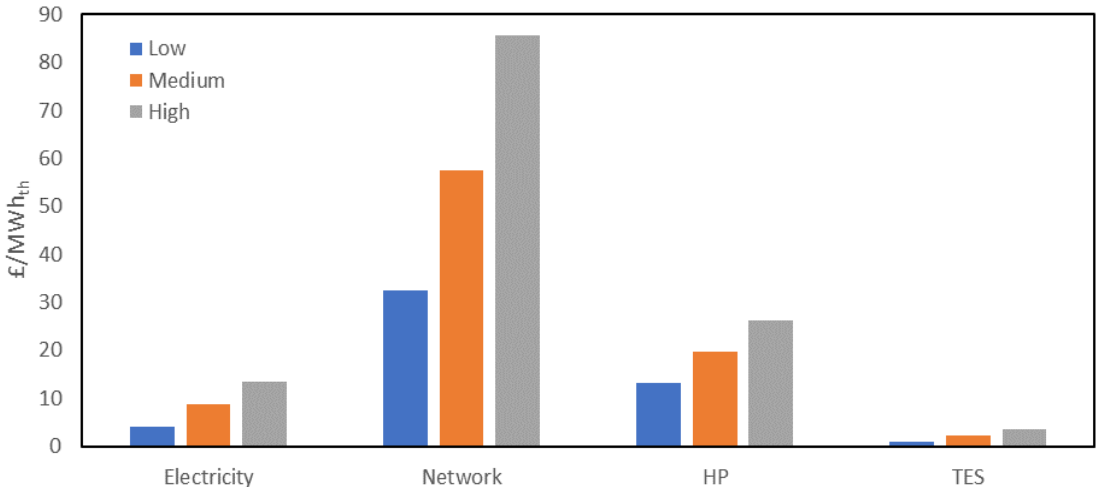

Figure 4.22 Comparison of annual component cost per MWh of delivered heat for Low, Medium and High cost sensitivity ranges

The component cost ranges are illustrated in Figure 4.22 where it can be seen that a large share of the costs come from the network itself. Previous estimates have shown that network costs amount to over 70% of total costs (ETI, 2018). The cost breakdown for the medium range in Figure 4.23 suggests that this is closer to 60% owing to the higher capital costs of HPs. Of the network costs, the majority of this comes from the cost of the heat connections, including the HIUs and heat meters. This has been found to be a key area of sensitivity with a wide cost range and the figures have been based on a limited number of UK installations. This is seen as a major barrier to deployment (DECC, 2015b). Other studies have shown the possibility for significant network cost reduction in the UK in comparison with Scandinavian DH systems. A report from Poyry proposes a possible 50% reduction (Macadam et al., 2009) while an ETI study shows up to 40% reduction through a combination of financing, experiential learning and supply chain management (ETI, 2018) and industry experts suggest a network capital cost reduction of at least 30% is a distinct possibility (BEIS, 2018b). With a 30% decrease in network costs in the medium cost range projections, the LCOH falls to £74 per MWh of delivered heat. By comparison, this is similar to a survey of heat prices from existing UK DH schemes where the average price charged for heat was £73 per MWh (DECC, 2015b).

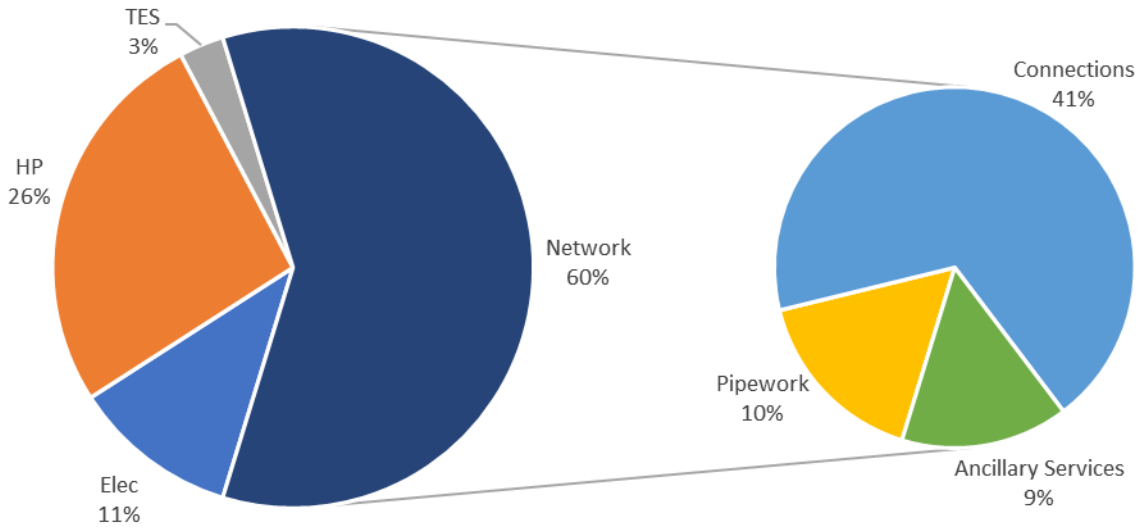

Figure 4.23 Medium case annual operating costs distribution

4.6 Discussion

This chapter documented the development of the District Heating Model – DiHeM, a DH energy model which enabled experimentation and optimisation of DH plant components. Various control strategies were trialled to operate the dispatch of heat from the HP and TES, ultimately settling on the implementation of a Model Predictive Control (MPC) operating algorithm. Existing DH studies were reviewed to identify appropriate methods and built upon in the modelling used for this study.

The modelling approach reduced the DH network to its fundamental components: a single heat load with fixed supply and variable return temperatures and physics-based representations of HPs and TES. This included thermal losses and dynamic COPs, both dependent on operating conditions. The DH model was designed to operate in three discrete modes per hourly timestep. While individual DH systems may indeed have higher source temperatures such as from sewage or waste heat, ground source temperatures have been used as a generic source temperature. These temperatures are less locationally dependent than other heat sources and are assumed to be representative of the average COP that may be achieved in the event of widespread DH deployment.

The flow and return temperatures have been modelled linearly assuming a variation between 50°C at peak and 15°C at no load, but rarely dropped below 30°C during the simulations. In reality, this relationship is never linear and there are many factors that are case specific, such as building internals, radiators, heat exchangers and the action of bypasses. Bypasses are used to maintain flow temperatures and normally result in heat losses being higher than assumed at low demand. This would result in higher return temperatures and would reduce the storage capacity of the TES. It also means that losses are a higher percentage of demand at low demand periods.

Distribution network losses were modelled as 12% multiplier of hourly demand. However, these losses should have been an additional constant loss to equal 12% annually rather than 12% of hourly demand. The impact of this would be negligible during the summer low demand periods as electricity prices are low and the TES does not operate but would lead to pessimistic results during high demand as it overestimates peak losses and therefore electricity consumption of HPs (when COP is typically lowest). Ultimately, further research is needed to model the dynamic network heat losses.

The inclusion of other sources such as geothermal or industrial waste heat in the modelling would result in superior COPs, reducing the electricity costs. The economics of other heat generators such as solar thermal have not been studied nor has the inclusion of cooling which was deemed outside the scope of this project.

4.6.1 Operation algorithm

Operational algorithms were explored for the control of TES and dispatch of heat. Heuristic based algorithms were first considered; the BSC algorithm which operated based on electricity grid conditions, and an improvement upon this was the TRG algorithm that uses electricity prices as the basis for control. The strength of these algorithms is the speed of simulation for modelling purposes. However, from analysis of hourly charging, the lack of any foresight used in these algorithms limited their performance.

Existing methods have been built upon to implement an MPC. This was used to both optimise dispatch with perfect foresight- DOA, and over a limited time horizon - RDOA. These algorithms used a type of MPC algorithm known as dynamic programming. Although it has several drawback including discretisation and computing requirements, it is particularly suited to the formulation used in DiHeM and could be easily adapted to operate the discrete modes of the model. The minimum achievable electricity cost is difficult to determine; however, a good indication of the theoretical minimum electricity costs can be estimated from the lowest hourly electricity costs

(during surplus hours, see Chapter 3.5) and average COPs attained by the system. In practice, this is difficult to achieve due to storage and HP limitations.

The RDOA provides a realistic assessment of the operating costs using a limited time horizon. It can be seen how close this is to the DOA costs and dependent on the weather year being simulated. Knowing the relative performance of the TRG compared to the RDOA can make it a useful algorithm to employ for quick results. The heuristic based algorithms can be improved upon extending it to use variable trigger price curves and including forecasting. This could easily extend to machine learning levels of sophistication where the algorithm continues to be refined based on continuing use data. With the use of the MPC algorithm, it was not worth pursuing such complexity and could easily be a doctoral research project itself. Meta-optimisation of the RDOA, both in terms of efficiency and accuracy, would also be a useful exercise. These limitations are relevant only to the modeller. DH operators will operate in real time and have access to greater computational power.

The results show that electricity costs rapidly fall with increasing TES capacity, up to around 1% of annual demand. Above 1%, costs continue to decline depending on the period measured but the reductions are diminished. TES capacities above 1% may be useful in bad weather years, where it was found that costs continue to diminish above 2% TES. If as a result of climate change, bad weather years and extreme winter weather were to become more common in the British Isles, then there may be a stronger case for larger capacities. This would require a better understanding of the local impacts of climate change and perhaps a complex statistical analysis of weather and costs. There are of course other options for storage with DH, such as biomass or hydrogen. With CHP, these have the wider benefit of producing electricity, but such an analysis was outside the scope of this project.

The electricity costs used are based on the assumptions of the marginal cost model – ElCoM for the NZ scenario. The reality of future costs and energy system are almost certainly going to differ from those presented here. The electricity costs do however simulate highly varying electricity costs. The modelling here shows that the majority of costs are concentrated in specific periods during the intersection of high costs and prolonged high demand. Larger TES capacities will help reduce these concentrated costs. This is also very dependent on the dynamic market structure, whether it operates on spot prices, day ahead prices and how far in advance contracting will be. DH operators may have separate contracts for electricity and there is the possibility that operators of smaller schemes with limited flexibility or TES may agree a Contracts for Difference (CfD) with electricity providers, protecting them from volatile electricity prices, but this would largely negate the benefits of flexibility gained via TES.

4.6.2 District heating cost and policy implications

The results have provided an indication for the range of LCOH that could be expected from DH in highly renewable scenarios as well as the expected operating costs for electricity import, which has rarely been accounted for in contemporary analysis. These figures could be used as input data to provide the basis for further analysis on the potential for DH along the lines of the studies presented in Table 1.2.

The current and projected capital costs of DH infrastructure show that TES costs account for a small fraction of this. There is some range in the annual electricity costs to achieve cost reductions but by far the largest determining factor are the network costs at around 60% of the LCOH. Various stakeholders suggest that this can be reduced by around 40% of current network costs. Depending on whether network costs decrease as projected, heat delivered by DH can still be financially competitive with consumer HPs and with current gas boiler heating assuming medium cost projections (Wang, 2018), although the latter is subject to the future cost of gas and associated emissions.

4.6.3 Practical Implications

Tank construction has a practical limit to due material properties and engineering constraints. Tank walls have to be built to withstand the pressure of a large volume of water. This pressure can be reduced by altering the ratio of height to diameter at the expense of land area. One way to avoid this is by partially burying the tanks, but this increase construction costs. With this method hybrid pit-tank TES with very large volumes on the order of 100,000 m^3 have been proposed (Ochs et al., 2020); but the largest tanks connected to DH remains around 15,000 m^3 while the largest PTES is 200,000 m^3. Underground TES may offer a route to larger storage capacities, albeit with high capital costs, and there has been shown to be substantial availability of underground stores in the UK, the locations of which, would have to be matched to areas of DH deployment (Gluyas et al., 2020).

The UK has historically used large gas holders built close to urban populations to store 'town gas' for use in buildings and the local gas distribution grid. They have become obsolete since the UK gas network transformed to use North Sea gas, but many still exist unused near town centres. At their peak, National Grid owned "over 500", SGN owned 110 and several other companies owned and operated gas cylinders around the UK with an estimated 750-1000 gas holders at their peak (Ram, 2015; SGN, 2021).

The UK now has many unused gas holders. The typical cylinder at full capacity was around 50,000 m^3. Assuming a DH network flow temperature difference of 55°C, a 15,000 m^3 TES stores just under 1 GWh and combined with an energy centre, could serve a DH with a 100 GWh annual demand. The large gas holder in Kennington, London (pictured in Figure 4.24) is 60m diameter with a minimum land area requirement of 2827 m^2. A TES of 1:2 ratio occupying the same land area would hold a TES of over 80,000 m^3. This would have a capacity of over 5 GWh (at 55°C temperature difference). The area occupied by 750 gas holders would allow construction of around 3.75 TWh worth of TES which can serve DH with aggregated heat demand of 375 TWh, which is over half of the low temperature annual space and hot water demand for buildings in Britain.

While it is highly unlikely that this level of DH will be constructed in the UK, and of course this needs to be spatially distributed and co-located with areas of high demand, it is an indication that the potential for low-cost DH networks is not limited by area for TES. The largest uncertainties arise from the cost of land to construct large TES. The costs of land in urban areas will not be trivial and these costs, including the cost of the building which house the energy centre have not been entirely factored in as these are highly location specific and may greatly impact the capital expenditure.

Figure 4.24 Aerial view of the Kennington gas holders (Google Maps, 2021)

4.6.4 Chapter conclusions

While TES capacity of around 1% of annual demand (corresponding to roughly 20 hours of peak demand) is found to minimise annual costs, the reality is that these costs represent a small fraction of the overall costs of heat from a DH system. The TES and associated electricity costs form around 12% of the final cost of delivered heat. As has been emphasised in the literature and by key stakeholders, there are far greater gains to be made by focusing on reducing network costs. This may be through better design and construction methods, supply chains or financing methods.

Minimum costs being achieved at 1% TES suggests that if this capacity is implemented and DH is widely deployed, then there is significant operational flexibility to be gained for the electricity system. This figure is also dependent on the fractions of wind and solar power deployment and the capacity factors they may be able to achieve in future. With the ability to shift demand by over 4 days at this TES capacity in the modelled NZ scenario, electricity peak loads can be reduced, and DH can facilitate the integration of variable renewable electricity.

The DH design and operation in this chapter has reflected the case of DH-HP operation being non-marginal upon the electricity system. If DH deployment is going to increase and become a major component of the GB energy system, then the operation of DH will at some stage become marginal on the electricity system, altering electricity costs and in turn, the operation of DH.

5 CONCLUSIONS: A SYSTEM PERSPECTIVE

5.1 Thesis Summary

The motivation of this research began with identifying the need to decarbonise heat supply in the UK. As a result of the electricity grid decarbonising, electrification of heat is a promising method of achieving this. With heat pumps, district heating can potentially deliver a considerable amount of electrified heat to urban areas. It can also provide a beneficial role in the electricity system by providing greater flexibility and COPs compared with individual heat pumps. To understand this role, we first needed to identify how DH may be designed and operated according to the requirements of a future system. With reference to the research aim and questions in section 1.4.1:

> *To what extent can DH with heat pumps and TES exploit the variability in demand and electricity prices to minimise operating costs and how should they be designed to achieve this?*

This has necessitated the development of a series of models where this thesis has:

1. Developed HeLoM to model the projected urban heat load for DH
    - Where the modelling comprised of building stock data and areas of highest heat demand density to provide an estimate of an urban DH demand load profile.
    - Similarly estimated the national (GB) heat load profile, contrasting the output to similar modelling of the 2010 total and peak demand.
    - Differences between the normalised urban and national demand duration profile were found and more significantly, the peak to trough ratio of the urban demand profile was lower than the national, indicating that the urban demand has a flatter demand curve.
2. Created ElCoM to simulate the electricity system
    - Utilising an existing net zero compatible scenario from National Grid which included a high fraction of electrified heat and DH deployment.
    - This was modified to 100% electrified heat and the generation and storage capacities were suitably adjusted to maintain the peak demand to renewable generation and storage capacity ratio such that it provided a security of supply where 98% of demand is met directly with renewable generation or via storage.

- A novel methodology was devised to simulate the variability in electricity prices based on marginal generation costs with distribution and transmission losses, finding strong seasonality in a highly renewable system.

3. Combined the outputs of HeLoM and ElCoM in DiHeM
   - And implemented an optimisation algorithm to control the dispatch of heat from the HP and TES with a finite time horizon. The finite time horizon resulted in costs 20% higher than a perfect foresight algorithm.
   - It was found that a TES capacity equivalent to around 1% of annual heat demand is sufficient to minimise operating costs with a HP sized to peak demand.

5.2 District Heating and the Electricity System

This thesis has achieved a modelling system that allows further exploration of DH for given scenarios. A question remains concerning how DH can fit into the wider system and what role it can play in it. We can explore the effects of large-scale DH deployment in several ways:

1. Replace Consumer heat pump electricity demand with an equivalent fraction of DH electricity demand. With this we can observe the impact on annual electricity consumption and peak electricity demand via:
   a. The effect of COP difference
   b. The effect of load shifting via TES
2. Integration of ElCoM and DiHeM to observe the impact on renewable generation surplus and deficits from:
   a. The co-operation of TES and grid storage
   b. Varying grid storage capacity on the system

5.2.1 Substitution of demand loads

By simply replacing a fraction of consumer HP electricity demand with the equivalent DH demand, we can begin to explore trends associated with the growth of DH. The ability to shift demand with TES means that the DH hourly load profile will not be a simple translation of the existing consumer HP profile attained through enhanced COPs. Figure 5.1 shows the impact of replacing 10% of consumer HP demand with DH. This results in a 3% decrease in annual demand of electricity for heating, due to a combination of enhanced COPs and lower transmission losses and 10% reduction of peak demand due to TES shifting the entire DH load away from the peak.

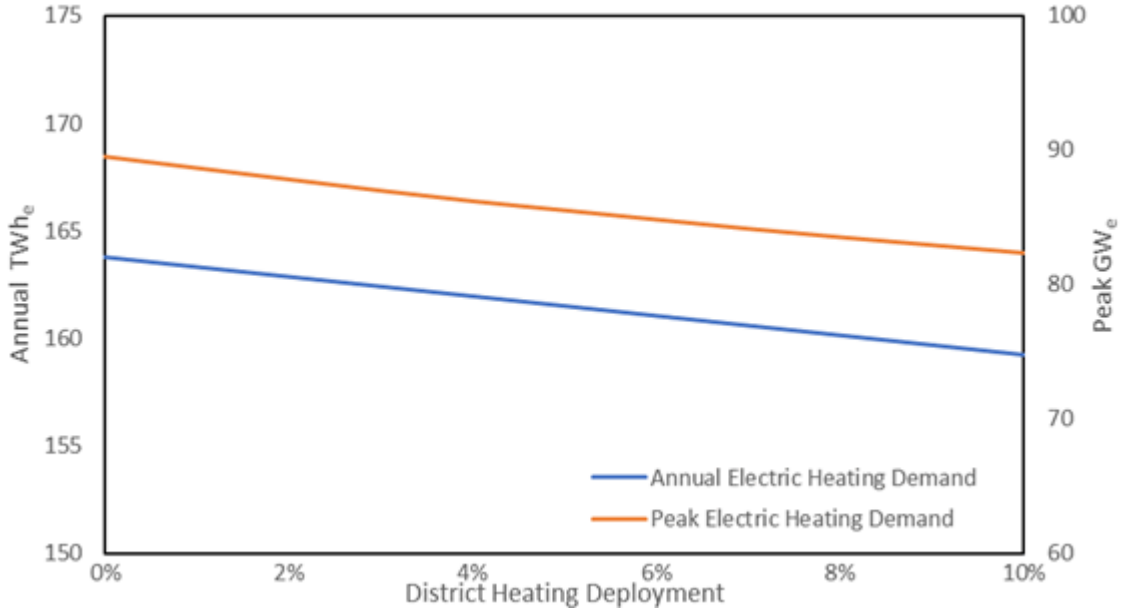

Figure 5.1 Peak and total electricity demand with DH deployment

5.2.2 System electricity costs

The resulting change in marginal electricity costs are shown in Figure 5.2 for each simulated year as DH expands to 10%. The annual mean marginal costs remain largely unchanged, but peak costs rise by varying amounts depending on the year as there are fewer dispatchable hours to recoup fixed operating costs (we can see in 2010, the year with most dispatchable hours, has the lowest peak generation costs). Around 80% of hours actually remained unchanged, these were almost exclusively surplus hours. Around 6% of hours reduced in costs and 14% increased. The average charge and discharge hour costs increased, as do the peak costs (maximum discharge hour costs). This is due to the reduced revenue from dispatch (flexibility) hours which constitute around 12% of all the hours. The increase of these costs is offset by the large decrease in costs during the extra surplus hours where the marginal generation costs are very low. Given most hours remain unchanged in cost and only the previously high-cost hours increase in cost, it may be that hourly DH operation, based on electricity price signals from the grid, would not be significantly altered given mass deployment other than during a minority of specific hours.

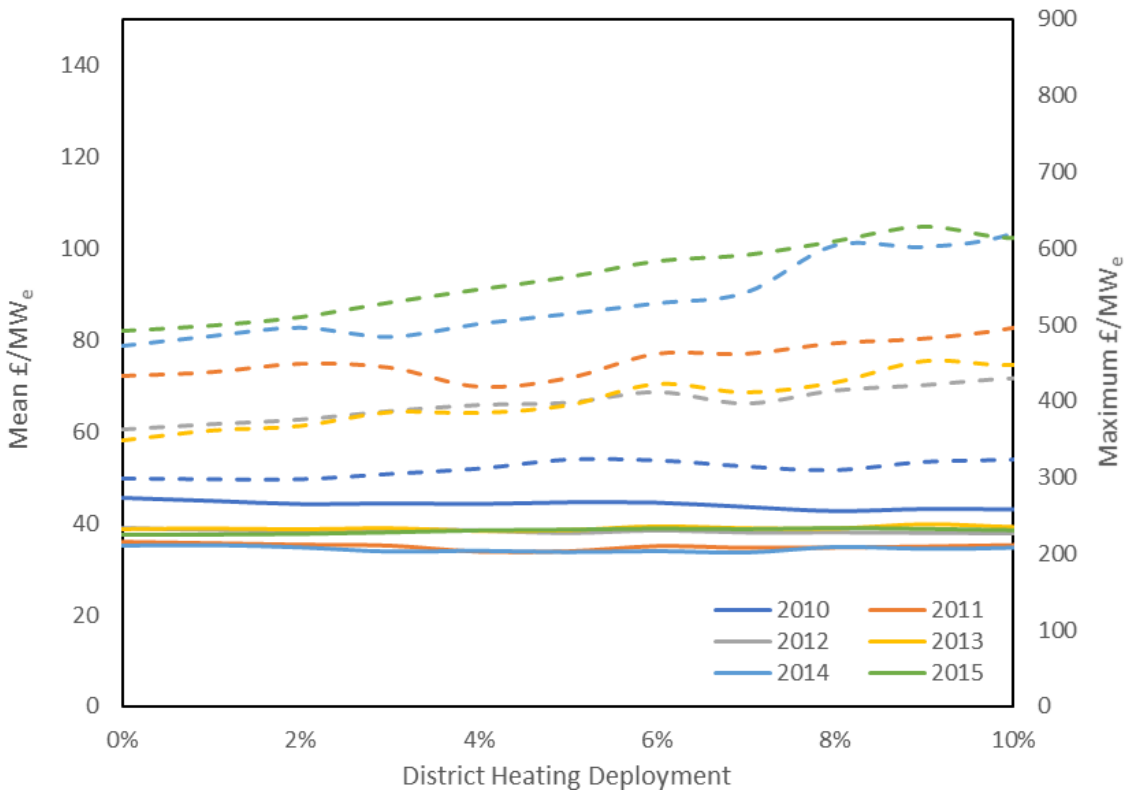

Figure 5.2 Change in the mean (solid) and maximum (dashed) marginal generation costs

5.2.3 Electrified heating costs

Both the average unit and total annual cost of electricity for heating falls with increasing DH deployment as shown in Figure 5.3. Using the modelled heat loads from Chapter 2, this corresponds to a total cost of between £10 billion and £18 billion per year for electric heating. As this is modelled from substituting demand loads, the difference in distribution costs is not taken into account here, and neither is the impact of TES on the need for battery storage. In Section 4.5 it was shown that the average annual cost of electricity for a non-marginal DH system was just under £9/MWh$_{th}$. As the fraction of DH deployment increases, the average cost would tend towards this number, this average will itself change as DH becomes marginal on the system.

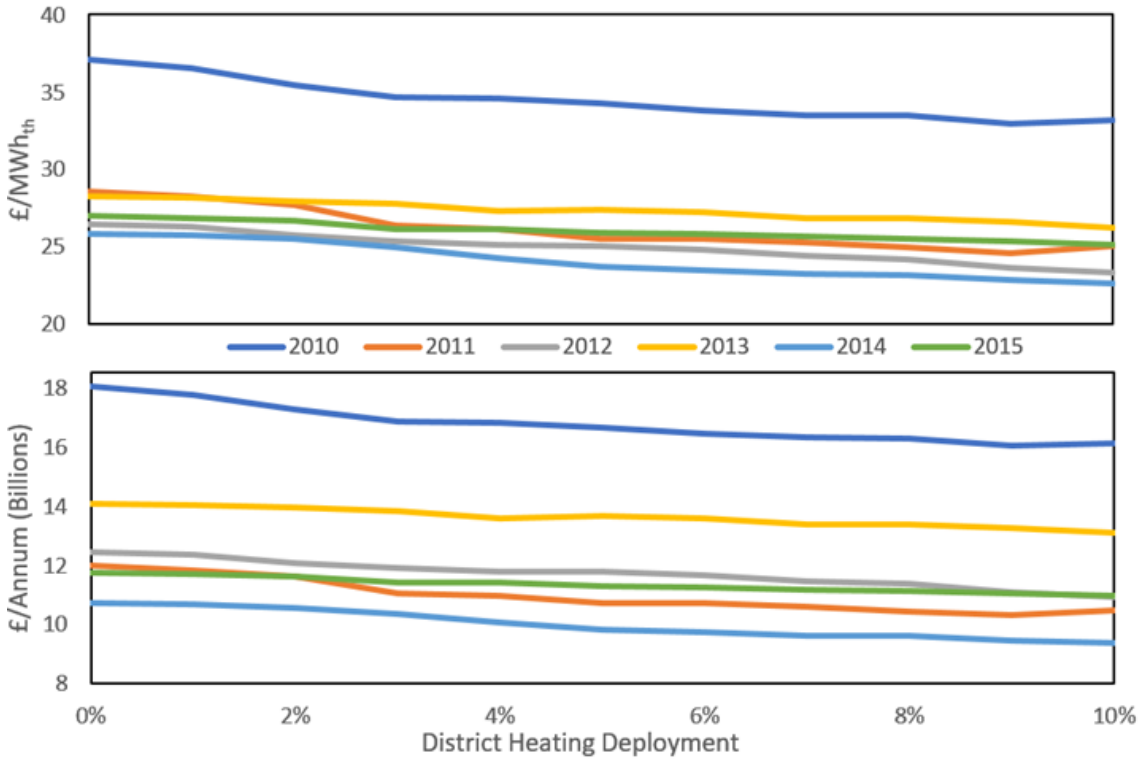

Figure 5.3 Change in the average unit (top) and total annual (bottom) cost of electric heating

5.2.4 Integrating ElCoM and DiHeM

An examination of how the flexibility of DH can be exploited by the electricity grid and utilise the extra storage capacity is more complex. The modelling methods used do not permit a robust hard integration of DiHeM and ElCoM without a fundamental redesign of the models. While the dispatch algorithm in ElCoM functions on an hourly basis, the evaluation of costs only occurs retrospectively on an annual basis. This presents an issue as the RDOA in DiHeM operates on the basis of known hourly electricity prices. When DH is significant on the system, the electricity demand will change and affect the marginal generation costs and hence the electricity price to the DH operator and in turn impact the operation of the DH. The resulting operation sequence could then be run again in ElCoM but there is no guarantee that this iteration will converge.

Furthermore, DH would impact on the optimal capacities of electricity generators and storage and so affect system costs and hourly prices. Properly then, the operation and system design would be optimised using an integrated model. Full integration of the models and optimisation would require a further research programme. One option to explore the coordinated operation of DH is on the basis of a centralised dispatch system. This effectively removes agency from the DH operator. By allowing the decisions in DiHeM to be controlled by the state of ElCoM, the dispatch model in ElCoM is set to treat DH TES as a secondary store after the grid's electrical storage has been fully utilised. This maximises the flexibility of the grid as electricity can be used for any purpose and minimises the use of dispatchable generators. The central dispatch is such that:

- When there is surplus power, priority is given to charging grid storage first, followed by the DH HPs, to first meet the DH load, and then to charge TES with the remaining excess HP capacity
- When there is a deficit of power, priority is given to switching off the DH HPs and the DH load is met from the TES, followed by discharging grid storage.

Figure 5.4 shows the comparison of DH to a counterfactual of full consumer HP based heating in the NZ Scenario. Surplus renewable generation slightly increases. However, the benefits of DH can be seen with a 60% reduction in the deficit at 10% DH deployment. The deficit would otherwise need to be made up from either dispatchable plant or other flexibility/storage in the system.

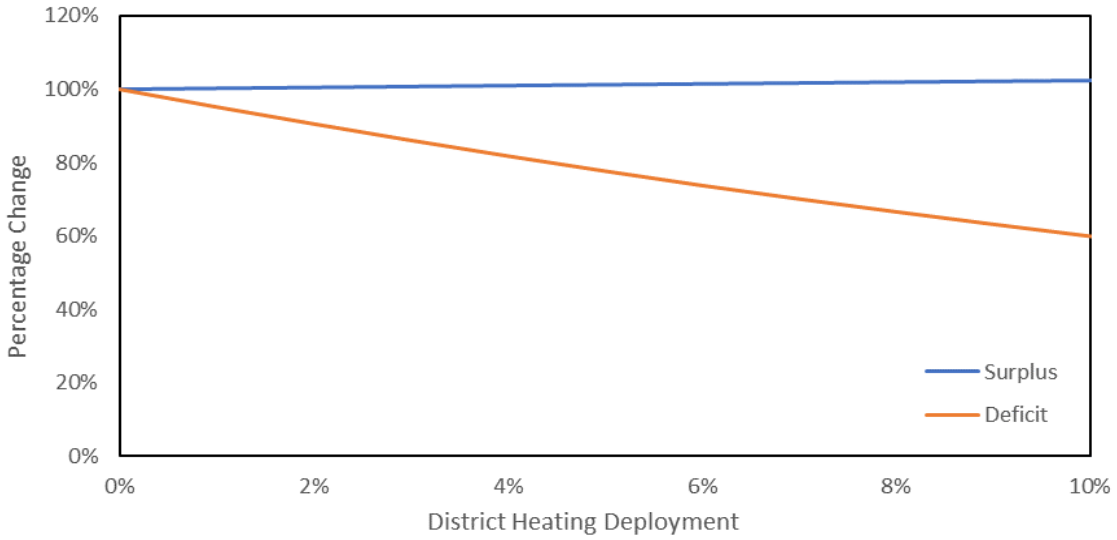

Figure 5.4 Change in renewable surplus and deficit after integration

5.2.5 Equating thermal and electrical storage

In Section 3.7 it was determined that 242 GWh_e of grid storage was necessary in 2010, the design year, to attain a security of supply where 2% of all demand was achieved via either dispatchable plant or other flexibility. For other weather years, the requirement was less than this.

The grid residual (generation minus demand) curve in Figure 5.5 shows the effect of grid storage and DH on the generation surplus and deficits using 2010 weather data. An ideal system should be perfectly balanced, the next best would be to eliminate the deficits. The orange curve represents hourly generation minus demand before the action of any grid storage. The addition of grid storage eliminates over 750 deficit hours (shown by the solid blue line). The dashed yellow line shows the addition of 10% DH on the system which further reduces the deficit. This level of DH deployment, assuming TES sized at 1.3% annual demand (as per results the findings in chapter 4), would have just under 550 GWh_{th} of connected TES (assuming a DH system temperature difference of 55°C) . The value of this extra storage on the system can be estimated by the cost of grid storage displaced without altering the deficit (dashed blue line).

For the 2010 weather year, this displacement is around 107 GWh_e of grid storage. 2010 was an exceptionally cold year which enhances the DH-TES system's ability to provide virtual storage for the grid (i.e. if heat demand were zero there would be no HP electricity demand to interrupt and the storage ability would be zero). Other years had a lower overall storage requirement than 2010 to attain the same security of supply (and hence a smaller displacement), despite DH being able to provide a greater level of virtual storage due to the higher heat demand in 2010.

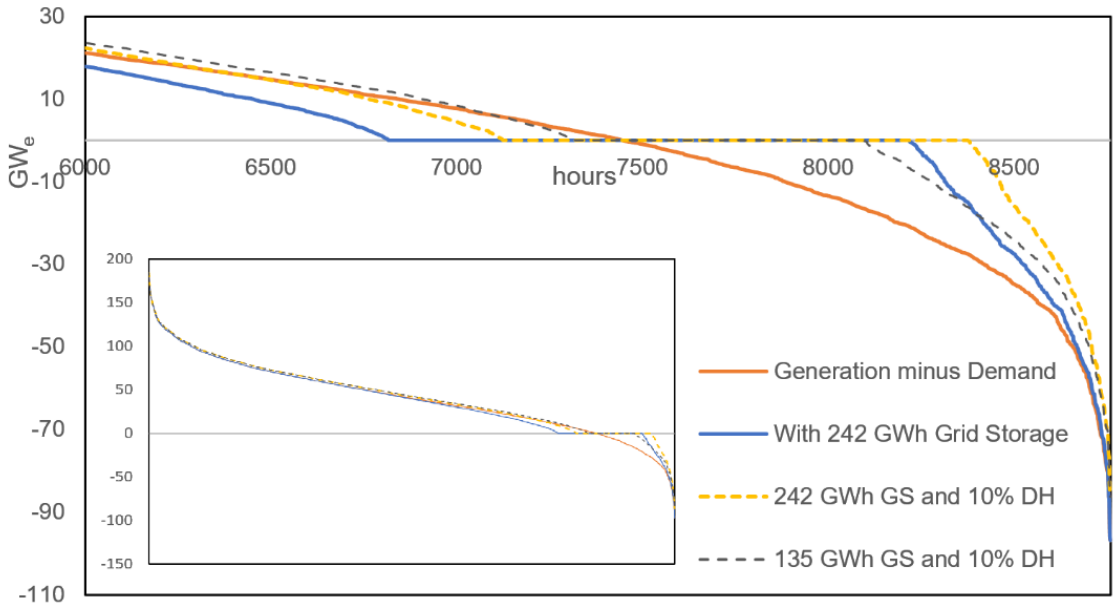

Figure 5.5 Grid residual duration curves for NZ scenario and integration of DH (2010)

For a 10% DH deployment, TES capacity and the corresponding capital costs were assumed with a reference DH temperature difference of 55°C. With a fixed volumetric capacity of TES, the actual stored energy varies with the temperature differential. The average winter DH temperature difference was 38°C which gives an effective winter TES capacity of around 380 GWh_{th}. The thermal storage electrical equivalence can then be estimated by the ratio of the effective winter capacity and maximum displacement (380/107). This is in the region of 3.5, that is 1 GWh_e of grid storage can be displaced by 3.5 GWh_{th} of TES (depending on the level of heat demand). This figure is essentially the average winter COP of the DH system, suggesting that the TES can be operated like grid storage provided that there is DH load on the system.

As per the capex assumptions from Chapter 3, 107 GWh_e of electrical storage represents a £36 billion capital investment. Using the medium range assumptions from Chapter 4, a 10% DH deployment would require an estimated £52 billion capital expenditure (network + HP + TES). The cost of the DH infrastructure needs to be factored in as a pre-requisite to be able to connect such quantities of TES to the system. TES represents less than 4% of the total capital of a DH network. Once the infrastructure is in place, the addition of further TES would require little further investment. Every 1 GWh_{th} of TES at a cost of £4.45 million potentially displaces up to 0.2 GWh_e of electrical storage, at a cost of £67.4 million (this is a 1:5 ratio at 55°C temperature difference as opposed to a 1:3.5 ratio at a 38°C difference).

The integration described here effectively assumes joint operation of the system and operates according to a surplus/deficit merit order which tries to maximally conserves exergy, but it is not price driven, though it may well minimise total system avoidable costs. However, the output from DH is assumed to be unavoidable as it is driven by demand, whereas grid storage output is optional. The level of displacement of grid storage presumably arises because of the inability of grid storage to meet demand in worst-case conditions due to insufficient charge. It is difficult to cover the extreme worst-case condition with the modelled decarbonised electricity system due the many variables involved. These include the state of charge of both grid storage and TES, the heat load and the electricity demand on the grid, and also the conditions and renewable output leading up to this. Because of these many uncertainties, small changes within the system could lead to large changes in the ability of TES to displace grid storage. While this result is a starting point, further analysis needs to be conducted with a more robustly integrated model. Experimentation on varying levels of TES and DH deployment levels is also needed to determine the minimum DH investment required to achieve grid benefits and how much TES can be supported at each level of DH deployment. The answers to all these questions are highly

dependent on the scenario, operating algorithm, and system design assumptions that any future analysis should consider.

5.2.6 Summary of model integration

This section has addressed the second main research aim which was to analyse how a significant DH presence may impact the electricity system. This was stated in section 1.4.1 as:

> *What is the impact of a significant DH deployment on the electricity system, how much flexibility can it provide and to what extent can it supplant grid storage?*

This required integrating ElCoM and DiHeM and coordinating the operation of the two models assuming a centralised dispatch. The results from this analysis at 10% DH deployment can be summarised as:

- A simple substitution of electricity demand loads shows that electricity demand for heating is reduced by 3% and peak demand is reduced by 10%.
- Annual mean electricity costs remain consistent and the costs in around 80% of hours in a year remain unchanged. However, peak marginal generation costs increase with fewer hours of dispatchable generation or other forms of flexibility.
- The total cost of electric heating for both individual HPs and DH was found to vary between £10 billion to £18 billion.
- The deficit in renewable generation is reduced by 60% while there is a slight increase in the surplus of renewable generation.
- DH can displace around 107 GWh_e of grid storage with every 1 GWh_{th} of TES able to displace 3.5 GWh_e of electrical battery storage (at a 38°C temperature difference).

5.3 Key Findings and Contributions

Each of the main chapters of this thesis has provided contributions to knowledge in their respective areas. Chapter 2 has drawn upon many existing sources to develop a method to model high spatiotemporal resolution heat loads on a large geographical scale. While various heat maps with high spatial resolution are in existence, the temporal dimension in HeLoM is novel. The modelling enabled disaggregation of urban loads at selected heat demand density thresholds as a proxy for DH load. The urban heat loads were shown to have a different temporal profile to the modelled national profile demonstrating that these cannot be simply interchanged. The output, both national and local urban load, can be used in various other research applications and model inputs.

Chapter 3 developed ElCoM which introduced a novel method for calculating marginal electricity generation costs from capital intensive systems. The modelling revealed that while intra-day variation of costs increases, the short-term variability decreases in high wind scenarios. The costs also show a strong seasonality, which was reinforced in the NZ scenario with the addition of fully electric heat loads. The NZ scenario itself was an adaptation of an existing national scenario where it was assumed that dispatchable generation can be eliminated through flexibility measures such as demand side response, interconnection and vehicle-to-grid (V2G). These flexibility measures amounted to 2% of annual demand in the stress case period, and represents a security of supply for the electricity system. The resulting generation mix shows ambitious renewable deployment capacities. This ambition, however, is in line with contemporary analysis in the field. Significantly, it was shown that the marginal cost of electricity supply in a highly renewable system with grid storage can be within a manageable range.

In Chapter 4, output from HeLoM and ElCoM are combined in DiHeM. The operational control of the HP – TES system was implemented with a novel application of an MPC algorithm, the RDOA. The RDOA has a finite time horizon corresponding to the accuracy of weather forecasts. This enables a practical grasp of the operating costs and can approximate within 20% of a perfect

foresight simulation. It was estimated that the levelised cost of heat from bulk DH systems would be in the region of £88 per MWh_{th}, of which around £9 per MWh_{th} are from fuel (electricity) costs. The model was used to determine the optimal TES capacities for the NZ scenario. It was determined that a TES capacity of 1.3% annual demand is sufficient to minimise electricity costs (with a heat pump sized to peak load). However, with the costs of current DH infrastructure, TES represents a small fraction of the capital investment.

This final section has shown that significant quantities of DH can be deployed with the result that electricity demand for heating and peak loads on the grid are reduced, as is the deficit in renewable generation without greatly impacting electricity costs. An attempt at integrating ElCoM and DiHeM reveals that the amount of grid storage that is displaced by TES is highly dependent on yearly weather conditions. This can be as much as 3.5 GWh_{th} of TES for every 1 GWh_e of grid storage on the system at significant cost savings.

5.3.1 Policy implications

DH costs are still very dependent on large capital investments and financing is a central issue. Reducing the cost of DH infrastructure is the subject of intense scrutiny among stakeholders. A reduction in DH capital costs of over 40% has been suggested (ETI, 2018), thereby increasing the areas in which deployment of DH is economical. There is uncertainty regarding the cost of land and space for TES, but the value to the grid that DH could provide merits further attention.

The modelling in this thesis has shown that the capacity requirements and therefore system capital costs are set by the worst-case period. In this research, this was the winter of 2010 which had a prolonged cold period with low renewable output. In Chapter 2, the peak simulated heat loads were seen during this period. The capacities in the NZ scenario in Chapter 3 were set by 2010 which was the year with the highest number of DSP hours. Chapter 4 also showed that the DH capacity requirements are determined by this period. If the 2010 meteorology year were not simulated, then the results here may look quite different. A fundamental question is whether a future system be designed according to this worst-case? How often will this worst case occur, particularly considering a changing climate with predicted milder winters? The NZ scenario was designed around a security of supply constraint but this may not be the grid operator's only constraint. It might also be to minimise the total cost of electricity to consumers. The marginal generation costs of electricity modelled here are largely driven by capital costs of both renewables and storage. Storage has a big impact on prices, and so this tends to favour prioritising its reduction over renewables. The whole system must be secure in worst-case conditions and the options are not limited to those discussed here.

It has also been shown that TES provides the highest benefits to the electricity system in the worst-case year. DH TES thereby offers the opportunity of greatly reducing system storage and dispatchable generator costs. This alone merits further investigation and any policy analysis or future scenario modelling should acknowledge this. Should DH then be designed and deployed according to this worst-case period at the expense of heating costs? If so, what incentives would be provided to DH owners and operators to provide this valuable flexibility? And importantly, who would be responsible for coordinating this?

The benefits of DH could be maximised with a co-ordinated system as the integrated modelling has illustrated. The design of such a system is a challenge of high complexity and raises further questions and challenges such as what signals are involved and who manages the system. The modelling here simulated a single large TES, effectively assuming that all stores are charged and discharged in unison. This is unlikely to be the case and something that could only be achieved via a centralised coordinated system operator. Alternatively, if the system is decentralised with competing agents, how is chaotic hunting avoided? We can only speculate on the configuration of the future energy system, and what the role of the National Grid or other operators may become. But in the absence of a central dispatch agent, would dynamic markets be able to recreate this behaviour? These are questions unanswered here.

The investment, ownership and operation of grid infrastructure is entirely separate from that of DH. A whole system cost minimisation would strengthen the case for DH. If a 10% DH deployment with a capital cost of £52 billion saved £36 billion in grid electricity storage, the effective spend on 10% DH deployment would be only £16 billion. Assuming that this level of deployment covers 3.5 million dwellings, this represents a spend of around £4,600 per dwelling (a conservative estimate considering that nondomestic buildings would form a large component of urban DH schemes). By comparison the typical cost of installing a domestic air source HP is around £10,000 (Vaughan, 2021). A £5,400 saving for 3.5m dwellings is £18.9billion and further savings could be achieved by considering the counterfactual costs of needing to reinforce the local electrical distribution network.

While observing these cost savings, it is important to remain cognizant of the declining costs of utility scale lithium-ion batteries and other form of grid storage. Some projections estimate a 2050 cost reduction of over 50% compared to the values used in this study (Cole et al., 2021). Though this reduces the impact of the cost savings from TES compared with lithium-ion batteries, TES is still significantly cheaper and of course these projections are based partly on historical trends and the continued availability of the required raw materials and associated supply chains.

The modelling of marginal generation costs shows that high levels of renewable deployment should not necessarily lead to high electricity prices in an efficient market. Average electricity generation costs remain in line with present costs, but these costs are seasonal. Increasing renewable deployment does however increase the costs of the few remaining dispatch or flexibility hours where there is a generation deficit, but this modelling has not reduced system capacities to avoid this. Tariff design will be vital to protect owners of consumer HPs from being exposed to the highest costs in winter, particularly as they are unlikely to have the load shifting abilities of TES. Large purchasers of electricity (electricity retailers and large consumers) may well enter into contracts-for-differences (CfDs) with wholesalers to fix their prices going forwards, and hence shield themselves from volatile and high short-run prices. The economics of storage however, depends on price volatility. Short-run prices need to be visible and accessible in the market, in order for storage to be properly rewarded. If they are not, then insufficient storage will be built, increasing volatility and threatening security of supply. Similarly, electricity retailers could offer a range of tariffs to small consumers - with a premium reflecting the extent to which the consumer is insulated from high and volatile prices.

5.3.2 Strengths and limitations

A strength and novel feature of the analysis in this thesis is that real weather underlines the primary data feeding into the simulated supply and demand. Weather data from the eleven GB regions provided by the Met Office (2019) directly fed into the heat load modelling in HeLoM. The renewable capacity factors from Staffell and Pfenninger (2016) were based on NASA Merra reanalysis data. This fundamentally linked the patterns of supply and demand, a link that is reinforced with higher renewable capacities. However, future weather and climate conditions will not be the same as the modelled past; in particular increased average ambient temperatures will reduce space heat loads and increase cooling demand, but episodes of extreme weather may impact on peak demands (Met Office, 2021).

The DH modelling rests on a single scenario. This scenario was based on a recent National Grid net zero scenario with a significant fraction of DH. Real world outcomes do not always follow the planned or most economic investments pathways. The purpose of this modelling is not to make a prediction, rather it is an exploration of future outcomes and a key challenge is to understand the uncertainties in these outcomes. How would these results change with lower renewable deployment or in a hydrogen dominated scenario? Compared to the National Grid scenarios, the NZ scenario adapted for this thesis had the highest level of heat electrification and DH deployment which made it most suitable for analysis. The largest departure from it was

the elimination of dispatchable hydrogen, this hydrogen is also a storage mechanism for the energy system.

The analysis of significant DH deployment in this concluding chapter effectively models a single large DH system with a single TES. In reality there would be many individual systems with different demand load profiles, HP COPs, etc. A rudimentary integration of ElCoM and DiHeM was attempted with an assumed merit order. But given that we know little about the composition of other storage and flexibility measures on the system, it is difficult to make any firm conclusions on this basis, but rather to create new avenues of exploration.

5.4 Future Work

A natural progression of this work is to extend the integration of ElCoM and DiHeM. This includes a co-optimisation of both electricity dispatch and storage in conjunction with TES. The challenge will come in the design of the optimisation and definition of the objective function which is being optimised. While a cost comparison between DH and grid storage has been attempted, a further addition is a comparison with consumer HPs. This would involve a comparison of not only the capital costs of installation but also the cost difference of the electricity consumption (inclusive of transmission losses). This would then tend towards a total system optimisation.

The heat loads from HeLoM are assumed to be inflexible in DiHeM. While attempts have been made to capture the effects of diversity and thermal inertia in the heat load modelling, there is no option in DiHeM to pre-heat or adjust temperature set-points. This increases the flexibility of the DH system. However, this would have required each building to be dynamically modelled, increasing computing demands.

Now that the modelling system is in place, further scenarios can be readily simulated. While a full system optimisation is beyond the capabilities of the modelling, an economic optimisation of DH deployment may be possible. Following from this, a central discussion point has been the matter of system design according to the worst-case period. This may require a full statistical analysis of the likely performance of the RDOA operational optimisation algorithm compared with perfect foresight in the face of an uncertain future. A statistical analysis of meteorology may be useful, but this may also require further climate modelling.

Including climate scenarios could enable a more robust analysis of heat loads as well as possible cooling loads. Cooling loads have only been captured indirectly through extrapolation of current electricity demands. Summer temperatures are projected to rise, and the frequency of heat waves may also increase. This cannot be simulated with the use of historical meteorological data and cooling loads may need to be explicitly derived. The question of cooling demand is certain to increase in importance in the coming years. The summer periods typically have high surpluses of electricity generation. Electric cooling loads could readily use this surplus and are unlikely to be as critical to system design as heating is. HPs and DH networks can also be used to provide cooling and the modelling can be extended to a district heating and cooling network. Substituting air-conditioning with district cooling is akin to replacing consumer HP with DH-HP resulting in lower electricity consumption. The provision of heating and cooling with HP could allow for the storage of both. An interseasonal TES could be used to store excess cold in the winter and heat in the summer. Indeed, concepts such as 'fifth generation district heating and cooling' systems are beginning to emerge that consider this proposition (Lund et al., 2021).

The results presented here show that the widespread deployment of DH can have an important function in the national energy system and warrants that it is thoroughly investigated as part of an energy system strategy. The issues directly impact organisations such as the electricity network operator, National Grid ESO, who should certainly examine these outcomes as well as being scrutinised by the appropriate government department and the Climate Change Committee who advise them and ultimately shape the direction of energy policy and research.

To summarise the scope of future work and extensions of the research presented in this thesis, this includes but is not limited to:

- Fully integrated electricity system and DH simulation including co-optimisation of dispatch, electrical and thermal storage, and a total system optimisation to contrast DH with consumer HPs.
- Inclusion of dynamic heat demand to capture the effect of varying temperature setpoints, pre-heating and thermal inertia.
- Addition of further national energy scenarios and economic optimisation of national DH deployment for each.
- Inclusion of summer cooling loads and potentially district cooling and cold stores

5.5 Epilogue

Since writing this thesis, the UK (and indeed the international) energy system has gone through a period of crisis. A perfect storm of low renewable generation coinciding with a nuclear power plant and interconnector outage and a period of volatility in the natural gas market has resulted in the collapse of several energy suppliers participating in the electricity retail market and threatened several more. Their losses will inevitably be passed onto consumers who could face higher electricity prices while the sustained high level of gas prices will likely lead to increased domestic heating costs. A further consequence of this is a possible increase in electricity generation from coal, thereby resulting in increased emissions.

This highlights the importance of some of the themes discussed in this thesis, particularly the need for long-term energy storage to provide system resilience and reduce exposure to an international commodity market. System design to ensure security of supply will be crucial as both the deployment of renewable generation and electrified demands such as heating increases. The need for appropriate market design is as vital as ever, to reduce the exposure of energy companies and consumers to high energy prices and volatility in the market while simultaneously allowing owners of storage access to this volatility to promote investment in storage and security of supply.

In this time, the UK government has published their Net Zero Strategy (2021b) and the Heating and Buildings Strategy (2021a) papers. While these are somewhat lacking in substance, they do signal support for domestic heat pumps via a (limited) capital grant scheme, with a role for hydrogen in industry and transport. For the power sector, the strategy confirms the intention for a mass deployment of offshore wind, with little comment however, on the storage and flexibility needed to accommodate this. Meanwhile, district heating continues to move up the agenda, with the completion of a recent consultation on zoning to support the development of new district heating networks (BEIS, 2021c) and a response to a consultation on regulatory frameworks for district heating markets (BEIS, 2021d). This illustrates the pace of development in this area and demonstrates that the topics covered in this thesis are going to remain relevant for the foreseeable future.

REFERENCES

Abu-Ebid, M., 2015. National Comprehensive Assessment of the Potential for Combined Heat and Power and District Heating and Cooling in the UK (Report for DECC). Ricardo Energy & Environment.

Ahmed, A., Mancarella, P., 2014. Strategic techno-economic assessment of heat network options for distributed energy systems in the UK. Energy 75, 182–193. https://doi.org/10.1016/j.energy.2014.07.011

Ancona, M.A., Bianchi, M., Branchini, L., Melino, F., 2014. District Heating Network Design and Analysis. Energy Procedia 45, 1225–1234. https://doi.org/10.1016/j.egypro.2014.01.128

Anderson, B.R. (Ed.), 2002. BREDEM-8: model description, 2001 update, Reprint. with corr. ed, BR. CRC.

Anna, V., Eduard, L., Maksim, A., Andres, S., 2018. Feasibility of thermal energy storage integration into biomass chp-based district heating system. Chem. Eng. Trans. 499–504. https://doi.org/10.3303/CET1870084

Apros, 2021. Dynamic Process Simulation Software for Nuclear and Thermal Power Plant Applications [WWW Document]. Dist. Heat. URL https://www.apros.fi/industries/district-heating/ (accessed 7.30.21).

Arababadi, R., 2012. Energy Use in the EU Building Stock-Case Study: UK. Linkoping University.

Armitage, P., Godoy-Shimizu, D., Palmer, J., 2015. The Cambridge Non-Domestic Energy Model.

Arran, J., Slowe, J., 2012. 2050 Pathways for Domestic Heat. Delta Energy & Environment Ltd.

ARUP, 2016. Review of Renewable Electricity Generation Cost and Technical Assumptions. Department of Energy and Climate Change.

Atabay, D., 2018. prodyn: Implementation of the dynamic programming algorithm for optimal system control. Institute for Energy Economy and Application Technology, Technische Universität München.

Atabay, D., 2016. Yabata/Prodyn: V0.1. Zenodo. https://doi.org/10.5281/ZENODO.166514

Atabay, D., Wagner, U., Reinhart, G., 2018. Comparison of Optimization Methods for Model Predictive Control: An Application to a Compressed Air Energy Storage System. Universitätsbibliothek der TU München.

Aunedi, M., Wills, K., Green, T., Strbac, G., 2021. Net-zero GB electricity: cost-optimal generation and storage mix. Imperial College London. https://doi.org/10.25561/88966

Averfalk, H., Ingvarsson, P., Persson, U., Gong, M., Werner, S., 2017. Large heat pumps in Swedish district heating systems. Renew. Sustain. Energy Rev. 79, 1275–1284. https://doi.org/10.1016/j.rser.2017.05.135

Averfalk, H., Werner, S., 2017. Essential improvements in future district heating systems. Energy Procedia 116, 217–225. https://doi.org/10.1016/j.egypro.2017.05.069

Aveva, 2018. District Energy Management - Software for district heating and cooling network operations [WWW Document]. URL https://sw.aveva.com/operate-and-optimise/continuous-process/district-energy-management (accessed 2.8.17).

Badyda, K., Dylik, M., 2017. Analysis of the Impact of Wind on Electricity Prices Based on Selected European Countries. Energy Procedia 105, 55–61. https://doi.org/10.1016/j.egypro.2017.03.279

Barone, G., Buonomano, A., Forzano, C., Palombo, A., 2020. A novel dynamic simulation model for the thermo-economic analysis and optimisation of district heating systems. Energy Convers. Manag. 220, 113052. https://doi.org/10.1016/j.enconman.2020.113052

Barrett, M., 2020. Private correspondance.

Barrett, M., 2014. Electricity Transmission and Distribution Losses: A Note. UCL Energy Institute.

Barrett, M., Spataru, C., 2013. Storage in Energy Systems. Energy Procedia 42, 670–679. https://doi.org/10.1016/j.egypro.2013.11.069

Beardsmore, G.R., Cull, J.P., 2001. Crustal heat flow: a guide to measurement and modelling. Cambridge University Press, Cambridge, UK;

BEIS, 2021a. Heat and Buildings Strategy. Department for Business, Energy and Industrial Strategy London.

BEIS, 2021b. Net Zero Strategy. Department for Business, Energy and Industrial Strategy London.

BEIS, 2021c. Heat Networks Zoning Consultation. Department for Business, Energy and Industrial Strategy London.

BEIS, 2021d. Heat Networks: Building a Market Framework. Department for Business, Energy and Industrial Strategy London.

BEIS, 2020a. Energy White Paper: Powering Our Net Zero Future.

BEIS, 2020b. Energy Consumption in the UK. Department for Business, Energy and Industrial Strategy London.

BEIS, 2020c. Sub-National Gas Consumption Data.

BEIS, 2018a. Business Energy Statistical Summary: How Energy Is Used and by Whom in the Non-Domestic Sector. Department for Business, Energy and Industrial Strategy London.

BEIS, 2018b. Estimating the Cost Reduction Impact of the Heat Networks Investment Project on Future Heat Networks. Carbon Trust.

BEIS, 2017a. The Clean Growth Strategy: Leading the way to a low carbon future. Department for Business, Energy and Industrial Strategy London.

BEIS, 2017b. Digest of UK Energy Statistics 2016. Department for Business, Energy and Industrial Strategy London.

BEIS, 2016a. Evidence gathering - Thermal energy storage. Delta Energy & Environment Ltd.

BEIS, 2016b. Government response: Heat Networks Investment Project consultation. Crown copyright 2016, London.

BEIS, 2016c. Building Energy Efficiency Survey (BEES). Department for Business, Energy and Industrial Strategy London, London.

BEIS, 2016d. Building Energy Efficiency Survey. Department for Business, Energy and Industrial Strategy London, London.

BEIS, 2016e. BEIS Electricity Generation Costs. Department for Business, Energy and Industrial Strategy London.

BEIS, 2010. Cambridge Housing Model and User Guide.

BEIS, DNV GL, 2019. Potential to improve Load Factor of offshore wind farms in the UK to 2035 (No. L2C156060-UKBR-R-05, Rev. D).

Ben Hassine, I., Eicker, U., 2013. Impact of load structure variation and solar thermal energy integration on an existing district heating network. Appl. Therm. Eng. 50, 1437–1446. https://doi.org/10.1016/j.applthermaleng.2011.12.037

Best, I., 2018. Economic comparison of low-temperature and ultra-low-temperature district heating for new building developments with low heat demand densities in Germany. Int. J. Sustain. Energy Plan. Manag. 45-60 Páginas. https://doi.org/10.5278/IJSEPM.2018.16.4

Bibri, S.E., 2018. Backcasting in futures studies: a synthesized scholarly and planning approach to strategic smart sustainable city development. Eur. J. Futur. Res. 6. https://doi.org/10.1186/s40309-018-0142-z

Boswarva, O., 2017. Profiling the age of housing stock in England and Wales [WWW Document]. URL https://www.owenboswarva.com/blog/archive/mg/20161213.htm (accessed 6.7.21).

Böttger, D., Götz, M., Lehr, N., Kondziella, H., Bruckner, T., 2014. Potential of the Power-to-Heat Technology in District Heating Grids in Germany. Energy Procedia 46, 246–253. https://doi.org/10.1016/j.egypro.2014.01.179

Brand, L., Calvén, A., Englund, J., Landersjö, H., Lauenburg, P., 2014. Smart district heating networks – A simulation study of prosumers' impact on technical parameters in distribution networks. Appl. Energy 129, 39–48. https://doi.org/10.1016/j.apenergy.2014.04.079

BRE, 2016. The Government's Standard Assessment Procedure for Energy Rating of Dwellings (SAP 2016). Building Research Establishment, Watford.

Bruhns, H., Steadman, P., Herring, H., 2000. A database for modeling energy use in the non-domestic building stock of England and Wales. Appl. Energy 66, 277–297. https://doi.org/10.1016/S0306-2619(00)00018-0

BSRIA, 2011. Rules of Thumb: Guidelines for Building Services. BSRIA, Bracknell.

Building Research Establishment, 2009. The Government's Standard Assessment Procedure for Energy Rating of Dwellings (SAP). Build. Res. Establ. 2005 Edition.

Burke, J., Byrnes, R., Fankhauser, S., 2019. How to price carbon to reach net-zero emissions in the UK. Policy Rep. Lond. Sch. Econ. Lond.

Burzynski, R., Crane, M., Yao, R., Becerra, V., 2012a. Space heating and hot water demand analysis of dwellings connected to district heating scheme in UK. J. Cent. South Univ. Technol. 19, 1629–1638. https://doi.org/10.1007/s11771-012-1186-z

Burzynski, R., Crane, M., Yao, R., Becerra, V., 2012b. Low temperature district heating network serving experimental zero carbon homes in Slough, UK, in: Proceedings of the 13th International Symposium on District Heating and Cooling, DHC13: Copenhagen.

Busby, J., 2015. UK shallow ground temperatures for ground coupled heat exchangers. Q. J. Eng. Geol. Hydrogeol. 48, 248–260. https://doi.org/10.1144/qjegh2015-077

Buttitta, G., Turner, W.J.N., Neu, O., Finn, D.P., 2019. Development of occupancy-integrated archetypes: Use of data mining clustering techniques to embed occupant behaviour profiles in archetypes. Energy Build. 198, 84–99. https://doi.org/10.1016/j.enbuild.2019.05.056

Calderón, C., James, P., Urquizo, J., McLoughlin, A., 2015. A GIS domestic building framework to estimate energy end-use demand in UK sub-city areas. Energy Build. 96, 236–250. https://doi.org/10.1016/j.enbuild.2015.03.029

Calikus, E., Nowaczyk, S., Sant'Anna, A., Gadd, H., Werner, S., 2019. A data-driven approach for discovering heat load patterns in district heating. Appl. Energy 252, 113409. https://doi.org/10.1016/j.apenergy.2019.113409

Caplin, J., 2017. Demand Forecasting.

Carbon Brief, 2018. What Next for UK Capacity Market After Surprise Eu Ruling? [WWW Document]. URL https://www.carbonbrief.org/qa-what-next-for-uk-capacity-market-after-surprise-eu-ruling (accessed 10.24.19).

Celsius, 2020. Case studies of Low Temperature District Heating systems [WWW Document]. URL https://celsiuscity.eu/case-studies-low-temperature-district-heating-systems/ (accessed 2.20.21).

Centre for Sustainable Energy, 2010. National Heat Map [WWW Document]. URL https://www.cse.org.uk/projects/view/1183

Challans, P., 2018. Hourly and Half Hourly Gas Data - Sustainable Energy Limited (private message).

Cheng, V., Steemers, K., 2011. Modelling domestic energy consumption at district scale: A tool to support national and local energy policies. Environ. Model. Softw. 26, 1186–1198. https://doi.org/10.1016/j.envsoft.2011.04.005

CIBSE (Ed.), 2015a. Environmental design: CIBSE guide A Chapter 6, Eighth edition. ed, CIBSE guide. Chartered Institution of Building Services Engineers, London.

CIBSE, 2015b. Heat Networks: Code of Practice for the UK. Chartered Institution of Building Services Engineers.

CIBSE (Ed.), 2007. Guide C: Reference Data, Eighth edition. ed, CIBSE guide. Chartered Institution of Building Services Engineers, London.

Claessens, B.J., Vanhoudt, D., Desmedt, J., Ruelens, F., 2017. Model-Free Control of Thermostatically Controlled Loads Connected to a District Heating Network. ArXiv170108074 Cs.

Clegg, S., Mancarella, P., 2019. Integrated electricity-heat-gas modelling and assessment, with applications to the Great Britain system. Part II: Transmission network analysis and low carbon technology and resilience case studies. Energy 184, 191–203. https://doi.org/10.1016/j.energy.2018.02.078

Climate Change Committee, 2016. Next steps for UK heat policy. Climate Change Committee, London.

Cole, W., Frazier, A., Augustine, C., 2021. Cost Projections for Utility-Scale Battery Storage: 2021 Update (No. NREL/TP--6A20-79236, 1786976, MainId:33462). https://doi.org/10.2172/1786976

Comaty, F., 2013. Modeling and Simulation of the European Power System using Power Nodes - Assessing the Value of Flexibility for High-Share Integration of Renewable Energies in Europe (Master Thesis). ETH Zurich.

Committee on Climate Change, 2019. Net Zero The UK's contribution to stopping global warming. London.

Committee on Climate Change, 2015. Sectoral scenarios for the Fifth Carbon Budget. London.

Connolly, D., 2017. Heat Roadmap Europe: Quantitative comparison between the electricity, heating, and cooling sectors for different European countries. Energy 139, 580–593. https://doi.org/10.1016/j.energy.2017.07.037

Connolly, D., Lund, H., Mathiesen, B.V., Pican, E., Leahy, M., 2012. The technical and economic implications of integrating fluctuating renewable energy using energy storage. Renew. Energy 43, 47–60. https://doi.org/10.1016/j.renene.2011.11.003

Connolly, D., Lund, H., Mathiesen, B.V., Werner, S., Möller, B., Persson, U., Boermans, T., Trier, D., Østergaard, P.A., Nielsen, S., 2014. Heat Roadmap Europe: Combining district heating with heat savings to decarbonise the EU energy system. Energy Policy 65, 475–489. https://doi.org/10.1016/j.enpol.2013.10.035

Cox, J., 2009. Impact of Intermittency. Pöyry Energy Consulting, Helsinki.

Crane, M., 2016. Energy efficient district heating in practice – the importance of achieving low return temperatures. Presented at the CIBSE Technical Symposium Edinburgh.

Dahl, M., Brun, A., Andresen, G.B., 2017. Using ensemble weather predictions in district heating operation and load forecasting. Appl. Energy 193, 455–465. https://doi.org/10.1016/j.apenergy.2017.02.066

Dalipi, F., Yildirim Yayilgan, S., Gebremedhin, A., 2016. Data-Driven Machine-Learning Model in District Heating System for Heat Load Prediction: A Comparison Study. Appl. Comput. Intell. Soft Comput. 2016, 1–11. https://doi.org/10.1155/2016/3403150

Danish Energy Agency, 2018. Technology Data for Energy Storage. Copenhagen.

Danish Energy Agency, 2016. Technology Data for Generation of Electricity and District Heating. Copenhagen.

David, A., Mathiesen, B.V., Averfalk, H., Werner, S., Lund, H., 2017. Heat Roadmap Europe: Large-Scale Electric Heat Pumps in District Heating Systems. Energies 10, 578. https://doi.org/10.3390/en10040578

DCLG, 2017. EHS English Housing Survey, 2008-English Housing Survey, 2011: Housing Stock Data. https://doi.org/10.5255/UKDA-SN-7386-4

DCLG, 2011. Zero carbon non-domestic buildings: phase 3 final report. Department for Communities and Local Government, London.

DECC, 2015a. Energy Consumption in the UK 2010.

DECC, 2015b. Assessment of the costs, performance, and characteristics of UK Heat Networks.

DECC, 2013. The Future of Heating: Meeting the Challenge. Department of Energy and Climate Change.

Denholm, P., Hand, M., 2011. Grid flexibility and storage required to achieve very high penetration of variable renewable electricity. Energy Policy 39, 1817–1830. https://doi.org/10.1016/j.enpol.2011.01.019

Dillig, M., Jung, M., Karl, J., 2016. The impact of renewables on electricity prices in Germany – An estimation based on historic spot prices in the years 2011–2013. Renew. Sustain. Energy Rev. 57, 7–15. https://doi.org/10.1016/j.rser.2015.12.003

Dogan, T., Reinhart, C., 2017. Shoeboxer: An algorithm for abstracted rapid multi-zone urban building energy model generation and simulation. Energy Build. 140, 140–153. https://doi.org/10.1016/j.enbuild.2017.01.030

Dominković, D.F., Bačeković, I., Sveinbjörnsson, D., Pedersen, A.S., Krajačić, G., 2017. On the way towards smart energy supply in cities: The impact of interconnecting geographically distributed district heating grids on the energy system. Energy 137, 941–960. https://doi.org/10.1016/j.energy.2017.02.162

Dong, S., Li, H., Wallin, F., Avelin, A., Zhang, Q., Yu, Z., 2019. Volatility of electricity price in Denmark and Sweden. Energy Procedia 158, 4331–4337. https://doi.org/10.1016/j.egypro.2019.01.788

Drysdale, B., Wu, J., Jenkins, N., 2015. Flexible demand in the GB domestic electricity sector in 2030. Appl. Energy 139, 281–290. https://doi.org/10.1016/j.apenergy.2014.11.013

Duarte, C., Van Den Wymelenberg, K., Rieger, C., 2013. Revealing occupancy patterns in an office building through the use of occupancy sensor data. Energy Build. 67, 587–595. https://doi.org/10.1016/j.enbuild.2013.08.062

Eames, P.C., Loveday, D., Haines, V., Romanos, P., 2014. The Future Role of Thermal Energy Storage in the UK Energy System: An Assessment of the Technical Feasibility and Factors Influencing Adoption - Research Report. UKERC, London.

Eckett, I., 2020. Private Correspondence with GEA.

Eggimann, S., Hall, J.W., Eyre, N., 2019. A high-resolution spatio-temporal energy demand simulation to explore the potential of heating demand side management with large-scale heat pump diffusion. Appl. Energy 236, 997–1010. https://doi.org/10.1016/j.apenergy.2018.12.052

EHPA, 2019. Large scale heat pumps in Europe - 2nd edition.

EKRC, 2014. Smart District Heating and Cooling.

Elexon, 2019. ELEXON Insights: Imbalance Prices Go Negative on 24 March 2019.

Energy Saving Trust, 2010. CE54: Domestic Heating Sizing Method.

Engineering ToolBox, 2005. Thermal Conductivity of Metals, Metallic Elements and Alloys. [WWW Document]. URL https://www.engineeringtoolbox.com/thermal-conductivity-metals-d_858.html (accessed 3.25.21).

ERP, 2016. Potential Role of Hydrogen in the UK Energy System.

EST, 2008. Measurement of Domestic Hot Water Consumption in Dwellings. Department for Environment, Food and Rural Affairs, Energy Saving Trust, London.

ETI, 2018. District Heat Networks in the UK: Potential Barriers and Opportunities. Energy Technologies Institute, Loughborough.

Evans, S., Liddiard, R., Steadman, P., 2017. 3DStock: A new kind of three-dimensional model of the building stock of England and Wales, for use in energy analysis. Environ. Plan. B Urban Anal. City Sci. 44, 227–255. https://doi.org/10.1177/0265813516652898

Evins, R., 2016. A Bi-Level Design and Operation Optimization Process Applied to an Energy Centre. J. Build. Perform. Simul. 9, 255–271. https://doi.org/10.1080/19401493.2015.1045034

Eyre, N., Baruah, P., 2015. Uncertainties in future energy demand in UK residential heating. Energy Policy 87, 641–653. https://doi.org/10.1016/j.enpol.2014.12.030

Fang, T., Lahdelma, R., 2016. Optimization of combined heat and power production with heat storage based on sliding time window method. Appl. Energy 162, 723–732. https://doi.org/10.1016/j.apenergy.2015.10.135

Fanti, M.P., Mangini, A.M., Roccotelli, M., Ukovich, W., 2015. A District Energy Management Based on Thermal Comfort Satisfaction and Real-Time Power Balancing. IEEE Trans. Autom. Sci. Eng. 12, 1271–1284. https://doi.org/10.1109/TASE.2015.2472956

Figueiredo, N.C., da Silva Pereira, P., 2017. The Price of Wind Power Generation in Iberia and the Merit-Order Effect. Int. J. Sustain. Energy Plan. Manag. 15, 87–96. https://doi.org/10.5278/ijsepm.2018.15.4

Firth, S.K., Lomas, K.J., Wright, A.J., 2010. Targeting household energy-efficiency measures using sensitivity analysis. Build. Res. Inf. 38, 25–41. https://doi.org/10.1080/09613210903236706

Fischer, D., 2017. Integrating heat pumps into smart grids: a study on system design, controls and operation, TRITA REFR report. KTH, Stockholm.

Fischer, D., Lindberg, K.B., Mueller, S., Wiemken, E., Wille-Haussmann, B., 2014. Potential for balancing wind and solar power using heat pump heating and cooling systems, in: Proceedings of the Solar Integration Workshop. Berlin: Energynautics GmbH. pp. 263–71.

Fischer, D., Madani, H., 2017. On heat pumps in smart grids: A review. Renew. Sustain. Energy Rev. 70, 342–357. https://doi.org/10.1016/j.rser.2016.11.182

Foster, S., Love, J., Walker, I., 2015. Research on District Heating and Local Approaches to Heat Decarbonisation. Element Energy Ltd, Cambridge.

Fraunhofer, 2019. REMod – National Energy System Model with Focus on Intersectoral System Development - Fraunhofer ISE [WWW Document]. Fraunhofer Inst. Sol. Energy Syst. ISE. URL https://www.ise.fraunhofer.de/en/business-areas/energy-system-technology/energy-system-analysis/energy-system-models-at-fraunhofer-ise/remod.html (accessed 1.20.19).

Fremouw, M., 2017. Quantifying urban energy potentials: Presenting three european research projects, in: Proceedings of the Smart & Sustainable Cities and Transport Seminar. CSIR.

Fuentes, E., Arce, L., Salom, J., 2018. A Review of Domestic Hot Water Consumption Profiles for Application in Systems and Buildings Energy Performance Analysis. Renew. Sustain. Energy Rev. 81, 1530–1547. https://doi.org/10.1016/j.rser.2017.05.229

Gakovic, B., 2000. Areas and Types of Glazing and other Openings in the Nondomestic Building Stock. Environ. Plan. B Plan. Des. 27, 667–694. https://doi.org/10.1068/bst09

Galatoulas, F., Frere, M., Ioakimidis, C., 2018. An Overview of Renewable Smart District Heating and Cooling Applications with Thermal Storage in Europe:, in: Proceedings of the 7th International Conference on Smart Cities and Green ICT Systems. SCITEPRESS - Science and Technology Publications, Funchal, Madeira, Portugal, pp. 311–319. https://doi.org/10.5220/0006785703110319

Gambino, G., Verrilli, F., Canelli, M., Russo, A., Himanka, M., Sasso, M., Srinivasan, S., Del Vecchio, C., Glielmo, L., 2016. Optimal operation of a district heating power plant with thermal energy storage, in: 2016 American Control Conference (ACC). IEEE, Boston, MA, USA, pp. 2334–2339. https://doi.org/10.1109/ACC.2016.7525266

GE, 2018. World's Largest Offshore Wind Turbine | Haliade-X [WWW Document]. URL https://www.ge.com/renewableenergy/wind-energy/offshore-wind/haliade-x-offshore-turbine (accessed 4.2.21).

Georges, E., Quoilin, S., Mathieu, S., Lemort, V., 2017. Aggregation of flexible domestic heat pumps for the provision of reserve in power systems. San Diego 12.

Gerdes, J., 2018. Design for 50MW Offshore Wind Turbine Inspired by Hurricane-Resilient Palm Trees [WWW Document]. URL https://www.greentechmedia.com/articles/read/design-for-50mw-offshore-wind-turbine-inspired-by-palm-trees (accessed 2.2.21).

Gils, H.C., 2015. Balancing of intermittent renewable power generation by demand response and thermal energy storage. https://doi.org/10.18419/OPUS-6888

Gissey, G.C., Grubb, M., Staffell, I., Agnolucci, P., Ekins, P., 2018. Wholesale cost reflectivity of GB and European electricity prices.

Gluyas, J.G., Adams, C.A., Wilson, I.A.G., 2020. The theoretical potential for large-scale underground thermal energy storage (UTES) within the UK. Energy Rep. 6, 229–237. https://doi.org/10.1016/j.egyr.2020.12.006

Google Maps, 2021. Kennington Oval Gas Holders (satellite).

Grainger, C., 2016. UK Spatial District Heating Analysis. London.

Grant, N., Clarke, A., 2014. Internal Gain Assumptions and Building Size. Presented at the 18th International Passivhaus Conference Aachen 2014.

Green, R., Vasilakos, N., 2011. The long-term impact of wind power on electricity prices and generating capacity, in: 2011 IEEE Power and Energy Society General Meeting. Presented at the Energy Society General Meeting, IEEE, Detroit, MI, USA, pp. 1–1. https://doi.org/10.1109/PES.2011.6039218

Green, R., Vasilakos, N., 2010. Market behaviour with large amounts of intermittent generation. Energy Policy 38, 3211–3220. https://doi.org/10.1016/j.enpol.2009.07.038

Greenleaf, J., Sinclair, D., 2012. Pathways for decarbonising heat Report for National Grid. Redpoint Energy.

Grubb, M., Drummond, P., 2018. UK Industrial Electricity Prices: Competitiveness in a low carbon world. UCL Inst. Sustain. Resour.

Grünewald, P.H., Cockerill, T.T., Contestabile, M., Pearson, P.J.G., 2012. The socio-technical transition of distributed electricity storage into future networks—System value and stakeholder views. Energy Policy 50, 449–457. https://doi.org/10.1016/j.enpol.2012.07.041

Gu, W., Wang, J., Lu, S., Luo, Z., Wu, C., 2017. Optimal operation for integrated energy system considering thermal inertia of district heating network and buildings. Appl. Energy 199, 234–246. https://doi.org/10.1016/j.apenergy.2017.05.004

Gudmundsson, O., Thorsen, J.E., Brand, M., 2018. The role of district heating in coupling of the future renewable energy sectors. Energy Procedia 149, 445–454. https://doi.org/10.1016/j.egypro.2018.08.209

Guelpa, E., 2020. Impact of network modelling in the analysis of district heating systems. Energy 213, 118393. https://doi.org/10.1016/j.energy.2020.118393

Guelpa, E., Marincioni, L., Capone, M., Deputato, S., Verda, V., 2019. Thermal load prediction in district heating systems. Energy 176, 693–703. https://doi.org/10.1016/j.energy.2019.04.021

Haas, R., Lettner, G., Auer, H., Duic, N., 2013. The looming revolution: How photovoltaics will change electricity markets in Europe fundamentally. Energy 57, 38–43. https://doi.org/10.1016/j.energy.2013.04.034

Hanmer, C., Shipworth, M., Shipworth, D., Carter, E., 2019. How household thermal routines shape UK home heating demand patterns. Energy Effic. 12, 5–17. https://doi.org/10.1007/s12053-018-9632-x

Hast, A., Rinne, S., Syri, S., Kiviluoma, J., 2017. The role of heat storages in facilitating the adaptation of district heating systems to large amount of variable renewable electricity. Energy 137, 775–788. https://doi.org/10.1016/j.energy.2017.05.113

Hedegaard, K., Mathiesen, B.V., Lund, H., Heiselberg, P., 2012. Wind power integration using individual heat pumps – Analysis of different heat storage options. Energy 47, 284–293. https://doi.org/10.1016/j.energy.2012.09.030

Helin, K., Zakeri, B., Syri, S., 2018. Is District Heating Combined Heat and Power at Risk in the Nordic Area?—An Electricity Market Perspective. Energies 11, 1256. https://doi.org/10.3390/en11051256

Henderson, J., Hart, J., 2013. BREDEM 2012–A technical description of the BRE Domestic Energy Model. Build. Res. Establ. BRE.

Hennessy, J., Li, H., Wallin, F., Thorin, E., 2018. Towards smart thermal grids: Techno-economic feasibility of commercial heat-to-power technologies for district heating. Appl. Energy 228, 766–776. https://doi.org/10.1016/j.apenergy.2018.06.105

Hermansson, K., Kos, C., Starfelt, F., Kyprianidis, K., Lindberg, C.-F., Zimmerman, N., 2018. An Automated Approach to Building and Simulating Dynamic District Heating Networks. IFAC-Pap. 51, 855–860. https://doi.org/10.1016/j.ifacol.2018.04.021

Hesaraki, A., Holmberg, S., Haghighat, F., 2015. Seasonal thermal energy storage with heat pumps and low temperatures in building projects—A comparative review. Renew. Sustain. Energy Rev. 43, 1199–1213. https://doi.org/10.1016/j.rser.2014.12.002

Hesse, H., Schimpe, M., Kucevic, D., Jossen, A., 2017. Lithium-Ion Battery Storage for the Grid—A Review of Stationary Battery Storage System Design Tailored for Applications in Modern Power Grids. Energies 10, 2107. https://doi.org/10.3390/en10122107

HM Government, 2020. The Ten Point Plan for a Green Industrial Revolution. London.

HM Treasury, 2018. The Green Book: appraisal and evaluation in central government. London.

Hohmann, M., Warrington, J., Lygeros, J., 2019. A two-stage polynomial approach to stochastic optimization of district heating networks. Sustain. Energy Grids Netw. 17, 100177. https://doi.org/10.1016/j.segan.2018.11.003

Huber, J., Nytsch-Geusen, C., 2011. Development of modeling and simulation strategies for large-scale urban districts. Proc. Build. Simul. 2011 1753–1760.

Hull, R., Kane, J., 2016. KPMG 2050 Energy Scenarios - The UK Gas Networks role in a 2050 whole energy system.

Idowu, S., Saguna, S., Åhlund, C., Schelén, O., 2016. Applied machine learning: Forecasting heat load in district heating system. Energy Build. 133, 478–488. https://doi.org/10.1016/j.enbuild.2016.09.068

Imam, S., Coley, D.A., Walker, I., 2017. The building performance gap: Are modellers literate? Build. Serv. Eng. Res. Technol. 38, 351–375. https://doi.org/10.1177/0143624416684641

Inenco Energy, 2016. Spotlight on the Capacity Market.

IRENA, 2019. Future of wind: Deployment, investment, technology, grid integration and socio-economic aspects (A Global Energy Transformation paper). International Renewable Energy Agency, Abu Dhabi.

IRENA, 2017. Electricity Storage and Renewables: Costs and Markets to 2030. International Renewable Energy Agency.

Jing, Z.X., Jiang, X.S., Wu, Q.H., Tang, W.H., Hua, B., 2014. Modelling and optimal operation of a small-scale integrated energy based district heating and cooling system. Energy 73, 399–415. https://doi.org/10.1016/j.energy.2014.06.030

Joos, M., Staffell, I., 2018. Short-term integration costs of variable renewable energy: Wind curtailment and balancing in Britain and Germany. Renew. Sustain. Energy Rev. 86, 45–65. https://doi.org/10.1016/j.rser.2018.01.009

Kallio, T., 2020. Development and validation of a dynamic simulation model of a district heating system; Kaukolämpöverkon dynaamisen simulointimallin kehitys ja validointi (G2 Pro gradu, diplomityö).

Kavgic, M., Mavrogianni, A., Mumovic, D., Summerfield, A., Stevanovic, Z., Djurovic-Petrovic, M., 2010. A review of bottom-up building stock models for energy consumption in the residential sector. Build. Environ. 45, 1683–1697. https://doi.org/10.1016/j.buildenv.2010.01.021

Keirstead, J., Jennings, M., Sivakumar, A., 2012. A review of urban energy system models: Approaches, challenges and opportunities. Renew. Sustain. Energy Rev. 16, 3847–3866. https://doi.org/10.1016/j.rser.2012.02.047

Kelly, S., Pollitt, M., 2010. An assessment of the present and future opportunities for combined heat and power with district heating (CHP-DH) in the United Kingdom. Energy Policy 38, 6936–6945. https://doi.org/10.1016/j.enpol.2010.07.010

Ketterer, J.C., 2014. The impact of wind power generation on the electricity price in Germany. Energy Econ. 44, 270–280. https://doi.org/10.1016/j.eneco.2014.04.003

Knight, I., Kreutzer, N., Manning, M., Swinton, M., Ribberink, H., 2007. European and Canadian non-HVAC electric and DHW load profiles for use in simulating the performance of residential cogeneration systems [A report of Subtask A of FC+ COGEN-SIM: The simulation of building-integrated fuel cell and other cogeneration systems: Annex 42 of the International Energy Agency, Energy Conservation in Buildings and Community Systems Programme].

Kondziella, H., Bruckner, T., 2016. Flexibility requirements of renewable energy based electricity systems – a review of research results and methodologies. Renew. Sustain. Energy Rev. 53, 10–22. https://doi.org/10.1016/j.rser.2015.07.199

Kong, L., WeixingYuan, Zhu, N., 2016. CFD Simulations of Thermal Stratification Heat Storage Water Tank with an Inside Cylinder with Openings. Procedia Eng. 146, 394–399. https://doi.org/10.1016/j.proeng.2016.06.419

Korolija, I., Marjanovic-Halburd, L., Zhang, Y., Hanby, V.I., 2013. UK office buildings archetypal model as methodological approach in development of regression models for predicting building energy consumption from heating and cooling demands. Energy Build. 60, 152–162. https://doi.org/10.1016/j.enbuild.2012.12.032

Kuosa, M., Kontu, K., Mäkilä, T., Lampinen, M., Lahdelma, R., 2013. Static study of traditional and ring networks and the use of mass flow control in district heating applications. Appl. Therm. Eng. 54, 450–459. https://doi.org/10.1016/j.applthermaleng.2013.02.018

Lake, A., Rezaie, B., Beyerlein, S., 2017. Review of district heating and cooling systems for a sustainable future. Renew. Sustain. Energy Rev. 67, 417–425. https://doi.org/10.1016/j.rser.2016.09.061

Lamont, A.D., 2008. Assessing the long-term system value of intermittent electric generation technologies. Energy Econ. 30, 1208–1231. https://doi.org/10.1016/j.eneco.2007.02.007

Lazard, 2019. Lazard's Levelized Cost of Energy Analysis - Version 13.0. N. Y. USA 20.

Leigh Fisher and Jacobs, 2016. Electricity Generation Costs and Hurdle Rates for DECC. Department of Energy and Climate Change.

Leitner, B., Widl, E., Gawlik, W., Hofmann, R., 2019. A method for technical assessment of power-to-heat use cases to couple local district heating and electrical distribution grids. Energy 182, 729–738. https://doi.org/10.1016/j.energy.2019.06.016

Leśko, M., Bujalski, W., Futyma, K., 2018. Operational optimization in district heating systems with the use of thermal energy storage. Energy 165, 902–915. https://doi.org/10.1016/j.energy.2018.09.141

Li, F., 2013. Spatially explicit techno-economic optimisation modelling of UK heating futures 311.

Li, Y., Rezgui, Y., Zhu, H., 2016. Dynamic simulation of heat losses in a district heating system: A case study in Wales, in: 2016 IEEE Smart Energy Grid Engineering (SEGE). Presented at the 2016 IEEE Smart Energy Grid Engineering (SEGE), IEEE, Oshawa, ON, Canada, pp. 273–277. https://doi.org/10.1109/SEGE.2016.7589537

Liddiard, R., 2020. Private correspondence.

Liddiard, R., 2018. CaRB2 [WWW Document]. UCL Energy Inst. Models. URL https://www.ucl.ac.uk/energy-models/models/carb2 (accessed 2.1.21).

Liddiard, R., Wright, A., Marjanovic-Halburd, L., 2008. A Review of Non-Domestic Energy Benchmarks and Benchmarking Methodologies. De Montfort University, Leicester, UK.

Lindberg, K.B., Bakker, S.J., Sartori, I., 2019. Modelling electric and heat load profiles of non-residential buildings for use in long-term aggregate load forecasts. Util. Policy 58, 63–88. https://doi.org/10.1016/j.jup.2019.03.004

Love, J., Smith, A.Z.P., Watson, S., Oikonomou, E., Summerfield, A., Gleeson, C., Biddulph, P., Chiu, L.F., Wingfield, J., Martin, C., Stone, A., Lowe, R., 2017. The addition of heat pump electricity load profiles to GB electricity demand: Evidence from a heat pump field trial. Appl. Energy 204, 332–342. https://doi.org/10.1016/j.apenergy.2017.07.026

Lowe, J.A., Bernie, D., Bett, P., Bricheno, L., Brown, S., Calvert, D., Clark, R., Eagle, K., Edwards, T., Fosser, G., others, 2018. UKCP18 National Climate Projections. Met Office Hadley Centre, Exeter.

Lowe, R., 2011. Combined heat and power considered as a virtual steam cycle heat pump. Energy Policy 39, 5528–5534. https://doi.org/10.1016/j.enpol.2011.05.007

Lund, H., 2018. Renewable heating strategies and their consequences for storage and grid infrastructures comparing a smart grid to a smart energy systems approach. Energy 151, 94–102. https://doi.org/10.1016/j.energy.2018.03.010

Lund, H., Hvelplund, F., Mathiesen, B.V., Østegaard, P.A., Connolly, D., Sperling, K., Möller, B., Nielsen, S., 2015. Sustainable Energy Planning Research Group Aalborg University, Denmark 36.

Lund, H., Möller, B., Mathiesen, B.V., Dyrelund, A., 2010. The role of district heating in future renewable energy systems. Energy 35, 1381–1390. https://doi.org/10.1016/j.energy.2009.11.023

Lund, H., Østergaard, P.A., Chang, M., Werner, S., Svendsen, S., Sorknæs, P., Thorsen, J.E., Hvelplund, F., Mortensen, B.O.G., Mathiesen, B.V., Bojesen, C., Duic, N., Zhang, X., Möller, B., 2018. The status of 4th generation district heating: Research and results. Energy 164, 147–159. https://doi.org/10.1016/j.energy.2018.08.206

Lund, H., Østergaard, P.A., Nielsen, T.B., Werner, S., Thorsen, J.E., Gudmundsson, O., Arabkoohsar, A., Mathiesen, B.V., 2021. Perspectives on fourth and fifth generation district heating. Energy 227, 120520. https://doi.org/10.1016/j.energy.2021.120520

Lund, H., Werner, S., Wiltshire, R., Svendsen, S., Thorsen, J.E., Hvelplund, F., Mathiesen, B.V., 2014. 4th Generation District Heating (4GDH). Energy 68, 1–11. https://doi.org/10.1016/j.energy.2014.02.089

Luo, X., Wang, J., Dooner, M., Clarke, J., 2015. Overview of current development in electrical energy storage technologies and the application potential in power system operation. Appl. Energy 137, 511–536. https://doi.org/10.1016/j.apenergy.2014.09.081

Macadam, J., Davies, G., Cox, J., Woods, P., Turton, A., 2009. The Potential and Costs of District Heating Networks. Pöyry Energy Consulting, Oxford.

Marina, A., Spoelstra, S., Zondag, H.A., Wemmers, A.K., 2021. An estimation of the European industrial heat pump market potential. Renew. Sustain. Energy Rev. 139, 110545. https://doi.org/10.1016/j.rser.2020.110545

Masatin, V., Latõšev, E., Volkova, A., 2016. Evaluation Factor for District Heating Network Heat Loss with Respect to Network Geometry. Energy Procedia 95, 279–285. https://doi.org/10.1016/j.egypro.2016.09.069

Mata, É., Sasic Kalagasidis, A., Johnsson, F., 2014. Building-stock aggregation through archetype buildings: France, Germany, Spain and the UK. Build. Environ. 81, 270–282. https://doi.org/10.1016/j.buildenv.2014.06.013

Maxwell, V., Sperling, K., Hvelplund, F., 2015. Electricity cost effects of expanding wind power and integrating energy sectors. Int. J. Sustain. Energy Plan. Manag. 6, 31–48. https://doi.org/10.5278/ijsepm.2015.6.4

McGlade, C., Bradshaw, M., Anandrajah, G., Watson, J., Ekins, P., 2014. A bridge to a low carbon future? Modelling the long-term global potential of natural gas.

Met Office, 2021. UK Climate Projections (UKCP) [WWW Document]. URL https://www.metoffice.gov.uk/research/approach/collaboration/ukcp/index (accessed 3.4.21).

Met Office, 2019. Met Office MIDAS Open: UK Land Surface Stations Data (1853-current). Centre for Environmental Data Analysis.

Met Office, 2017. Weather Guides: About our forecasts [WWW Document]. URL https://www.metoffice.gov.uk/weather/guides/about-forecasts (accessed 3.4.21).

MHCLG, 2018. English Housing Survey - Floor Space in English Homes – Main Report. https://doi.org/10.5255/UKDA-SN-6106-2

MHCLG, 2016. English Housing Survey. https://doi.org/10.5255/UKDA-SN-6106-2

Mikkola, J., Lund, P.D., 2014. Models for generating place and time dependent urban energy demand profiles. Appl. Energy 130, 256–264. https://doi.org/10.1016/j.apenergy.2014.05.039

Millar, M.-A., Burnside, N., Yu, Z., 2019. District Heating Challenges for the UK. Energies 12, 310. https://doi.org/10.3390/en12020310

Morales, J.M., Conejo, A.J., Perez-Ruiz, J., 2011. Simulating the Impact of Wind Production on Locational Marginal Prices. IEEE Trans. Power Syst. 26, 820–828. https://doi.org/10.1109/TPWRS.2010.2052374

Moustakidis, S., Meintanis, I., Halikias, G., Karcanias, N., 2019. An Innovative Control Framework for District Heating Systems: Conceptualisation and Preliminary Results. Resources 8. https://doi.org/10.3390/resources8010027

Müsgens, F., 2006. Quantifying Market Power in the German Wholesale Electricity Market Using a Dynamic Multi-Regional Dispatch Model. J. Ind. Econ. 54, 471–498. https://doi.org/10.1111/j.1467-6451.2006.00297.x

Nageler, P., Zahrer, G., Heimrath, R., Mach, T., Mauthner, F., Leusbrock, I., Schranzhofer, H., Hochenauer, C., 2017. Novel validated method for GIS based automated dynamic urban building energy simulations. Energy 139, 142–154. https://doi.org/10.1016/j.energy.2017.07.151

National Grid, 2020. Future Energy Scenarios.

National Grid, 2017a. Future Energy Scenarios.

National Grid, 2017b. The Impact of Locational Transmission Losses on Transmission Charges.

National Grid ESO, 2019. Historic Demand Data [WWW Document]. Data Explor. URL https://demandforecast.nationalgrid.com/efs_demand_forecast/faces/DataExplorer

Neshat, N., Amin-Naseri, M.R., Danesh, F., 2014. Energy models: Methods and characteristics. J. Energy South. Afr. 25, 101–111.

Netsim, 2017. Grid Simulation Software NetSimGrid Simulation Software NetSim [WWW Document]. URL http://www.gssnetsim.com/ (accessed 8.15.17).

Nielsen, K.M., Andersen, P., Pedersen, T.S., 2013. Aggregated control of domestic heat pumps, in: 2013 IEEE International Conference on Control Applications (CCA). pp. 302–307. https://doi.org/10.1109/CCA.2013.6662775

Noussan, M., Cerino Abdin, G., Poggio, A., Roberto, R., 2014. Biomass-fired CHP and heat storage system simulations in existing district heating systems. Appl. Therm. Eng. 71, 729–735. https://doi.org/10.1016/j.applthermaleng.2013.11.021

Nouvel, R., Mastrucci, A., Leopold, U., Baume, O., Coors, V., Eicker, U., 2015. Combining GIS-based statistical and engineering urban heat consumption models: Towards a new framework for multi-scale policy support. Energy Build. 107, 204–212. https://doi.org/10.1016/j.enbuild.2015.08.021

Nuytten, T., Claessens, B., Paredis, K., Van Bael, J., Six, D., 2013. Flexibility of a combined heat and power system with thermal energy storage for district heating. Appl. Energy 104, 583–591. https://doi.org/10.1016/j.apenergy.2012.11.029

Ochs, F., Dahash, A., Tosatto, A., Bianchi Janetti, M., 2020. Techno-economic planning and construction of cost-effective large-scale hot water thermal energy storage for Renewable District heating systems. Renew. Energy 150, 1165–1177. https://doi.org/10.1016/j.renene.2019.11.017

Ochs, F., Heidemann, W., Müller-Steinhagen, H., 2021. Modeling Large-Scale Seasonal Thermal Energy Stores, in: Proceedings of Effstock.

Ochs, F., Heidemann, W., Müller-Steinhagen, H., 2009. Performance of Large-Scale Seasonal Thermal Energy Stores. J. Sol. Energy Eng. 131, 041005. https://doi.org/10.1115/1.3197842

Office for National Statistics, 2020. Census Statistics.

Ofgem, 2018. State of the Energy Market Report.

Oikonomou, E., Davies, M., Mavrogianni, A., Biddulph, P., Wilkinson, P., Kolokotroni, M., 2012. Modelling the relative importance of the urban heat island and the thermal quality of dwellings for overheating in London. Build. Environ. 57, 223–238. https://doi.org/10.1016/j.buildenv.2012.04.002

Oreszczyn, T., Lowe, R., 2010. Challenges for energy and buildings research: objectives, methods and funding mechanisms. Build. Res. Inf. 38, 107–122. https://doi.org/10.1080/09613210903265432

Palmer, J., Cooper, I., 2013. United Kingdom Housing Energy Fact File. Department of Energy and Climate Change.

Palyvos, J.A., 2008. A survey of wind convection coefficient correlations for building envelope energy systems' modeling. Appl. Therm. Eng. 28, 801–808. https://doi.org/10.1016/j.applthermaleng.2007.12.005

Patronen, J., Kaura, E., Torvestad, C., 2017. Nordic heating and cooling, TemaNord. Nordic Council of Ministers. https://doi.org/10.6027/TN2017-532

Pfenninger, S., Hawkes, A., Keirstead, J., 2014. Energy systems modeling for twenty-first century energy challenges. Renew. Sustain. Energy Rev. 33, 74–86. https://doi.org/10.1016/j.rser.2014.02.003

Pfenninger, S., Staffell, I., 2016. Long-term patterns of European PV output using 30 years of validated hourly reanalysis and satellite data. Energy 114, 1251–1265. https://doi.org/10.1016/j.energy.2016.08.060

Piddington, J., Nicol, S., Garret, H., Custard, M., 2020. The Housing Stock of The United Kingdom. BRE Trust.

Pieper, H., Ommen, T., Elmegaard, B., Brix Markussen, W., 2019. Assessment of a combination of three heat sources for heat pumps to supply district heating. Energy 176, 156–170. https://doi.org/10.1016/j.energy.2019.03.165

Pikk, P., Viiding, M., 2013. The dangers of marginal cost based electricity pricing. Balt. J. Econ. 13, 49–62. https://doi.org/10.1080/1406099X.2013.10840525

Pirkandi, J., Jokar, M.A., Sameti, M., Kasaeian, A., Kasaeian, F., 2016. Simulation and multi-objective optimization of a combined heat and power (CHP) system integrated with low-energy buildings. J. Build. Eng. 5, 13–23. https://doi.org/10.1016/j.jobe.2015.10.004

Pirouti, M., Bagdanavicius, A., Ekanayake, J., Wu, J., Jenkins, N., 2013. Energy consumption and economic analyses of a district heating network. Energy 57, 149–159. https://doi.org/10.1016/j.energy.2013.01.065

Powell, K.M., Kim, J.S., Cole, W.J., Kapoor, K., Mojica, J.L., Hedengren, J.D., Edgar, T.F., 2016. Thermal energy storage to minimize cost and improve efficiency of a polygeneration district energy system in a real-time electricity market. Energy 113, 52–63. https://doi.org/10.1016/j.energy.2016.07.009

Prieto, I., Sonvilla, P.M., Munguet, M.C., Wilson, J., Kęsik, M., Rieksts-Riekstins, V., Wenzel, T., Dinis, J., Wyke, S., Seeman, M.-E., 2018. THERMOS - Baseline Replication Assessment Report (No. D4.1).

Quiggin, D., Buswell, R., 2016. The implications of heat electrification on national electrical supply-demand balance under published 2050 energy scenarios. Energy 98, 253–270. https://doi.org/10.1016/j.energy.2015.11.060

Radov, D., Klevnäs, P., Lindovska, M., Abu-Ebid, M., Barker, N., Stambaugh, J., others, 2010. Decarbonising heat: low-carbon heat scenarios for the 2020s. Lond. UK NERA Econ. Consult. AEA.

Ram, E., 2015. Will the UK's gas holders be missed? [WWW Document]. BBC News. URL https://www.bbc.co.uk/news/magazine-30405066 (accessed 2.4.21).

Reinhart, C.F., Davila, C.C., 2016. Urban building energy modeling – A review of a nascent field. Build. Environ. 97, 196–202. https://doi.org/10.1016/j.buildenv.2015.12.001

Reynolds, J., Ahmad, M.W., Rezgui, Y., 2018. District Heating Energy Generation Optimisation Considering Thermal Storage, in: 2018 IEEE International Conference on Smart Energy Grid Engineering (SEGE). IEEE, Oshawa, ON, pp. 330–335. https://doi.org/10.1109/SEGE.2018.8499509

Rezaie, B., Rosen, M.A., 2012. District heating and cooling: Review of technology and potential enhancements. Appl. Energy 93, 2–10. https://doi.org/10.1016/j.apenergy.2011.04.020

Rintamäki, T., Siddiqui, A.S., Salo, A., 2017. Does renewable energy generation decrease the volatility of electricity prices? An analysis of Denmark and Germany. Energy Econ. 62, 270–282. https://doi.org/10.1016/j.eneco.2016.12.019

Rismanchi, B., 2017. District energy network (DEN), current global status and future development. Renew. Sustain. Energy Rev. 75, 571–579. https://doi.org/10.1016/j.rser.2016.11.025

Robinson, D., Haldi, F., Leroux, P., Perez, D., Rasheed, A., Wilke, U., 2009. CitySim: Comprehensive micro-simulation of resource flows for sustainable urban planning, in: Proceedings of the Eleventh International IBPSA Conference. pp. 1083–1090.

Robinson, I., 2018. Design Guide: Stored Hot Water Solutions in Heat Networks (No. HWA/DG1). Hot Water Association.

Romanchenko, D., Odenberger, M., Göransson, L., Johnsson, F., 2017. Impact of electricity price fluctuations on the operation of district heating systems: A case study of district heating in Göteborg, Sweden. Appl. Energy 204, 16–30. https://doi.org/10.1016/j.apenergy.2017.06.092

Rosser, J.F., Long, G., Zakhary, S., Boyd, D.S., Mao, Y., Robinson, D., 2019. Modelling Urban Housing Stocks for Building Energy Simulation using CityGML EnergyADE. ISPRS Int. J. Geo-Inf. 8, 163. https://doi.org/10.3390/ijgi8040163

Ruhnau, O., Hirth, L., Praktiknjo, A., 2019. Time series of heat demand and heat pump efficiency for energy system modeling. Sci. Data 6, 189. https://doi.org/10.1038/s41597-019-0199-y

Rylatt, R.M., Gadsden, S.J., Lomas, K.J., 2003. Methods of predicting urban domestic energy demand with reduced datasets: a review and a new GIS-based approach. Build. Serv. Eng. Res. Technol. 24, 93–102. https://doi.org/10.1191/0143624403bt061oa

Saletti, C., Zimmerman, N., Morini, M., Kyprianidis, K., Gambarotta, A., 2020. A Scale-Free Dynamic Model for District Heating Aggregated Regions (preprint). https://doi.org/10.20944/preprints202006.0320.v1

Salpakari, J., Lund, P., 2016. Optimal and rule-based control strategies for energy flexibility in buildings with PV. Appl. Energy 161, 425–436. https://doi.org/10.1016/j.apenergy.2015.10.036

Sameti, M., Haghighat, F., 2017. Optimization approaches in district heating and cooling thermal network. Energy Build. 140, 121–130. https://doi.org/10.1016/j.enbuild.2017.01.062

Sanders, D., Hart, A., Ravishankar, M., Brunert, J., Strbac, G., Aunedi, M., Pudjianto, D., 2016. An Analysis of Electricity System Flexibility for Great Britain. Imperial College London, Carbon Trust.

Sansom, R., 2014. Decarbonising low grade heat for low carbon future. https://doi.org/10.25560/25503

Sansom, R., Strbac, G., 2012. The impact of future heat demand pathways on the economics of low carbon heating systems. Presented at the BIEE – 9th Academic Conference, Oxford.

Sarbu, I., 2021. Modelling, Optimisation and Modernisation of Heating Systems, in: Advances in Building Services Engineering. Springer International Publishing, Cham, pp. 87–208. https://doi.org/10.1007/978-3-030-64781-0_3

Sarwar, A., 2020. Private Correspondance with BU-UK.

Sayegh, M.A., Danielewicz, J., Nannou, T., Miniewicz, M., Jadwiszczak, P., Piekarska, K., Jouhara, H., 2017. Trends of European research and development in district heating technologies. Renew. Sustain. Energy Rev. 68, 1183–1192. https://doi.org/10.1016/j.rser.2016.02.023

Schweiger, G., Rantzer, J., Ericsson, K., Lauenburg, P., 2017. The potential of power-to-heat in Swedish district heating systems. Energy 137, 661–669. https://doi.org/10.1016/j.energy.2017.02.075

Scottish Government, 2018. Scotland's Non-Domestic Energy Efficiency Baseline. Edinburgh.

Scottish Government Statistics, 2020. Small Area Statistics on Households and Dwellings [WWW Document]. URL https://statistics.gov.scot/ (accessed 6.1.20).

Seel, J., Mills, A.D., Wiser, R.H., 2018. Impacts of high variable renewable energy futures on wholesale electricity prices, and on electric-sector decision making.

SGN, 2021. Gas Holders [WWW Document]. URL https://www.sgn.co.uk/about-us/more-than-pipes/gas-holders (accessed 4.10.21).

Shakoor, A., Davies, G., Strbac, G., 2017. Roadmap for Flexibility Services to 2030. Rep. Comm. Clim. Change Lond. Pöyry.

Shipworth, M., Firth, S.K., Gentry, M.I., Wright, A.J., Shipworth, D.T., Lomas, K.J., 2010. Central heating thermostat settings and timing: building demographics. Build. Res. Inf. 38, 50–69. https://doi.org/10.1080/09613210903263007

Silva Monroy, C.A., Christie, R.D., 2011. Energy storage effects on day-ahead operation of power systems with high wind penetration, in: 2011 North American Power Symposium. Presented at the 2011 North American Power Symposium (NAPS 2011), IEEE, Boston, MA, USA, pp. 1–7. https://doi.org/10.1109/NAPS.2011.6025193

Simonsson, J., Atta, K.T., Schweiger, G., Birk, W., 2021. Experiences from City-Scale Simulation of Thermal Grids. Resources 10, 10. https://doi.org/10.3390/resources10020010

Smith, S.T., 2009. Modelling thermal loads for a non-domestic building stock: associating a priori probability with building form and construction - using building control laws and regulations.

Sneum, D.M., Sandberg, E., 2018. Economic incentives for flexible district heating in the Nordic countries. Int. J. Sustain. Energy Plan. Manag. Vol. 16 (2018)-. https://doi.org/10.5278/ijsepm.2018.16.3

Sørensen, P.A., Schmidt, T., 2018. Design and Construction of Large Scale Heat Storages for District Heating in Denmark. Presented at the 14th International Conference on Energy Storage, p. 15.

Sorknæs, P., Djørup, S.R., Lund, H., Thellufsen, J.Z., 2019. Quantifying the influence of wind power and photovoltaic on future electricity market prices. Energy Convers. Manag. 180, 312–324. https://doi.org/10.1016/j.enconman.2018.11.007

Sousa, G., Jones, B.M., Mirzaei, P.A., Robinson, D., 2017. A review and critique of UK housing stock energy models, modelling approaches and data sources. Energy Build. 151, 66–80. https://doi.org/10.1016/j.enbuild.2017.06.043

Staffell, I., Pfenninger, S., 2016. Using bias-corrected reanalysis to simulate current and future wind power output. Energy 114, 1224–1239. https://doi.org/10.1016/j.energy.2016.08.068

Stamp, S.F., 2016. Assessing uncertainty in co-heating tests: Calibrating a whole building steady state heat loss measurement method (PhD Thesis). UCL (University College London).

Steadman, P., 1997. The non-domestic building stock of England and Wales. Struct. Style Conserv. 20th Century Build.

Steadman, P., Bruhns, H.R., Gakovic, B., 2000. Inferences about Built Form, Construction, and Fabric in the Nondomestic Building Stock of England and Wales. Environ. Plan. B Plan. Des. 27, 733–758. https://doi.org/10.1068/bst13

Steadman, P., Evans, S., Batty, M., 2009. Wall area, volume and plan depth in the building stock. Build. Res. Inf. 37, 455–467. https://doi.org/10.1080/09613210903152531

Steadman, P., Evans, S., Liddiard, R., Godoy-Shimizu, D., Ruyssevelt, P., Humphrey, D., 2020. Building stock energy modelling in the UK: the 3DStock method and the London Building Stock Model. Build. Cities 1, 100–119. https://doi.org/10.5334/bc.52

Strbac, G., Aunedi, M., Pudjianto, D., Djapic, P., Teng, F., Sturt, A., Jackravut, D., Sansom, R., Yufit, V., Brandon, N., 2012. Strategic assessment of the role and value of energy storage systems in the UK low carbon energy future. Rep. Carbon Trust.

Strbac, G., Aunedi, M., Pudjianto, D., Teng, F., Djapic, P., Druce, R., Carmel, A., Borkowski, K., 2015. Value of flexibility in a decarbonised grid and system externalities of low-carbon generation technologies. Imp. Coll. Lond. NERA Econ. Consult.

Strbac, G., Djapic, P., Pudjianto, D., Konstantelos, I., Moreira, R., 2018a. Strategies for reducing losses in distribution networks. London.

Strbac, G., Konstantelos, I., Aunedi, M., Pollitt, M., Green, R., 2016. Delivering future-proof energy infrastructure 54.

Strbac, G., Pudjianto, D., Aunedi, M., Djapic, P., Teng, F., Zhang, X., Ameli, H., Moreira, R., Brandon, N., 2020. Role and value of flexibility in facilitating cost-effective energy system decarbonisation. Prog. Energy 2, 042001. https://doi.org/10.1088/2516-1083/abb216

Strbac, G., Pudjianto, D., Sansom, R., Djapic, P., Ameli, H., Shah, N., Brandon, N., Hawkes, A., Qadrdan, M., 2018b. Analysis of Alternative UK Heat Decarbonisation Pathways. Imperial College London.

Talebi, B., Mirzaei, P.A., Bastani, A., Haghighat, F., 2016. A Review of District Heating Systems: Modeling and Optimization. Front. Built Environ. 2. https://doi.org/10.3389/fbuil.2016.00022

Taylor, S., Fan, D., Rylatt, M., 2014a. Enabling urban-scale energy modelling: a new spatial approach. Build. Res. Inf. 42, 4–16. https://doi.org/10.1080/09613218.2013.813169

Taylor, S., Firth, S.K., Wang, C., Allinson, D., Quddus, M., Smith, P., 2014b. Spatial mapping of building energy demand in Great Britain. GCB Bioenergy 6, 123–135. https://doi.org/10.1111/gcbb.12165

Tereshchenko, T., Nord, N., 2018. Future Trends in District Heating Development. Curr. Sustain. Energy Rep. 5, 172–180. https://doi.org/10.1007/s40518-018-0111-y

The Crown Estate, 2019. Offshore wind operational report. London.

Thomsen, P.D., Overbye, P.M., 2016. Energy Storage for District Energy Systems, in: Advanced District Heating and Cooling (DHC) Systems. Elsevier, pp. 145–166. https://doi.org/10.1016/B978-1-78242-374-4.00007-0

Tian, W., Choudhary, R., 2012. A probabilistic energy model for non-domestic building sectors applied to analysis of school buildings in greater London. Energy Build. 54, 1–11. https://doi.org/10.1016/j.enbuild.2012.06.031

UK Parliament, 2019. The Climate Change Act 2008 (2050 Target Amendment) Order 2019.

UK Parliament, 2008. The Climate Change Act c.27.

UKPN, 2020. Use of System Charging Statement.

Valuation Office Agency, 2020. VOA.

Van Beeck, N., 2000. Classification of energy models. Tilburg University, Faculty of Economics and Business Administration.

Vandermeulen, A., van der Heijde, B., Helsen, L., 2018. Controlling district heating and cooling networks to unlock flexibility: A review. Energy 151, 103–115. https://doi.org/10.1016/j.energy.2018.03.034

Vanhoudt, D., Claessens, B.J., Salenbien, R., Desmedt, J., 2018. An active control strategy for district heating networks and the effect of different thermal energy storage configurations. Energy Build. 158, 1317–1327. https://doi.org/10.1016/j.enbuild.2017.11.018

Vaughan, A., 2021. Priming the heat pump. New Sci. 252, 9. https://doi.org/10.1016/S0262-4079(21)01864-9

Vega, F.J., 2018. Development of a systems approach for studying decarbonisation pathways of heat demand in the UK. https://doi.org/10.25560/61337

Verrilli, F., Srinivasan, S., Gambino, G., Canelli, M., Himanka, M., Del Vecchio, C., Sasso, M., Glielmo, L., 2017. Model Predictive Control-Based Optimal Operations of District Heating System With Thermal Energy Storage and Flexible Loads. IEEE Trans. Autom. Sci. Eng. 14, 547–557. https://doi.org/10.1109/TASE.2016.2618948

Vesterlund, M., Sandberg, J., Lindblom, B., Dahl, J., 2013. Evaluation of Losses in District Heating System, a Case Study. Presented at the Proceedings Of Ecos 2013 - The 26th International Conference On Efficiency, Cost, Optimization, Simulation And Environmental Impact Of Energy Systems, Guilin, China.

Villavicencio, M., 2017. The value of electric energy storage in electricity systems with high shares of wind and solar PV. https://doi.org/10.13140/rg.2.2.19063.11681

Wang, H., Mancarella, P., 2016. Towards sustainable urban energy systems: High resolution modelling of electricity and heat demand profiles, in: 2016 IEEE International Conference on Power System Technology (POWERCON). Presented at the 2016 IEEE International Conference on Power System Technology (POWERCON), IEEE, Wollongong, Australia, pp. 1–6. https://doi.org/10.1109/POWERCON.2016.7754005

Wang, H., Yin, W., Abdollahi, E., Lahdelma, R., Jiao, W., 2015. Modelling and optimization of CHP based district heating system with renewable energy production and energy storage. Appl. Energy 159, 401–421. https://doi.org/10.1016/j.apenergy.2015.09.020

Wang, Z., 2018. Heat pumps with district heating for the UK's domestic heating: individual versus district level. Energy Procedia 149, 354–362. https://doi.org/10.1016/j.egypro.2018.08.199

Wang, Z., Crawley, J., Li, F.G.N., Lowe, R., 2020. Sizing of district heating systems based on smart meter data: Quantifying the aggregated domestic energy demand and demand diversity in the UK. Energy 193, 116780. https://doi.org/10.1016/j.energy.2019.116780

Watson, S.D., Lomas, K.J., Buswell, R.A., 2019. Decarbonising domestic heating: What is the peak GB demand? Energy Policy 126, 533–544. https://doi.org/10.1016/j.enpol.2018.11.001

Wernstedt, F., Davidsson, P., Johansson, C., 2003. Simulation of district heating systems for evaluation of real-time control strategies. Presented at the European Simulation and Modelling Conference.

Weron, R., 2014. Electricity price forecasting: A review of the state-of-the-art with a look into the future. Int. J. Forecast. 30, 1030–1081. https://doi.org/10.1016/j.ijforecast.2014.08.008

Wilson, I.A.G., Rennie, A.J.R., Ding, Y., Eames, P.C., Hall, P.J., Kelly, N.J., 2013. Historical daily gas and electrical energy flows through Great Britain's transmission networks and the decarbonisation of domestic heat. Energy Policy 61, 301–305. https://doi.org/10.1016/j.enpol.2013.05.110

Wilson, M., 2019. Lazard's Levelized Cost of Storage Analysis - Version 13.0.

Woods, P., 2012. ETI Macro Distributed Energy Project Summary Report. Energy Technologies Institute.

Wozabal, D., Graf, C., Hirschmann, D., 2016. The effect of intermittent renewables on the electricity price variance. Spectr. 38, 687–709. https://doi.org/10.1007/s00291-015-0395-x

Yao, R., Steemers, K., 2005. A method of formulating energy load profile for domestic buildings in the UK. Energy Build. 37, 663–671. https://doi.org/10.1016/j.enbuild.2004.09.007

Zehnder, M., 2005. Efficient air-water heat pumps for high temperature lift residential heating, including oil migration aspects. https://doi.org/10.5075/EPFL-THESIS-2998

APPENDICES

APPENDIX A - CHAPTER 1 136
APPENDIX B - CHAPTER 2 141
APPENDIX C - CHAPTER 3 146
APPENDIX D - CHAPTER 4 148

Appendix A - Chapter 1

Table A-1 Review of models integrating heat and electricity sectors

Model	Classification	Focus	Area	Scenarios length	Electricity	Heating	District heating	Resolution	Optimisation and operation	Availability
Dynemo	Exploration Accounting	Whole system model - Integration of REN	UK (and France)	Current to 2050	Set by defining 2050 installed capacity with a transition from current	Building thermal model, Option for synthesis weather or actual location data	Included with HP and TES	Pre defined - minutes to years	Heuristic Based operational control	Academic dept.
Balmorel	Exploration Accounting Bottom up Deterministic	Long term planning and short-term operation analysis of sectors in a whole system	International regional subdivision	various up to 50 years	Simulated power gen, Renewables stochastic, Includes transmission, variable marginal costs	Defined by total annual heat load and inter-year variability	Emphasis on CHP integration	Hourly	Optimised hourly dispatch of DHN-CHP, heuristic based power model	Open source
Enneralt	Forecasting	Simulate electricity market operation	Nordic	Yearly	Uses known gen capacities, VRE simulated by mean level but varying generation by the standard deviation (stochastic)	Using input data or heating degree hours for regional/district level	CHP and storage modelled with regional heat loads	Hourly	Myopic operation cost optimisation	Academic dept.

UK Times	Exploration Accounting Bottom up	Economic policy and planning energy systems	Global National regional	Up to 2100	Simulated by capacity and capacity factors in time slices	Predefined annual demand. Based on day/nighttime slices with seasonal variation	Full range of DH technologies	Hourly Daily Monthly	Global optimisation	Free source code, requires commercial solver
SIVAEL	Forecasting Simulation Bottom up	Electricity and DH simulation	National regional district	Daily to Annual	Simulates using forecast with stochastic renewable generation	Known DH load profiles	Mainly CHP district heating	Hourly	economic optimisation of operation	Discontinued
RAMSES	Forecasting Simulation	Danish Energy forecast and simulation for electricity and DH	National Denmark	Up to 30-year analysis	Electricity cost for Scandinavian market based on marginal costs	Simulated heat loads	DH-CHP modelled with heat revenues included	Hourly to daily	Linear optimisation of plant investments	Not commercially available
EnergyPlan	Forecasting and Exploration Simulation Bottom up	National whole system analysis	Localised to many countries	Annual pre-defined	Deterministic power generation set by defined install capacities	Pre-defined heat load profiles	Comprehensive DH plant components	Hourly	Heuristic based	Free to download

energyPRO	Forecasting Simulation Bottom up	Project simulation and optimisation	Region/district within national system	Up to 40 years plant/project life	Pre-load wholesale prices (i.e., from elexon)	Based on degree days with various demand profiles	All thermal plant except nuclear	Hourly	Mathematical optimisation based on electricity market cost	Commercial
REMod-D	Forecasting Simulation Deterministic	German whole system scenario analysis and planning	National Germany	Up to 2050	Based on normalised annual generation profile	Using ambient temperature and a single aggregated correlation for national heat demand	Includes DH connected heat loads with CHP and thermal storage	Hourly	Particle swarm optimisation for least cost whole system	Not commercially available
OSeMOSYS	Exploration	Flexible open-source whole system scenario planning	Various	Long term scenario	Based on technology and capacity factors, aggregated over time slices	Modelled in fractions of year of similar demand levels based on annual demand	Not modelled but modular structure allows future addition	5 year of 3 seasons	Economic optimisation of technologies	Open source
RESOM	Exploration Accounting Bottom up	Whole system planning	National UK	Up to 2050	Using technology data and average load factors	Detailed segmented heat demand	HP, CHP(+CCS), fuel cells, TES, No interseasonal Tes	5 year of 5 characteristic days of 4-hour blocks	Global system costs optimised with perfect or partial foresight	Private

ESME	Exploration Optimisation Bottom up	National whole system design and planning	National Localised version	Up to 2050	Using technology data and average load factors with constraints to meet demand	Regional heat load per time slice	Included as a solution but no evidence of TES - spatially explicit	5 year of 2 seasons consisting of 5 diurnal time slices	Pathway cost optimisation with stochasticity	Private/Academic
GTMax	Forecasting Simulation Bottom up Deterministic	National electricity generation and transmission	National Localised versions available	Annual or flexible	Full detailed recreation of electricity sector with spot prices	Selected as predefined heat loads	Included as a CHP load	Hourly	Cost and operational optimisation of power plants	Commercial

Table A-2 Summary of main modeling assumption

Section	Assumption
2.1	District heating loads are entirely consisted of urban heat demand which have the highest heat demand density as these are likely the most economic areas for DH deployment.
2.5	The national heat load profile can be extrapolated from the consumption profile of the top 10% gas consumption areas.
2.3	All buildings of the same archetype exhibit the same physical characteristics.
2.3.2	HeLoM models all building with a (gas boiler) heating power input efficiency of 85%.
2.3.3	All domestic archetypes exhibit the same occupancy pattern.
2.3.7	Nondomestic MSOA gas data for urban areas is predominantly service and commercial sector rather than industrial use.
2.4	The temperature of the building thermal mass and internal wall surface are equal to the internal air temperature
2.4	Wind forced convection acts only on one side of a building.
2.4	The building thermal model assumes steady state heat transfer.
2.4.1	Nondomestic hot water demand has a constant flat hourly distribution.
2.4.2	Age distributions of domestic buildings is evenly spread across archetypes.
3.3	The GB electricity network is an isolated island with no interconnection. Baseload generation is constant and dispatchable would be lower in the merit order than renewable generation.
3.4	A dispatch merit order would include a carbon emission tax as well as direct cost.
3.5	Electricity prices reflect marginal costs with additional transmission and distribution costs.
3.5.4	Grid batteries all charge and discharge in unison, effectively a single large store.
3.5.6	Lithium-ion batteries are assumed for grid electrical storage.
3.7	Non heating and transport demand variations can be estimated by extrapolating existing demand. EV charging demand is the inverse of traffic flows with no vehicle to grid service.
3.7.3	Individual domestic and nondomestic heat pumps operate with a fraction of Carnot efficiency of 0.40 and 0.45 respectively.
3.7.3	UKPN electricity losses for London and South East are representative of the country.
3.7.5	2050 offshore wind capacity factors will average 0.55, higher than the present average.
4.2.2	The DH operates with a fixed 70°C flow temperature and a return varying linearly between 50°C at peak load and 20°C at zero load.4.2.3Hourly distribution losses are 12% of the hourly load on the DH network.
4.2.6	DH HPs are connected at high voltage and therefore avoid LV distribution losses.
4.2.6	Generic HP source temperatures vary seasonally as ground temperatures at 3m depth.
4.2.5	TES are pressure connected with the DH network and stratified in two layers and designed with a height/diameter ratio of 0.5. Thermal losses are simplified by using the average tank temperature as representative of the surface temperature.
4.2.6	DH has a single stage heat pump with a Carnot efficiency of 65% and negligible ramp limits. A generic source temperature is used based on ground temperature variations.
4.3	A back up electrical resistance boiler is able to provide any unmet thermal load.
4.3.5	The rolling dynamic optimisation algorithm has perfect foresight in the finite time horizon periods specified.
5.2.5	A centralised dispatch agent or market controls the storage on the electrical system and TES in DH. The model implicitly has a single large DH system with HP and TES which act upon the electrical system rather than smaller DH systems with unique load profiles and multiple smaller TES.

Appendix B - Chapter 2

Table B-1 Domestic characterisation: Assumptions and parameters

Dwelling type	Built period	Floor Area m^2	Height m	Wall U W/m^2K	Ground U W/m^2K	Loft floor U W/m^2K	Glazing U W/m^2K	Glazing area m^2	Glazing Trans %	ACH $hour^{-1}$	∑UA W/K	TMP kJ/m2K	ThM kWh/K	Boiler kW	Mean Occu-pancy
Terraced	Pre 1918	87.0	4.70	2.10	0.8	0.16	3.1	21.75	0.85	0.56	311.79	612	14.8	23.95	3.0
Terraced	1918–1964	78.0	4.70	2.10	0.6	0.16	3.1	19.50	0.75	0.76	294.93	500	10.8	23.02	2.9
Terraced	1965–1980	78.0	4.70	1.30	0.6	0.16	3.1	19.50	0.75	0.64	248.90	400	8.7	20.49	2.9
Terraced	1981–1990	68.0	4.70	0.60	0.6	0.30	3.1	17.00	0.75	0.64	204.77	300	5.7	18.06	2.9
Terraced	Post 1990	77.0	4.70	0.45	0.3	0.16	3.1	19.25	0.75	0.51	174.20	200	4.3	16.38	2.9
Semi-det	Pre 1918	126.0	4.70	2.10	0.8	0.16	3.1	31.50	0.85	0.56	576.37	612	21.4	33.50	3.1
Semi-det	1918–1964	91.0	4.70	1.60	0.6	0.16	3.1	22.75	0.75	0.76	414.54	500	12.6	26.60	3.0
Semi-det	1965–1980	85.5	4.70	1.30	0.6	0.16	3.1	21.38	0.75	0.64	348.98	400	9.5	21.99	3.0
Semi-det	1981–1990	74.0	4.70	0.60	0.6	0.30	3.1	18.50	0.75	0.64	255.66	300	6.2	17.86	2.9
Semi-det	Post 1990	79.5	4.70	0.45	0.3	0.16	3.1	19.88	0.75	0.51	206.10	300	6.6	18.14	2.9
Detached	Pre 1918	197.0	4.70	2.10	0.8	0.16	3.1	49.25	0.85	0.56	965.33	550	30.1	49.89	2.8
Detached	1918–1964	151.0	4.70	1.60	0.6	0.16	3.1	37.75	0.75	0.76	720.80	450	18.9	36.44	2.3
Detached	1965–1980	135.0	4.70	1.30	0.6	0.16	3.1	33.75	0.75	0.64	582.68	350	13.1	31.85	2.5
Detached	1981–1990	134.0	4.70	0.60	0.6	0.30	3.1	33.50	0.75	0.64	469.28	250	9.3	32.61	2.3
Detached	Post 1990	166.0	4.70	0.45	0.3	0.16	3.1	41.50	0.75	0.51	427.97	200	9.2	37.34	2.2
Flat	Pre 1918	67.0	2.35	2.10	0.0	0.0	4.8	16.75	0.85	0.56	375.38	300	5.6	27.45	2.2
Flat	1918–1964	56.0	2.35	2.10	0.0	0.0	3.1	14.00	0.75	0.76	257.42	250	3.9	20.96	1.9
Flat	1965–1980	52.5	2.35	1.30	0.0	0.0	3.1	13.13	0.75	0.64	255.75	250	3.6	20.87	1.8
Flat	1981–1990	57.0	2.35	0.60	0.0	0.0	3.1	14.25	0.75	0.64	191.39	200	3.2	17.33	1.9
Flat	Post 1990	60.0	2.35	0.45	0.0	0.0	3.1	15.00	0.75	0.51	141.93	200	3.3	14.61	2.0

Table B-2 Nondomestic Archetype parameters

CaRB2 Class	Floor Area m^2	Storey Height m	Depth m	Width Ext %	Glaze %	Glaze Trans %	Wall U W/m^2K	Glaze U W/m^2K	Roof U W/m^2K	Floor U W/m^2K	AirCh hr^{-1}	SHL kW/K	ThM kWh/K	Boiler kW	Int Gain W/m^2
Office	276.0	3.0	8.0	0.9	0.4	0.5	1.0	3.8	0.7	0.4	3.5	1.1	19.2	19.3	32
Shop	201.7	3.0	15.0	0.9	0.5	0.5	1.0	3.8	0.7	0.4	5.0	1.2	14.0	20.2	46
Factory	737.3	5.0	20.0	0.9	0.1	0.7	1.0	3.8	0.7	0.4	3.0	4.9	51.2	59.0	90
Warehouse	922.9	8.0	25.0	0.9	0.1	0.7	1.0	3.8	0.7	0.4	1.5	5.5	64.1	46.2	27
Hospitality	365.9	3.0	8.0	0.9	0.2	0.7	1.0	3.8	0.7	0.4	5.0	1.9	25.4	22.0	47
ArtsLeisure	437.1	3.0	8.0	0.9	0.2	0.7	1.0	3.8	0.7	0.4	5.0	2.5	30.4	43.7	30
Sports	668.6	6.0	15.0	0.9	0.1	0.7	1.0	3.8	0.7	0.4	5.0	6.2	46.4	24.9	60
Education	1291.0	3.5	10.0	0.9	0.1	0.7	1.0	3.8	0.7	0.4	3.5	6.0	89.7	112.3	75
Health	1477.7	4.0	15.0	0.9	0.2	0.7	1.0	3.8	0.7	0.4	5.0	7.9	102.6	73.9	69
Transport	408.2	5.0	20.0	0.9	0.1	0.7	1.0	3.8	0.7	0.4	5.0	3.8	28.3	20.4	26
Community	295.7	3.0	7.0	0.9	0.1	0.7	1.0	3.8	0.7	0.4	5.0	1.7	20.5	20.7	40
Emergency	2496.1	4.0	7.0	0.9	0.1	0.7	1.0	3.8	0.7	0.4	5.0	18.6	173.3	124.8	40

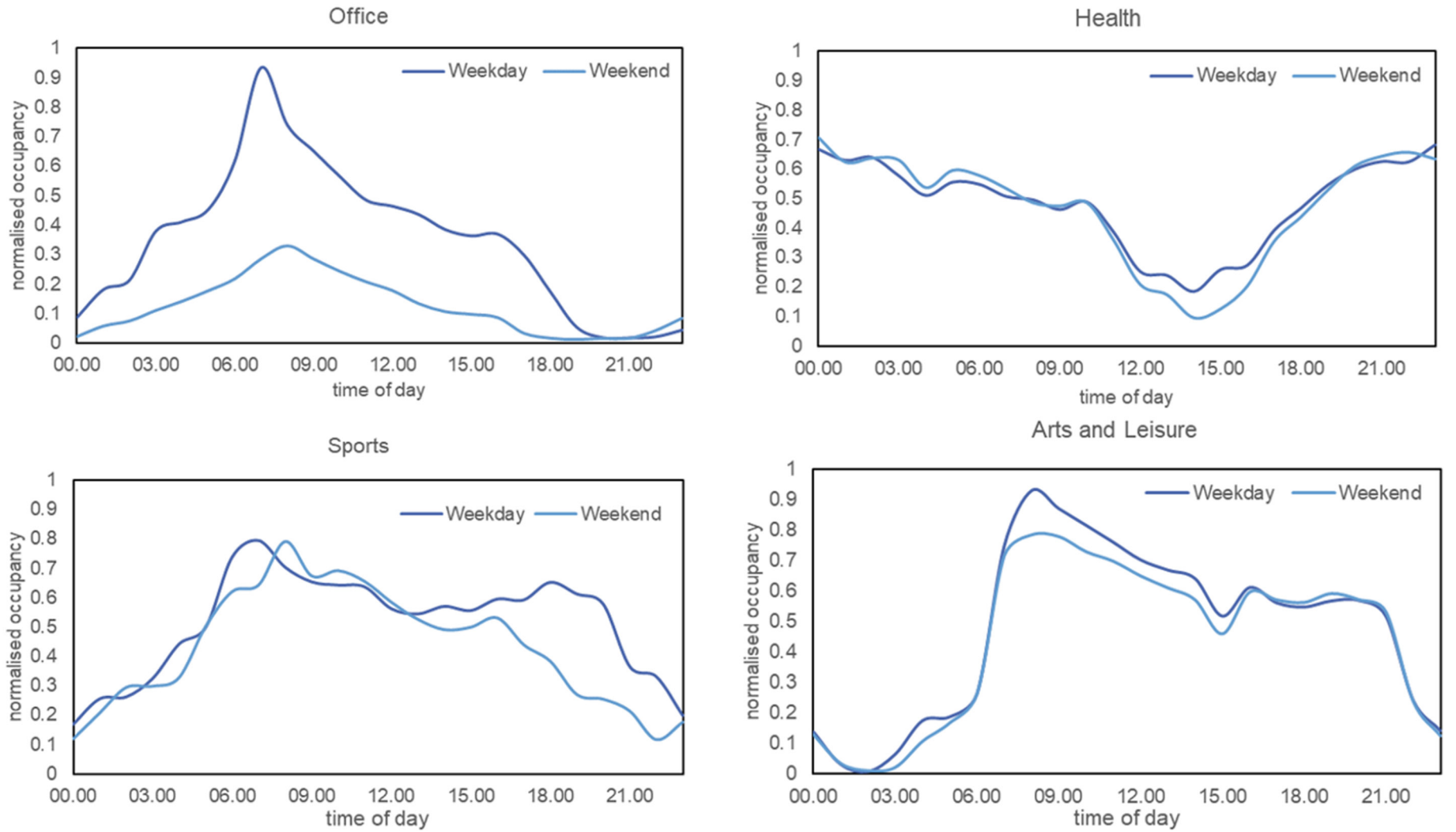

Figure B-1 24-hour occupancy factors derived from measured hourly gas consumption (a) from data provided by Sustainable Energy Ltd (Challans, 2018)

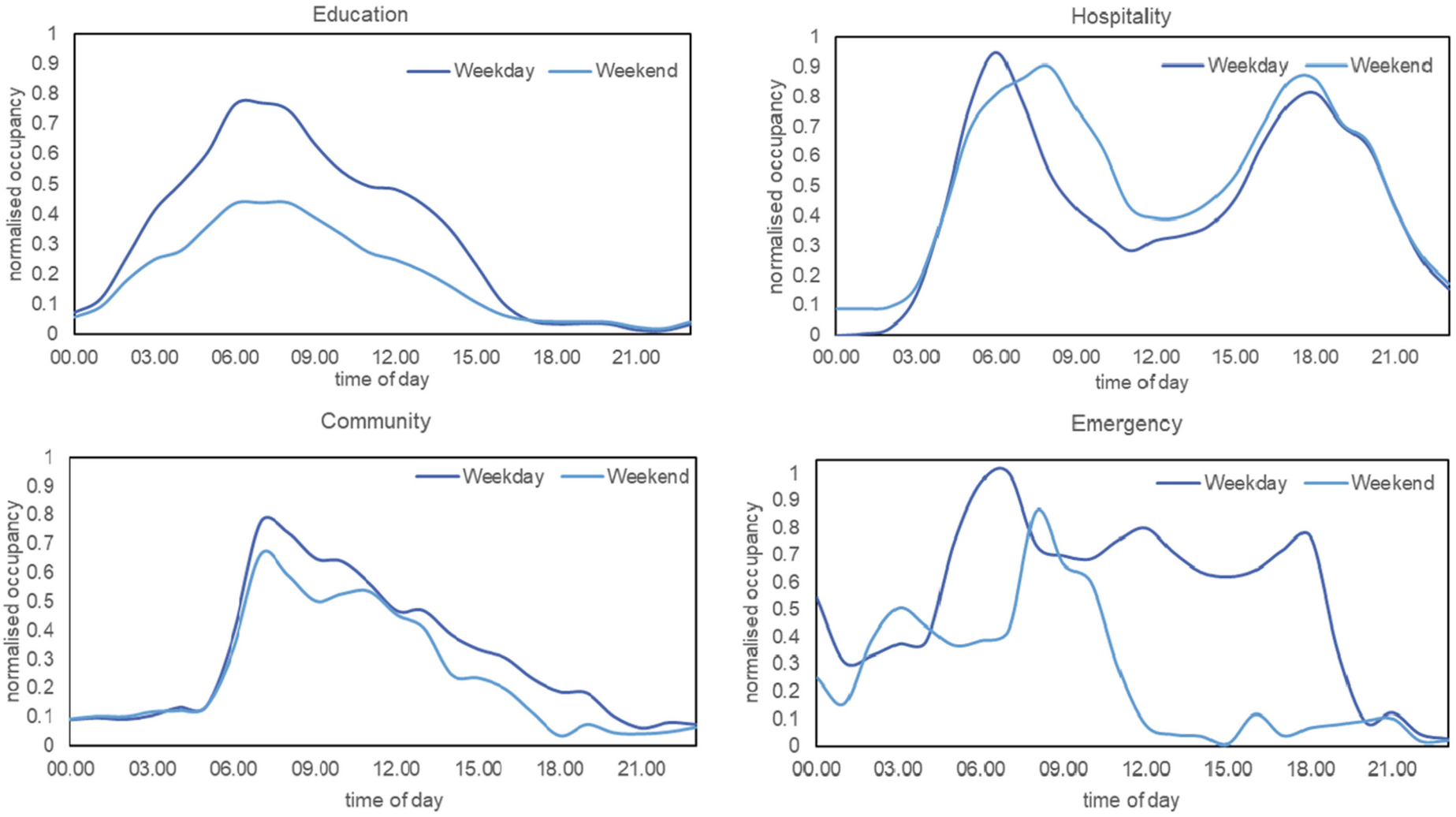

Figure B-2 24-hour occupancy factors derived from measured hourly gas consumption (b) from data provided by Sustainable Energy Ltd (Challans, 2018)

Table B-3 Details of hourly nondomestic gas consumption from data provided by Sustainable Energy Ltd (Challans, 2018)

CaRB2 Class	Building sources	Data Length	Further Information	Estimated Active Occupancy
Offices	5	2011-2015	5 office	7-5 weekday, 8-15 weekend
Hospitality	2	2015-2017	2 hotels	6-23
Arts Leisure	3	2013-2014	3 theatres	8-21
Sports	5	2010-2015	5 leisure centres	7-20
Education	16	2011-2015	10 primary, 5 secondary, 1 college	6-17 weekday, 6-15 weekend
Health	2	2011-2015	1 hospital, 2 care homes	24hr
Community	2	2013-2015	1 Library, 1 day centre	7-18
Emergency	1	2013-2014	Fire station	24hr weekday, 12hr weekend

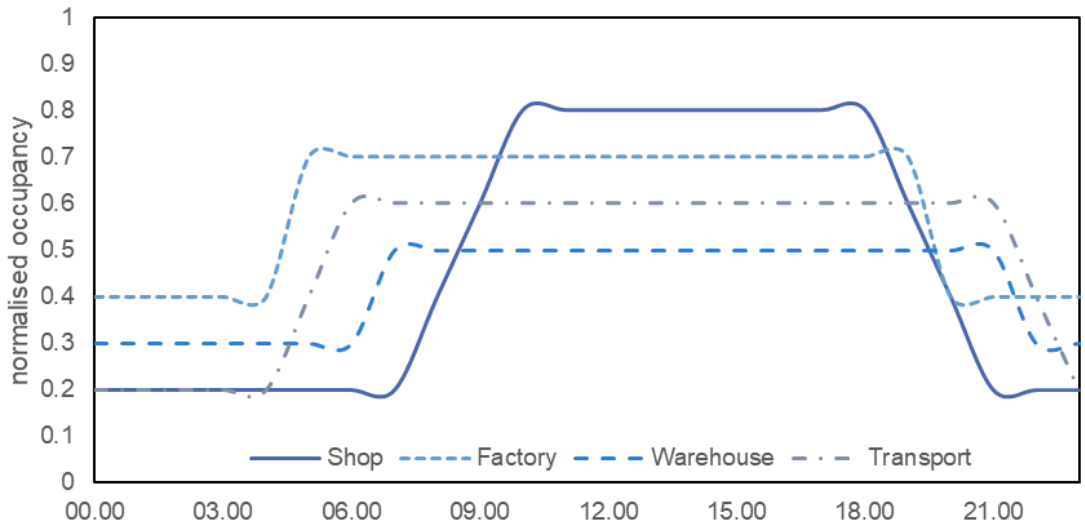

Figure B-3 Hourly estimated nondomestic occupancy factors

Table B-4 Estimated activity classifications

CaRB2 Class	Estimated Active Occupancy	Further information
Shop (retail)	9-20	(Duarte et al., 2013)
Factory	24hr	Reduced overnight
Warehouse	24hr	Reduced overnight
Transport	24hr	Reduced weekend

Appendix C - Chapter 3

Table C-1 Input cost assumptions used in cost modelling*

Generator	CAPEX £/kW	Fixed O&M £/MW/a	Var O&M £/MWh	Efficiency %	Fuel cost £/MWh	Carbon cost £/MWh	Lifetime years	Source
CCGT Class H	526.8	15,520	1.5	0.6	35	19**	25	(BEIS, 2016e; Leigh Fisher and Jacobs, 2016)
Offshore. Wind	1860	45,715	3.5	0	0	0	25	(ARUP, 2016; BEIS, 2016e)
Onshore. Wind	1395	22,100	5	0	0	0	23	(ARUP, 2016; BEIS, 2016e)
Solar PV	652	4,792	0.1	0	0	0	25	(ARUP, 2016; BEIS, 2016e)
Li-Ion	337 (£/kWh)	2,120 (£/MWh/a)	2	0.9	0	0	15	(IRENA, 2017; Wilson, 2019)

* All costs have been adjusted for inflation to 2020 figures

**Calculated assuming a carbon price of £300/tCO_2e (Burke et al., 2019)

Table C-2 National Grid FES 2020 Scenarios

Generation / Demand	CT	ST	LW	SP
Baseload - GW	24.32	22.52	15.05	8.79
Offshore Wind - GW	82.72	87.87	83.97	64.73
Onshore Wind - GW	47.74	28.82	41.52	25.28
Solar PV - GW	75.36	56.17	71.13	30.77
Other Renewables - GW	15.77	15.69	7.32	8.02
Other capacity - GW	33.02	45.32	23.05	10.09
Fossil fuel - GW	0.07	0.24	0.5	43.19
Battery - GWh	51.9	21.1	56.2	23.9
Other storage - GWh	142.2	125.2	146.7	91.5
Total Annual demand TWh	451	374	386	394
Electric Vehicle Annual demand - TWh	87	82.5	81.1	82.2
Domestic Electrified Heat - TWh	83	44	74	47

Table C-3 National Grid FES 2020 Heating Scenarios

Heating method	2019	CT	ST	LW	SP
ASHP	0%	57%	13%	42%	8%
Electric storage heaters	5%	5%	5%	5%	6%
GSHP	0%	7%	1%	6%	0%
Direct Electric Heating	2%	2%	2%	3%	3%
Gas boilers	85%	0%	0%	0%	68%
Hybrid boilers (Natural gas)	0%	0%	0%	0%	6%
Hybrid boilers (Hydrogen)	0%	10%	13%	26%	0%
Oil, LPG, & solid fuel boilers	5%	0%	0%	0%	3%
Hydrogen boilers	0%	0%	53%	0%	0%
Biomass boilers [Biofuels]	0%	0%	0%	1%	0%
District Heat	2%	16%	10%	13%	5%
Biofuels (Off gas Grid)	0%	3%	2%	3%	1%
Others	0%	0%	0%	2%	0%

Appendix D - Chapter 4

Table D-1 Assumptions and sources used for DHN costs*

	Low	Medium	High	Source
Network Capital non-bulk £/ MWh	456	1043	1699	(DECC, 2015b)
Network Fixed OM £/ MWh_{th}/yr		13.1		(Wang, 2018)
Network Lifetime Years		50		
HP Capital £ /MW_{th}	435,000	652,500	870,000	(Danish Energy Agency, 2016)
HP Fixed OM £/ MW_{th}/yr	900	1750	2600	(Marina et al., 2021)
HP Var OM (exc elec) £/MWh_{th}	1.3	1.52	1.74	
HP Lifetime Years		25		
TES Capital £/MWh	1900	4450 or $107{,}198(TES)^{-0.47}$	7000	(Danish Energy Agency, 2018)
TES Fixed OM £/MWh/yr	4.35	16.52	28.7	(BEIS, 2016a)
TES Lifetime Years		40		

* All costs have been adjusted for inflation to 2020 figures